RESPONSE OF A SLOTTED PLATE FLOW METER TO

HORIZONTAL TWO PHASE FLOW

A Thesis

by

VASANTH MURALIDHARAN

Submitted to the Office of Graduate Studies of
Texas A&M University
in partial fulfillment of the requirements for the degree of

MASTER OF SCIENCE

December 2003

Major Subject: Mechanical Engineering

RESPONSE OF A SLOTTED PLATE FLOW METER TO

HORIZONTAL TWO PHASE FLOW

A Thesis

by

VASANTH MURALIDHARAN

Submitted to Texas A&M University
in partial fulfillment of the requirements
for the degree of

MASTER OF SCIENCE

Approved as to style and content by:

Gerald L. Morrison (Chair of Committee)	David Rhode (Member)
Kenneth R. Hall (Member)	Dennis O' Neal (Head of Department)

December 2003

Major Subject: Mechanical Engineering

ABSTRACT

Response of a Slotted Plate Flow Meter to
Horizontal Two Phase Flow. (December 2003)
Vasanth Muralidharan, B.E., Madurai Kamaraj University
Chair of Advisory Committee: Dr. Gerald L. Morrison

The slotted plate flow meter has been widely tested as an obstruction flow meter during the past several years. It has been tested for both single-phase flows as well as for two-phase flows. Previous studies have revealed that the slotted plate flow meter is always better in performance and accuracy than the standard orifice plate flow meter. This study is primarily based on how a slotted plate responds to horizontal two-phase flow with air and water being used as the working fluids. The plates under consideration are those with beta ratios of 0.43 and 0.467. Experiments have been performed with six different configurations of the slotted plate test sections. The performances of the slotted plate flow meters will be compared to that of a standard orifice plate flow meter and then with a venturi. The effects of varying the upstream quality of the two-phase flow on the differential pressure and the coefficient of discharge of the slotted plates, the standard orifice plate and the venturi will be evaluated. Response characteristics at low differential pressures will be investigated. Tests for repeatability will be performed by studying the effects of the gas Reynolds number and the upstream quality on the differential pressure. The differential pressures across the slotted plates, the standard orifice plate and the venturi will be compared. Reproducibility will be evaluated by comparing the data obtained from all six different configurations. One of the main objectives of this study is to arrive at the best suitable procedure for accurately measuring the flow rate of two-phase flow using the slotted plate flow meter.

DEDICATION

To my family for their unlimited love and support in helping me achieve my goals.

ACKNOWLEDGEMENTS

TABLE OF CONTENTS

NOMENCLATURE

A1	Area of cross section of the pipe section upstream of the orifice plate
A2	Area of cross section of the vena contracta
$A_{orifice}$	Area of cross section of the orifice
A_{pipe}	Cross sectional area of the pipe taking the inner diameter into account
A_{slots}	Total area of the slots (open)
β	Beta ratio
C_c	Contraction coefficient
C_d	Coefficient of discharge
C_v	Velocity coefficient
d or $d_{orifice}$	Diameter of the orifice
D_{pipe}	Diameter of the pipe
dP or ΔP	Differential pressure
F_a	Factor to account for the thermal expansion of the primary element
g	Acceleration due to gravity
γ_{G1}	Specific weight of gas at the orifice outlet
γ_{L1}	Specific weight of the liquid at the orifice outlet
h_{wTP}	Head produced by the two phase flow through the orifice
H1	Vertical position of the flange tap
H2	Vertical position of the vena contracta
K	Flow coefficient

$K_G Y_G$	Product of flow coefficient and expansion factor for gas flow
K_L	Flow coefficient for liquid flow
KY	Calibration coefficient
$\dot{m}$	Mass flow rate
$\dot{m}_{air}$	Mass flow rate of air
$\dot{m}_{actual}$	Actual mass flow rate of the two-phase flow mixture through the slotted plate
$\dot{m}_{lwater}$	Flow rate of water flowing through the large Coriolis flow meter
$\dot{m}_{mixture}$	Mass flow rate of the two-phase flow mixture
$\dot{m}_{swater}$	Flow rate of water flowing through the small Coriolis flow meter
$\dot{m}_{water}$	Mass flow rate of water
μ_{air}	Absolute viscosity for air
P1	Pressure upstream of the orifice plate at the flange tap
P2	Downstream pressure at the vena contracta
P_{air}	Air pressure
Q_{air}	Volumetric flow rate
R_{air}	Gas constant for air
Re_{air}	Air Reynolds number
ρ	Density of the fluid
ρ_{air}	Density of air

ρ_{actual}	Actual density of the fluid mixture flowing through the plate under consideration
$\rho_{mixture}$	Density of the two-phase flow mixture
ρ_{water}	Density of water
T_{air}	Air temperature
V1	Bulk averaged velocity at the flange tap
V2	Bulk averaged velocity at the vena contracta
w_h	Weight flow rate of the two-phase flow
X	Quality
$X_{0.43}$	Quality downstream of the 0.43 beta ratio slotted plate
$X_{0.467}$	Quality downstream of the 0.467 beta ratio slotted plate
X_{up}	Quality upstream of the slotted plate section
y	Liquid weight fraction which is the ratio of the weight of the liquid during two-phase flow to that of the total flow
Y	Expansion factor

INTRODUCTION

Flow measurement is a very important requirement in industries dealing with oil, natural gas, chemicals, processing, and steam as well as nuclear and conventional power plants. Most of these industries deal with fluid flow and in reality this fluid flow is generally multi-phase. In the past, several different types of equipment were used to measure multi-phase flow. These have turned out to be either inaccurate or are not suited to a real time industrial environment. It was only in the recent past few years; multi-phase flow meters have started to be used as flow measuring devices. These devices are cheaper, more accurate, easier to use, and time saving when used to measure the individual quantities of fluids mixed together in a two-phase flow.

For industries dealing with multi-phase flows, profit and loss is directly governed by the accuracy in the measurement of the various components. Thus it is necessary to use a flow metering device which is accurate. There are several advantages in using a multi-phase flow metering device, especially in the oil and gas industry where the flow is mostly multi-phase. Knowledge of the flow rates of water, oil and gas is needed to monitor the amount of oil and gas produced. An increased accuracy means greater control over the production process and hence wells can satisy the regulated guidelines. In steam and nuclear power, accuracy is an important keyword as it largely decides the efficiency of the plant and the extent to which the process could be controlled. Maximum efficiency could be attained with improved accuracy. A significant amount of research has been performed to develop a multi-phase flow metering device capable of satisfying industry standards. Conventional single phase flow metering devices such as the standard orifice plate, the venturi meter, the turbine meter, the vortex shedding flow meter, the ultrasonic Coriolis flow meter and the Pitot probe have been

---

This thesis follows the style and format of the Journal of Flow Measurement and Instrumentation.

tested with multi-phase flow to observe their capabilities. New methods of instrumentation for multi-phase flow such as the true mass flow meter which makes independent direct measurements of each phase, the vibrating pendulum flow meter, the crossed beam correlation with lasers, the pulsed neutron activation method, the capacitance method and a multi-phase flow meter which uses gamma rays have also been developed.

The standard orifice plate flow meter, which consists of a plate with a circular orifice at the center, was the first of the flow meters to be used for multi-phase flow. Further research has led to the development of a slotted plate flow meter. Unlike its predecessor, the slotted plate has an array of radial slots instead of a circular orifice. The porosity of each ring of slots can be kept the same by changing the number of slots. This disperses the flow over the entire cross section of the pipe and also eliminates swirl. In the last few years it has been tested for single-phase flow and found to be more accurate and repeatable than the standard orifice plate. It can be used both as a flow metering device as well as a flow conditioner.

The main purpose of this study is to show how the slotted plate responds to two-phase flow consisting of air and water. A literature review was performed to investigate previous research completed on the slotted plate flow meter and other flow measuring equipment. Several experiments were carried out using air and water to observe if the data collected shows repeatability and if the plates are capable of reproducing similar data. The effects of varying the gas flow rate and the quality of the two-phase flow at different upstream pressures on the coefficient of discharge of the slotted plate were also observed. This was done for different arrangements of the slotted plate test section. Slotted plates with beta ratios of 0.43 and 0.467 were used in the experiments. They were tested in conjunction with a standard orifice plate having a beta ratio of 0.508 and later with a venturi having a beta ratio of 0.527 to observe how well the slotted plate responded to two-phase flow compared to other devices. The response of the slotted

plate at low differential pressures was also studied to determine whether it was good enough for low pressure measurement. In reality oil and natural gas pipelines deal with pressures characterized by heavy fluctuations ranging from an extreme high to very low pressures and it should be ensured that the slotted plate responds well in such scenarios.

Motivation behind the Study

A standard orifice plate essentially consists of a thin metallic circular disc having a hole (orifice) drilled at the the center. The inlet side of the orifice is flat whereas the outlet side is bevelled. The orifice can be circular or square depending on the application. It is mounted in between flanges in such a way that the orifice is concentric to the pipe. The flow downstream of the orifice plate is axisymmetric. Pressure measurement using an orifice plate consists of determining the difference in pressure from the upstream side to the downstream side. This difference in pressure is attributed to the orifice plate which acts as an obstruction that narrows the pipe cross section and forces the fluid to constrict. This fluid constriction creates a differential pressure.

A fully developed flow through a circular pipe, accelerates as it approaches the orifice plate flow meter and migrates towards the pipe centerline. This flow is axially symmetric on the upstream side of the plate. As it reaches close to the plate surface it attains significant radial momentum as the fluid accelerates through the orifice. The energy required to produce the acceleration, both axial and radial is provided by the differential pressure across the plate. This combination of axial as well as radial velocities makes the fluid to flow through the orifice. As it reaches the downstream surface of the plate the flow seperates. A recirculation zone is created close to the downstream side. The cross sectional area of the fluid flowing out of the orifice reaches a minimum some distance downstream of the orifice plate. This point is called as the vena contracta and is characterized by minimum jet diameter. Its presence is due to the large inward radial velocity required for the fluid to enter the orifice. The left over

momentum causes the vena contracta. After the vena contracta has been reached the fluid velocity starts decreasing and reattachment takes place on the downstream side. Once the fluid has reattached with the pipe walls, the fluid velocity becomes predominantly axial as the radial component decreases. A difference in pressure is created between the upstream side and the downstream side of the orifice plate and this difference is proportional to the flow rate of the fluid. This phenomenon is the main motivation behind the study of orifice plate flow meters. The mass flow rate of the fluid flowing through the orifice plate is derived using Bernoulli's equation. The flow is assumed to be steady, frictionless, uniform, incompressible with no body forces. Two locations, point (1) on the upstream side where the orifice plate does not have any effect on the flow and point (2) at the vena contracta where the pressure is minimum, are considered for this analysis. The Bernoulli's equation is written as,

$$\frac{P_1}{\rho} + \frac{V_1^2}{2} + gH_1 = \frac{P_2}{\rho} + \frac{V_2^2}{2} + gH_2 \qquad (1)$$

where P_1 (Pa) and P_2 (Pa) are the pressures at points (1) and (2), V_1 (m/s) and V_2 (m/s) are the bulk averaged velocities at points (1) and (2), H_1 (m) and H_2 (m) are the vertical positions of points (1) and (2) from the datum, ρ (kg/m^3) is the density of the fluid, and g (m/s^2) is the acceleration due to gravity. Assuming both points (1) and (2) are at the same height, then

$$H_1 = H_2 \qquad (2)$$

Using the continuity equation, the mass flow rate of fluid through the pipe is given by

$$\dot{m} = \rho A_1 V_1 = \rho A_2 V_2 \qquad (3)$$

where $\dot{m}$ (kg/s) is the mass flow rate of fluid flowing through the pipe, and A_1 (m^2) and A_2 (m^2) are the cross sectional areas at points (1) and (2). Solving equation (3) for V_1 and substituting it in equation (1),

$$V_2 = \sqrt{\frac{2(P_1 - P_2)}{\rho\left[1 - \left(\dfrac{A_2}{A_1}\right)^2\right]}} \tag{4}$$

Substituting the expression for V_2 in equation (3),

$$\dot{m} = \rho A_2 V_2 = \rho A_2 \sqrt{\frac{2(P_1 - P_2)}{\rho\left[1 - \left(\dfrac{A_2}{A_1}\right)^2\right]}} = \frac{A_2}{\sqrt{1 - \left(\dfrac{A_2}{A_1}\right)^2}}\sqrt{2\rho\Delta P} \tag{5}$$

In reality the cross sectional area at point (2) is very difficult to measure and hence it is replaced by the area of cross section of the orifice. This is done by intoducing a correction factor called as the contraction coefficient C_c. This also brings in the beta ratio of the pipe into picture. The beta ratio is given by,

$$\beta = \sqrt{\frac{A_{orifice}}{A_1}} = \frac{d_{orifice}}{D_{pipe}} \tag{6}$$

where β is the beta ratio of the orifice plate, $A_{orifice}$ (m^2) is the area of cross section of the orifice, $d_{orifice}$ (m) is the diameter of the orifice and D_{pipe} (m) is the diameter of the pipe. The differences in velocities between the two points is corrected by introducing yet another correction factor called the velocity coefficient C_v. Substituting C_c and C_v in equation (5) and replacing A_2 with the area of the orifice, the mass flow rate is given by,

$$\dot{m} = C_c C_v A_{orifice}\left(\frac{1}{\sqrt{1 - \beta^4}}\right)\sqrt{2\rho\Delta P} \tag{7}$$

Equation (7) can further be simplified as,

$$\dot{m} = C_d A_{orifice} \left(\frac{1}{\sqrt{1-\beta^4}} \right) \sqrt{2\rho\Delta P} \tag{8}$$

$$C_d = \frac{4\dot{m}\sqrt{1-\beta^4}}{\pi(D_{pipe}\beta)^2\sqrt{2\rho\Delta P}} \tag{9}$$

where C_d is called the coefficient of discharge of the orifice plate flow meter and ΔP is the difference between P1 and P2. Experimental investigations have revealed that for standard orifice plates operated using flange tap differential pressures, the coefficient of discharge ranges from about 0.6 to 0.7.

LITERATURE REVIEW

One of the most important factors, which determine the reliability of the data associated with multi-phase flow, is accuracy. It characterizes the capability of a measuring instrument to indicate that the measurement taken is close to the true value. Repeatability refers to the closeness of agreement between independent results obtained in the normal and correct operation of the same method on identical test material, in a short space of time, and under the same test conditions (such as the same operator, same apparatus, and same laboratory). Reproducibility refers to the closeness of agreement between individual results obtained in the normal and correct operation of the same method on identical test material, but under different test conditions (such as different operators, different apparatus, and different laboratories). To test for the repeatability and the reproducibility of the flow meters it is necessary to study the flow regimes that the instrument can handle.

Multi-phase flow is a complex phenomenon. It is difficult to understand, predict and model. Most of the characteristics that are associated with single-phase flows such as velocity profile, turbulence and boundary layers are inapplicable for describing two-phase flows. In general the structure of the flow is classified into regimes and these are in turn governed by a number of parameters. Each flow regime is different from the other in terms of phase distribution in space and time and they are largely influenced by the operating conditions, fluid properties, flow rates and the orientation and geometry of the pipes [1].

Formation of flow regimes is governed by mechanisms such as transient effects, geometry/terrain effects, hydrodynamic effects and combinations of all these effects. Transients occur as a result of the changes in boundary conditions of the system. Opening and closing of valves is an example, which causes transient effects. Geometry/terrain effects are caused when there is a change in the pipeline geometry or

inclination. Severe riser slugging is an example of this effect and it can prevail for kilometers mainly in sea lines. When there are no transient effects or geometry/terrain effects the flow is steady and it is entirely dependent on the flow rates, fluid properties, pipe diameter and inclination. Such regimes are encountered in pipes that are purely straight and they are also called as hydrodynamics effects.

Flow regimes can be classified into the following groups: dispersed flow, separated flow, intermittent flow or a combination of these three. Dispersed flow is one in which there is a uniform phase distribution in both the radial and axial directions. Bubble and mist flows are examples of such flows. The flow is said to be separated when there is a non-continuous phase distribution in the radial direction and a continuous phase distribution in the axial direction. Stratified and annular flows are examples of such flows. Intermittent flow is characterized by being non-continuous in the axial direction and therefore exhibits unsteady behaviour. Elongated bubble, churn and slug flows are examples of such flows.

Martinelli et al. [2] studied the static differential pressure associated with the isothermal two-phase two-component flow of air and eight different liquids. The static differential pressures were measured for different flow conditions varying from all air to all liquid in a 0.0254 m (1 inch) glass pipe and a 0.0127 m (0.5 inch) galvanized iron pipe. The flow patterns at various flow rates were visually studied and photographed. The following trends were visible,

1. Static differential pressure for two-phase flow is always greater than the differential pressure when each phase is flowing alone at the same mass flow rate as that of the two-phase flow.

2. At a particular gas flow rate, the differential pressure increases as more liquid is added.

3. When the gas flow rate is decreased to zero, keeping the liquid flow rate constant, a static differential pressure due to flow of the pure liquid is attained.

Therefore the static differential pressure lines of constant liquid flow rate become horizontal when the gas flow rate is reduced.

4. When the gas flow is increased, keeping the liquid flow rate constant, the static differential pressure increases and it becomes asymptotic with the 100% gas line.

5. The differential pressure is also influenced by the viscosity of the liquid. The greater the viscosity, the greater is its effect on the differential pressure.

It was concluded that microscopic behaviour of a two-phase flow system is very complex and so it is best to study macroscopic behaviour, which would yield results useful from an engineering standpoint.

Murdock [3] presented a practical method for measuring two-phase flows through standard orifice flow meters to a tolerance of 1.5 percent. An existing single-phase metering equation was used to develop a rational expression by introducing an experimentally determined constant. Data from previous publications of the ASME fluid meters research was used for this purpose. The experimental constant was derived by analyzing 90 data points for two-phase flow of steam-water, air-water, natural gas-water, natural gas-salt water, and natural gas-distillate mixtures. Orifices with beta ratios varying from 0.25 to 0.5 were used. Absolute pressures ranging from atmospheric to 920 psia, differential pressures ranging from 2.5 to 125 kPa (10 to 500 inches) of water and liquid mass fractions ranging from 2 to 89 percent were considered. Temperatures ranged from 10 to 260 °C (50 to 500 °F) and Reynolds numbers from 50 to 50,000 for the liquid phase and 15,000 to 1,000,000 for the gaseous phase. The data for the gas phase was computed assuming that only the gas phase was flowing. Therefore the differential pressure which was calculated would be that obtained if only gas was flowing through the flow meter. The same treatment was applied to the liquid phase. An expression for computing two-phase flow to a tolerance of 1.5 percent was derived. It is given by,

$$w_h = \frac{359 K_G Y_G F_a d^2 \sqrt{h_{wTP}\gamma_{G1}}}{(1-y)+1.26y\frac{K_G Y_G}{K_L}\sqrt{\frac{\gamma_{G1}}{\gamma_{L1}}}} \qquad (10)$$

where, w_h (lb/hr) is the weight flow rate of the two-phase flow, $K_G Y_G$ is the product of flow coefficient and expansion factor for gas flow only, d (in) is orifice diameter, F_a is the factor to account for the thermal expansion of the primary element, h_{wTP} (in) is the head produced by the two phase flow through the orifice, y is the liquid weight fraction which is the ratio of the weight of the liquid during two-phase flow to that of the total flow, K_L is the flow coefficient for liquid flow only, γ_{G1} (lb/ft^3) is the specific weight of gas at the orifice outlet and γ_{L1} (lb/ft^3) is the specific weight of the liquid at the orifice outlet.

Brennan et al. [4] studied the performance of a turbine flow meter by comparing it with a standard orifice plate flow meter for clockwise and anti-clockwise swirling flows. Single phase flow was used. Four different beta ratio plates ranging from 0.43 to 0.73 in addition to two different turbine meters were used. Testing was done using 0.1 m (4 inch) pipes at Reynolds number ranging from 40,000 to 160,000 using nitrogen pressurized at 4 MPa (580 psia). The errors associated with orifice plates were as high as 8% for swirling flows. It was observed that as the beta ratio was decreased, the error increased. Results from one of the turbine meters showed that the meter factors increased with an increase in clockwise swirl and decreased with an increase in anti-clockwise swirl. The second turbine meter remained unaffected. It was concluded that the magnitude and the sign of the errors related to the orifice plate depend on the amount and direction of swirl, location of pressure taps and the beta ratio of the plate. Turbine meter errors were found to largely dependent on the design of the turbine meter.

Wenran and Yunxian [5] devised a new method for two-phase flow measurement by analyzing the noise associated with orifice plate differential pressure. A theoretical model was developed for measurement of mass flow rate as well as steam quality. It was

based on the Murdock's [3] separated flow model. The model was found to satisfy a set of orifice experiments in a two-phase flow system at pressures varying from 5.8-12.1 MPa and steam qualities varying from 0.05-0.95. The root mean square values of the mass flow rate and steam quality estimated by this new model were 9.0 and 6.5% respectively. These studies resulted in the development of a method to measure the mass flow rate as well as steam quality for two-phase flow using only one orifice plate. The characteristic of the noise associated with the differential pressure, due to the flow of a two-phase mixture through an orifice was found to be related to the behavior of the flow. The test data was in exact accordance with the theoretical model.

Ferreira [6] investigated a method of applying spectral analysis on the differential pressure due to two-phase flow of air and water through an orifice plate. The intensity of the power spectrum function was found to increase when a second phase was introduced. The power spectrum density of the differential pressure signal was integrated in order to determine the increment caused when the second phase was added. The integral of the power spectrum density was found to have a linear dependence on the water flow rate. It was finally concluded that there was a possible correlation between the liquid flow rate and the total two-phase flow.

Classification of Multi-Phase Flow Meters

The need for developing multi-phase flow meters increased from around 1980 when the oil and natural gas industry starting taking serious interest into it [7]. Since then considerable amount of time and resources have been spent in joint testing, development and field performance evaluations by manufacturers of multi-phase meters. This has led to the accumulation of sufficient data based on their performance. One of the primary challenges associated with multi-phase flow metering is the speed with which it can measure flow compared to seperation units, the accuracy of the data obtained, and repeatablity and reproducibility of the data obtained. Multi-phase flow

meters can be broadly classified into three different categeries namely separation meters, in-line meters and others.

Separation type meters are characterised by complete or partial seperation of the multi-phase flow stream, followed by in-line measurement of each of the individual phase. The test seperator found on nearly every production platform is basically a three phase meter. It seperates the three phases and carries out flow measurements of the oil, water and gas. Separation type meters are further classified into two categories. One of them is called as a full seperation meter. Conventionally it consists of a vertical test seperator which isolates the various components of the mixture. The test seperator consists of a stage of inlet baffles and a stage of mist eliminator banks. When wet gas is passed through the seperator the entrained liquid is removed in stages. The gas forces its way through the top of the seperator while the liquid gets collected in the bottom of the seperator. The gas is then metered using a single phase flow meter, especially the standard orifice plate. The liquid flow rate is measured using a liquid flow rate meter. An on-line water fraction meter is used to measure the water-in-liquid ratio. However this method is only moderately accurate (typically ±5 to 10% of each phase flow rate).

A second type of separation type meter called partial seperation based meter is characterized by the partial seperation of the flow into predominantly liquid and predominantly gas streams before measurement. Each flow stream only needs to be measured over a limited range of component fractions. In a typical partial seperation type meter the three-phase mixture of gas, water and oil is seperated into two streams one mainly gas and the other mainly liquid. A flow divertor diverts most of the gas into a gas bypass loop. The volumetric flow rate of the wet gas stream is measured with an accuracy of 10% using a two-phase flow meter. The liquid stream which still may contain traces of gas is passed through a section consisting of a positive displacement flow meter, a venturi meter and a microwave component fraction meter. The outputs of these three devices are combined to obtain the volumetric flow rate of the oil, water and

gas components in the liquid stream. The uncertainty in the measurement of component volumetric flow rates in the liquid stream is around ±2% of full scale. The gas and the liquid stream are then mixed together again before they leave the measurement system. This type of a flow meter is intended for metering flows containing a high gas fraction. Such type of instruments have been tested and have found to measure oil, water and gas flow rates with an uncertainty of better than ±10% at gas fractions of upto 99.4%.

However, the seperation type flow meter was found unsuitable for practical purposes because of the following reasons.

1. Conventional separators especially when used offshore are expensive and they occupy huge space.

2. Consistency and the accuracy of the data collected is in most cases inaccurate and has to be improved by increasing the testing time and employing more field personal. The test setup also requires heavy maintenance.

3. Whenever there are problems due to foaming or formation of tight emulsions in the fluid flow, the use of chemical or mechanical means to correct them becomes difficult. This in turn affects the seperation process. On the whole the results obtained are inaccurate and there is no repeatability.

In-line multi-phase flow meters are characterized by the complete measurement of phase fractions and phase flow rates performed directly on the multi-phase flow line, without any flow seperation. At least a minimum of six parameters need to be known to measure a gas, oil, water mixture. In most cases either two or all the three phases are assumed to flow with the same velocity. This reduces the required number of measurements. Such a case would require either the use of a mixer or establishing a set of calibration factors. In-line multi-phase meters generally use a combination of two or more of the following techniques: microwave technology, capacitance, gamma absorption, neutron interrogation, cross-correlation using radiocative, acoustic or electrical signals, differential pressure using differential pressure meters and positive displacement meters.

There are also other categories of multi-phase flow meters which include advanced signal processing systems, estimating phase fractions and flow rates from analysis of the time-variant signals from sensors in the multi-phase flow line [8]. These sensors could be acoustic, pressure or other types. The signal processing systems used could either be based on neural networks or other pattern recognition or statistical signal-processing systems. Process simulation programs combined with techniques for parameter estimation have also been used for developing multi-phase metering systems. The pressure and temperature at the arrival point can be measured and input into the simulation program instead of predicting the state of the flow at the arrival point. The pressure and temperature at points at a location upstream and downstream must also be measured. The phase fractions and the flow rates can be estimated when the pipe line configuration is known along with the properties of the fluid.

Off late a great deal of work has been performed by a number of industries with a view to study the performance of multi-phase meters and to determine whether they are reliable enough to yield accurate results. These studies showed that multi-phase meters are capable of measuring oil, water and gas flow rates with accuracies within ±10%. In certain applications accuracies as good as ±5% have been achieved.

Slotted Plate History

Industries often deal with multi-phase flows which need to be accurately measured. However the task of measuring such types of flow is still in a stage of infancy. There are various aspects that must be considered while adopting a suitable multi-phase flow metering method, such as cost, accuracy, amount of space occupied, ease of use, installation and maintenance. Substantial study has been done in the past on the slotted plate flow meter and this will be continued until a meter with all the desirable qualities has been developed. The following paragraphs will discuss the history of the slotted plate and the past studies performed. Multi-phase metering technology in

development and that, which is currently available, will also be discussed to chart out a plan for present and future slotted plate flow metering research.

The concept of a slotted plate was first conceived and developed by Dr.Kenneth Hall and Dr.James Holste of the Department of Chemical Engineering at Texas A&M University, for the Dansby Power Plant in Bryan, Texas. The main purpose was to set up a differential pressure to sample gas and then send it back to the pipeline without using a pump or a compressor. Initially the slotted plate was used as a proportional flow splitter, but later it was used as a flow conditioner and currently it is being marketed as a flow meter.

The initial evaluation of the slotted plate as a flow meter was carried out by Macek [9] under the supervision of Dr.Gerald Morrison. The slotted plate was tested as a single-phase flow meter and the results were compared with those obtained from a standard orifice plate flow meter. The slotted plate demonstrated a greater consistency by having a lower differential pressure, faster pressure recovery on the downstream side of the plate, and comparatively lesser dependence on the upstream flow conditions such as swirl and axial velocity profiles than the standard orifice flow meter. This paved the way for further study of the slotted plate as a flow-measuring device.

Ihfe [10] and Dr.Gerald Morrison tested the slotted plate as a flow conditioner at the Department of Mechanical Engineering at Texas A&M University. The plate was subjected to both numerical and experimental investigation. The purpose of the project was to develop a new type of flow conditioner that was capable of creating a fully developed turbulent flow profile in a short pipe length. It was found that, by varying the porosity of the plate across the pipe radius, fully developed flow could be obtained in a shorter pipe length than is possible with commercially available flow conditioners. However, the head loss was higher in the slotted plate compared to other standard flow conditioning devices. Hence the slotted plate was not accepted as a flow conditioner.

Further research on the slotted plate as a flow meter was performed by Terracina [11] and Dr.Gerald Morrison to investigate the behaviour of the slotted plate when subjected to single phase flow. The study included both numerical and experimental investigation to observe the effects of velocity profile distortions, line pressure, mass flow rate, tube bundle location, and pipe size scaling. A numerical study was done to design the inlet edge contours of the slots based upon the performance of the plate. It was found that with respect to ill-conditioned flows the slotted plate possessed better accuracy than the standard orifice plate. This effect was optimized when a slot width to plate thickness ratio of 0.25 is used. The flow meter showed greater immunity to the variation in upstream flow conditions with increasing plate thickness thereby eliminating the need for a tube bundle. The thickness of the plate was determined in such a way that the pressure loss across the plate was kept below that of the standard orifice plate. It was found that the discharge coefficient of the slotted plate was almost constant (±0.25%) whereas the discharge coefficient for the standard plate varied from +6% to −1% under the influence of various amounts of distorted velocity profiles. It was also concluded that a plate having a square contour for the slot inlet produced the best accuracy compared to round contours or beveled contours.

Round inlets resulted in high differential pressures and so they were totally ruled out. But the square inlet and the beveled inlet showed comparable differential pressure. This meant that they were more immune to the perturbations in the incoming flow as compared to round inlets. It was finally decided that the square contour for slot inlet would be used in future research. Pressure recovery took place within one pipe diameter after all the three slotted plates. This inferred to the fact that having pipe taps 2.5 pipe diameters upstream and 8 pipe diameters downstream would be appropriate than having flange taps 0.0254 m (1 inch) upstream and 0.0254 m (1 inch) downstream. Later Brewer along with Dr. Gerald Morrison proved that the use of flange taps for a slotted was more suitable than using pipe taps.

Brewer [12], under the direction of Dr.Gerald Morrison, developed a two-phase flow facility using air and water to study the response of slotted plates having beta ratios of 0.5 and 0.43, with flow qualities varying from 100%(pure air) to 20% of air (slug flow). Beta ratio, β is defined as,

$$\beta = \sqrt{\frac{A_{slots}}{A_{pipe}}} \qquad (11)$$

where, A_{slots} (m^2) is the area of the slots in the slotted plate,

A_{pipe} (m^2) is the area of the pipe taking the inner diameter into account.

The investigation was performed to determine the appropriate locations of pressure taps for measuring the differential pressure across the slotted plate. The study also investigated the behaviour of the new plate to horizontal and vertical orientation when subjected to two-phase flow. Video documentaries featuring various flow regimes encountered during the course of the study were also prepared. Flange taps and pressure taps located 2.5 pipe diameters upstream and downstream of the slotted plate were found to be very accurate for the study. Compressibility effects were found to be different for the two different slotted plates which were tested. At low Reynolds numbers, slotted plates homogenized the flow hence making them good mixers for two-phase flow mixture. It was recommended that employing stacked pressure transducers could increase accuracy of the flow meter since it appeared to work well at low differential pressures but the pressure transmitter low end accuracy was questionable.

Flores [13] along with Dr.Gerald Morrison studied the performance of the slotted plate in terms of repeatability and reproducibility of the data for wet steam flows. The data acquired from the water and steam facility displayed a maximum of 10% change in quality and this change did not have any effect on the curve fit equation used for predicting the calibration coeffiecient. The calibration coefficient is given by,

$$KY = \frac{4\dot{m}}{\pi(D_{pipe}\beta)^2 \sqrt{2\rho\Delta P}} \qquad (12)$$

where, K is the flow coeffcient, Y is the expansion factor, $\dot{m}$ (kg/s) is the mass flow rate, β is the beta ratio, D_{pipe} (m) is the inner diameter of the pipe, ρ (kg/m^3) is the density and ΔP (Pa) is the differential pressure across the plate. Of all the data obtained using the water and steam slotted plate study, the same trends were displayed as the quality, steam Reynolds number, and beta ratios were changed. These trends were the same as those displayed in the water and air study done by Brewer. It was seen that as the gas Reynolds number was increased the differential pressure across the slotted plate increased. The differential pressure again increased when the quality was decreased. A third trend showed that at constant gas Reynolds number and quality the slotted plate having the smallest beta ratio displayed the highest differential pressure. This is due to a decrease in the area through which the fluid flows. The current study will make use of the coefficient of discharge instead of making use of the calibration coefficient. The coefficient of discharge is given by,

$$C_d = \frac{4\dot{m}\sqrt{1-\beta^4}}{\pi(D_{pipe}\beta)^2 \sqrt{2\rho\Delta P}} \qquad (13)$$

where C_d is the coefficient of discharge, $\dot{m}$ (kg/s) is the mass flow rate, β is the beta ratio, D_{pipe} (m) is the inner diameter of the pipe, ρ (kg/m^3) is the density and ΔP (Pa) is the differential pressure across the plate.

Reproducibility was confirmed when different sets of data from all the three slotted plates (beta ratio of 0.43, 0.467 and 0.5), working fluids, instrumentation and line pressures were found to be independent of mixture Reynolds number when the calibration factor was plotted as a function of Euler number (function of mixture density, mixture mass flow rate, and differential pressure across the slotted plate). For the water

and steam facility the differential temperature across the slotted plates had the same trend as the differential pressure across the slotted plates. The differential temperature across each beta ratio decreased when the quality was increased.

Uncertainty analysis on the calibration coefficient for the water and steam test facility revealed that the uncertainty in the beta ratio was the largest contributor for the total uncertainty. This contribution from the beta ratio was about 90% to the uncertainty in the calibration coefficient. The second and third largest uncertainties were from the mixture density and the mixture mass flow rate respectively.

OBJECTIVES

The main objective of this study is to study the response of the slotted plate as a two-phase flow meter with air and water as the working fluids. The data that is obtained through the experiments will be compared with other standardized flow meter data. Slotted plates with beta ratios of 0.43 and 0.467 will be tested on different arrangements of the slotted plate test section. A standard orifice plate flow meter and a venturi will also be included in the orifice run and the results obtained will be compared with those corresponding to the slotted plate. The following objectives will be investigated to develop the calibration of these plates.

1. Determine the effects of varying the quality of the two-phase flow on the differential pressure and the coefficient of discharge of the slotted plates.
2. Test the slotted plates with beta ratios of 0.43 and 0.467, the standard orifice plate and the venturi in an air and water facility to evaluate repeatability.
3. Compare the performance of the slotted plates when used in conjunction with a standard orifice plate and later a venturi. This will be done to ascertain the fact that the slotted plate is superior in accurately measuring two-phase flow compared to the standard orifice plate and the venturi.
4. Study the behaviour of the coefficient of discharge at low differential pressures.
5. Compare the differential pressure across the 0.43 and 0.467 β ratio slotted plates, the standard orifice plate and the venturi.
6. Study the effects of the gas Reynolds number on the differential pressure and the coefficient of discharge.
7. Investigate the reproducibility of the slotted plates when used under different arrangements of the test facility.
8. Deduce a suitable procedure for accurately measuring the flow rate of the two phase flow mixture on this test facility using the slotted plate flow meter.

EXPERIMENTAL APPARATUS

An air and water test facility was designed by modifying the existing water and steam facility. This facility was used to test the slotted plate flow meter. It consists of the control room, the air metering section, the water metering section and the horizontal slotted plate section. The control room houses the computer and the hardware for data acquisition and the electronic valve controllers for regulating the flow through the test rig. Air is supplied to the air metering section by the compressors located outside the test cell. The air metering section and the water metering section serve the purpose to determine the temperatures, pressures and flow rates of each stream separately. The slotted plate section is instrumented to measure the temperature, differential pressure and flow rates of the two-phase flow as it passes through the slotted plate. All of this information was used to analyze the response of the slotted plate flow meter in two-phase flow.

Air Metering Section

One of the components of the two-phase flow mixture was air. Air was found to be more suitable than steam. Steam temperatures showed very large fluctuations. This was not so in the case of air. It was possible to compress air to a variety of pressures, but steam was produced over a restricted range of pressures. The use of air was safer and less hazardous as compared to steam and so it was favoured over steam. A schematic diagram of the air metering section is shown in Figure 2. Ambient air was compressed by a Sullair Model 25-150 (17.0 m^3/hr at 860 kPa, 600 SCFM at 125 psig) screw type air compressor. The humidity of the air was fixed by a pair of desiccant dryers, which filtered and dried the compressed air to a dewpoint temperature of -40 °C (-40 °F).

The air was brought into the test rig through a 0.102 m (4 inch) pipe and was controlled by a gate valve. Once the gate valve was opened to allow air supply into the

test facility, air passed through a 0.051 m (2-inch) rubber hose to the stainless steel pipes. The volumetric flow rate (in ACFM), pressure and temperature of the incoming air were measured before it was mixed with the water. A turbine meter manufactured by Quantum Dynamics having a rating of 0.00236 m^3/s to 0.118 m^3/s (5-250 ACFM) was used for measuring the flow rate of the air. This turbine meter was however calibrated only for a range of 0 to 0.038 m^3/s (0 to 1.333 ft^3/s). Calibration was performed using the compressed air from the compressor and three sonic nozzles (Model N24018-SI (150), N240127-SI (150), and N240255-SI) mounted in parallel to each other. These nozzles were initially calibrated by the Colorado Engineering Experiment Station, Incorporated (CEESI) which made use of standards comparable to the National Institute of Standards and Technology (NIST). A range of flow rates was achieved for the calibration data by using different combinations of the sonic nozzles.

Air temperature was measured by an Omega T-type thermocouple located downstream of the turbine meter. A Rosemount Model 3051 SMART pressure transducer (0 to 1 MPa, 0 to 150 psig span) measured the pressure of the incoming air. This pressure transducer was calibrated using a dead weight pressure tester. Once the pressure, temperature and the volumetric flow rate are measured, air flows through a stainless steel pipe through an electromechanical control valve (Masoneilan Dresser Varimax 3000 Series). This valve was used to regulate the flow of air and for varying the upstream pressures during the calibration of the slotted plate. The valve requires compressed air to be actuated, which is supplied by a separate compressor in the compressor room. This valve is controlled from the control room by means of an electronic valve controller. The flow rate is regulated by turning the knob on the controller that sends a current signal in the range of 4-20 mA, where 4 mA signifies fully closed position and 20 mA signifies fully open position. The air regulated by the control valve flows through a brass check valve (0.051 m, 2 in N.P.T), which prevents water from entering the air metering section. Once the air crosses the check valve, it is sent to the two-phase meter run where it mixes with water to form a two-phase flow mixture.

Water Metering Section

The water metering system, Figure 3, measures the characteristics of the water supplied to the test rig. It essentially consists of a brass gear pump (Sherwood Model MBN6) driven by an electric motor, which supplies water at a volumetric flow rate from 0 to 0.00123 m^3/s (0 to 0.043 ft^3/s) at a maximum pressure of 0.862 MPa (125 psig). The pump draws water from a stainless steel tank 0.757 m^3 (26.7 ft^3). This tank is also used to collect the water exiting from the test facility. It is designed to drain any water if the volume of water in the tank exceeded 0.0379 m^3 (13.3 ft^3). The pump has a pressure relief valve, which recirculates the water back to the tank in case there is an excessive pressure build up on the downstream side of the pump. This prevents the pump from being damaged, in case the pump is running and the valves downstream of the pump are closed. The relief valve is also used for adjusting the pump pressure. The water flowing out of the pump passes through a pipe, which branches into two parallel pipes. Two brass pressure regulators, one rated for 0-345 kPa (0-50 psi) and the other for 172-517 kPa (25-75 psi) were fitted along these two pipes to maintain a constant pressure in the water flowing out. The pressure on these regulators were generally set at 333 to 400 MPa (50 to 60 psig) depending upon the upstream air pressure.

Two Coriolis flow meters manufactured and donated by Micro Motion are each connected to a pressure regulator. The purpose of these flow meters is to accurately measure the flow rate and density of the water. Each Coriolis flow meter is accompanied by a transmitter (Model RFT9739) that converts the flow rate measured into a current signal ranging from 4-20 mA. This transmitter is responsible for measuring the mass flow rate, volumetric flow rate and density. One of the Coriolis (Small) flow meters (Model CMF010) has a range of 0.001512 to 0.03 kg/sec (0.2-4 lb/min). The flow rate of the water in this flow meter is adjusted by using needle valves connected to an AC motor by a rigid coupling. The opening and closing of the valves was accomplished from the control room by means of a toggle switch. This allows setting the flow rates accurately.

The other Coriolis (Large) flow meter (Model CMF025) has a range of 0.03 to 0.65 kg/sec (4-80 lb/min). An automatic control valve (Masoneilan Model 2800 series) is used to control the flow rate of water through this flow meter. An Omega T-type thermocouple is used to measure the temperature of water. The small Coriolis flow meter is used for regulating small flow rates of water whereas the large Coriolis flow meter is used to attain large flow rates. The water exiting both these flow meters passes through a common rubber hose provided with a ball valve, which carries it to be mixed with air from the air metering section before entering the slotted plate section.

Slotted Plate Section

This test section was designed to install up to three slotted plate flow meters in series and observe each meter's response to the horizontal two-phase flow of air and water through each one of them and the effect of the flow meters upon each other. Air entering from the air metering section and water from the water metering section mix with each other to form a two-phase flow mixture, which is then passed through the slotted plates. Figures 4, 5 and 6 contain a schematic of the slotted plate test section in different configurations.

A Rosemount Model 3051 pressure transducer was used to measure the pressure of the flow on the upstream side of the first flow meter. This transducer is specifically designed to measure absolute pressure. A T-type thermocouple is used to measure the upstream temperature at the same location. The slotted plate test section used for measuring two phase flow is 25 pipe diameters in length. In this case, the pipe has an inner diameter of 0.051 m (2 in) and is referred by D. This section consists of five spools of two-inch stainless steel pipes with flanges. Each pipe spool is at least five-pipe diameters long and has stainless steel flanges (68.039 kg) at each end. A 0.00317 m coupling is welded to the 5D length pipe at the center and a 0.00317 m tap is provided at the center of each flange. There are four spools, which contain flanges whose raised face

were removed, and an O-ring groove machined in the face. The remaining spools have the same configuration as the other four, but they do not have an O-ring groove. Each plate is placed in between two spools. The plates are placed after the thermocouples. Initially the slotted plates were arranged from upstream to downstream with beta ratios of 0.43 and 0.467. The order of the plates was then changed, wherein slotted plates with beta ratios of 0.43 and 0.467 were used in combination with a Daniel standard orifice plate flow meter having a beta ratio of 0.508. Later the standard orifice plate flow meter was removed and a venturi of beta ratio 0.527 was used instead. This section consisted of two stainless steel pipe spools, 5 pipe diameters long, with the venturi sliding through them such that a part of the venturi was in each of the spool. A pressure tap was made at the center of one of the spool just above the vena contracta of the venturi and a quick disconnect was plumbed to it. The differential pressure across each slotted plate was measured simultaneously by three stacked Rosemount Model 3051C pressure transducers connected to the flange taps located on the flanges of the spools. The transducers can be connected and disconnected from the flange taps by means of using quick disconnects. Couplings for measuring temperatures were provided 2.5 D from the side of each orifice plate and located at the center of each spool. An automatic control valve (Masoneilan Model 3000 series) was located downstream of the slotted plates. This valve is controlled manually or by a PID controller (Omega CN 4421CV-F1). The controller opens and closes the valve to maintain the pressure upstream of the first plate. This valve was also referred to as the backpressure valve. The upstream pressures were varied from 100 kPa to 600 kPa. It was also possible to set the upstream pressure using the PID controller to any value. The PID controller was used to set upstream pressure at 98 kPa, 150 kPa, 204 kPa, 255 kPa, 360 kPa, 415 kPa, 470 kPa and 575 kPa for the experiments to be performed. The upstream pressure can be monitored by the absolute pressure transducer located upstream of the slotted plates. The two-phase flow mixture after passing through the Masoneilan valve is collected in the stainless steel tank. The water settled down in the tank while the air escaped into the atmosphere through the vent provided in it.

Slotted Plates

Two slotted plates having beta ratios of 0.43 and 0.467 as seen in Figure 7 and Figure 8, were mounted in series in the test section. The 0.43 and 0.467 beta ratio plates were then tested with their positions interchanged. They were also compared with a 0.508 beta ratio standard orifice plate, Figure 9, and later with a 0.527 beta ratio venturi meter, Figure 10. Macek showed that a slotted plate 0.006 m (0.236 in) thick ensured that the pressure distribution on the pipe walls was consitent and was independent of the upstream flow conditions. Such plates demonstrated lower differential pressures than plates which were 0.003 m (0.118 in). The slotted plate which was used for two-phase flow measurement was 0.003 m thick. In order to reduce the differential pressure, two such plates were placed together such that the new plate thickness became 0.006 m. Locaters pins or dowel pins were provided to ensure that the slots of the plates aligned with each other when they were combined. These pins also ensured that the plates held to each other in the same position through out the experimentation process. Silicon vacuum grease was applied between these plates to make them leak proof to two-phase flow.

Pressure and Temperature Instrumentation

The orifice plate test section consisted of nine differential pressure transducers, one absolute pressure transducer and five thermocouples. Each orifice plate had three stacked pressure transducers (Rosemount Model 3051C) to measure the differential pressure across it. These pressure transducers contained a high-pressure port and a low pressure port connection. There was a flange tap on one side of the orifice plate 0.5 D distance apart and this was used for measuring the pressure on the high-pressure port of the transducer. There was a second flange tap located downstream of the orifice plate, the same distance apart which measured the lower pressure port of the transducer. Brewer determined this distance. He also found out that a flange tap 0.5 D from the

orifice plate is as accurate as a pressure tap 2.5 D from the orifice plate. Each of these flange taps was connected to a 0.00635 m copper tube which ran vertically up a distance of 0.0254 m, then 0.0762 m horizontally and then about 0.3048 m (1 ft) downward. The first row of three pressure transducers was connected at this point. This was repeated for the second row of pressure transducers following the first row with a distance of 0.3048 m (1 ft) between them. The third row of transducers were placed at a distance of 0.3048 m (1 ft) from the second row. Before running the tests it was ensured that the transducers were filled with water. This was done to prevent the transducers from getting damaged and to improve its accuracy. The setting was later changed with the first row of transducers moved to a location 0.508 m (20 inches) above the orifice run. In such a case it was no longer needed to fill the transducers with water.

One of the significant features of these pressure transducers was its ability to automatically provide temperature compensation. This was useful to counter the uncertainties created when there was a temperature difference between the time of calibration and the time when the experiments are performed. The data for both cases were analyzed in the same way. The first row of pressure transducers was calibrated at the highest pressure range. It had a span of 0 to 250 kPa (0 to 1000 inches) H_2O. The second row of pressure transducers was calibrated for the middle range of an experiment. They had a span of 0 to 62.25 kPa (0 to 250 inches) H_2O. The third row of pressure transducers measure the lowest range for an experiment and its span was 0 to 12.45 kPa (0 to 50 inches) H_2O. An absolute pressure transducer (Rosemount Model 3051C) having a span of 0 to 1 MPa (0 to 150 psig) was used for measuring the pressure upstream of the slotted plates. This transducer had only one pressure port and this was connected to a pressure tap located at the center of a spool. The main reason for using this transducer was to monitor the upstream pressure and to make sure that it was constant. The thermocouples were Omega T-type thermocouples and they were inserted at the center of the spools, 2.5 D away from the slotted plates.

EXPERIMENTAL PROCEDURE

The experimental procedure involved during this study consists of several different tasks which must be carried out precisely to ensure that the calibration of the slotted plate is accurate. Setting up the data acquisition system was the preliminary task involved in the experimental procedure. This was done to record the temperatures, pressures, densities and flow rates of the two-phase flow throughout the water and steam facility. To ensure that the correct measurements were recorded, the pressure transducers, turbine meters and the Coriolis flow meters were calibrated. Once recorded, these raw data were reduced and analyzed using suitable data reduction techniques.

Data Acquisition System

The data acquisition system plays a very important role in any experimental procedure. The main purpose of the data acquisition system is to monitor the experiment, to ensure that all the required parameters are satisfied and to record data for the process. The data that is recorded gives the true picture of the exact conditions in the test facility when the experiment is carried out. For this study, a computer powered by the Pentium II processor formed the heart and soul of the data acquisition system.

Hardware used for Data Acquisition

The computer housed two data acquisition boards (DAQ) manufactured and supplied by Measurement Computing, Inc. These boards were used for converting analog signals into a digital form. One of the boards had 8 analog inputs. Each one of these inputs had a resolution of 16 bits (CIO-DAS802/16). Out of the 8 inputs only 4 were used. Three of them were designated as 0, 1 and 7 respectively and were connected to a CIO-EXP32 expansion board also manufactured by Measurement Computing, Inc. Of the 32 channels on the expansion board 16 channels corresponded to 0 and the

remaining 16 channels corresponded to 1 on the CIO-DAS802/16 board. Six out of the 16 channels contained in 0 were used for temperature measurement by the T-type thermocouples located in the air metering facility, water metering facility and the slotted plate section. Of the 16 channels contained in 1, eleven channels were used for reading pressure (six), density (two) and flow rates (three). Temperature of the screw terminal on the computer board also known as the cold junction compensation was recorded by Channel 7 of the CIO-DAS802/16 board. The fourth channel from the CIO-DAS802/16 board was used in measuring pressure. A connection was established from the expansion board to the CIO-DAS802/16 board in the computer through a 37 pin connector. Also the CIO-DAS802/16 board could only detect a voltage signal. The instrumentation in the test facility consisted of nine differential pressure transducers, two absolute pressure transducers, a large Coriolis flow meter and a small Coriolis flow meter. These flow meters were also able to measure densities. But however the output signals from all these instruments were in the form of a current in a range of 4-20 mA. These signals had to be passed through a resistor to create a voltage drop, which was supplied as an input to the CIO-DAS802/16 board.

Software used for Data Acquisition

The LabVIEW graphical program developed and marketed by National Instruments, Inc. was used for designing a virtual instrument program used in data acquisition. This program was used for monitoring the pressures, densities, temperatures and flow rates and can also be used for observing the changes in them. Calibration was performed on each instrument to represent every variable (pressures, densities, temperatures and flow rates) as a linear function of voltage. This was represented by the straight line equation given by y = mx +c, where y was the quantity to be measured, x was the voltage signal produced by the measuring instrument, 'm' was the slope of the linear curve fit and 'c' was the intercept of the linear curve fit for the instrument calibration.

There was a module in the program where the calibration equations were input. There were nine inputs for the differential pressure transducers, two for the absolute pressure transducers, two for the water flow rates, two for the water densities, and one for the air flow rate. These input values could be changed at will, whenever the instrument calibration changed. Each variable input was assigned a channel number, which corresponded to a certain channel on the expansion board. The data that was recorded by the program comprised of the mean, average standard deviation and the percentage error for all the variables mentioned above. Apart from this, the data also comprised the mean, average standard deviation and the percentage error for the six thermocouples used in the test facility.

When the program was executed, it gave the user a choice to either set the flow rates or to directly start recording data. The viscosity of air was supplied to the program to calculate the gas Reynolds number. The viscosity of air did not vary much because of the low fluctuations in the air temperature. There was also a provision for entering the gas density, which was calculated manually from the upstream temperature and pressure. There was a button provided in the program which when pressed started taking data. This button was pressed when all the correct values were entered.

The number of data points and the rate at which data was being recorded could be manipulated. The number of data points to be recorded was set to 100 at a rate of 500 milliseconds between each data point. This process was done twice. Mean and standard deviation for each of these 100 data points were calculated and averaged. The percentage error was calculated by subtracting the mean of the first point from the mean of the second point and dividing this difference by the mean of the first point. This percentage error was compared against the maximum allowable percentage error specified in the program. If the percentage error was within the permissible limit, the program prompted the user to save the data in a file. If the percentage error was found to be very high, an error message was displayed and data had to be retaken.

The program also has visual aides in the form of plots for pressures, temperatures, densities and flow rates. These plots popped up in a separate window once data was being taken. The main use of these plots is that they allow the operator to visually monitor the changes in pressures, temperatures, densities and flow rates. The operator can come to a conclusion that the data was erroneous, when there were heavy fluctuations in any of the variables listed above. Fine adjustments could then be made until the error was within the specified limit.

Calibration of Measuring Instruments

The accuracy of the data obtained from the air-water test facility by and large depends on the measuring instruments used. These instruments need to be calibrated periodically. This is due to the fact that their performance may vary with time. The following paragraphs give a detailed picture of the calibration of pressure transducers, and the Coriolis flow meters.

Pressure Transducer Calibration

A total of nine differential pressure transducers and two absolute pressure transducers were used. The differential transducers were calibrated en masse. The absolute pressure transducers were calibrated separately. The calibration of these instruments was done without removing them from their fixed positions. An Ametek Model RK-300 pneumatic dead weight pressure tester was used to calibrate the Rosemount pressure transducers.

Each slotted plate (beta ratio of 0.43 and 0.467) had a stack of three pressure transducers connected to the flange taps. The dead weight pressure tester was attached to a common line designed in such a way that it applied equal pressure on all the high pressure port legs, one for each plate. In this way, the high pressure ports of all the

transducers were pressurized. The common line allowed the high pressure port to be pressurized without letting any gas into the slotted plate section. The low pressure port leg connected to the low pressure ports of all the nine transducers was opened to the atmosphere.

Each plate had three pressure transducers and they were calibrated for three different ranges. These transducers were arranged from top to bottom in the range of high, medium to low pressures, respectively. The zero and span of each row of transducers is set. Zero corresponded to the minimum differential pressure measured by the transducer. Any differential pressure below the zero value would result in the same voltage signal as that was produced at the zero value. Applying the maximum desired differential pressure and then pushing the span button set the span of the transducer. This differential pressure became the maximum differential pressure, which the transducer could measure, although it was capable of measuring higher differential pressures.

A LabVIEW program was made specifically for the purpose of calibrating the pressure transducers. This program recorded the value of the average voltage signal over 200 data points corresponding to the pressure applied on the dead weight tester. Calibration was done by first placing the holder which corresponded to a differential pressure of 1kPa (4 inches of water/0.144 psi). The weights were then added in increasing order. Addition of the weights resulted in an increase in the pressure applied on the transducers, which in turn produced higher voltages. This was done until the maximum differential pressure corresponding to the top row of transducers with the highest range was applied through the dead weight tester. The voltages for each row of transducers were sorted and were then plotted against the pressure applied. Linear curve fits were made to express the differential pressures as a function of the voltage output for each transducer. These linear curve fits were then entered into the air and water data acquisition program used to record data for slotted plate two-phase flow meter.

Calibration of the absolute pressure transducers differed slightly from the differential pressure transducers. Unlike the previous ones, the absolute pressure transducers had only one port leg. The dead weight pressure tester was used to calibrate each transducer for a range of 0 to 689 kPa (0 to 100 psig). This was done by applying pressure in an increasing order. Care was taken to ensure that there were at least ten points for the total range considered. Pressure was plotted against voltage for each transducer. Linear curve fits were obtained representing the pressure as a function of the voltage. These curve fits were entered into the air and water data acquisition program used to record data for slotted plate two-phase flow meter.

Coriolis Flow Meter Calibration

The Coriolis flow meters were used in the water metering section to measure the flow rate and density of the water that was mixed with air to form the two-phase flow mixture. There were two such flow meters. One of them was capable of metering volumetric flow rates in the range of 0.001512 to 0.03 kg/sec (0.2-4 lb/min) and it was referred to as the small Coriolis flow meter. The other one measured volumetric flow rates in the range of 0.03 to 0.65 kg/sec (4-80 lb/min) and was referred to as the large Coriolis flow meter. A Sherwood Model MBN6 gear pump driven by an electric motor acted as the flow source supplying water at flow rates ranging from 0 to 0.00123 m^3/s (0 to 0.043 ft^3/s) at a maximum pressure of 0.862 MPa (125 psig). The outlet of the pump was split into two parallel lines. One of them carried the flow to the small Coriolis flow meter and the other to the large Coriolis flow meter. Pressure regulators provided upstream of these flow meters maintained the pressure of water flowing through them constant. Calibration was first done on the small Coriolis flow meter. The pump was started to supply water. The small Coriolis flow meter was connected to the common hose, which supplied water to be mixed with air, through two needle valves one large and one small. These needle valves were connected in parallel. They were used to increase and decrease the flow rate of water flowing through this flow meter. The large

needle valve was used for varying water flows in large quantities while the small needle valve was used for fine adjustments in the flow rate. A bucket was used for collecting water, which flowed out of the small Coriolis flow meter. This bucket was weighed before the calibration. The air and water data acquisition program used to record data for slotted plate two-phase flow meter was used for this purpose. A flow rate was set using the needle valves. Water was allowed to flow into the bucket once the program was started. At the end of data acquisition the bucket was removed. The time taken for the data to be recorded was simultaneously measured using a stopwatch. The bucket was again weighed this time with water in it. The weight of the water was calculated from this. The voltage corresponding to this flow rate was measured simultaneously. From the weight of the water collected in the bucket and the time taken for filling the bucket, the flow rate of water could be calculated. This procedure was repeated for different flow rates. The flow rates thus obtained were plotted against voltages and a linear curve fit was obtained from this plot. This equation was then used in the same data acquisition program replacing the old equation.

The calibration process for large Coriolis flow meter was similar to the small Coriolis flow meter. The only difference was the use of an automatic control valve (Masoneilan Model 2800 series) instead of the needle valves. This valve enabled large flow rates. The procedure was the same as before. At the end of the calibration, the flow rates were plotted against voltage values to obtain the curve fit equation. This equation was later used in the data acquisition program replacing the existing equation.

Testing Parameters

This study is entirely dedicated to analyze the response of the slotted plate flow meter for horizontal two-phase flow. The slotted plate section was hence mounted horizontally. The gate valve controlling the flow of air from the compressor to the test facility was opened. The air supply to the pneumatic control valves was turned on so that

they could be opened and closed. The back pressure valve was controlled by the PID controller. This device was responsible for maintaining the required pressure in the slotted plate test section. Tests were performed by maintaining the upstream line pressure at values of 98 kPa, 150 kPa, 204 kPa, 257 kPa, 310 kPa, 360 kPa, 415 kPa, 470 kPa and 575 kPa. This was done by setting voltages of 1.25 V (98 kPa), 1.5 V (150 kPa), 1.75 V (204 kPa), 2.0 V (255 kPa), 2.25 V (310 kPa), 2.5 V (360 kPa), 2.75 V (415 kPa), 3.0 V (470 kPa) and 3.5 V (575 kPa). The air valve (Masoneilan Dresser Varimax 3000 Series) was opened to send in air through the slotted plate test section. Different flow rates of air such as 0.085, 0.125, 0.165, 0.205, 0.244, 0.276 m^3/sec were considered. Depending on the flow rate, the PID controller controlled the back pressure valve to set a constant inlet pressure to the flow meter run.

The data acquisition program has an indicator which monitors the Reynolds number in the system. Typically, for air flow rates ranging from 0.085 to 0.276 m^3/sec, the Reynolds number varied from 118000 to 384000. Reynolds number is defined by,

$$\text{Re}_{air} = \frac{4\,\dot{m}_{air}}{\pi D_{pipe}\,\mu_{air}} \qquad (14)$$

where $\dot{m}_{air}$ (kg/s) is the mass flow rate of air, D_{pipe} (m) is the inner diameter of the pipe, and μ_{air} (kg/ms) is the absolute viscosity for air. The inner diameter of the pipe was 0.051 m (2 in) and the viscosity of air was taken at room temperature. The mass flow rate of air is given by the following expression,

$$\dot{m}_{air} = Q_{air}\rho_{air} \qquad (15)$$

where ρ_{air} (kg/m^3) is the density of air, which is calculated from the upstream air pressure and temperature and Q_{air} (m^3/s) is the volumetric flow rate of air recorded by the data acquisition program. The gear pump (Sherwood Model MBN6) was turned on

to supply water to the water metering facility. The pump pressure was set at about 760-860 kPa (110-125 PSI). The pressure on the regulators fitted on the two lines exiting of the pump was set at 345-485 kPa (50-70 PSI).

Quality is an important parameter considered during the experiment. It was varied throughout the experiment. This was done because a change in quality implied a change in the water flow rate. Quality is given by the formula,

$$X = \frac{\dot{m}_{air}}{\dot{m}_{mixture}} = \frac{\dot{m}_{air}}{\dot{m}_{air} + \dot{m}_{water}} \qquad (16)$$

where $\dot{m}_{air}$ (kg/s) is the mass flow rate of air, $\dot{m}_{water}$ (kg/s) is the mass flow rate of water, and $\dot{m}_{mixture}$ (kg/s) is the sum of the mass flow rate of air and water. The Coriolis flow meters output a voltage equivalent to the mass flow rate of water which the data acquisition program recorded. The small Coriolis flow meter was used for low flow rates of water and flow through this was controlled by the needle valves. The large Coriolis flow meter was used when larger flow rates of water were needed and flow through this controlled by the automatic control valve (Masoneilan Model 2800 series).

The quality of water could be varied from 0% (pure water) to 100 % (pure air). Maintaining the upstream pressure and the air mass flow rate at a certain fixed value the quality of the flow was varied from 25% to 95%. Qualities below 25% were not considered. This was repeated for different mass flow rates of air at the same pressure. Once this was done, the pressure was changed to the next required value and the entire process was repeated again. It was not possible to reach the total range of qualities in some cases. This was because the flow rates were either too high or too low to allow the back pressure valve to open or close in order to maintain the constant upstream pressure. After setting the quality at a certain fixed value, approximately 2 to 5 minutes of settling

time was allowed for the flow to equilibriate. Data was taken after this. Typically, the time taken for running a single experiment varied some where between 8 hrs to 20 hrs.

Data Reduction

Data reduction is the technique of converting raw data into a more useful form. It can be done by methods such as grouping, summing, averaging etc. For this particular study a data reduction was written using MathCAD. This reduced the raw data obtained from the air-water two-phase flow test facility. The data was separated into spreadsheets containing the test runs for upstream line pressure at values of 98 kPa, 150 kPa, 204 kPa, 255 kPa, 310 kPa, 360 kPa, 415 kPa, 470 kPa and 575 kPa. This new data files were supplied to the data reduction program to determine the coefficients of discharge, actual Reynolds numbers, mass fractions, mass flow rates, differential pressures, densities and the ratios of the differential pressure to the upstream line pressure. This procedure was carried out for the slotted plates (beta 0.43 and 0.467), the standard orifice plate and the venturi. The variables that were determined by data reduction were used in the calibration of the slotted plate flow meter for horizontal two-phase flow.

The Quantum Dynamics turbine meter installed in the air metering facility was used for measuring the flow rate of air entering into the test rig. It was calibrated for volumetric flow rates using air and sonic nozzles. The mass flow rate of the air entering the facility was computed using the density and the volumetric flow rate of the air. The density of air ρ_{air} (kg/m^3) was calculated using the formula,

$$\rho_{air} = \frac{P_{air}}{R_{air} T_{air}} \tag{17}$$

where P_{air} (kPa) is the pressure of the incoming air measured also known as upstream pressure, R_{air} (J/mol K) is the gas constant for air, and T_{air} (K) is the temperature of the incoming air.

The volumetric flow rate of air obtained from the test facility was used for computing the mass flow rate of air using the equation given below,

$$\dot{m}_{air} = \rho_{air} Q_{air} \tag{18}$$

where $\dot{m}_{air}$ (kg/s) is the mass flow rate of air and Q_{air} (m³/s) is the volumetric flow rate of air. Water flow rates were directly read from the data acquisition program using either the large or the small Coriolis flow meter. Since these flow meters also acted as densitometers, the density of water ρ_{water} (kg/m³) flowing through them was also recorded. The flow rates of water flowing through the large Coriolis flow meter and the small Coriolis flow meter are given by $\dot{m}_{lwater}$ (kg/s) and $\dot{m}_{swater}$ (kg/s) respectively.

The Reynolds number of the two-phase flow mixture Re_{air} was computed next.

$$Re_{air} = \frac{\dot{m}_{air} D_{pipe}}{\mu_{air} A_{pipe}} \tag{19}$$

where μ_{air} (kg/ms) is the viscosity of air, D_{pipe} (m) is the inner diameter of the pipe which was 0.051 m (2 in) and A_{pipe} (m²) the area of the pipe which was found to be 0.002027 m² (3.142 in²).

Quality was an important parameter used in analyzing the data obtained from the experiments. One of the key objects of this study was to identify the effect of two-phase flow of air and water on the differential pressure across each slotted plate. This implied that the quality upstream of the slotted plate section X_{up} and the qualities behind each plate $X_{0.43}$ and $X_{0.467}$ needed to be found. Quality or mass fraction X of the flow was defined by,

$$X = \frac{\dot{m}_{air}}{\dot{m}_{air} + \dot{m}_{water}} \tag{20}$$

The differential pressure across each plate was obtained from the raw data acquired from the test facility during the different test runs. Using the knowledge of the pressure upstream of the slotted plate section and the individual differential pressures across each plate, the pressure upstream of each plate was calculated. These pressures were used to calculate the density of the air in front of each plate, which in turn was used to calculate the density of the two-phase flow mixture through each plate.

$$\rho_{mixture} = \frac{\rho_{air}}{X + (1-X)\dfrac{\rho_{air}}{\rho_{water}}} \tag{21}$$

where $\rho_{mixture}$ (kg/m^3) is the density of the two-phase flow, ρ_{air} (kg/m^3) is the density of air upstream of each slotted plate, X is the quality of the two-phase flow mixture, and ρ_{water} (kg/m^3) is the density of water.

Once all the required parameters were calculated, the coefficient of discharge C_d of the slotted plate was computed for each plate. The coefficient of discharge C_d is defined by,

$$C_d = \frac{\dot{m}_{actual}\sqrt{1-\beta^4}}{\dfrac{\pi}{4}\left(D_{pipe}\beta\right)^2 \sqrt{2\rho_{actual}\Delta P}} \tag{22}$$

where $\dot{m}_{actual}$ (kg/s) is the actual mass flow rate of the two-phase flow mixture through the slotted plate under consideration, β is the beta ratio of the slotted plate under consideration, D_{pipe} (m) is the inner diameter of the pipe which is 0.051 m (2 in), ρ_{actual}

(kg/m^3) is the actual density of the fluid mixture flowing through the plate under consideration and ΔP (Pa) is the differential pressure across the slotted plate.

Instrument Accuracies and Uncertainties

The outcome of an experiment largely depends on the accuracy of the instruments used for measurement. A bad instrument could lead to highly erroneous results. Especially in the case of experiments dealing with large amounts of data inaccurate measurements can result in a loss of valuable time and resource. Therefore the accuracies and the uncertainties of the instruments used need to be studied to make sure that they do not affect the experiment. The span of a measuring instrument is the values it can measure, ranging from a maximum to a minimum. The uncertainty of an instrument is calculated by multiplying its accuracy by the span.

The accuracies of the Rosemount Model 3051C smart differential pressure transducers used in the stacked pressure transducer system were found to be 0.075%. The uncertainties were $\pm$ 0.1875 kPa ($\pm$ 0.75 in of H$_2$O) for the transducers with a span of 0 – 250 kPa (0 – 1000 in of H$_2$O), $\pm$ 0.0462 kPa ($\pm$ 0.186 in of H$_2$O) for the transducers with a span of 0 – 62.25 kPa (0 – 250 in of H$_2$O), and $\pm$ 0.00933 kPa ($\pm$ 0.0375 in of H$_2$O) for the transducers with a span of 0 – 12.5 kPa (0 - 50 in of H$_2$O). It can be seen that the first row of transducers had the highest uncertainty. This resulted in an uncertainty in the differential pressure measured. The uncertainty in the upstream pressure measurement depended on the uncertainty of the Rosemount Model 3051 absolute pressure transducer. Its accuracy was 0.075%. Therefore the uncertainty of this transducer came out to be $\pm$ 0.7755 kPa ($\pm$ 0.1125 PSI) for a span of 0 – 1034 kPa (0 – 150 PSI). The uncertainty in the temperature of the air was the same as the uncertainty of the thermocouple which is $\pm$ 1° K. The uncertainty in the air flow rate was found by multiplying the uncertainty in the sonic nozzles (0.25%) by the air flow rate measured by the Quantum Dynamics gas turbine meter.

The water flow rates were measured by the large and the small Coriolis flow meters and their uncertainties were found to be ± 0.00062 kg/s (± 0.076 lb/s) and ± 0.0000285 kg/s (± 0.0038 lb/s) respectively. The uncertainty in the density of the water measured by these two flow meters was ± 0.5 kg/m^3. The uncertainty in the diameter of the 0.051 m (2 in) pipe was ± 2.54×10^{-5} m (± 0.001 in). The uncertainties of the measuring instruments can then be used to determine the uncertainties in the differential pressure, upstream quality, gas Reynolds number and the coefficient of discharge.

RESULTS AND DISCUSSION

The success of an experiment depends not only on how accurately it was conducted but also on how well the data is interpreted into meaningful results. Results that have been obtained from the air water two-phase flow test facility are presented in this section. Data taken from different arrangements of the test facility will be discussed in the form of six different test cases. The effects of upstream quality on the differential pressure and the coefficient of discharge of the two slotted plates (beta ratios of 0.43 and 0.467), the standard orifice plate and the venturi will be shown in the form of contour plots. Contour plots portraying the effect of the gas Reynolds number on the differential pressure will also be discussed. This section focuses primarily on the response of the slotted plates to upstream line pressures of 150 kPa, 255 kPa and 360 kPa. Repeatability of the slotted plates will be evaluated in each test case for the above mentioned line pressures. Data pertaining to other line pressures of 100 kPa, 200 kPa, 310 kPa, 415 kPa, 470 kPa and 575 kPa will also be discussed. Plots comparing the differential pressure across the slotted plates, the standard orifice plate and the venturi will be discussed. Reproducibility of the slotted plates will be studied. The effects of low differential pressure on the estimation of the coefficient of discharge will also be discussed.

The back pressure valve (V1, refer to Figure 4) on the slotted plate test section was controlled by a PID controller. Setting a voltage on the PID controller ensured a constant pressure on the upstream side of the slotted plate section. However, opening the airflow control valve (V2, refer to Figure 2) beyond a certain extent, increased the pressure on the upstream side to a level that it was not possible for the PID controller to bring the pressure down to the required value. Therefore each upstream line pressure could accommodate only certain values of the air flow rates. X_{up} will represent the incoming upstream quality of the flow as it approaches the meter run and the C_d will represent the coefficient of discharge in the forthcoming discussions.

Case 1

Two slotted plates with beta ratios of 0.43 and 0.467, shown in Figure 7 and Figure 8 were considered for this case. The slotted plate with beta ratio of 0.467 was placed 5D downstream of the 0.43 beta ratio slotted plate. Testing was performed at upstream line pressures of 98 kPa, 150 kPa, 204 kPa, 255 kPa, 310 kPa, 360 kPa and 415 kPa. Industries dealing with petroleum and natural gas often encounter multi-phase flow phenomenon where the quality of the flow is highly erratic. Keeping this in mind the quality of the two-phase flow mixture was varied to study the response of the slotted plates to different types of flows. Only the large Coriolis flow meter was used for metering the water flow. Temperatures were measured by thermocouples marked T2 (air temperature), T3 (temperature upstream of 0.43 plate), T4 (temperature between 0.43 and 0.467 plate), and T5 (temperature downstream of 0.467 plate).

Quality Effects on the Coefficient of Discharge and Differential Pressure

The effect of quality upon the differential pressure and the coefficient of discharge of the slotted plates for various gas flow rates will be discussed in this section. Contours plots were made to establish a relationship between the differential pressure measured across each plate, upstream quality and the coefficient of discharge. These plots contain information pertaining to all the gas flow rates corresponding to each upstream line pressure. Figures 11 to 17 show the relation between the differential pressures across the 0.43 β ratio slotted plate, X_{up} and C_d for upstream line pressures of 98 kPa, 150 kPa, 204 kPa, 255 kPa, 310 kPa, 360 kPa and 415 kPa respectively. Each line pressure accommodated certain gas flow rates.

Figure 11 shows the quality effects on the differential pressure at an upstream line pressure of 98 kPa. It was observed that by keeping X_{up} fixed at a certain value and by increasing the overall mass flow rate and hence the differential pressure, a decrease in

C_d was caused. This is analogous to an orifice plate where C_d decreases with increasing mass flow rate. Varying the gas flow rate so that the differential pressure is constant while increasing X_{up} results in a decrease in C_d. It can be observed that in general an increase in differential pressure and X_{up} results in a decrease in C_d. Also C_d was found to increase as the flow changed from mist flow (high quality) to slug flow (low quality). A similar trend is observed for subsequent plots at 150 kPa, 204 kPa, 255 kPa, 310 kPa, 360 kPa and 415 kPa.

Figures 18 to 24 represent the effect of the upstream quality on the differential pressure across the 0.467 β ratio slotted plate and the coefficient of discharge of that plate. The trends are similar to that observed in the case of the 0.43 β ratio slotted plate. At 98 kPa upstream line pressure, the contours appear to show a slight distortion after the flow has achieved a quality of 0.8. These distortions appear more pronounced at 150 kPa, 204 kPa, 255 kPa, 310 kPa, 360 kPa and 415kPa. It is also seen that with an increase in upstream line pressure, the distortions in the contours is more drastic. These distortions could be attributed to many factors. One of them was the fluctuations in the pump pressure. It was found that the pressure regulator on the pump did not function effectively and at very high qualities when the water flow rate is very low, the pressure of the water supplied by the pump is subjected to large fluctuations. This in turn affected the quality which could not be fixed at a certain desired value under such conditions. It also caused large fluctuations in the differential pressures. The second factor was the inaccuracy of the large Coriolis flow meter in measuring low water flow rates. The large Coriolis flow meter is capable of measuring flow rates only in the range of 0.03 to 0.65 kg/sec (4-80 lb/min). At qualities greater than 0.8 it can be seen that the water flow rate is less than 0.03 kg/sec. This renders the large Coriolis flow meter incapable of measuring these low flow rates accurately. The data for the differential pressure showed a scatter at very high values. This caused a scatter in C_d at low values. This was also partially responsible for the distortions in the contours.

For both the slotted plates (β ratio of 0.43 and 0.467), it can be seen that, at low quality flows with X_{up} ranging from 0.4 to 0.5, the value of C_d showed an increasing trend with an increase in upstream line pressures. It was already shown in previous sections that C_d is directly proportional to the mass flow rate and inversely proportional to the square root of the differential pressure. At these qualities the mass flow rate increase is greater than the square root of the increase in differential pressure. This mass flow rate becomes much higher as the upstream line pressure is increased from 98 kPa to 415 kPa. This is the reason why the coefficient of discharge was found to increase as the upstream line pressure was increased from 98 kPa to 415 kPa.

The coefficient of discharge of the slotted plate flow meter is a measure of the accuracy with which the flow meter estimates the mass flow rate of the fluid flowing through it. It can be expressed as,

$$C_d = \frac{\dot{m}_{real}}{\dot{m}_{ideal}} \tag{23}$$

where $\dot{m}_{real}$ (kg/s) is the actual flow rate of the fluid measured by the slotted plate and $\dot{m}_{ideal}$ (kg/s) is the flow rate that the slotted plate would measure under ideal conditions. C_d becomes unity when the real mass flow rate and the ideal mass flow rate are equal. In reality, the real mass flow rate is always lesser than the ideal mass flow rate and the maximum C_d values for a slotted plate are in the range of 0.8 to 1.0. This is the case when the flow of fluid through the plate is single-phase. However a two-phase flow phenomenon is entirely different from single-phase flow. Figures 13, 14, 15, 16, 17, and 24 indicate that the maximum C_d values reached are more than 1.0. This leads to a scenario in which the flow rate measured by the slotted plate is more than the actual flow rate of fluid flowing through the slots. This is partially due to the fact that the mass flow rate used in the calculation of C_d is a sum of the mass flow rates of air and water metered by the air and water metering systems respectively. The experiments have been

performed keeping the upstream line pressure constant and then varying the flow rate of air. At each airflow rate the quality of the flow is varied from about 0.95 to 0.4 and back to 0.95. A quality of 0.95 implies that the two-phase flow mixture comprises 95% of air and 5% of water and a X_{up} of 0.4 implies the flow mixture is made of 40% of air and 60% of water. The figures mentioned above show that, at low values of X_{up} and low differential pressures, the C_d value seems to be above 1.0. Low X_{up} implies high mass flow rate of water and so the mass flow rate of the mixture is high. Since C_d is directly proportional to the mass flow rate and inversely proportional to the square root of the differential pressure, the value of C_d is greater than 1.0 in these regions.

Repeatability

Repeatability of the slotted plate flow meters readings in this case was studied at different upstream line pressures of 98 kPa, 150 kPa, 204 kPa, 255 kPa, 310 kPa, 360 kPa and 415 kPa, by plotting the differential pressure as a function of upstream quality with seven different ranges of gas Reynolds number. These gas Reynolds number ranges were from 117600 to 141400 for an upstream line pressure of 98 kPa, 122600 to 173400 for an upstream line pressure of 150 kPa, 122000 to 221000 for an upstream line pressure of 204 kPa, 133000 to 284200 for an upstream line pressure of 255 kPa, 128300 to 314700 for an upstream line pressure of 310 kPa, 182000 to 333200 for an upstream line pressure of 360 kPa and 131400 to 347600 for an upstream line pressure of 415 kPa. These plots portray the variation of the differential pressure at different gas Reynolds numbers. Repeatability will be confirmed for the 0.43 β ratio slotted plate if the trends showed by it at each upstream line pressure are similar. This condition is also applicable for the 0.467 β ratio slotted plate. This implies that the trends corresponding to the slotted plates at a particular upstream line pressure must be in close agreement with those at every other upstream line pressure to ensure repeatability.

Contour plots of differential pressure as a function of upstream quality were evaluated for the air and water data for this particular configuration of the slotted plate test section at an upstream line pressure of 98 kPa for both the slotted plates (0.43 and 0.467). These are shown in Figure 25 and Figure 26. The contour plots are similar to each other. When the quality is increased keeping the gas Reynolds number fixed, the differential pressure across each plate decreases. It can also be inferred from the plots that at constant quality an increase in the gas Reynolds number causes an increase in the differential pressure across the plates. Figure 27 and Figure 28 show the functional dependence of the differential pressure across the slotted plates on the upstream quality and the gas Reynolds number for an upstream line pressure of 150 kPa. The plots are again very similar to each other and they showed a smooth decrease in the differential pressure with an increase in quality at a certain fixed gas Reynolds number, though the differential pressure for the 0.467 β ratio slotted plate showed a steep decline initially. Figures 29 to 38 show the relation between the differential pressure, the upstream quality and the gas Reynolds number for upstream line pressures of 204 kPa, 255 kPa, 310 kPa, 360 kPa and 415 kPa respectively. The trends in the variation of the differential pressure with quality and gas Reynolds number are the same just as mentioned above. This suggests that the slotted plates (0.43 and 0.467) demonstrate good trends in this particular test case. Repeatability in the trends shown by the slotted plates is observed as the contour plots for each upstream line pressure show a close resemblance. The range of gas Reynolds number shows an increase with an increase in upstream line pressure. This is due to the fact that the PID controller allows more air flow rates as the line pressure is increased.

For upstream line pressures of 98 kPa, 150 kPa, 255 kPa, 310 kPa and 360 kPa the maximum differential pressure across the 0.467 β ratio slotted plate is greater than that across the 0.43 β ratio slotted plate. But this does not imply that all values of differential pressures across the 0.467 β ratio slotted plate are greater than that across the 0.43 β ratio slotted plate. Figure 39 shows the differential pressure across the 0.43 β

ratio slotted plate as a function of the differential pressure across the 0.467 β ratio slotted plate. At the upstream line pressure of 98 kPa, the differential pressure across the 0.43 β ratio slotted plate is initially greater than that across the 0.467 β ratio slotted plate. However at higher flow rates which result in larger differential pressures, the differential pressure across the 0.467 plate becomes slightly greater than the differential pressure across the 0.43 plate. As the upstream line pressure is increased beyond 98 kPa to values such as 150 kPa, 255 kPa, 310 kPa and 360 kPa this effect becomes very significant. Each upstream line pressure has a set of corresponding gas flow rates associated with it. This effect is observed only at the highest gas flow rates with low upstream qualities when the mass flow rate of the two-phase flow is predominantly high. At 415 kPa the differential pressure across the 0.43 plate is at all times greater than that across the 0.467 plate.

Figures 40 and 41 show the relation between C_d and the gas Reynolds number for various upstream line pressures and upstream qualities. As the upstream line pressure is increased, there is an increase in the value of the gas Reynolds numbers reached. This is due to the fact that the PID controller allows higher flow rates at large line pressures also increasing the gas density. Also the range of C_d decreases as the gas Reynolds number is increased. This could be understood from figures 42 and 43. At low gas Reynolds numbers, the differential pressures are very low. Since C_d is inversely proportional to the square root of the differential pressure, it is not affected at low differential pressures. The high range in the values of C_d is due to the fact that it is directly proportional to the mass flow rate of the mixture which is varied over a wide range of values. In other words it is possible to achieve a higher range of upstream qualities at low gas Reynolds numbers. At higher Reynolds numbers the differential pressures become higher and more dominant than the mass flow rate of the mixture. Also the range of upstream qualities becomes smaller as at high gas flow rates the opposition to the flow of water is higher. The mixture predominantly consists of air. This is the reason why the range of variation of C_d becomes small at these values.

Case 2

The two slotted plates with beta ratios of 0.43 and 0.467 were again used for this case. They were arranged with the 0.467 β ratio slotted plate placed on the upstream side of the 0.43 β ratio slotted plate. The two plates were separated by a distance of five pipe diameters. Testing was done at upstream line pressures of 150 kPa, 255 kPa, and 360 kPa. T4 thermocouple in this case measured the temperature between 0.467 and 0.43 plates, and T5 thermocouple measured the temperature downstream of 0.43 plate. In the previous test case the contour plots of differential pressure, upstream quality and the coefficient of discharge, showed distortions in the contours at high values of upstream quality. It was also shown that at high quality flows the results obtained from the 0.467 β ratio slotted plate showed distortions and these increased with increasing upstream line pressure.

It was earlier discussed that there were large fluctuations in the pump pressure. This resulted in large-scale variations in the mass flow rate of water, especially when it was low. This in turn affected the quality of the mixture, which could not be set constant at a certain value. Low differential pressures were observed at these high qualities. Also It should be noted that the differential pressures measured by the transducers across the 0.467 β ratio slotted plate is less than 10 kPa (1.5 PSI) for low gas flow rates, at high upstream qualities for each upstream line pressure. This means that under such conditions the water flow rate is very low (less than 0.03 kg/s). The pressure transducer calibration showed that the stacked pressure transducer system was inaccurate in measuring differential pressures below 10 kPa (1.5 PSI). This test case was performed to observe the effect of the above mentioned factors on the data obtained from the slotted plates and also to see if the response of the slotted plates was affected by exchanging their positions.

Quality Effects on the Coefficient of Discharge and Differential Pressure

Figures 44 to 46 show the relationship between the differential pressure across the 0.43 β ratio slotted plate, X_{up} and the C_d of the 0.43 β ratio slotted plate. Figure 44 shows the quality effects at an upstream line pressure of 150 kPa. It is shown that keeping X_{up} constant and increasing the differential pressure caused a decrease in C_d. Also keeping the differential pressure constant and increasing X_{up} showed a decrease in C_d. An increase in differential pressure and X_{up} resulted in a decrease in the C_d. The C_d was found to increase as the flow changed from mist flow (high quality) to slug flow (low quality). A similar trend is observed for other upstream line pressures at 255 kPa and 360 kPa.

Figures 47 to 49 represent the dependence of the differential pressure across the 0.467 β ratio slotted plate on the coefficient of discharge of that plate and the upstream quality. The general performance of this plate is similar to the 0.43 β ratio slotted plate. However the shape of the contour plots in Figure 44 and Figure 47 are not alike, though the variation of the differential pressure with quality is the same in both the plots. When examined closely it can be seen that the contours of Figure 44 are smoother at higher qualities than those in Figure 47. Figures 44 and 47 are contour plots corresponding to an upstream line pressure of 150 kPa. Referring to Figure 56, it can be seen that there are only two gas flow rates associated with this line pressure. At the higher gas flow rate the differential pressure across the 0.43 and the 0.467 β ratio slotted plates are very much higher than 20 kPa. However for the low gas flow rate it can be observed that most of the differential pressures across the 0.43 β ratio slotted plate is higher than 10 kPa whereas the entire set of differential pressures across the 0.467 β ratio slotted plate is less than 10 kPa. It has already been shown that the stacked pressure transducers are inaccurate in measuring differential pressures below 10kPa (1.5 PSI). Previous research conducted by Terracina [11] showed that the slotted plate with the lowest β ratio was less sensitive to upstream flow conditions than the plates with higher

β ratios. This could probably be one of the reasons why the 0.467 plate was affected when it was subjected to non-homogenized two-phase flow in this case. These are the reason for the contours in Figure 44 to be smoother than those in Figure 47. Figure 48 shows the appearance of distortions at higher qualities and these distortions appear to have been increased in Figure 49. These characteristics of the 0.467 β ratio slotted plate are similar to those observed in the previous case. Irregardless of its location, whether it is upstream or downstream of the 0.43 β ratio slotted plate, the 0.467 β ratio slotted plate shows distortions at high qualities as the upstream line pressure is increased.

Though the pressure upstream of the slotted plate section is maintained at a constant value, the pressure upstream of the 0.43 β ratio slotted plate is not constant. As the two-phase flow mixture initially passes through the 0.467 β ratio slotted plate there is a pressure differential created across it, which reduces the pressure of the flow mixture. Therefore the pressure upstream of the 0.43 plate is influenced by the pressure differential across the 0.467 plate which in turn is governed by the mass flow rate of the two-phase flow. This pressure can be calculated by subtracting the differential pressure across the first plate from the upstream line pressure. However this is a very crude method of calculating the pressure upstream of the second plate as there is some amount of pressure recovery as the mixture exits the first plate. As the mass flow rate is increased the differential pressure across the 0.467 β ratio slotted plate increases and this reduces the pressure upstream of the 0.43 β ratio slotted plate and vice versa.

It can be confirmed from this test case that at high qualities, when the air flow rate is very high compared to the water flow rate, the response of the 0.467 β ratio slotted plate flow meter is not as good as the 0.43 β ratio slotted plate. This was due to the inaccuracy of the large Coriolis flow meter to measure the flow rate of the water flowing through it accurately; particularly when the water flow rate is less than 0.03 kg/sec. Added to this the stacked pressure transducer system was unable to measure low differential pressures (less than 10 kPa / 1.5 PSI). In order to overcome this difficulty of

measuring low flow rates, the small Coriolis flow meter with a measurement range of 0.001512 to 0.03 kg/sec (0.2-4 lb/min) was incorporated into the water metering facility. This arrangement will be dealt with in the next test case.

At low values of X_{up} varying from 0.4 to 0.5, C_d values show an increase with an increase in the upstream line pressure. This is in exact accordance to what was seen in the previous test case. The reasons for such an increase in C_d have already been explained in the previous test case. The maximum values of C_d in Figures 46 to Figure 49 are more than 1.0. This is again similar to the previous test case where the C_d value exceeded 1.0 for certain line pressures. In all the differential pressure effects on the coefficient of discharge of the two slotted plates (β ratio of 0.43 and 0.467) are similar in both the test cases and it is unaffected by the location of the slotted plates.

Repeatability

Repeatability of the slotted plates for this particular test case was evaluated by plotting the differential pressure as a function of upstream quality and gas Reynolds number. This was performed for three upstream line pressures of 150 kPa, 255 kPa and 360 kPa. Each upstream line pressure was associated with a corresponding gas Reynolds number range. They were 125000 to 175000 for an upstream line pressure of 150 kPa, 128000 to 275000 for an upstream line pressure of 255 kPa and 132000 to 328000 for an upstream line pressure of 360 kPa. The 0.43 and the 0.467 β ratio slotted plates are capable of exhibiting repeatability if the trends showed by each of them are similar to the trends shown by them at other upstream line pressures.

Figure 50 and Figure 51 shows the relationship between the differential pressure, upstream quality and the gas Reynolds number for an upstream line pressure of 150 kPa for the 0.43 and 0.467 β ratio slotted plates. These plots are similar to each other. At a certain fixed gas Reynolds number, the differential pressure across each plate decreased

smoothly with increasing quality. This is because an increase in quality at constant gas Reynolds number implies a decrease in the mass flow rate of the mixture. This in turn reduces the differential pressure. Also keeping the quality fixed, the differential pressure was found to increase with increase in the gas Reynolds number across the plates. Under such a scenario, when the value of the quality is fixed and the gas Reynolds number is increased, the mass flow rate of the mixture also increases proportionally so as to maintain the quality constant. This in turn increases the differential pressure. These trends were just similar to the previous case.

Figure 52 and Figure 53 shows the functional relation between the differential pressure across the slotted plates on the upstream quality and the gas Reynolds number for an upstream line pressure of 255 kPa. The plots are very similar to each other and they showed a smooth decrease in the differential pressure with an increase in quality at a certain fixed gas Reynolds number, though the differential pressure for the 0.43 β ratio slotted plate shows a steep decline initially.

Figure 54 and Figure 55 shows the relation between the differential pressure, the upstream quality and the gas Reynolds number for an upstream line pressure of 360 kPa. The performances of the slotted plates in these plots are again very similar to the upstream line pressures mentioned above. The slotted plates (β ratio of 0.43 and 0.467) show good repeatability. The performance of the two plates (β ratio of 0.43 and 0.467) is unaffected by the location of the plate. The range of gas Reynolds number increases with an increase in upstream line pressure, as the PID controller allows more air flow rates as the line pressure is increased. The trends showed by the 0.43 β ratio slotted plate are similar to each other for all the three line pressures considered. This is the same for the 0.467 β ratio slotted plate. This similarity in trends ensures repeatability.

Figure 56 shows the differential pressure across the 0.43 plate as a function of the differential pressure across the 0.467 plate. For upstream line pressures of 150 kPa, 255

kPa and 360 kPa differential pressures across the 0.43 β ratio slotted plate is always greater than that of the 0.467 β ratio slotted plate. Since the 0.43 β ratio slotted plate has a smaller open area compared to the 0.467 β ratio slotted plate, the differential pressure across it is greater. Figures 57 and 58 show the variation in C_d with gas Reynolds number for different upstream line pressures and qualities. Figures 59 and 60 show the differential pressure across each slotted plate as a function of the gas Reynolds number. The trends are similar to those discussed in the previous test case.

Case 3

A standard orifice plate flow meter, Figure 9, was incorporated into the slotted plate test section. The 0.43 β ratio slotted plate was placed 5D upstream of the 0.467 β ratio slotted plate. The standard orifice plate flow meter of β ratio 0.508 manufactured by Daniel Flow Products was installed 5D downstream of the 0.467 plate. Previous research has shown that the standard orifice plate is extremely sensitive to upstream flow conditions and it requires a flow conditioner to perform satisfactorily. This was the reason why it was placed downstream of the two slotted plates. The slotted plates were less sensitive to upstream flow conditions and they homogenized the flow to a good extent. The 0.43 plate was placed ahead of the 0.467 plate as it was more accurate, less sensitive to upstream conditions and homogenized the flow better than the 0.467 plate. Testing was done in two stages. The first stage dealt with the use of the small Coriolis flow meter for metering the water flow rates. This flow meter with a range of 0.001512 to 0.03 kg/sec (0.2-4 lb/min) was well suited for high quality flows and was a good replacement for the large Coriolis flow meter under such conditions. The experiments were performed for upstream line pressures of 150 kPa, 255 kPa and 360 kPa for both the stages. Thermocouple T6 (temperature downstream of standard orifice plate) was added to the slotted plate test section.

Quality Effects on the Coefficient of Discharge and Differential Pressure – High Quality Flow

Contour plots are shown relating the differential pressure across the slotted plates and the standard orifice plate with the upstream quality and the coefficient of discharge. Figures 61 to 63 show such plots for the 0.43 β ratio slotted plate. Upstream quality was varied in the range of 0.78 to 0.97. This is due to the use of the small Coriolis flow meter, which allows only low water flow rates. The plots show a decline in the differential pressure with increasing quality. Increasing the upstream line pressure increases the differential pressure as well as the C_d. Figures 64 to 66 show the contour plots for the 0.467 β ratio slotted plate. Keeping C_d fixed at some value, the differential pressure in Figure 64 decreases smoothly up to a certain extent and then falls sharply, with increasing quality. In Figure 65 and Figure 66 the differential pressure decreases smoothly, but after reaching $X_{up} = 0.9$ the contours show large distortions. This is due to the presence of low differential pressures (less than 10 kPa) at these low mass flow rates. Figures 67 to Figure 69 show the contour plots for the 0.508 β ratio standard orifice plate. In Figure 67 the differential pressure decreases sharply with increasing quality for a certain fixed value of C_d. The plot becomes highly distorted after X_{up} is increased beyond 0.9. Figure 68 and Figure 69 are plots for 255 kPa and 360 kPa respectively. These are the pressures upstream of the 0.43 plate. When X_{up} is increased, the differential pressure decreases slowly, but after crossing a value of $X_{up} = 0.9$, the contours become distorted. This is due to two main reasons. When the quality was set at 0.95, it never stayed at 0.95 but fluctuated from 0.92 to 0.97. At such low water flow rates, the gear pump was unable to maintain a constant water flow rate. Added to this the pump pressure was fluctuating at such flow rates. The second reason was due to the inaccuracy of the stacked pressure transducers to measure differential pressures less than 10 kPa (1.5 psi). The increase in the C_d values with increasing upstream line pressure for the 0.467 β ratio slotted plate was marginal. For the standard orifice plate the C_d values did not change when the upstream line pressure was increased.

Quality Effects on the Coefficient of Discharge and Differential Pressure – Low Quality Flow

The needle valves across the small Coriolis flow meter were closed. The large Coriolis flow meter was brought into operation. Figures 70 to 72 show the contour plots for the 0.43 β ratio slotted plate. Upstream quality was varied from 0.4 to 0.74. This was due to the capability of the large Coriolis flow meter to allow large water flow rates. The contour plots show a sharp decrease in the differential pressure with increasing upstream quality at fixed C_d values. Figures 73 to 75 show the contour plots for the 0.467 β ratio slotted plate. Figures 76 to 78 show the contour plots for the 0.508 β ratio standard orifice plate. All the figures mentioned above show a steady decrease in the differential pressure across each plate with an increase in the upstream quality.

When the upstream line pressure was increased the values of the coefficient of discharge of the 0.43 and 0.467 β ratio slotted plates also showed an increase. But the standard orifice plate did not show such a trend. The standard orifice plate flow meter has a low coefficient of discharge which is responsible for the high differential pressure. The quality range for upstream line pressures of 150 kPa and 255 kPa varies from 0.4 to 0.75, but for 360 kPa it was varied from 0.4 to 0.975. However only the zones between 0.4 and 0.8 are of significance. As it was in the previous cases the maximum differential pressure across the three plates shows a steady increase with increasing upstream line pressure.

Repeatability

The data obtained from the small and large Coriolis flow meters were combined to evaluate the repeatability in this test case. The upstream quality of the two-phase flow was varied from 0.37 to 0.97. Three upstream line pressures of 150 kPa, 255 kPa and 360 kPa were considered. Reynolds numbers were in the range of 119500 to 170000 for

the upstream line pressure of 150 kPa, 125500 to 269000 for the upstream line pressure of 255 kPa, and 125500 to 328000 for the upstream line pressure of 360 kPa. From the last two test cases it was proved that the 0.43 and the 0.467 β ratio slotted plates demonstrated good repeatability. Contour plots were made to evaluate the standard orifice plate. Repeatability will be confirmed for the standard orifice plate if the trends shown by it for each upstream line pressure are the same.

Figures 79, 80 and 81 show the dependence of the differential pressure on the gas Reynolds number and upstream quality for the 0.43, 0.467 slotted plates and the standard orifice plate respectively at an upstream line pressure of 150 kPa. The contour plots look exactly alike. The decrease in the differential pressure is steady and gradual with increasing upstream quality, at a fixed gas Reynolds number. Also when the gas Reynolds number is increased keeping the quality constant the differential pressure shows an increase. There are no distorted contours anywhere. Figures 82 to 84 show the functional relation between the differential pressure, the upstream quality and the gas Reynolds number for an upstream line pressure of 255 kPa. Figures 85 to 87 show the relation between the differential pressure, the upstream quality and the gas Reynolds number for an upstream line pressure of 360 kPa. At each upstream line pressure, the shape of the contour plots is more or less the same for the two slotted plates (0.43 and 0.467) and the standard orifice plate. This shows that the data corresponding to all the three plates agree well with each other. Also the trends showed by each plate at the three upstream line pressures considered are the same thereby confirming repeatability.

Figures 88 and 89 show the differential pressures across the 0.43 β ratio slotted plate and the standard orifice plate as a function of the 0.467 β ratio slotted plate, respectively. Differential Pressure across the 0.43 and 0.467 plates are close to each other, but the differential pressure across the standard orifice plate is very much higher when compared to the slotted plates. Figures 90, 91 and 92 show C_d as a function of the gas Reynolds number for the 0.43, 0.467 slotted plates and the standard orifice plate

respectively at different upstream line pressures and qualities. While the C_d values for the two slotted plates are close to each other, the standard orifice plate shows a much lower range of C_d values. Figures 93, 94 and 95 show the differential pressure as a function of the gas Reynolds number.

Case 4

Case 4 is slightly different from Case 3. The 0.467 β ratio slotted plate was removed from the slotted plate test section. The 0.43 β ratio slotted plate and the 0.508 β ratio standard orifice plate were used for the test, with the slotted plate placed 5D upstream of the standard plate. The slotted plate is always placed ahead of the standard plate as it is less sensitive to flow instabilities upstream of the slotted plate section and is not affected much due to the presence of elbows, bends and other pipe fittings on the upstream side. It also acts as a flow conditioner by homogenizing the flow. Testing was performed in the same way as in Case 3. The experiments were performed for upstream line pressures of 150 kPa, 255 kPa and 360 kPa. Thermocouple T4 measured the temperature between the 0.43 plate and the standard orifice plate and T5 measured the temperature downstream of the standard orifice plate.

Quality Effects on the Coefficient of Discharge and Differential Pressure – High Quality Flow

Figures 96 to 98 show the contour plots for the 0.43 β ratio slotted plate. Upstream quality was varied from 0.8 to 0.97. The plots show the differential pressure decreasing with increasing quality when C_d was fixed at a certain value, for a line pressure of 150 kPa. As the upstream line pressure is increased to 255 and 360 kPa, the differential pressures become higher compared to the previous line pressure. C_d increases with increasing upstream line pressure. The contour plots for the standard orifice plate is shown in Figures 99, 100 and 101. The plot for 150 kPa upstream line

pressure shows a very steep decrease in differential pressure with a small increase in quality for fixed values of C_d. A change in C_d with a change in differential pressure is marginal whereas it changes largely with changing quality. This implies that C_d is more dependent on the upstream quality than the differential pressure or in other words the differential pressure has very little impact on C_d for this line pressure. At 255 kPa and 360 kPa the differential pressure decreases almost proportionally with increasing quality when C_d is fixed. The contours lose their smoothness below a differential pressure value of 20 kPa. This is due to the effect of the fluctuating pump pressure. Similar to the previous test case the C_d values of the standard orifice plate does not show any change with changing upstream line pressure.

Quality Effects on the Coefficient of Discharge and Differential Pressure – Low Quality Flow

Differential pressure effects on the slotted plate and the standard plate at lower qualities are discussed below. Figures 102 to 104 illustrate the quality effects on the differential pressure for the 0.43 β ratio slotted plate. Upstream quality is varied from about 0.4 to 0.75. Similar to the previous cases, at fixed values of C_d the differential pressure shows a decrease with increasing quality. Another trend common for the slotted plate is the increase in the values of C_d with increasing upstream line pressure. The differential pressure across the slotted plates show an increase with increasing upstream line pressure. Figures 105 to 107 show the variation of the differential pressure with changing upstream quality and coefficient of discharge for the standard orifice plate flow meter. At 150 kPa, C_d is almost unaffected by the differential pressure. It only changes slightly with differential pressure. However C_d shows great dependency on the upstream quality. Plots for 255 kPa and 360 kPa show the differential pressure decreasing rapidly when upstream quality is increased keeping C_d fixed. It can be understood that C_d is more influenced by the mass flow rate than by the differential pressure for the standard orifice plate flow meter. This is because C_d is directly proportional to the mass flow rate

and mass flow rate is inversely proportional to the upstream quality. A decrease in quality would increase the mass flow rate and this in turn would increase C_d. The same can also be inferred from the contour plots. At low values of upstream quality the coefficient of discharge is very high.

Repeatability

The data obtained from the small and large Coriolis flow meters were combined to evaluate the repeatability in this test case. Upstream quality was varied from 0.4 to 0.95. Reynolds numbers were in the range of 118500 to 167700 for the upstream line pressure of 150 kPa, 125700 to 275400 for the upstream line pressure of 255 kPa, and 131000 to 323300 for the upstream line pressure of 360 kPa. The 0.43 β ratio slotted plate and the standard orifice plate demonstrate repeatability if the trends showed by each one of them at a particular upstream line pressure are similar to the trends at other line pressures.

Figures 108 and 109 show the dependence of the differential pressure on the gas Reynolds number and upstream quality for the 0.43 β ratio slotted plate and the standard orifice plate respectively at an upstream line pressure of 150 kPa. Figures 110 and 111 show the functional relation between the differential pressure, the upstream quality and the gas Reynolds number for an upstream line pressure of 255 kPa. Figures 112 and 113 show the relation between the differential pressure, the upstream quality and the gas Reynolds number for an upstream line pressure of 360 kPa. The contour plots show a similarity. At each contour level the decrease in the differential pressure is very slow and gradual with increasing upstream quality. Also when the gas Reynolds number is increased the differential pressure shows an increase. As the quality is increased the change in the differential pressure is very small at a certain fixed gas Reynolds number. But with the quality fixed the differential pressure increases rapidly with an increase in the gas Reynolds number. The contour plots for the slotted plate show similar trends for

each upstream line pressure. This is the same for the standard orifice plate. Both the plates show good repeatability.

Figure 114 shows the differential pressure across the 0.43 plate as a function of the differential pressure across the standard orifice plate. The slope of the line plot is almost unity which implies that the differential pressures across the two plates are quite close to each other. Figures 115 and 116 show the functional relation between C_d and the gas Reynolds number for the 0.43 β ratio slotted plate and the 0.508 β ratio standard plate at different upstream line pressures and qualities. Though the differential pressures are almost the same, C_d values for the standard plate are comparatively lower than the slotted plate. This is due to the difference in the β ratios and the density of the two-phase flow mixture across the two plates. Figures 117 and 118 show the differential pressures across the two plates as a function of the gas Reynolds number. The plots agree well with each other.

Case 5

The venturi with a beta ratio of 0.527 shown in Figure 10 was used in this test case along with the 0.43 and 0.467 β ratio slotted plates. The arrangement was similar to the one in Case 3, but the standard orifice plate flow meter was replaced by the venturi. Figure 5 shows the slotted plate section along with the venturi. The slotted plates were placed upstream of the venturi to homogenize the flow. Again the 0.43 plate was placed upstream of the 0.467 plate as it homogenized the flow better and it was less sensitive to upstream flow conditions. Testing was done at upstream line pressures of 150 kPa, 255 kPa, 360 kPa, 470 kPa and 575 kPa respectively. The thermocouple T5 was used to measure the temperature between the 0.467 β ratio slotted plate and the venturi.

Quality Effects on the Coefficient of Discharge and Differential Pressure – High Quality Flow

Figures 119 to 123 show the dependence of the differential pressure across the 0.43 β ratio slotted plate on the upstream quality. In Figure 119 at a certain set value of C_d the differential pressure reduces with increasing upstream quality. The highest value of C_d is attained when both the differential pressures as well as the upstream quality are at their lowest and vice versa. As the upstream line pressure is increased to 255 kPa, 360 kPa, 470 kPa and 575 kPa the differential pressure across the plate increases and then decreases. Figures 124 to 128 show the contour plots for the 0.467 β ratio slotted plate. The contour plot in Figure 124 is similar to that in Figure 119. As the upstream line pressure is increased further, the contours become highly distorted. These distortions are more when the quality is above 0.9 and when the differential pressures are low. This is due to the fluctuation of the quality at high values. Also the inability of the pressure transducers to measure low pressure (below 10 kPa) accurately is one of the contributing factors.

Figures 129 to 133 show the plots for the venturi. At 150 kPa the contours are almost horizontal. This implies that upstream quality has no effect on C_d. The values of C_d are solely governed by the differential pressure. The contours corresponding to rest of the line pressures are highly distorted. This reflects upon the inability of the venturi to measure the correct data accurately at such high qualities. A common trend observed in most of the previous cases was an increase in the differential pressure with increasing upstream line pressure. There is a similar trend in this case too. But once the upstream line pressure is increased to 575 kPa, the differential pressure lowers compared to the previous line pressure. This is because the differential pressure decreases gradually when the gas flow rate is fixed and the upstream line pressure is increased. However when the upstream line pressure was increased from 150 kPa to 470 kPa, higher gas flow rates were achieved which resulted in higher differential pressures at successive upstream line

pressures. For 575 kPa it was not possible to achieve a higher gas flow rate as the back pressure valve was almost closed. Therefore the differential pressure across the plates and the venturi is lower for this line pressure compared to the previous one. The values of C_d increased when the upstream line pressure was increased for both the slotted plates. But for the venturi the values of C_d shows a decrease with increasing line pressure. The differential pressure for each line pressure were in the order of 0.43 > 0.467 > venturi.

Quality Effects on the Coefficient of Discharge and Differential Pressure – Low Quality Flow

Upstream quality was varied from 0.38 to 0.85. This was possible by using the large Coriolis flow meter. The valves connected to the small Coriolis flow meter were shut. Figure 134 through Figure 138 shows the contour plots for the 0.43 β ratio slotted plate at upstream line pressures of 150 kPa, 255 kPa, 360 kPa, 470 kPa and 575 kPa. The contour plots show a steady decrease in the differential pressure with increasing upstream quality. This trend is not affected much when the upstream line pressure is increased. The value of C_d at a fixed differential pressure increases as upstream quality is decreased and vive versa. It also increases with upstream line pressure.

Figure 139 through Figure 143 shows the contour plots for the 0.467 β ratio slotted plate. The contour plots for each line pressure for the 0.467 β ratio slotted plate is similar to those corresponding to 0.43 β ratio slotted plate. This suggests that the data taken using the slotted plates at each line pressure agree well with each other. Figures 144 to Figure 148 show the contour plots for the venturi. As the upstream line pressure was increased the data corresponding to the venturi started to get bad. It can be seen that at high upstream line pressures, the performance of the venturi does not in anyway correspond to that of the slotted plates. The slotted plates show a steady decrease in the differential pressure across each plate with an increase in the upstream quality. But it

becomes unpredictable in the case of the venturi. This implies that the mass flow rate measured by the venturi for two-phase flow of air and water is not as accurate as that measured by the slotted plate flow meters. The coefficient of discharge of the 0.43 and 0.467 β ratio slotted plates showed an increase when the upstream line pressure was increased. For the venturi the coefficient of discharge increased up to a line pressure of 360 kPa and then it started to decrease. As it was in the previous cases the maximum differential pressure across the slotted plates and the venturi shows a steady increase with increasing upstream line pressure. However at 575 kPa the differential pressure is lower than what it was for the previous line pressure. This will be discussed in detail.

Repeatability

Data obtained using both the large and the small Coriolis flow meters were combined to evaluate the repeatability of the slotted plates and the venturi for this test case. Upstream quality of the two-phase flow was varied from 0.38 to 0.97. Five upstream line pressures of 150 kPa, 255 kPa, 360 kPa, 470 kPa and 575 kPa were considered. Reynolds numbers were in the range of 116000 to 168700 for the upstream line pressure of 150 kPa, 122900 to 262100 for the upstream line pressure of 255 kPa, 129500 to 360500 for the upstream line pressure of 360 kPa, 137000 to 424400 for the upstream line pressure of 470 kPa, and 132000 to 382100 for the upstream line pressure of 575 kPa. The contour plots corresponding to the venturi for each line pressure would be compared and if they show a similarity in trends then repeatability is confirmed.

Figures 149, 150 and 151 show the dependence of the differential pressure on the gas Reynolds number and upstream quality for the 0.43, 0.467 slotted plates and the venturi respectively at an upstream line pressure of 150 kPa. The contour plots are similar to each other. The differential pressure shows a steady and gradual decrease with increasing upstream quality at fixed gas Reynolds number. Also when the gas Reynolds number is increased the differential pressure shows an increase. Figure 152 through

Figure 163 shows the functional relation between the differential pressure, the upstream quality and the gas Reynolds number for upstream line pressures of 255 kPa, 360 kPa, 470 kPa and 575 kPa respectively. The contours become horizontal as the upstream line pressure is increased. The influence of the gas Reynolds number on the differential pressure becomes stronger. This is due to the higher gas flow rates achieved as the upstream line pressure is increased. At each upstream line pressure, the shape of the contour plots is more or less the same for the two slotted plates (0.43 and 0.467) and the venturi. The Reynolds number range shows an increase with increasing upstream line pressure. But at 575 kPa it decreases. As can be seen from the contour plots for the venturi, the trends demonstrated by the venturi at the upstream line pressures considered above are similar to each other and this proves that the venturi is capable of repeatability.

Figures 164 and 165 show the differential pressures across the 0.43 plate and the venturi respectively as a function of the differential pressure across the 0.467 plate. The differential pressure across the 0.43 plate is almost close to that across the 0.467 plate. The differential pressure across the venturi is very much lower than that across the slotted plates. Figures 166, 167 and 168 show the relation between C_d and the gas Reynolds number for the slotted plate and the venturi at different upstream line pressures and qualities. The plots for the slotted plates show that at low gas Reynolds number, the range of values attained by C_d is high and it shows a decline when the gas Reynolds number is increased. This is due to the high range of qualities obtained at these low gas Reynolds numbers. The plot for the venturi does not show any such trend. Figures 169, 170 and 171 show the differential pressures as a function of the gas Reynolds number. The plots for the two slotted plates are similar. Keeping the gas Reynolds number fixed the differential pressure across the slotted plates decreases with an increase in the upstream line pressure. At a gas Reynolds number of 170000 in Figure 226, the differential pressure across the plate at each line pressure are in the order of 150 kPa > 255 kPa > 360 kPa > 415 kPa > 575 kPa. The upstream line pressure is largely governed

by the extent to which the back pressure valve is open which in turn depends on the PID controller. This affects the differential pressure. Increasing the upstream line pressure closes down the back pressure valve further thereby reducing the differential pressure. This is the reason why the differential pressure across the slotted plates is zero at 690 kPa (back pressure valve completely closed) even though the air flow control valve is fully open.

Case 6

The previous five test cases have shown that the response of the slotted plates (0.43 and 0.467) to horizontal two phase flow is good for low quality flows (high water flow rates). The data obtained from both these plates showed good correspondence to each other. They were also tested along with a standard orifice plate flow meter and a venturi. In all the cases the slotted plates have shown superior performance. In this test case the 0.43 β ratio slotted plate was used along with the 0.467 β ratio slotted plate and the venturi like in the previous case. The testing was performed only for high quality flows (low water flow rates). A minor change was made in the slotted plate test section. The first row of the stacked pressure transducer system was shifted to a location 0.508 m (20 inches) above the orifice run. Figure 6 gives a schematic representation of the new slotted plate test section. Two water pressure regulators were incorporated in the water metering system, each along the pipe lines to the large and the small Coriolis flow meters respectively, but only the small Coriolis flow meter was used. The prime reason for using these regulators was to stabilize the pressure of the water entering into the Coriolis flow meters from the pump. This was mainly done to prevent the upstream quality from fluctuating at high values. Apart from these two changes everything else remained the same.

Quality Effects on the Coefficient of Discharge and Differential Pressure

Figures 172 to 175 show the plots representing the differential pressure as a function of the upstream quality and coefficient of discharge for the 0.43 β ratio slotted plate at upstream line pressures of 100 kPa, 150 kPa, 200 kPa and 255 kPa respectively. The upstream quality was varied from 0.85 to 0.975. Figure 172 shows the contour plot for a line pressure of 100 kPa. The contours are smooth and the differential pressure decreases with increasing quality. Also an increase in differential pressure resulted in a decrease in the coefficient of discharge. This is due to the fact that C_d is inversely proportional to the square root of the differential pressure. The change in the differential pressure is comparatively larger than the change in the mass flow rate of the mixture and hence it has more influence on the C_d. Plots for 150 kPa and 200 kPa show similar trends. However the plot for 255 kPa was very different. At qualities around 0.975 the contours were almost vertical. However this plot cannot be considered authentic as much of the data falls in the low pressure range (less than 10 kPa) which the stacked pressure transducers fail to measure accurately. This was one of the reasons why testing was not performed for line pressures higher than 255 kPa. Figure 176 through 179 shows the contour plots for the 0.467 β ratio slotted plate. The nature of the plots are similar to those for the 0.43 β ratio slotted plate. Figure 180 through 183 shows the contour plots for the venturi. No visible trend can be seen.

Repeatability

Contour plots relating the differential pressure with upstream quality and gas Reynolds number are shown. Gas Reynolds number ranges from 120000 to 171400 for an upstream line pressure of 100 kPa, 120750 to 173250 for an upstream line pressure 150 kPa, 125000 to 228700 for an upstream line pressure 200 kPa and 122000 to 175200 for an upstream line pressure 255 kPa were considered. Figure 184 through 186 shows the relationship between the differential pressure, upstream quality and the gas Reynolds

number for an upstream line pressure of 100 kPa for the slotted plates and the venturi. These three plots show similar trends. The decrease in differential pressure with increasing quality at a fixed value of gas Reynolds number is very slow. An increase in the gas Reynolds number causes an increase in differential pressure. The plots also show that changing the gas Reynolds number does not change the quality much. This implies that the mass flow rate of water is very low compared to the mass flow rate of air, that the quality is not affected much when the mass flow rate of air is increased.

Figure 187 through 195 shows the contour plots for line pressures of 150 kPa, 200 kPa and 250 kPa. All these plots have similar characteristics. Figures 196 and 197 represent the differential pressures across the 0.43 β ratio slotted plate and the venturi as functions of the differential pressure across the 0.467 β ratio slotted plate. While the differential pressures across the 0.43 and the 0.467 plates are comparable, the differential pressure across the venturi is very low compared to the two slotted plates. Figures 198, 199 and 200 show C_d as a function of the gas Reynolds number. The C_d values for the 0.43 slotted plate are higher than that for the 0.467 plate and the venturi. This is due to the low beta ratio of that plate. Figures 201, 202 and 203 show plots representing the differential pressure as a function of the gas Reynolds number. The trends observed are similar to the previous test cases.

Reproducibility

Reproducibility was evaluated for the 0.43 and 0.467 β ratio slotted plates, the standard orifice plate and the venturi for all test cases. This was done by combining the entire set of data for each plate from the six test cases discussed before. Data from both the high and low quality flows were also combined. The main reason this was performed was to observe if the data obtained from the slotted plates, the standard orifice plate and the venturi were unaffected by the various changes applied to the test facility. Reproducibility will be established if the results produced by each plate are similar in all

the test cases. This implies that the response of that particular plate is unaffected by changes in the test facility. The performance of such an instrument will not change from one test facility to another. A good way to evaluate reproducibility is to plot the differential pressure against upstream quality and the coefficient of discharge. If all the data points corresponding to a particular plate lie on one surface plot, then reproducibility is established. Surface plots with dP (differential pressure), X_{up}, C_d will be discussed in the following cases. Plots with dP/P (ratio of the differential pressure to upstream line pressure), X_{up}, C_d are also shown. Plots were made with gas Reynolds number being used instead of C_d. But they were not good enough as the previous plots and hence are not shown.

Figure 204 shows the surface plot for the 0.43 β ratio slotted plate. Differential pressure is plotted against upstream quality and coefficient of discharge. It can be inferred from the plot that almost all data points lie on the surface. There are a few data points at high differential pressures and high upstream qualities which do not fall on the surface. This is because of the scatter in the data observed in all the test cases discussed before at high differential pressure values and high upstream qualities. This could be due to the fluctuation of the upstream quality at high values. But otherwise the 0.43 β ratio slotted plate shows good reproducibility. Figure 205 shows the surface plot for the 0.467 β ratio slotted plate. The plot shows trends similar to the previous plot. However the number of data points which do not collapse on the surface plot are more for this slotted plate. The r^2 value for the 0.43 β ratio slotted plate is greater than that for 0.467 β ratio slotted plate. Also the standard error of the fit is higher for the 0.467 β ratio slotted plate than for the 0.43 β ratio slotted plate. This shows that the reproducibility of the 0.43 plate is better than the 0.467 plate.

The two-phase flow mixture passing through the standard orifice plate and the venturi was well homogenized and mixed since they were placed downstream of the 0.43 and the 0.467 β ratio slotted plates. Figure 206 shows the surface plot for the

standard orifice plate. The distribution of the data points on the surface is better than those for the 0.43 and the 0.467 β ratio slotted plates. This can be inferred from the r^2 values for the plot. It is very much higher for the standard orifice plate than for the slotted plates. Also the standard error of the fit is lower for the standard plate than for the slotted plates. As far as the reproducibility is concerned the standard plate shows a better performance than the slotted plates. Figure 207 shows the surface plot for the venturi. There is no visible trend observed in the plot. More than half the data points do not lie on the surface. This can be understood as the r^2 values are very low compared to the previous three plots. The standard error of the fit is the highest for the venturi. This shows that the venturi has the least reproducibility.

Figures 208 to 211 show the surface plots for the slotted plates, the standard plate and the venturi. This plot is slightly different from the previous ones because the differential pressure is replaced by dP/P (ratio of the differential pressure to upstream line pressure). The plots for the slotted plates and standard plate have a better r^2 value than the previous plots. Also the standard error of the fit is lower for these plots. The trends shown by these plots are the same for each plate. The surface plot for the venturi again shows half the points out of the fit. It can be concluded that the standard orifice plate shows the best reproducibility. It is followed by the 0.43 β ratio slotted plate and then by the 0.467 β ratio slotted plate. The venturi has the least reproducibility of all. This is also evident from the contour plots discussed in the previous sections. Results from test cases 5 and 6 show that there is no correlation in the response of the venturi between the two test cases.

CONCLUSIONS

An experimental study was conducted to determine the response of a slotted plate as a two-phase flow meter. This study focused mainly upon the performance of the slotted plate flow meter in the horizontal orientation using air and water as the working fluids. Two slotted plates with beta ratios of 0.43 and 0.467 were tested for different arrangements of the slotted plate test section. A standard orifice plate flow meter with a beta ratio of 0.508 and a venturi with a beta ratio of 0.527 were included in the orifice run. The data obtained from them were compared with the data obtained from the slotted plates. The experiments performed were categorized into six different test cases. Each test case corresponded to a particular arrangement of the slotted plate test section. The two slotted plates were first tested by placing the 0.43 β ratio slotted plate upstream of the 0.467 β ratio slotted plate. They were tested again by exchanging their positions. The response of the slotted plates remained unaffected. The slotted plates were then tested in conjunction with a standard orifice plate flow meter. Later the standard orifice plate was removed and a venturi was used instead.

Effects of upstream quality on the differential pressures and the coefficient of discharge were studied. A common trend observed in all the test cases was the decrease in the differential pressure when the upstream quality was increased. An increase in upstream quality caused a decrease in the coefficient of discharge when the differential pressure was maintained constant. These characteristics were found to be common for all the test cases. From the calibration of the pressure transducers, it was observed that the transducers were inaccurate in measuring differential pressures below 10 kPa (1.5 PSI). This had an adverse effect on the values obtained for the coefficient of discharge especially when the quality of the flow is very high. The fluctuations in the pump pressure at high qualities compounded this effect. The fluctuations were later reduced by using pressure regulators.

Repeatability was evaluated by studying the contour plots which depicted the effect of gas Reynolds number on the differential pressure at changing upstream qualities. An increase in the upstream line pressure resulted in an increase in the gas Reynolds number. It was possible to achieve higher gas flow rates as the line pressure was increased and this resulted in differential pressures across the plates higher than those obtained in the previous test case. At constant coefficient of discharge when density of the mixture was decreased the differential pressure showed an increase. When the gas Reynolds number was fixed constant at a certain value and the upstream line pressure increased the differential pressure across the plates showed a decrease. This was because at very high upstream line pressures the amount of water supplied by the water metering system was very low as the water pressure was not high enough to overcome the gas pressure. So at high line pressures the quality of the flow corresponding to each gas flow rate was high compared to lower line pressures. The range of values attained by the coefficient of discharge at each upstream line pressure decreased with an increase in the gas Reynolds number. It was also possible to achieve a higher range of qualities at low gas Reynolds number. The two slotted plates (beta ratios of 0.43 and 0.467) along with the standard orifice plate and the venturi showed good repeatability.

Experiments were performed in two stages. One for high air qualities (low water flow rates) using the small Coriolis flow meter and the other for low air qualities (high water flow rates) using the large Coriolis flow meter. The differential pressures were in the order of standard orifice plate > 0.43 > 0.467 > venturi. The standard orifice plate had the lowest coefficient of discharge while the slotted plates had high coefficients of discharge. However when tested only with the 0.43 β ratio slotted plate, the standard orifice plate produced different results. The differential pressure across the standard orifice plate was less than the 0.43 β ratio slotted plate at high gas flow rates and higher at low gas flow rates. The standard orifice plate flow meter is known to be sensitive to upstream flow conditions and this affected its performance drastically from one case to another. The response of the venturi is unpredictable though it shows repeatability. This

can be observed from the contour plots relating the differential pressure with the coefficient of discharge and the upstream quality. No visible trend can be seen in the plots.

Reproducibility was evaluated by consolidating the data obtained from the slotted plates, the standard orifice plate and the venturi from all the six test cases. Surface plots were made for each plate by plotting differential pressure against upstream quality and the coefficient of discharge. Reproducibility for a particular plate can be established when all the data corresponding to it collapses on one single surface. The standard orifice plate showed the best reproducibility for this selection of independent variables. It was followed by the 0.43 β ratio slotted plate and then by the 0.467 β ratio slotted plate. The venturi had poor reproducibility.

The performance of the slotted plates was enhanced when the water pressure regulators were installed in the water metering section. This stabilized the water pressure which in turn prevented the quality of the two-phase flow mixture from fluctuating. The response of the slotted plates was good especially for high quality flows and this could be observed in test case 6. Though the standard orifice plate shows excellent reproducibility its performance as a whole is not as good as the slotted plates. The slotted plates have several advantages over the standard plate such as high C_d values, lower differential pressures, and low sensitivity to upstream flow conditions, high accuracy, good repeatability and reproducibility. These factors make it a better choice for metering two-phase flows.

RECOMMENDATIONS

1. The calibration of the stacked pressure transducer system revealed that the accuracy was lost at low differential pressures (less than 10 kPa / 1.5 PSI). This affects the response of the slotted plates at low differential pressures as the data is not measured accurately. Transducers capable of measuring low differential pressures can be added to the stack to improve the accuracy.

2. The pressure upstream of the first plate is maintained constant. But the pressure upstream of the second plate is not constant and it changes with changing quality. This is because the differential pressure across the first slotted plate varies with quality. The line pressure upstream of the second plate is deduced by subtracting the differential pressure across the first plate from the upstream line pressure. But this not the right way as it does not include the effects of pressure recovery downstream of the first slotted plate. Absolute pressure transducers should be used to measure the line pressure upstream of the second plate. Multivariable pressure transducers can also be used as they are capable of measuring both the differential as well as absolute pressures.

3. When the water mixes with the air to form a two-phase flow mixture there is a possibility that some of the water may get vaporized and saturate the air. This changes the mass flow rate of the air and water which in turn affects the quality. The results obtained in this study did not take these effects into account as the upstream line pressures considered were higher than the saturation pressure of air. However these effects will become more significant at low upstream pressures and hence have to be considered.

4. The slotted plates should be tested at low upstream line pressures. This is to study the response of the slotted plates for low differential pressures.

5. The slotted plates should be tested for three-phase flow, comprising of air, water and a third fluid (either oil or steam). This would increase the capability of the slotted plates to measure any type of multi-phase flow.

6. Experiments should be performed with different types of flows such as slug flows, bubble flows and abrasive flows. This should be done to observe whether the slotted plate is capable of metering such types of flow accurately.

REFERENCES

[1] J. Amdal, H. Danielsen, E. Dykesteen, D. Flolo, J. Grendstad, H.O. Hide, H. Moestue, B.H. Torkildsen, Handbook of Multi-Phase metering, The Norwegian Society for Oil and Gas Measurements, Available: http://www.nfogm.no/docup/dokumentfiler /Handbook.PDF, 1999, pp. 20-30.

[2] R.C. Martinelli, L.M.K. Boelter, T.H.M. Taylor, E.G. Thomsen, E.H. Morrin, Isothermal pressure drop for two-phase two-component flow in a horizontal pipe, heat transfer division, Transactions of the ASME, 66, 1943, pp.139-151.

[3] J.W. Murdock, Two-phase flow measurement with orifices, Journal of Basic Engineering, (12), (1962), pp.419-433.

[4] J.A. Brennan, S.E. McFaddin, C.F. Sindt, K.M. Kothari, The influence of swirling flow on orifice and turbine flow meter performance, Flow Measurement and Instrumentation, 1, (10), (1989), pp.5-8.

[5] Wenran W, Yunxian T, A new method of two-phase flow measurement by orifice plate differential pressure noise, Flow Measurement and Instrumentation, 6, (4), (1995), pp.265-270.

[6] V.C.S. Ferreira, Differential pressure spectral analysis for two-phase flow through an orifice plate, International Journal of Pressure Vessels and Piping, 73, (1997), pp.19-23.

[7] A.W. Jamieson, Multi-Phase Metering – The challenge of implementation, 16th North Sea Flow Measurement Workshop, London, U.K., 1998.

[8] R. Thorn, G.A. Johansen, E.A. Hammer, Recent developments in three-phase flow measurement, Measurement Science and Technology, 8, (1997), pp.691-701.

[9] M.L. Macek, A slotted orifice plate used as a flow measurement device, M.S. Thesis, Texas A&M University, College Station, 1993.

[10] M.L. Ihfe, Development of slotted orifice flow conditioner, M.S. Thesis, Texas A&M University, College Station, 1994.

[11] D.P. Terracina, The experimental and numerical development of a slotted orifice meter and its design parameters, Ph.D. Dissertation, Texas A&M University, College Station, 1996.

[12] C.V. Brewer, Evaluation of the slotted orifice plate as a two phase flow meter, M.S. Thesis, Texas A&M University, College Station, 1999.

[13] A.E. Flores, Evaluation of a slotted orifice plate using horizontal two phase flow, M.S. Thesis, Texas A&M University, College Station, 2000.

[14] G.L. Morrison, K.R. Hall, J.C. Holste, R.E. DeOtte Jr., M.L. Macek, L.M. Ihfe, Slotted orifice flowmeter, AIChE Journal, 40, (10), (1994), pp.1757-1760

[15] G.L. Morrison, K.R. Hall, J.C. Holste, M.L. Macek, L.M. Ihfe, R.E. DeOtte Jr., D.P. Terracina, Comparison of orifice and slotted plate flowmeters, Flow Measurement and Instrumentation, 5, (2), (1994), pp.71-77.

[16] J.R. Fincke, Performance characteristics of an extended throat flow nozzle for the measurement of high void fraction multi-phase flows. Proc. NETL Oil and Gas Conference, Dallas, USA, Paper P.7, 1999

[17] S.J. Kline, F.A. McClintock, Describing uncertainties in simple-sample experiments, Mechanical Engineering, 75, (1953), pp.3-10.

APPENDIX

FIGURES
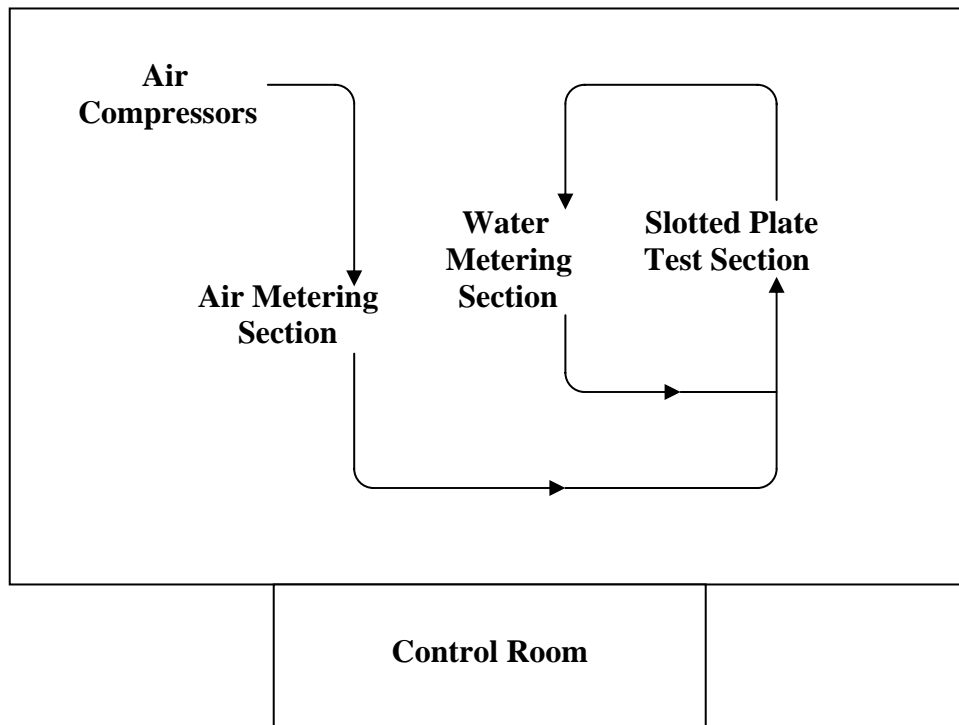
Figure 1, Air and Water Two Phase Flow Slotted Plate Test Facility
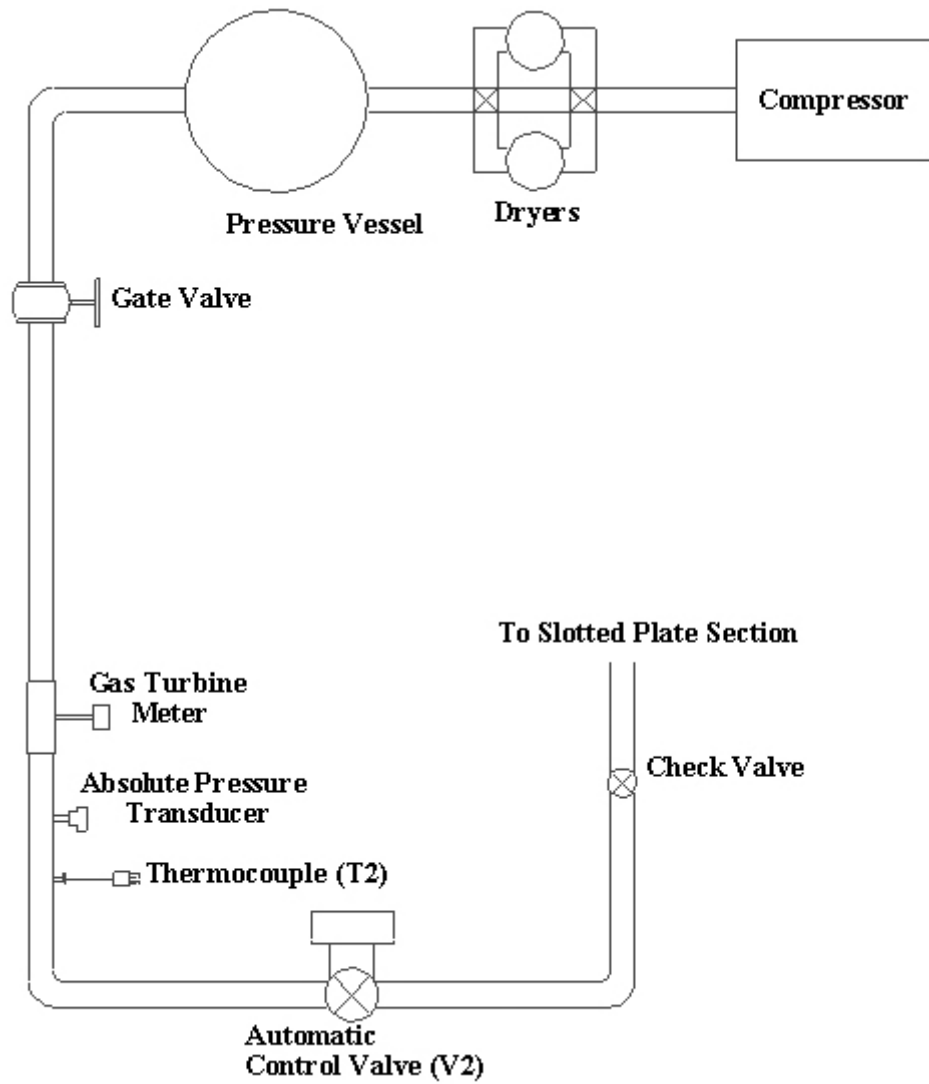
Figure 2, Air Metering Section
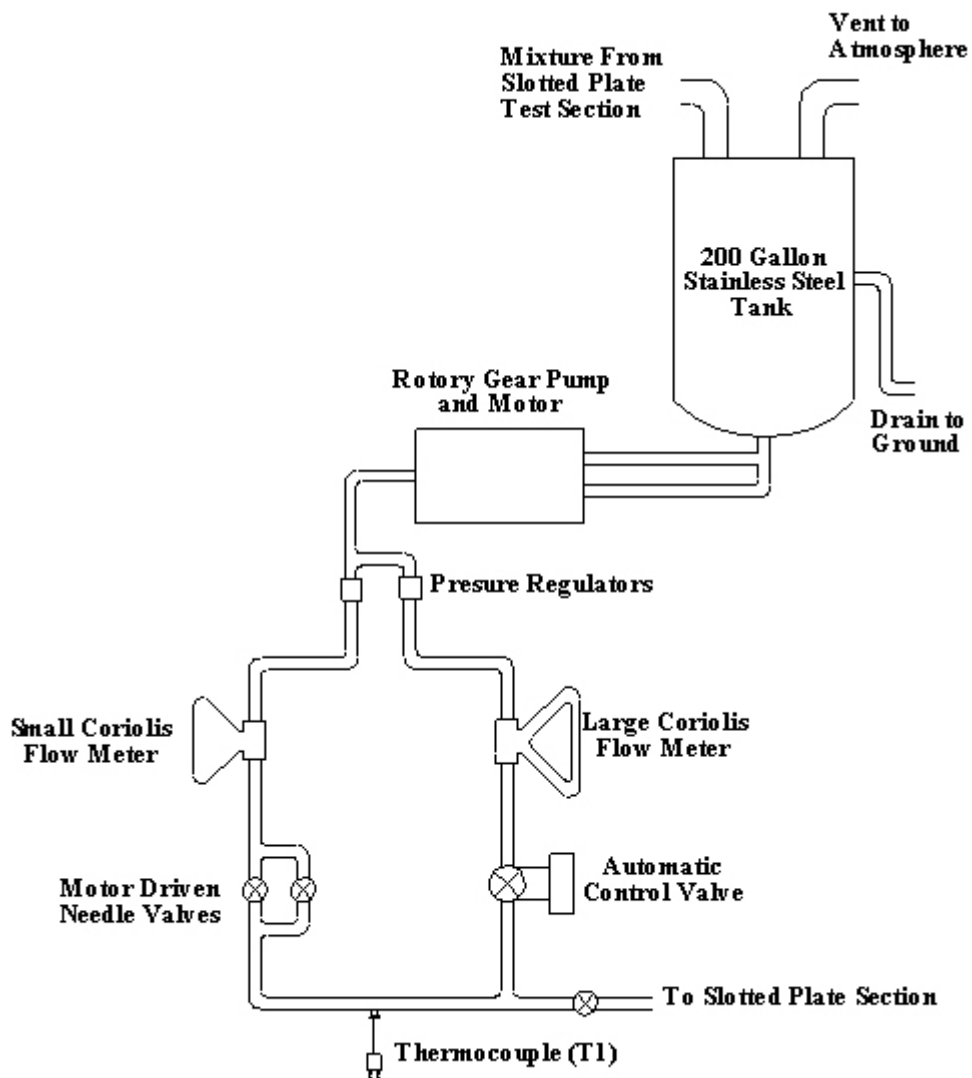
Figure 3, Water Metering Section
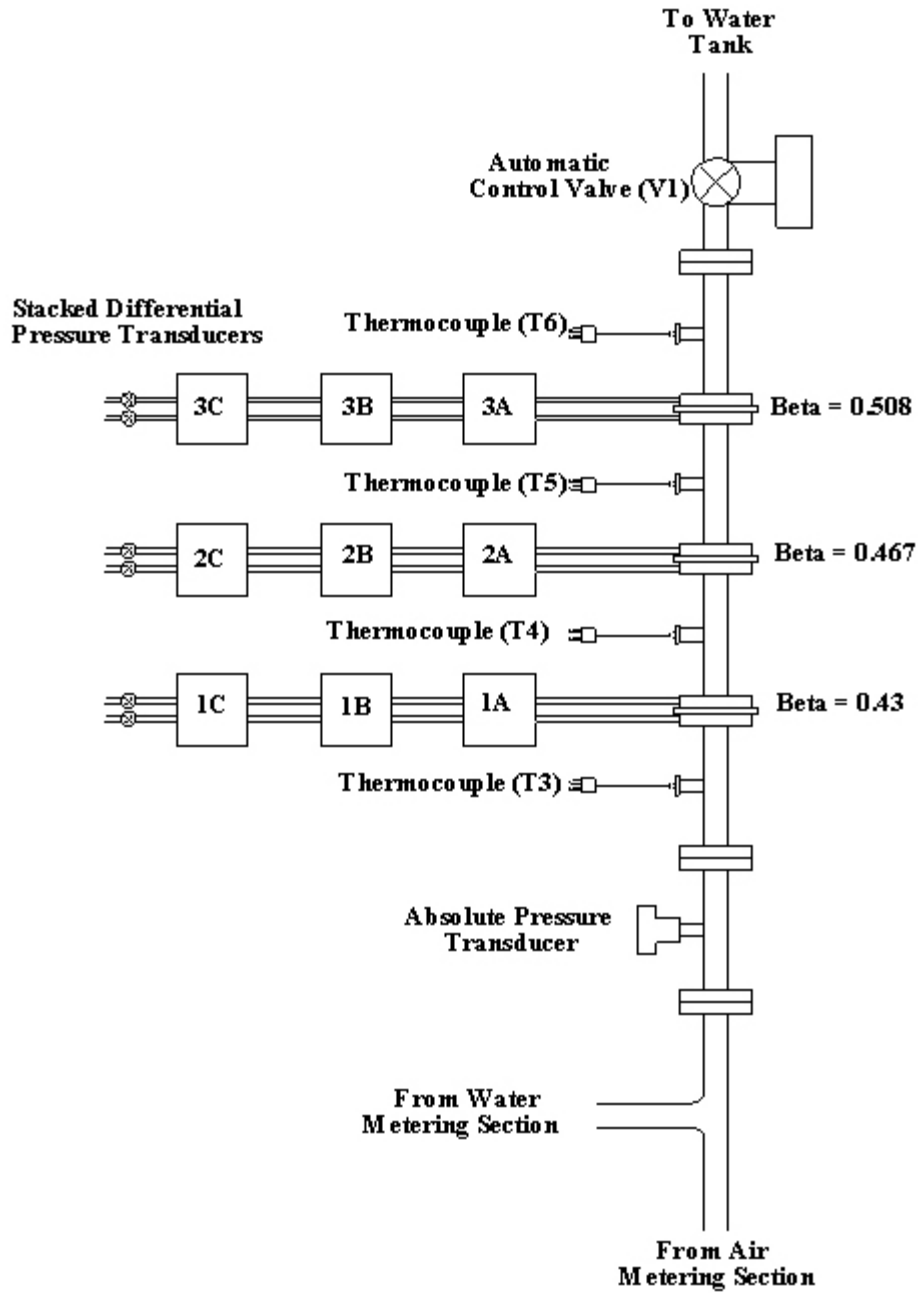
Figure 4, Slotted Plate Test Section with Standard Orifice Plate Flow Meter
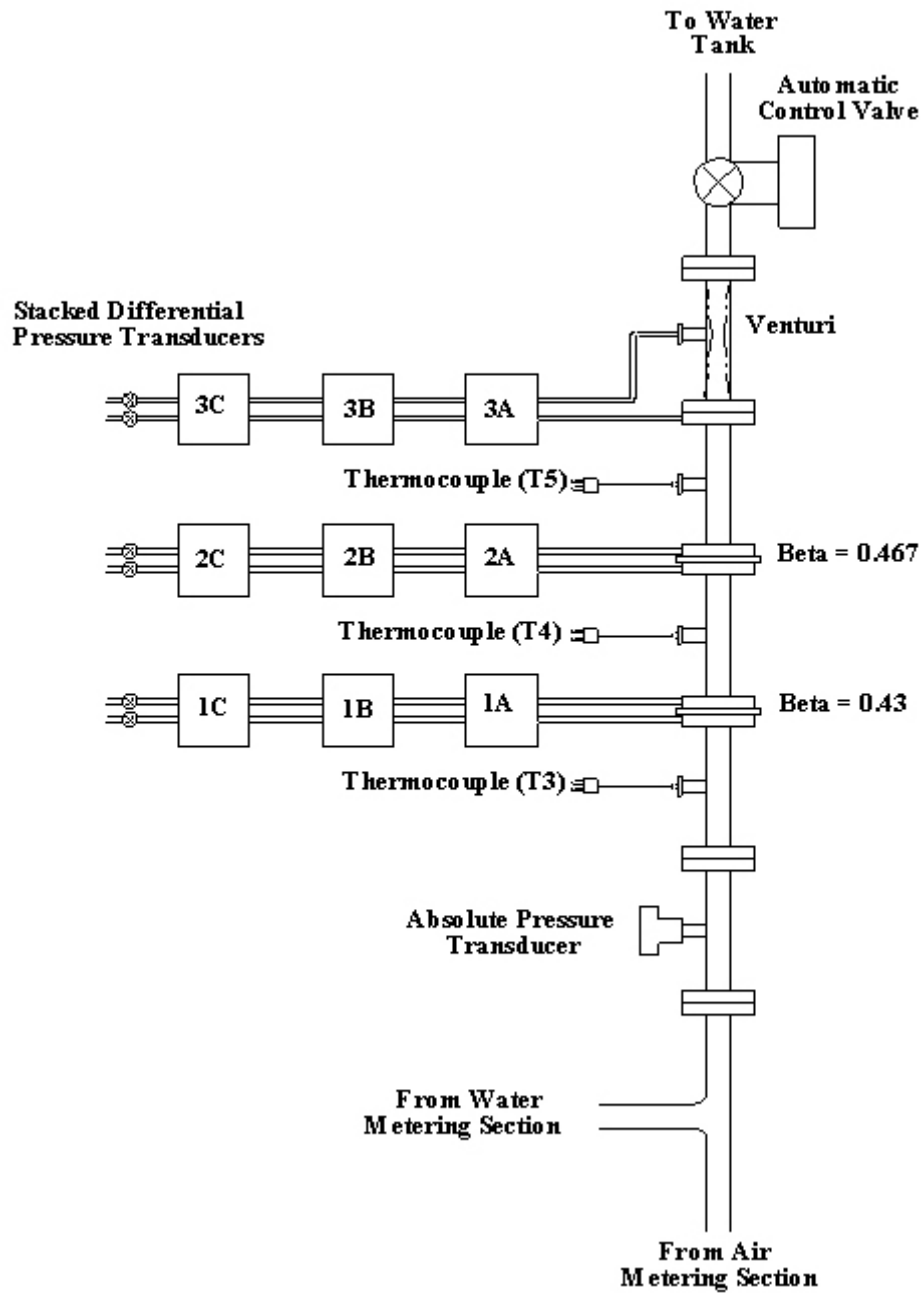
Figure 5, Slotted Plate Test Section with Venturi
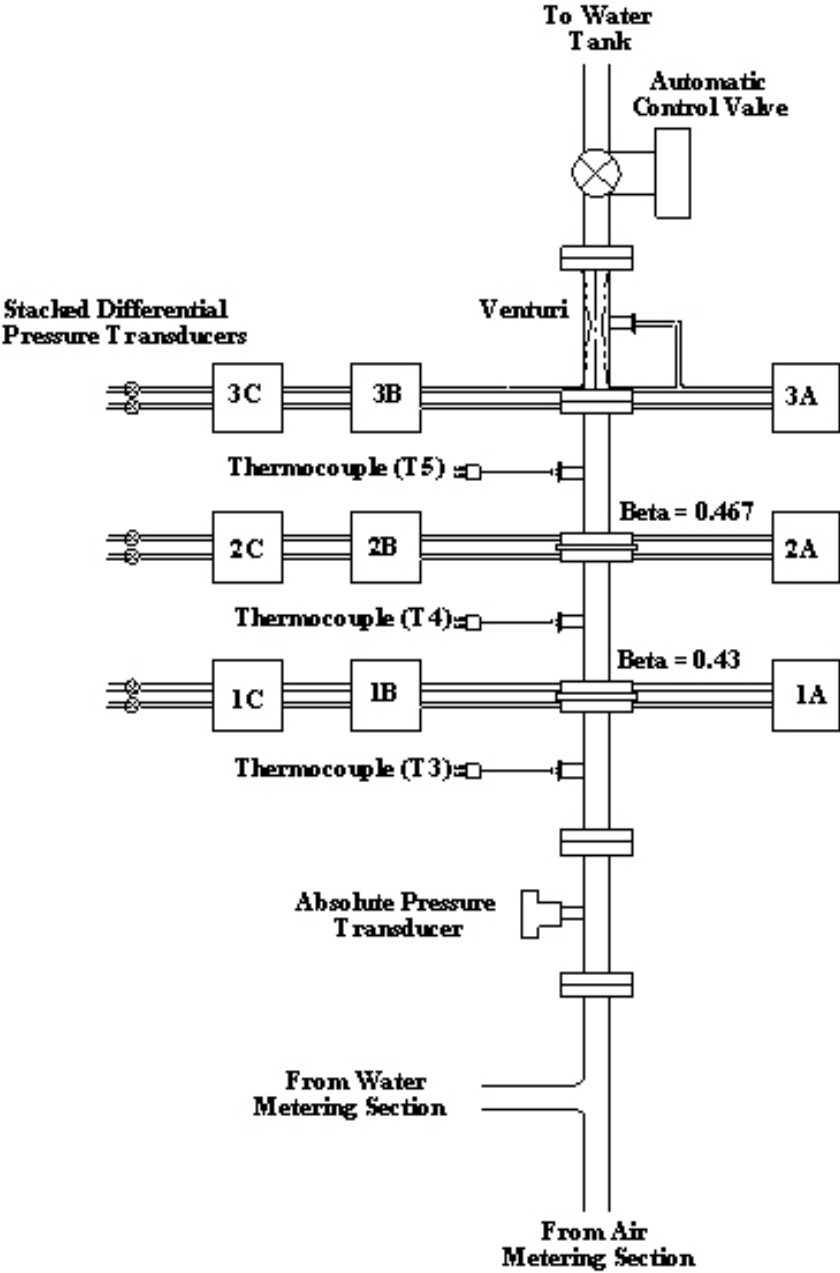
Figure 6, Modified Slotted Plate Test Section with Venturi
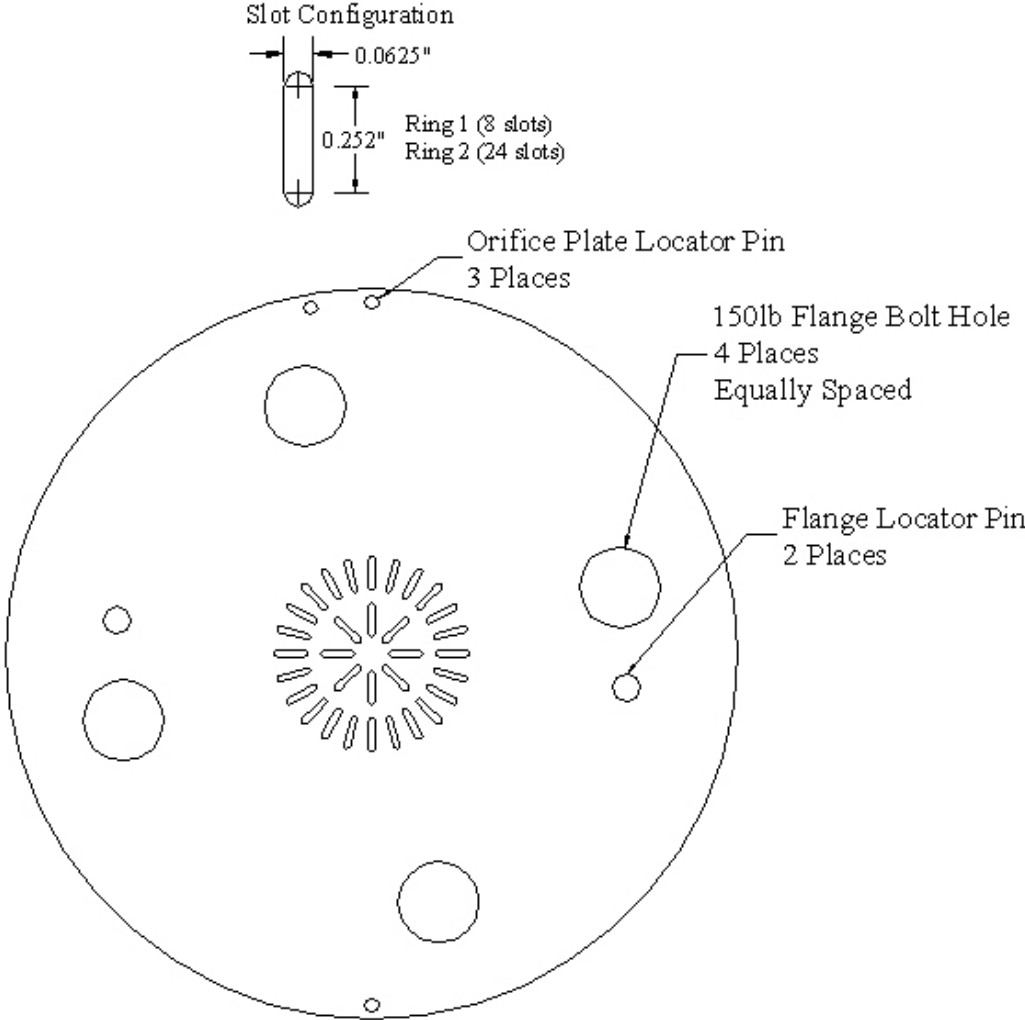
Figure 7, 0.43 Beta Slotted Plate

Beta = 0.467
Slotted Plate (2 Ring)

Slot Configuration

0.0625"

0.374"   Ring 1 (8 slots)
Ring 2 (18 slots)

Orifice Plate Locator Pin
3 Places

150lb Flange Bolt Hole
4 Places
Equally Spaced

Flange Locator Pin
2 Places
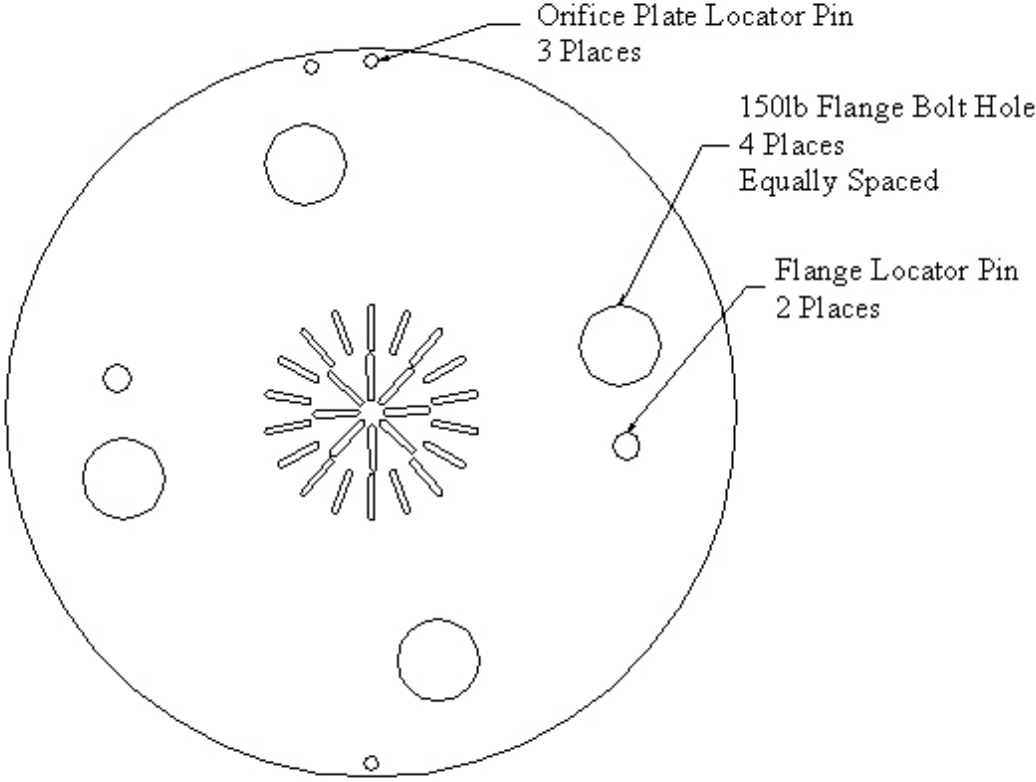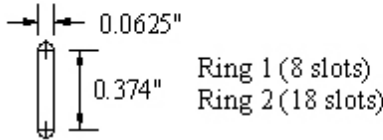
Figure 8, 0.467 Beta Slotted Plate

Standard Orifice Plate
Beta = 0.508

∅1.017"

1.00"

R2.00"
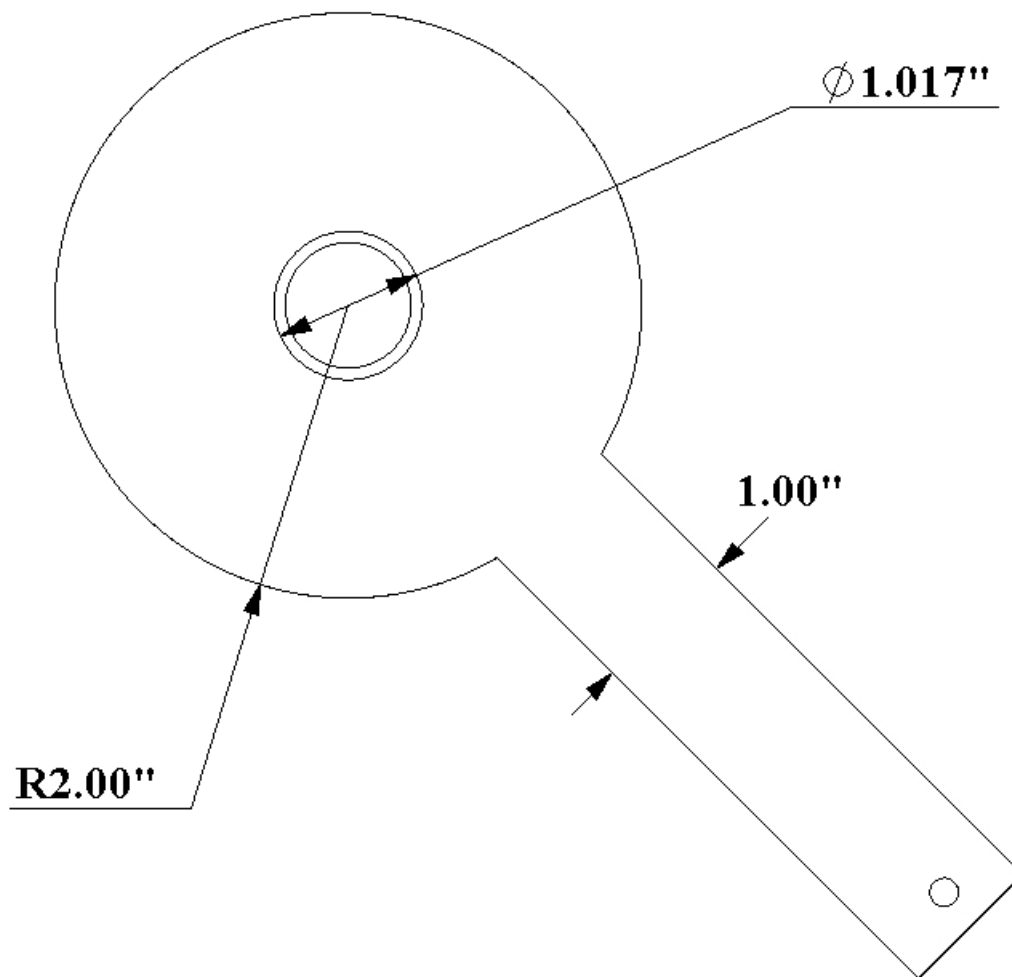
Figure 9, Standard Orifice Plate

Beta = 0.527
Venturi
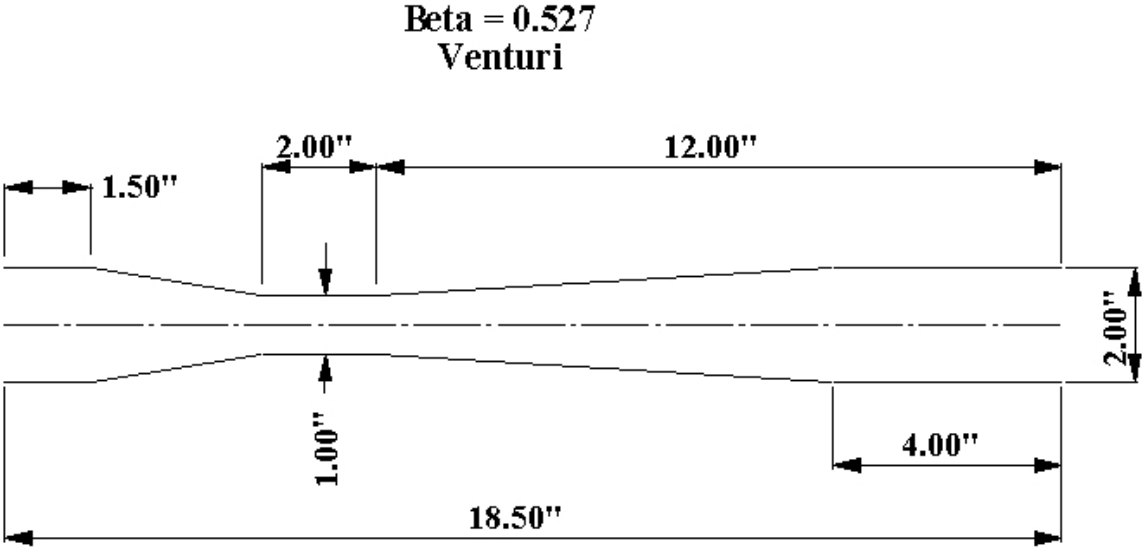
Figure 10, Venturi

Case 1 Quality Effects

98 kPa Line Pressure
Beta = 0.43
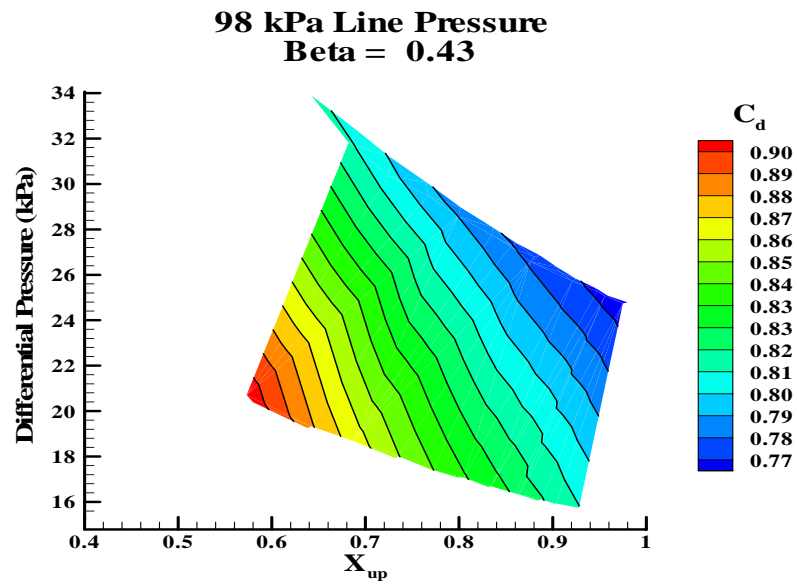
Figure 11   Differential Pressure as a Function of Upstream
Quality and Coefficient of Discharge,
98 kPa Upstream Line Pressure, $\beta = 0.43$

150 kPa Line Pressure
Beta = 0.43
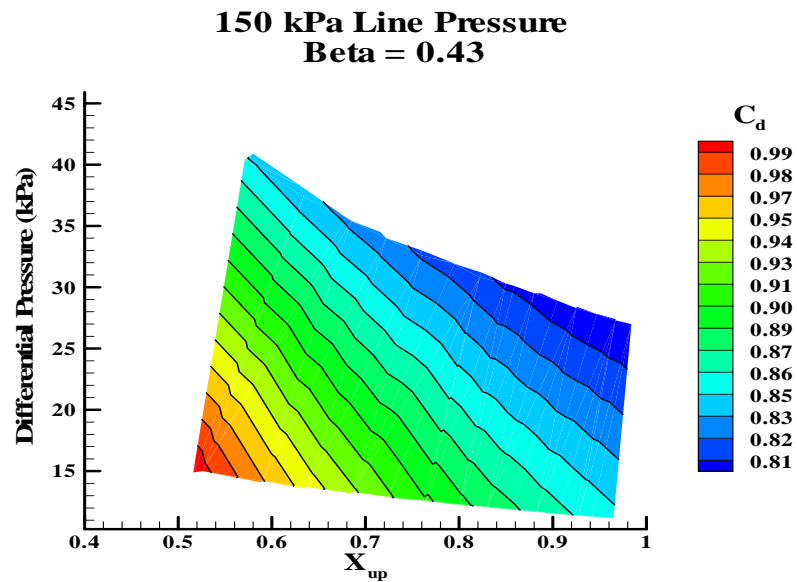
Figure 12   Differential Pressure as a Function of Upstream
Quality and Coefficient of Discharge,
150 kPa Upstream Line Pressure, $\beta = 0.43$

204 kPa Line Pressure
Beta = 0.43
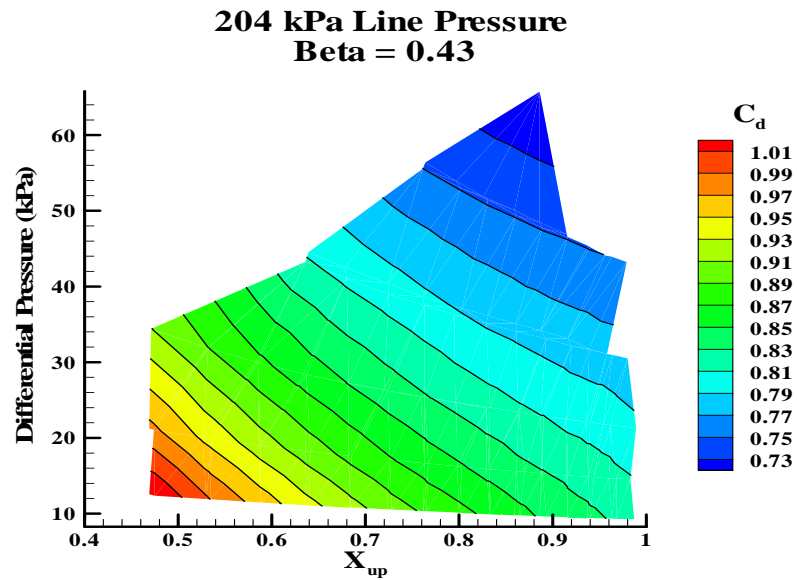
Figure 13   Differential Pressure as a Function of Upstream
Quality and Coefficient of Discharge,
204 kPa Upstream Line Pressure, $\beta = 0.43$

255 kPa Line Pressure
Beta = 0.43
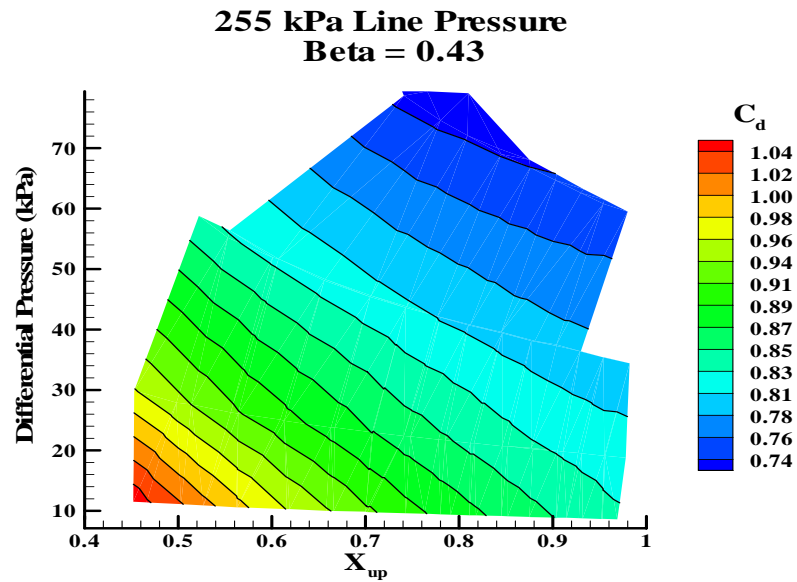
Figure 14   Differential Pressure as a Function of Upstream
Quality and Coefficient of Discharge,
255 kPa Upstream Line Pressure, $\beta = 0.43$
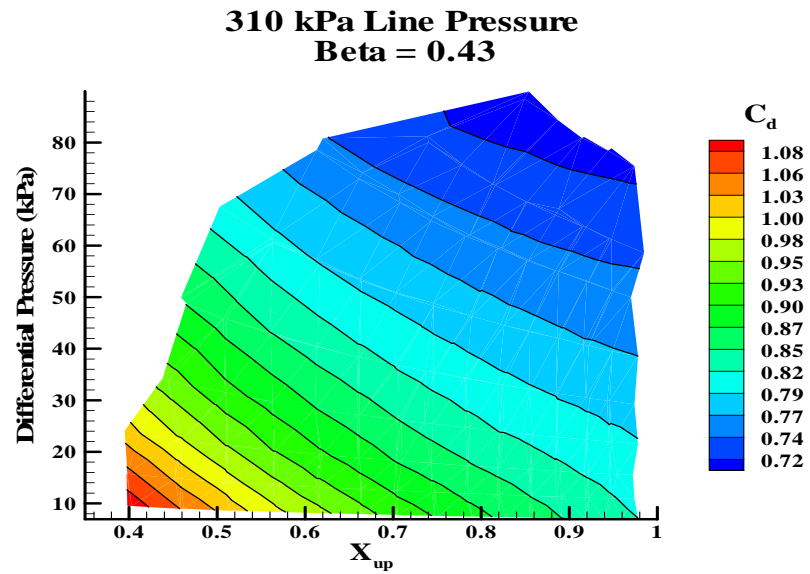
Figure 15   Differential Pressure as a Function of Upstream
Quality and Coefficient of Discharge,
310 kPa Upstream Line Pressure, $\beta = 0.43$
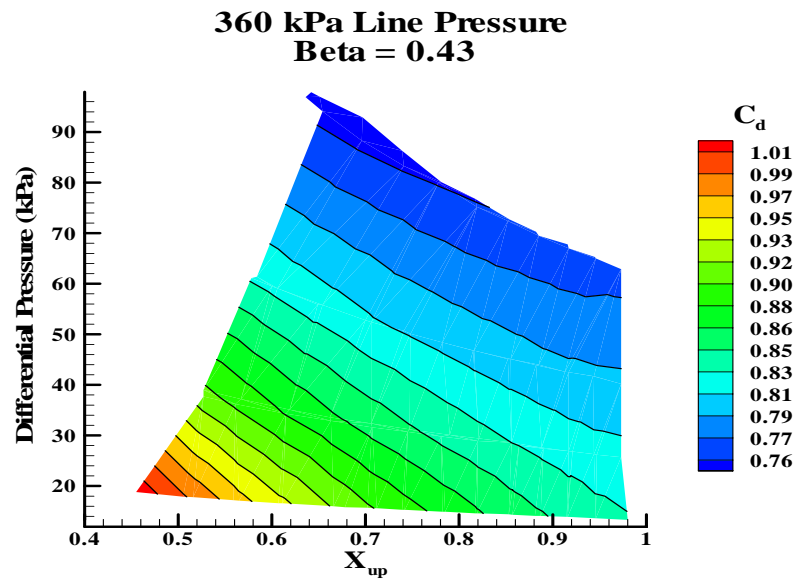
Figure 16   Differential Pressure as a Function of Upstream
Quality and Coefficient of Discharge,
360 kPa Upstream Line Pressure, $\beta = 0.43$

415 kPa Line Pressure
Beta = 0.43
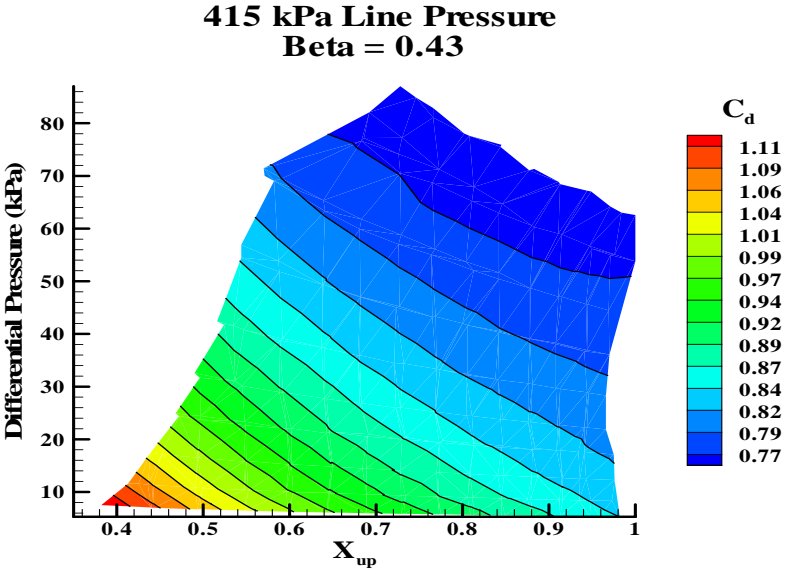
Figure 17   Differential Pressure as a Function of Upstream Quality and Coefficient of Discharge, 415 kPa Upstream Line Pressure, β = 0.43

98 kPa Line Pressure
Beta = 0.467
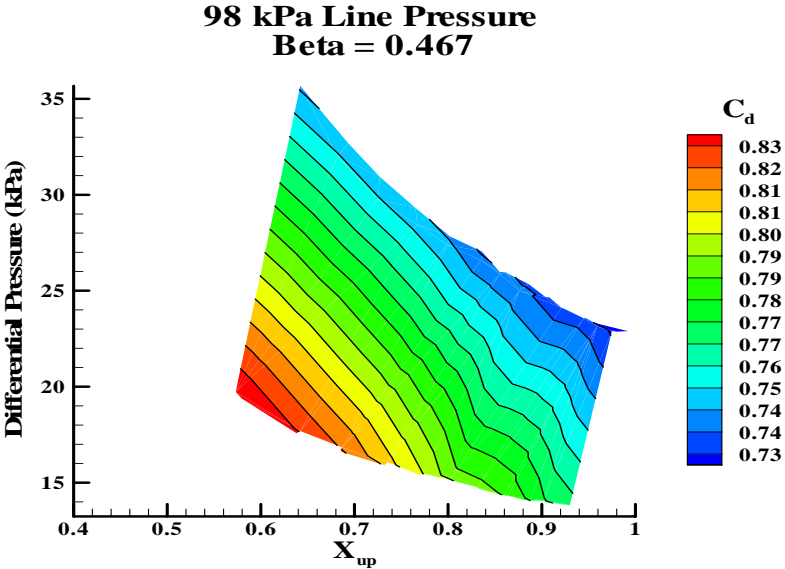
Figure 18   Differential Pressure as a Function of Upstream Quality and Coefficient of Discharge, 98 kPa Upstream Line Pressure, β = 0.467
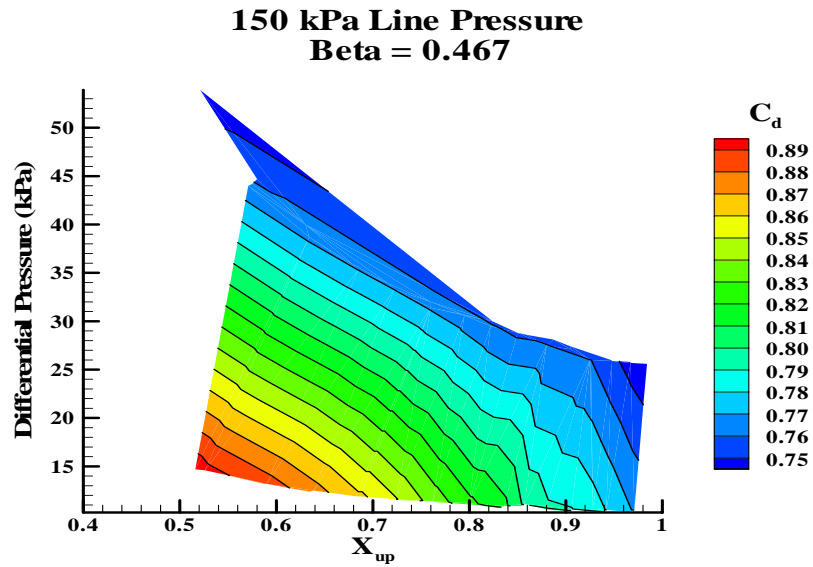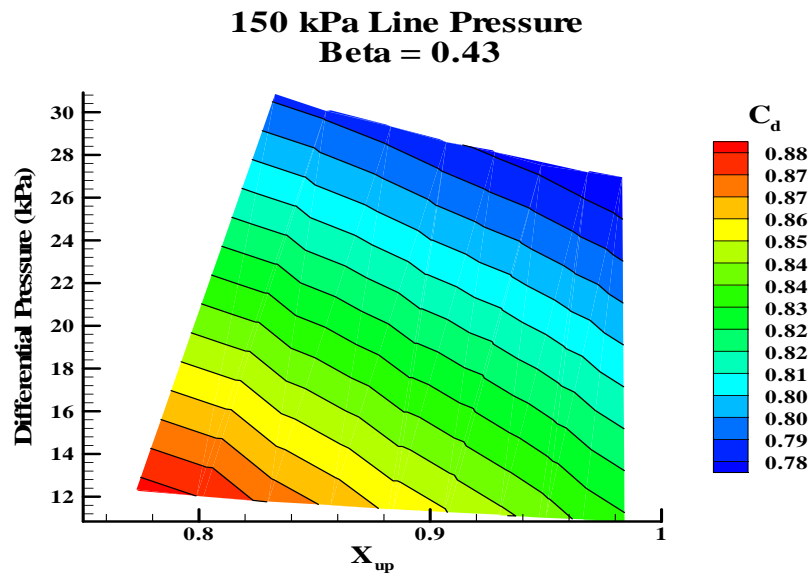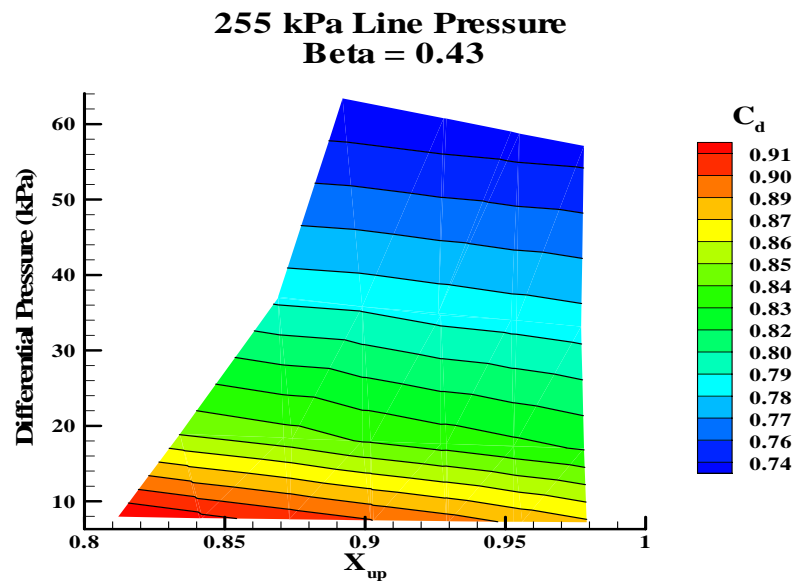
Figure 19   Differential Pressure as a Function of Upstream Quality and Coefficient of Discharge, 150 kPa Upstream Line Pressure, β = 0.467
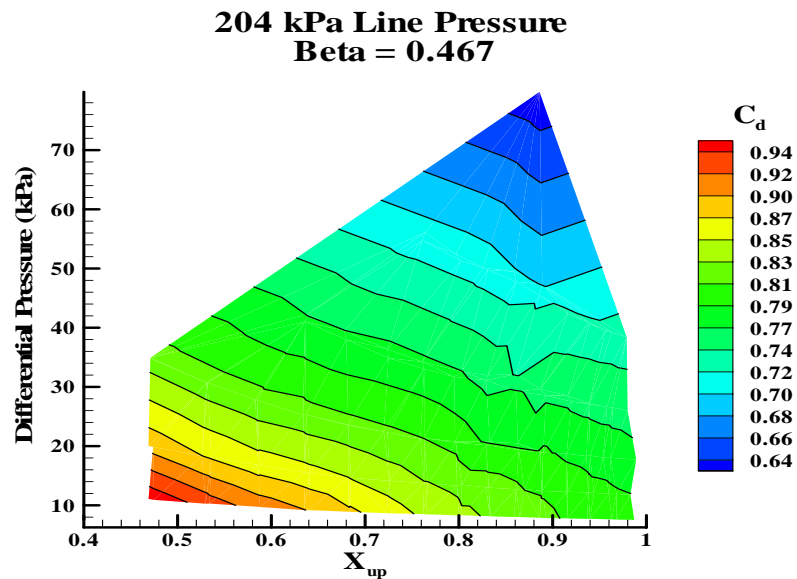
Figure 20   Differential Pressure as a Function of Upstream Quality and Coefficient of Discharge, 204 kPa Upstream Line Pressure, β = 0.467

255 kPa Line Pressure
Beta = 0.467
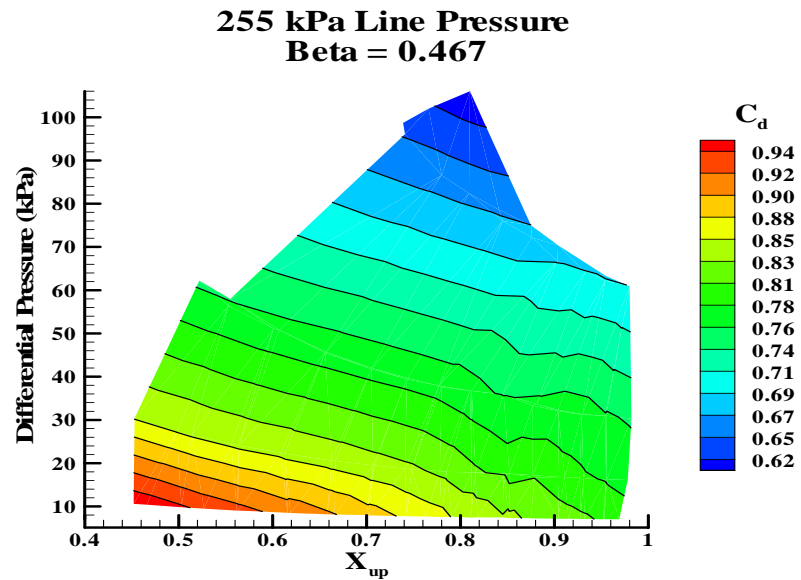
Figure 21   Differential Pressure as a Function of Upstream
             Quality and Coefficient of Discharge,
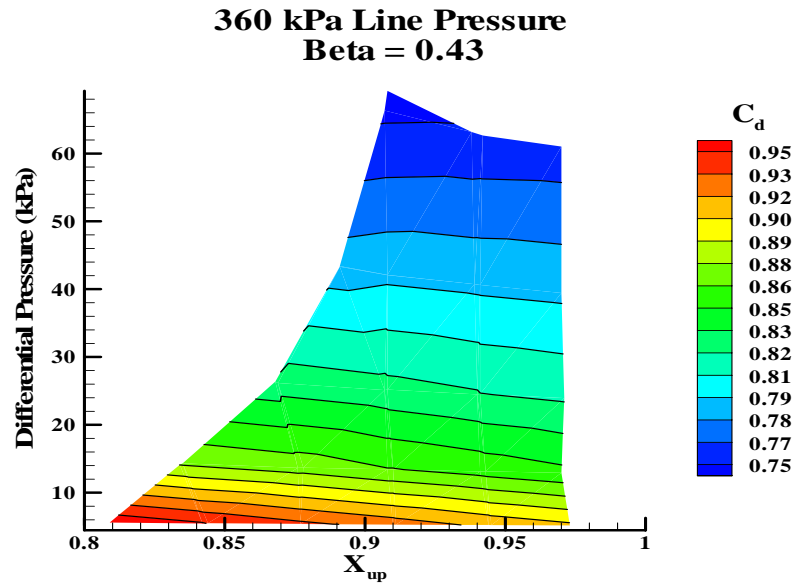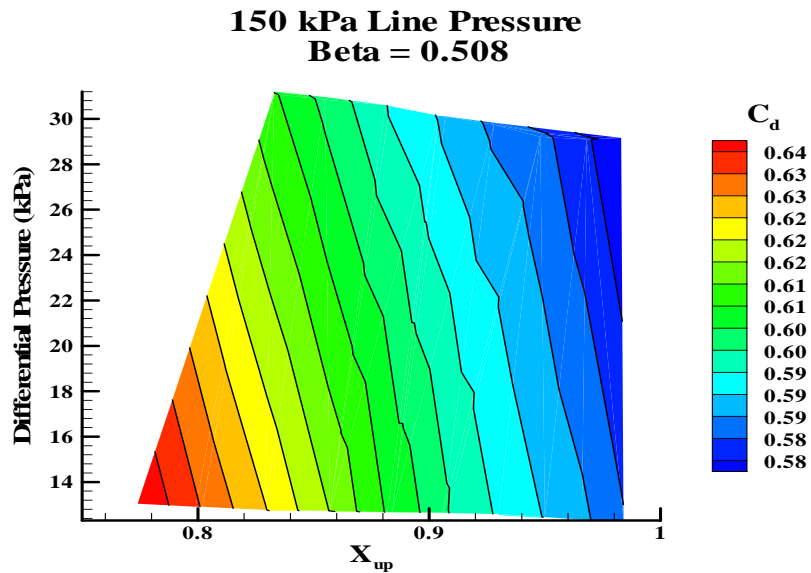   255 kPa Upstream Line Pressure, β = 0.467

310 kPa Line Pressure
Beta = 0.467
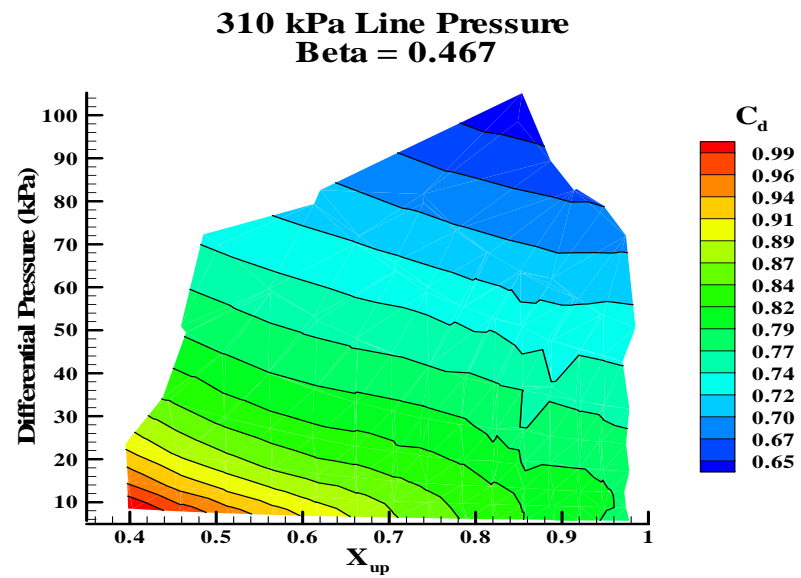
Figure 22   Differential Pressure as a Function of Upstream
             Quality and Coefficient of Discharge,
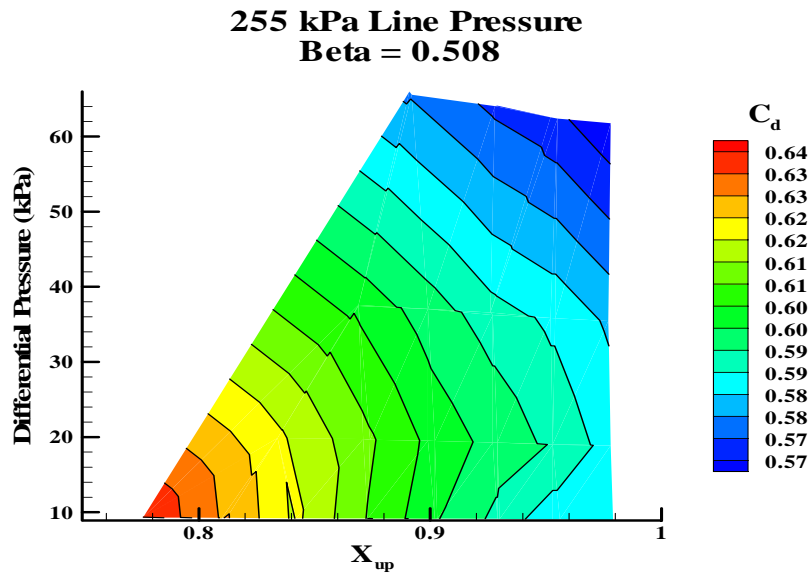   310 kPa Upstream Line Pressure, β = 0.467

360 kPa Line Pressure
Beta = 0.467
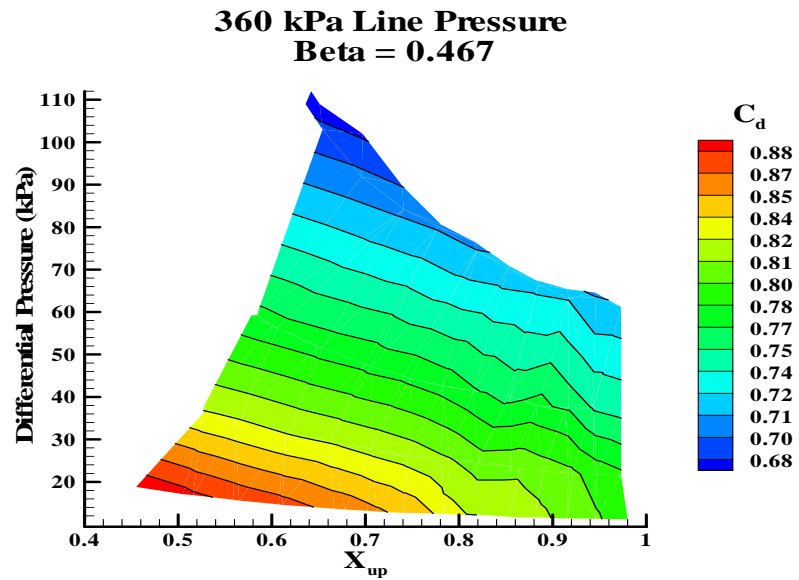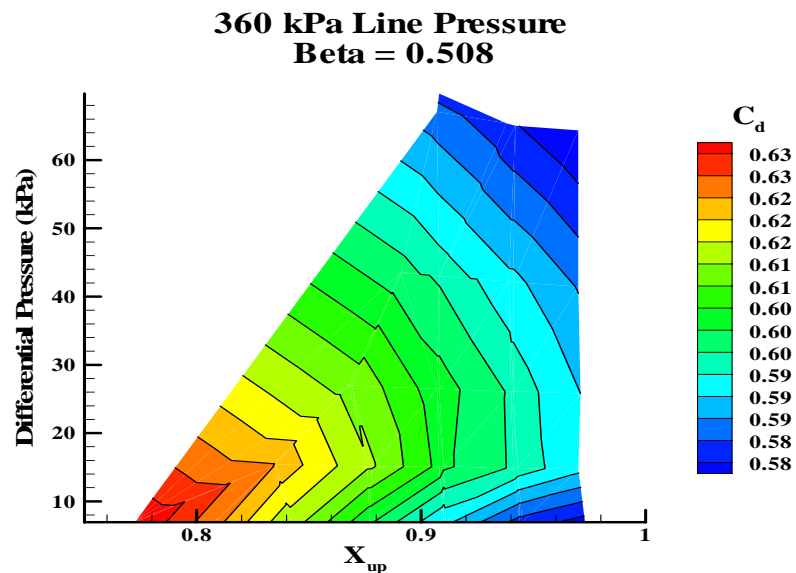

Figure 23   Differential Pressure as a Function of Upstream
Quality and Coefficient of Discharge,
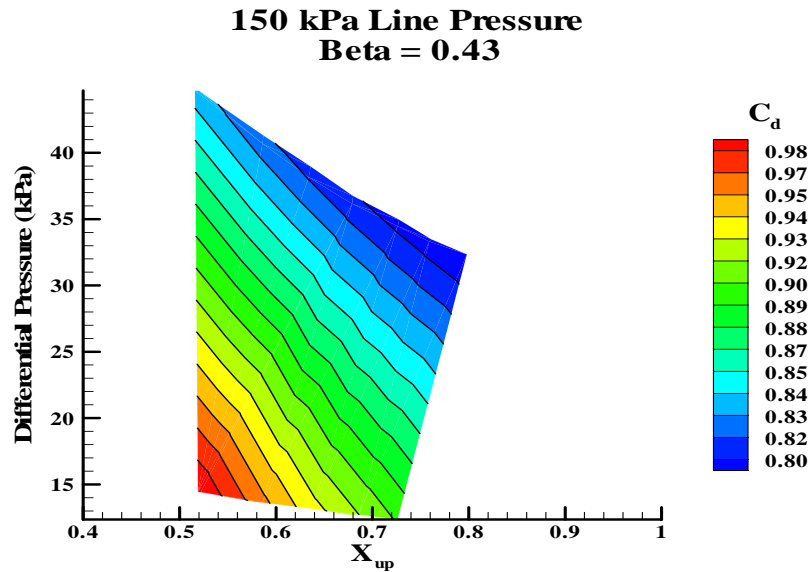360 kPa Upstream Line Pressure, β = 0.467

415 kPa Line Pressure
Beta = 0.467
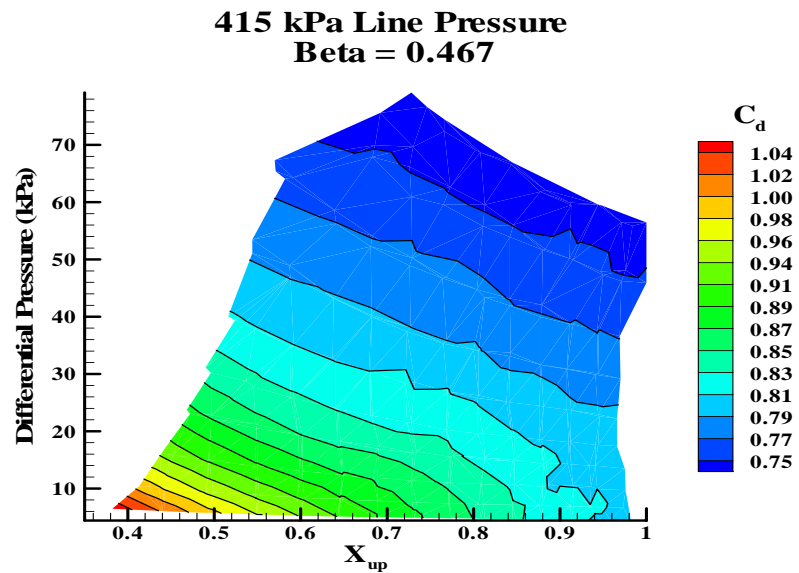
Figure 24   Differential Pressure as a Function of Upstream
Quality and Coefficient of Discharge,
415 kPa Upstream Line Pressure, β = 0.467

Case 1 Repeatability
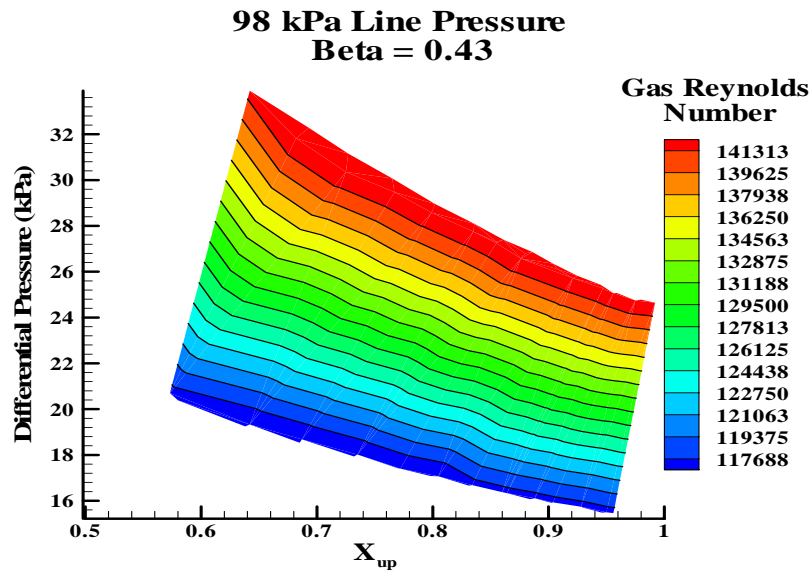
Figure 25   Differential Pressure as a Function of Upstream
Quality and Gas Reynolds Number,
98 kPa Upstream Line Pressure, $\beta = 0.43$
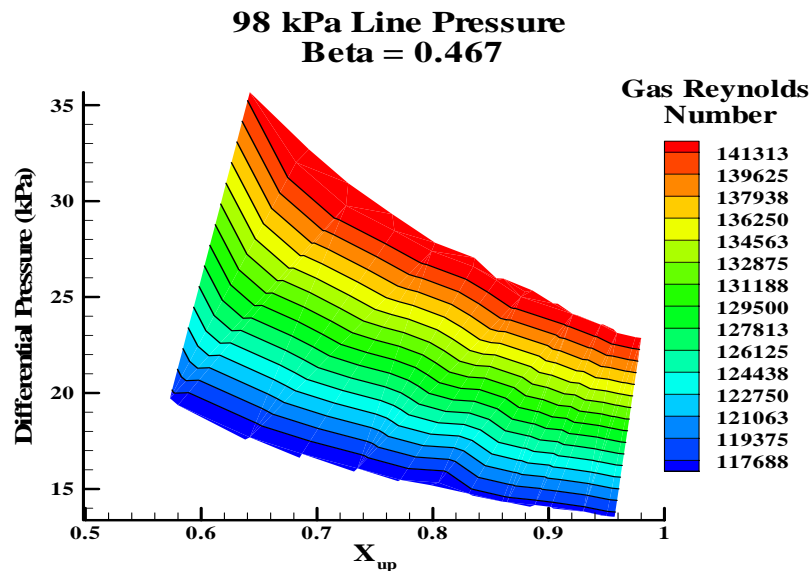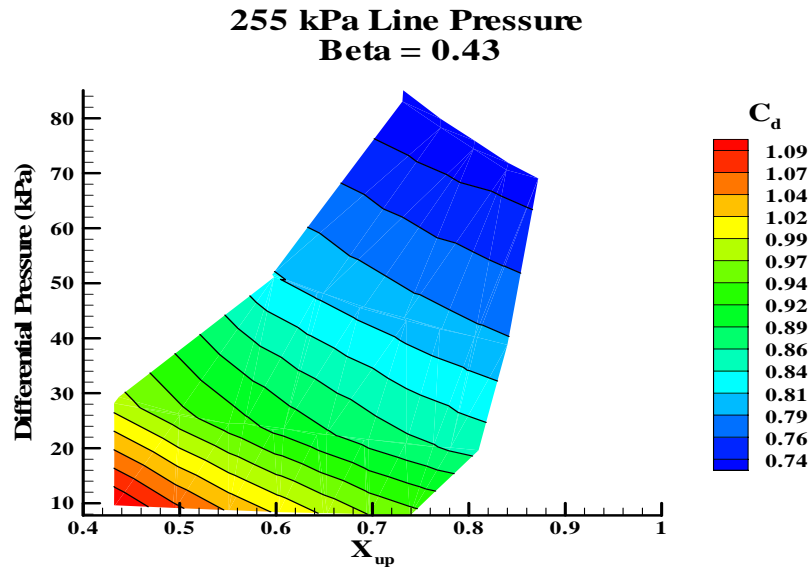

Figure 26   Differential Pressure as a Function of Upstream
Quality and Gas Reynolds Number,
98 kPa Upstream Line Pressure, $\beta = 0.467$
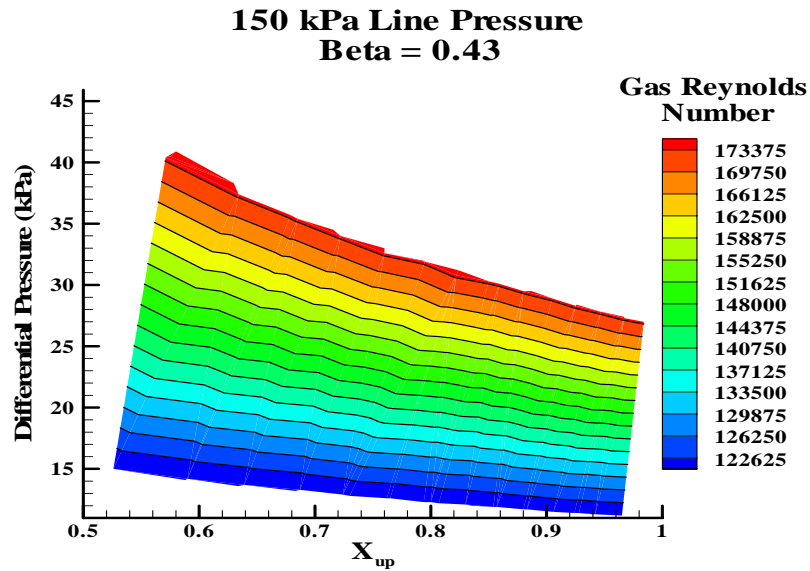
Figure 27   Differential Pressure as a Function of Upstream
Quality and Gas Reynolds Number,
150 kPa Upstream Line Pressure, β = 0.43
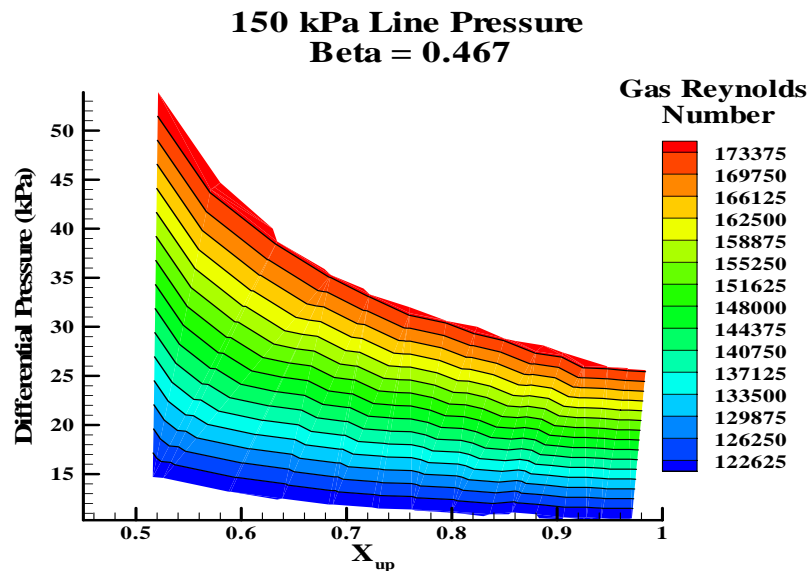
Figure 28   Differential Pressure as a Function of Upstream
Quality and Gas Reynolds Number,
150 kPa Upstream Line Pressure, β = 0.467

204 kPa Line Pressure
Beta = 0.43
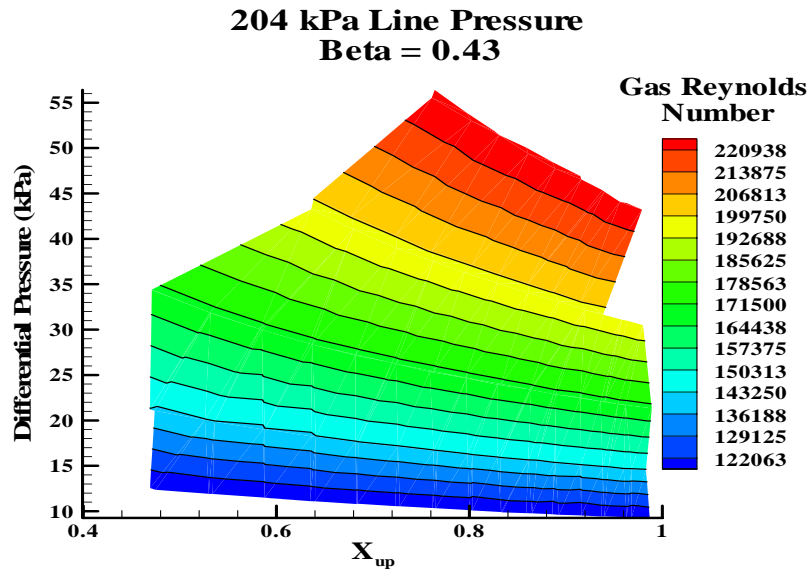
Figure 29   Differential Pressure as a Function of Upstream
Quality and Gas Reynolds Number,
204 kPa Upstream Line Pressure, β = 0.43

204 kPa Line Pressure
Beta = 0.467
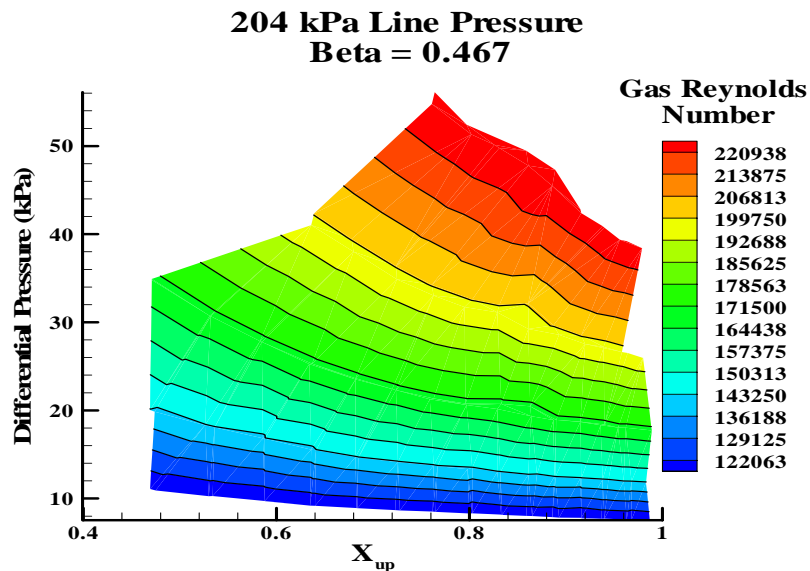
Figure 30   Differential Pressure as a Function of Upstream
Quality and Gas Reynolds Number,
204 kPa Upstream Line Pressure, β = 0.467

255 kPa Line Pressure
Beta = 0.43
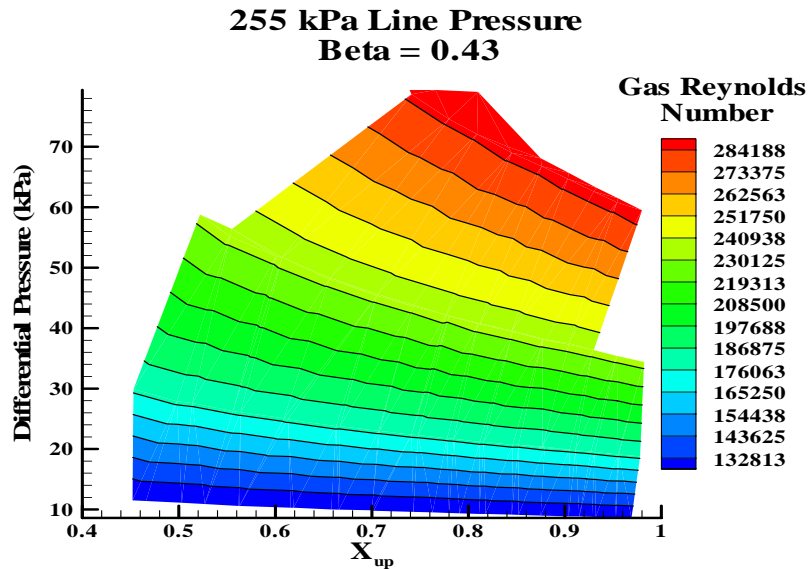
Figure 31   Differential Pressure as a Function of Upstream
                   Quality and Gas Reynolds Number,
                   255 kPa Upstream Line Pressure, β = 0.43

255 kPa Line Pressure
Beta = 0.467
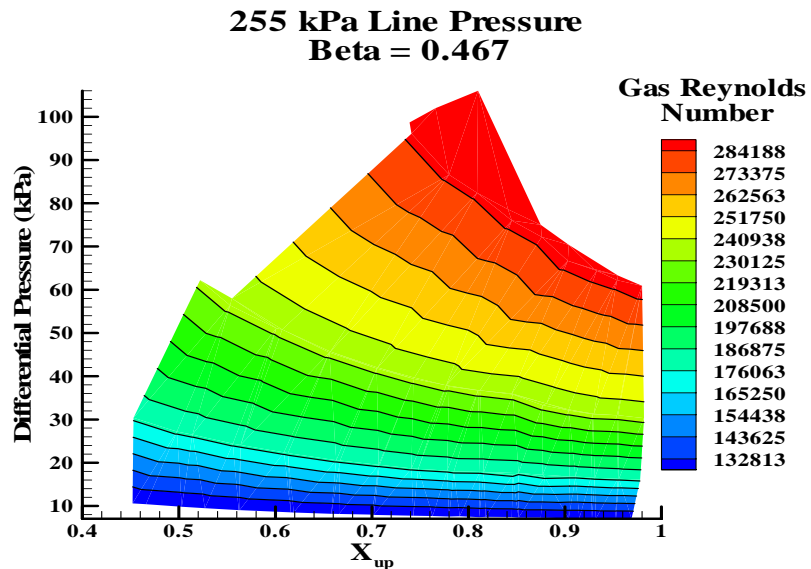
Figure 32   Differential Pressure as a Function of Upstream
                   Quality and Gas Reynolds Number,
                   255 kPa Upstream Line Pressure, β = 0.467
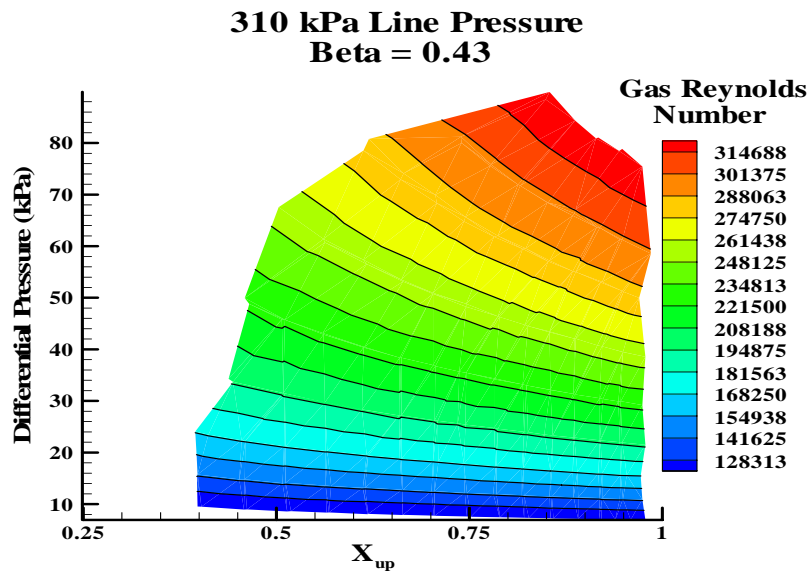
Figure 33   Differential Pressure as a Function of Upstream
Quality and Gas Reynolds Number,
310 kPa Upstream Line Pressure, β = 0.43
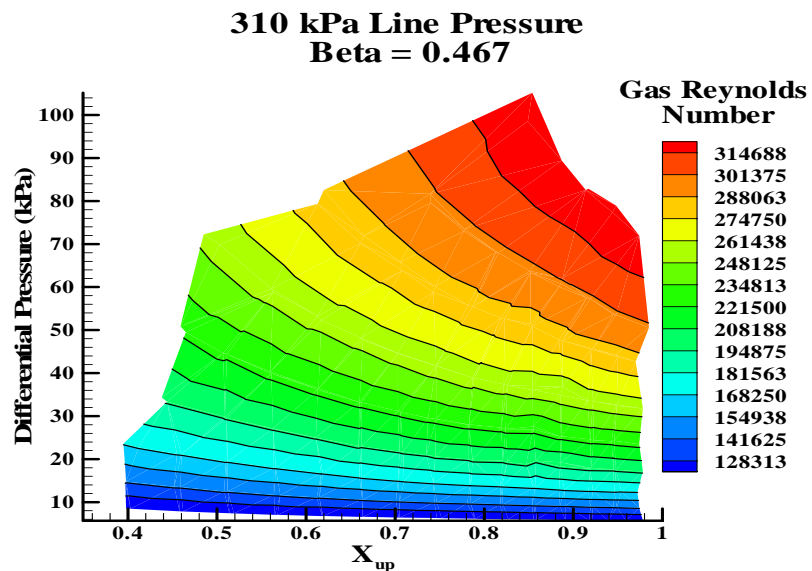
Figure 34   Differential Pressure as a Function of Upstream
Quality and Gas Reynolds Number,
310 kPa Upstream Line Pressure, β = 0.467

360 kPa Line Pressure
Beta = 0.43
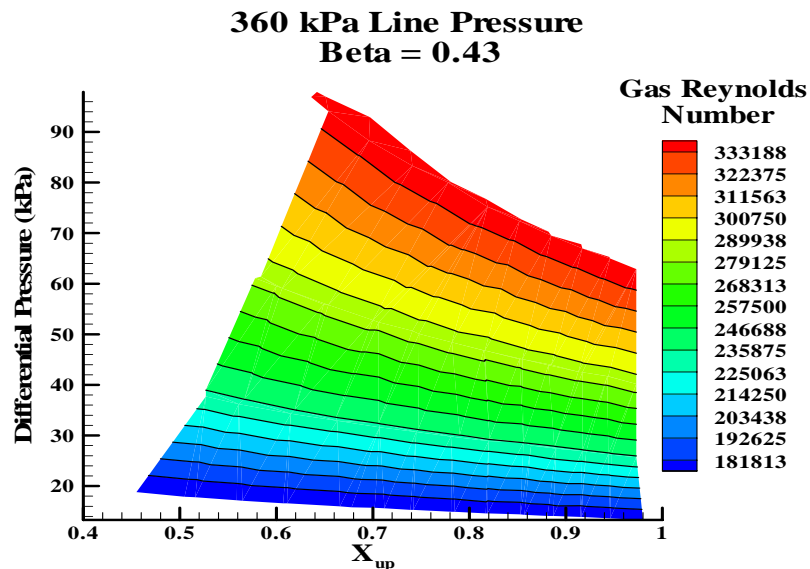
Figure 35   Differential Pressure as a Function of Upstream
Quality and Gas Reynolds Number,
360 kPa Upstream Line Pressure, $\beta = 0.43$
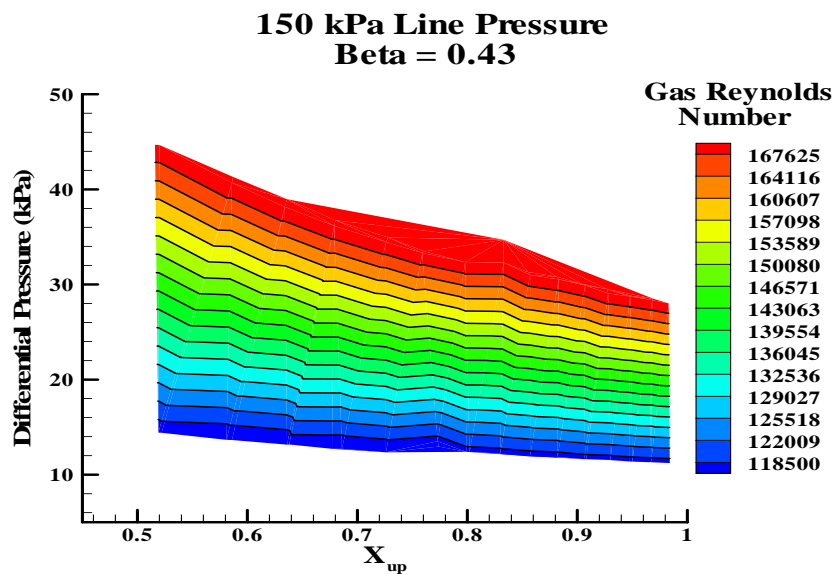
360 kPa Line Pressure
Beta = 0.467
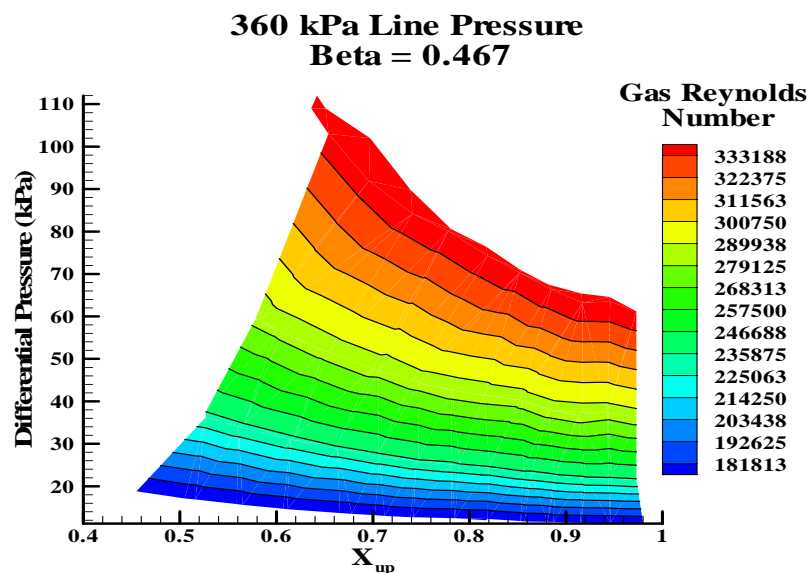
Figure 36   Differential Pressure as a Function of Upstream
Quality and Gas Reynolds Number,
360 kPa Upstream Line Pressure, $\beta = 0.467$

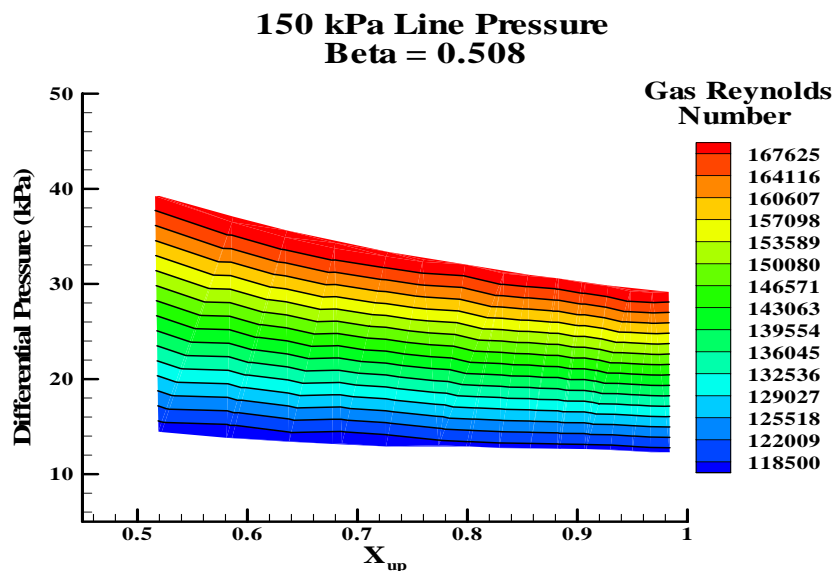**415 kPa Line Pressure**
Beta = 0.43
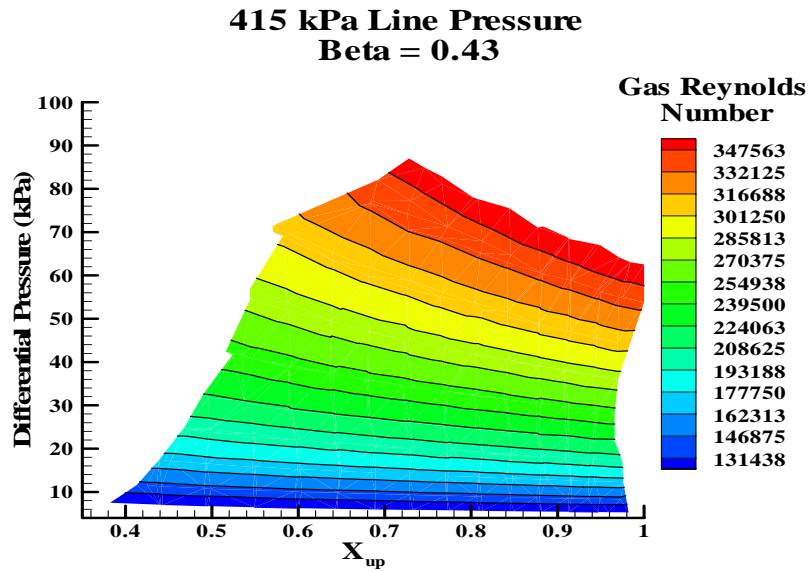
Figure 37   Differential Pressure as a Function of Upstream
             Quality and Gas Reynolds Number,
             415 kPa Upstream Line Pressure, β = 0.43

415 kPa Line Pressure
Beta = 0.467
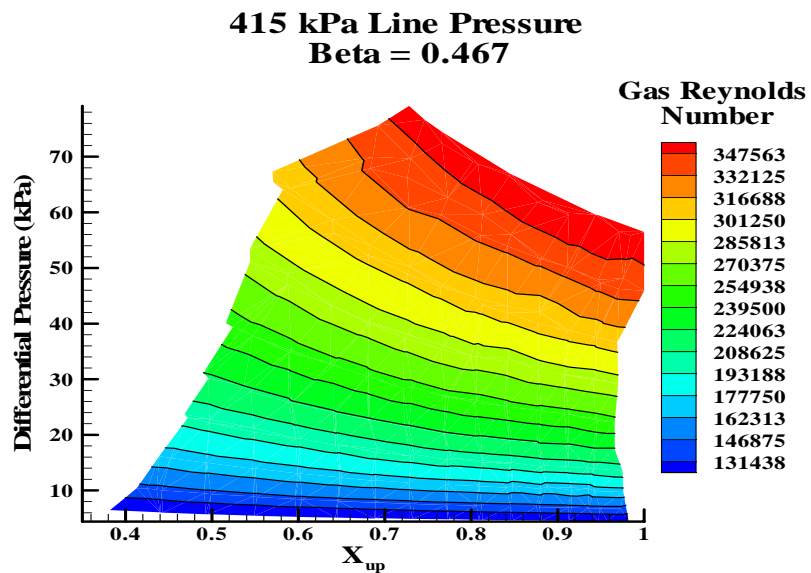
Figure 38   Differential Pressure as a Function of Upstream
             Quality and Gas Reynolds Number,
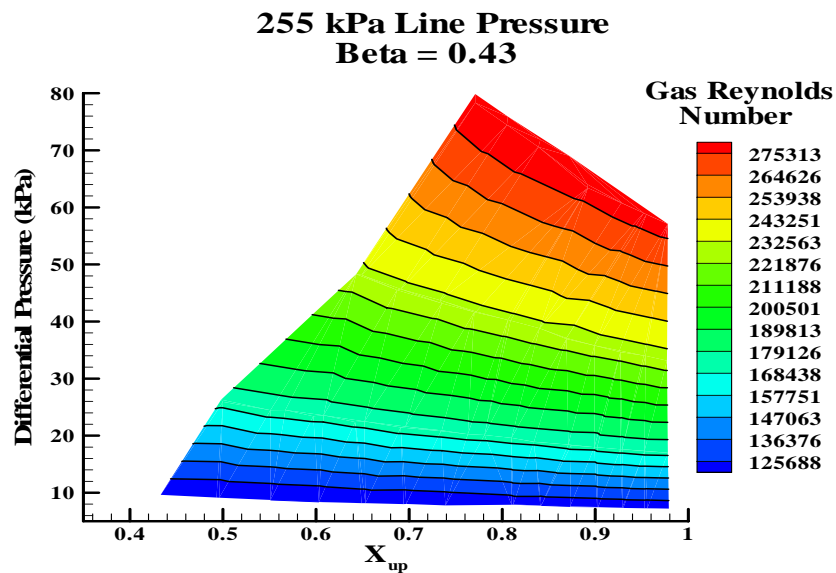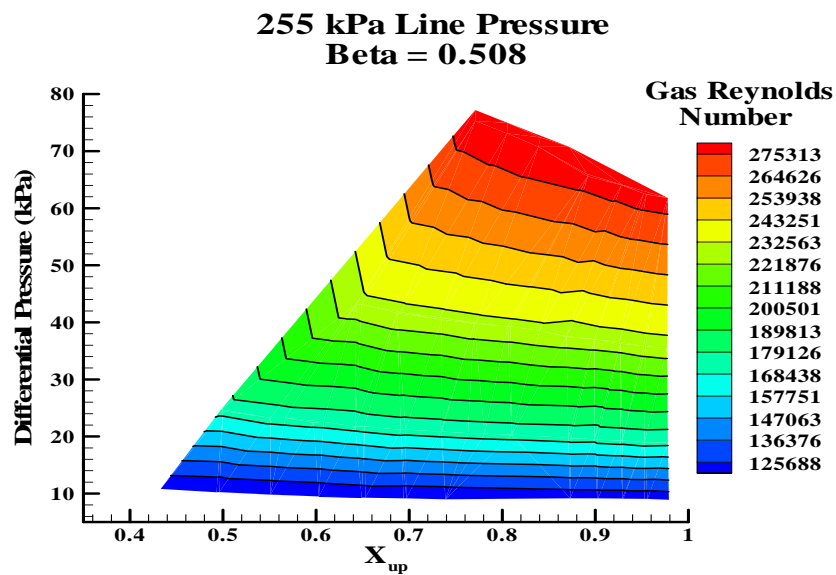   415 kPa Upstream Line Pressure, β = 0.467

dP 0.43 vs dP 0.467
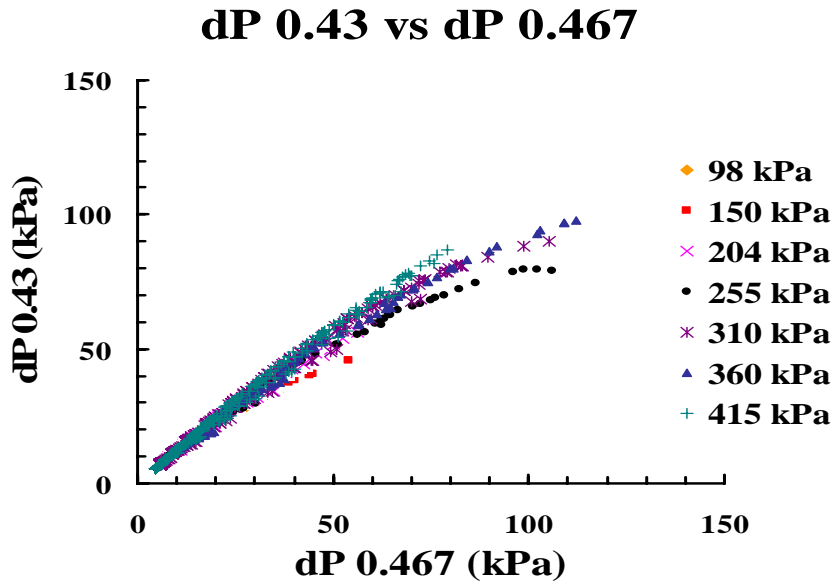
Figure 39　Differential Pressure across β = 0.43 plate as a function of the Differential Pressure across β = 0.467 plate
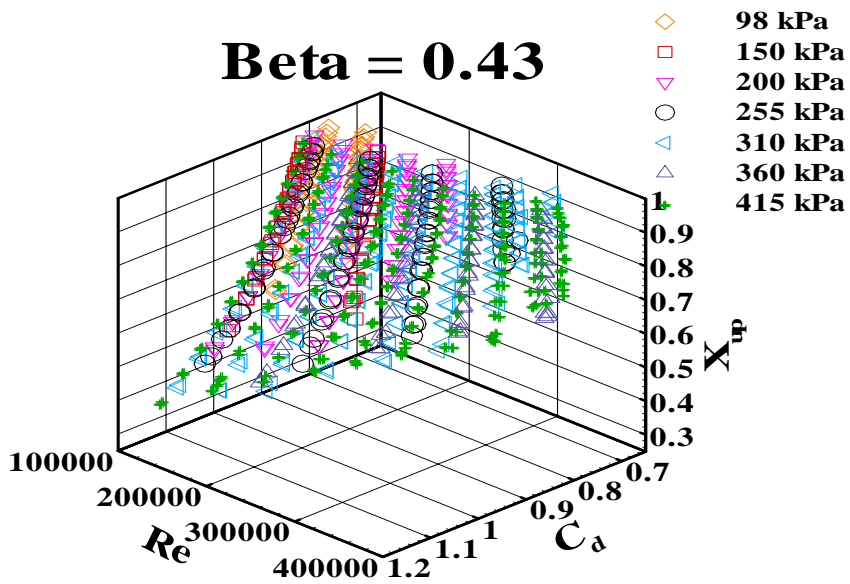
Figure 40　Coefficient of Discharge as a function of Gas Reynolds Number and Upstream Quality at different upstream line pressures, β = 0.43
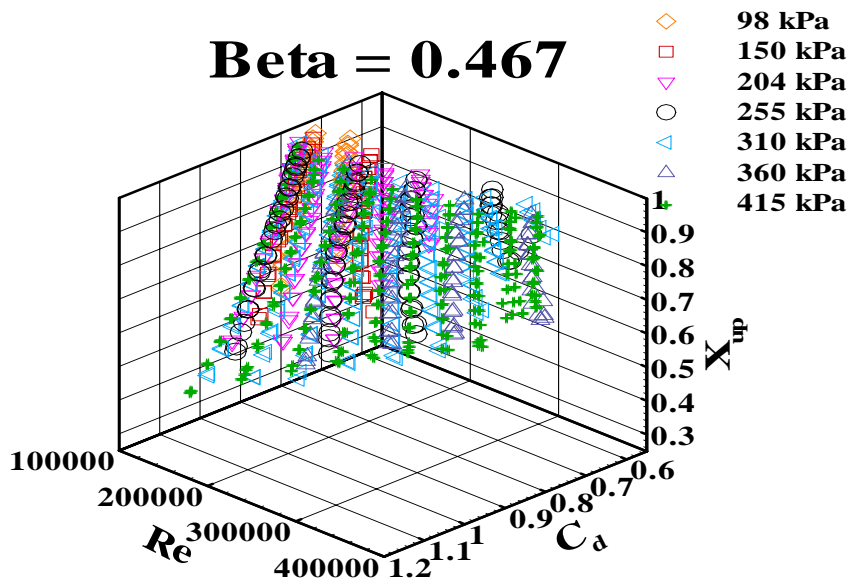
Figure 41   Coefficient of Discharge as a function of
Gas Reynolds Number and Upstream Quality
at different upstream line pressures, β = 0.467
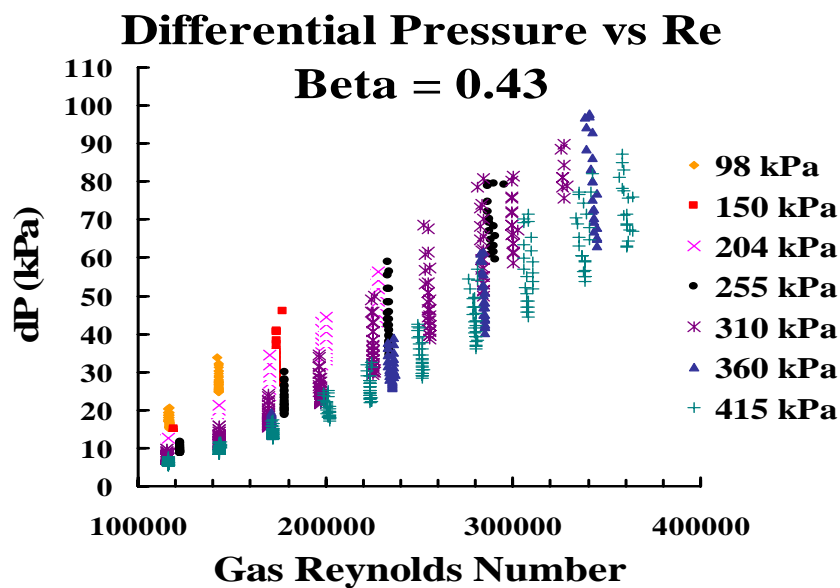
Figure 42   Differential Pressure as a function of
Gas Reynolds Number, β = 0.43
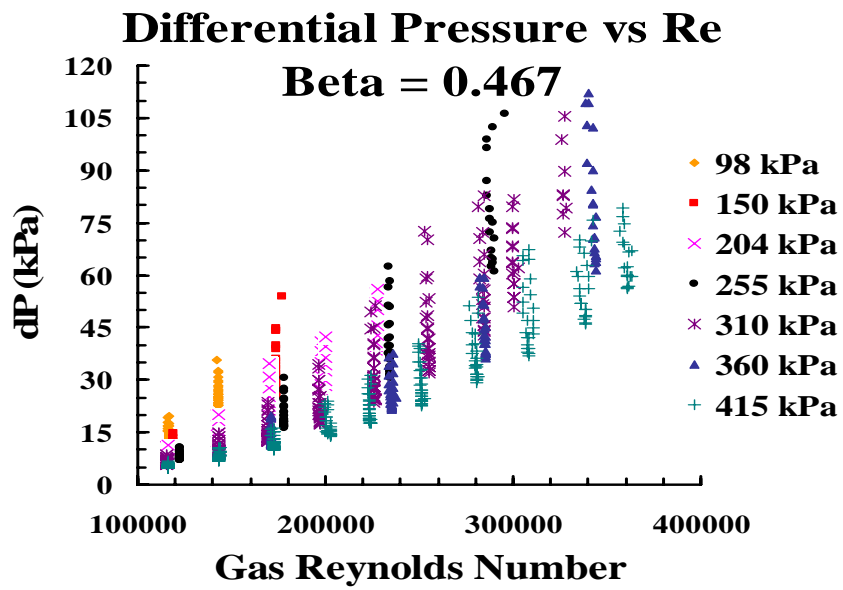
Figure 43   Differential Pressure as a function of
Gas Reynolds Number, $\beta = 0.467$

Case 2 Quality Effects
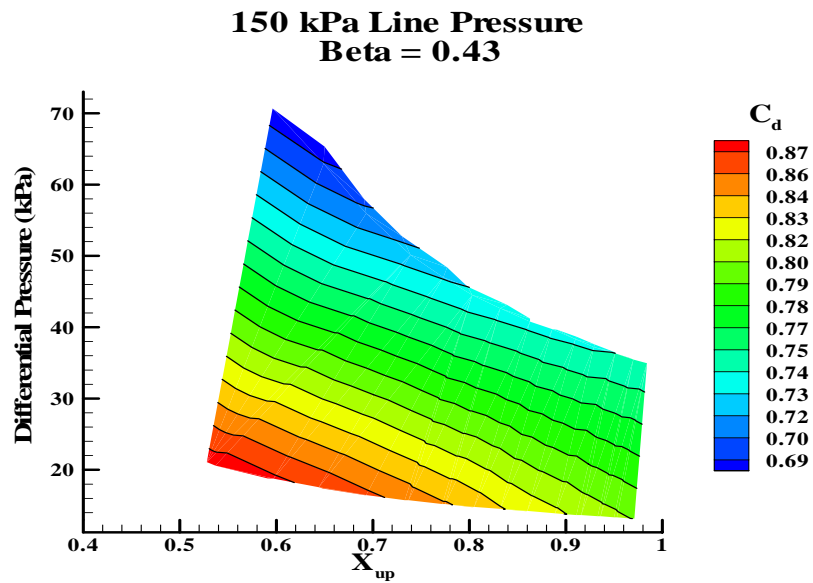
Figure 44   Differential Pressure as a Function of Upstream
Quality and Coefficient of Discharge,
150 kPa Upstream Line Pressure, $\beta = 0.43$
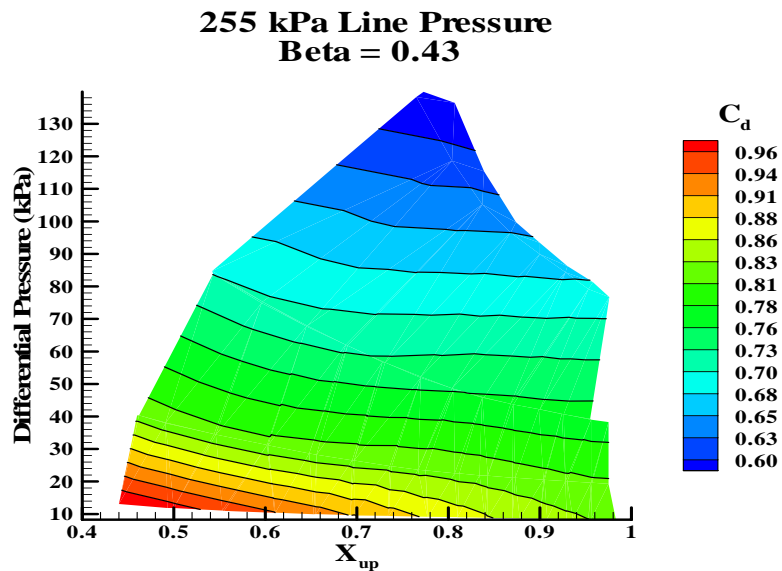
Figure 45   Differential Pressure as a Function of Upstream
Quality and Coefficient of Discharge,
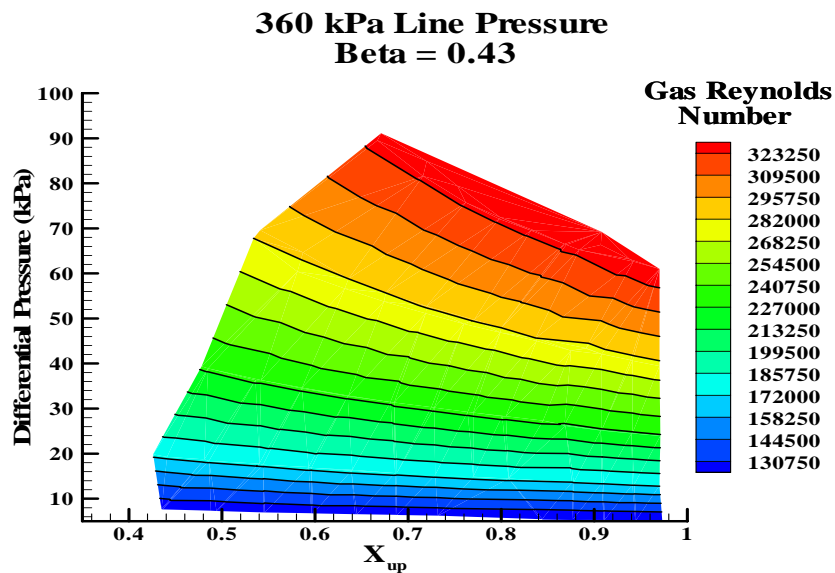255 kPa Upstream Line Pressure, $\beta = 0.43$
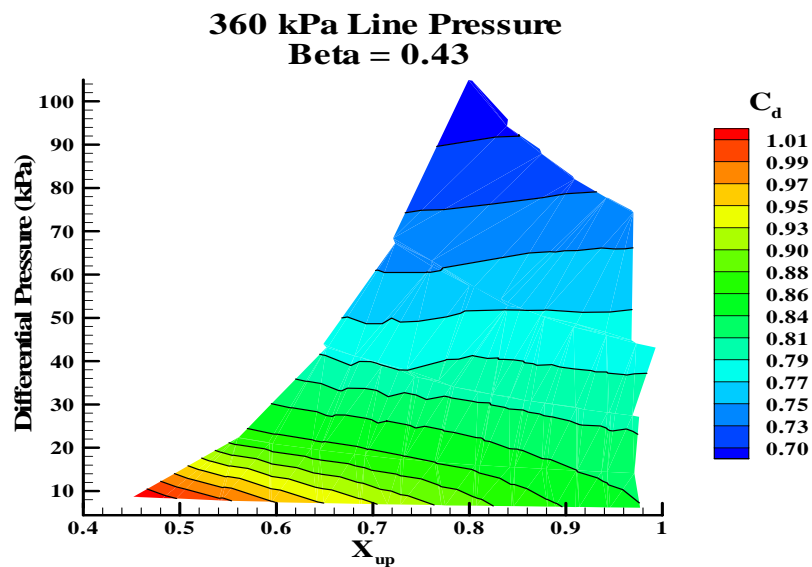
Figure 46   Differential Pressure as a Function of Upstream
Quality and Coefficient of Discharge,
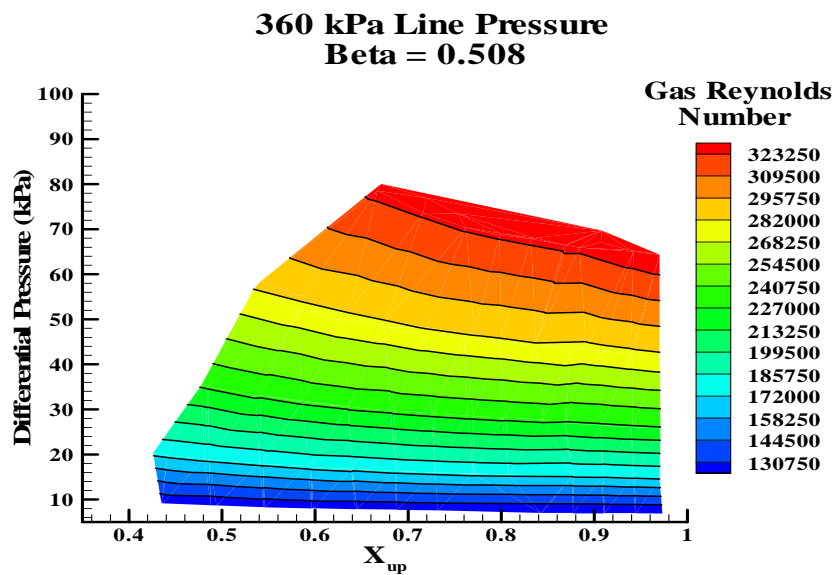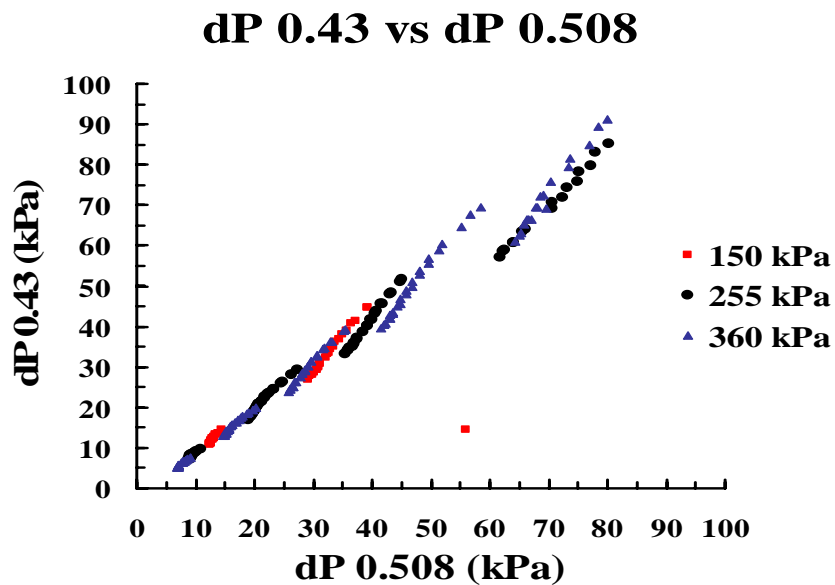360 kPa Upstream Line Pressure, $\beta = 0.43$
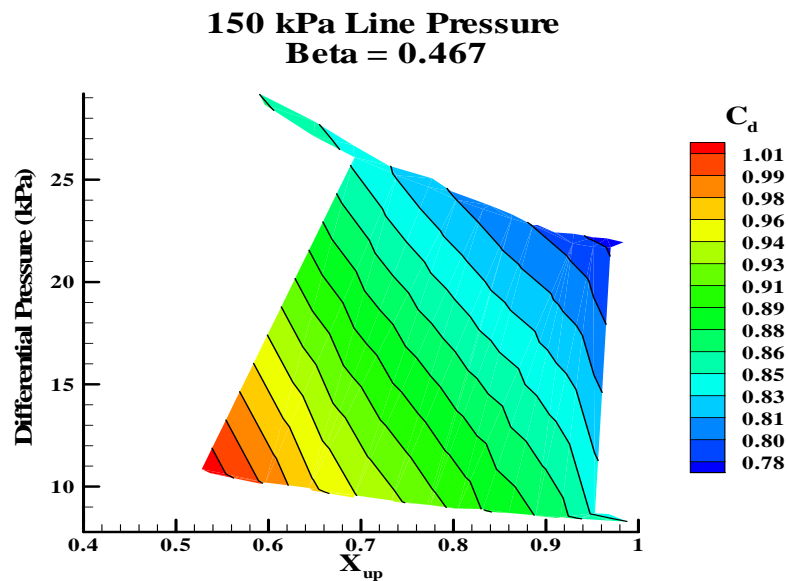
Figure 47   Differential Pressure as a Function of Upstream
Quality and Coefficient of Discharge,
150 kPa Upstream Line Pressure, $\beta = 0.467$

255 kPa Line Pressure
Beta = 0.467
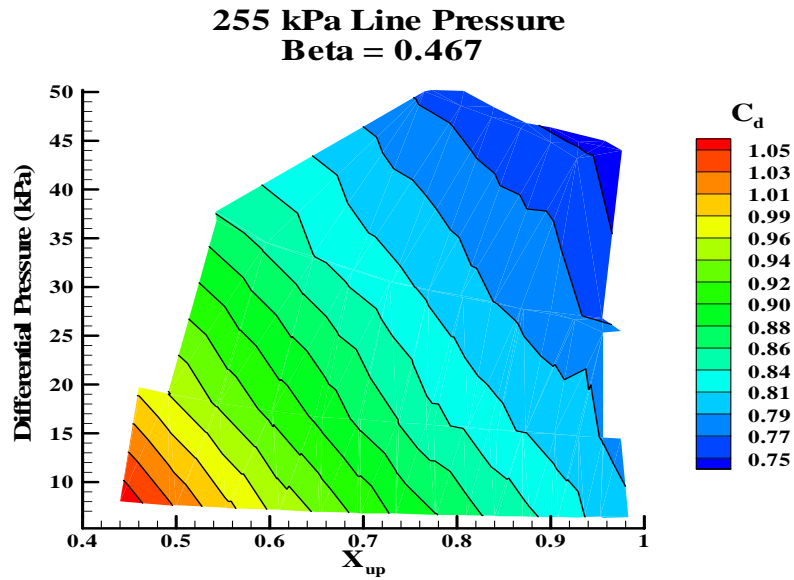
Figure 48   Differential Pressure as a Function of Upstream
             Quality and Coefficient of Discharge,
             255 kPa Upstream Line Pressure, β = 0.467

360 kPa Line Pressure
Beta = 0.467
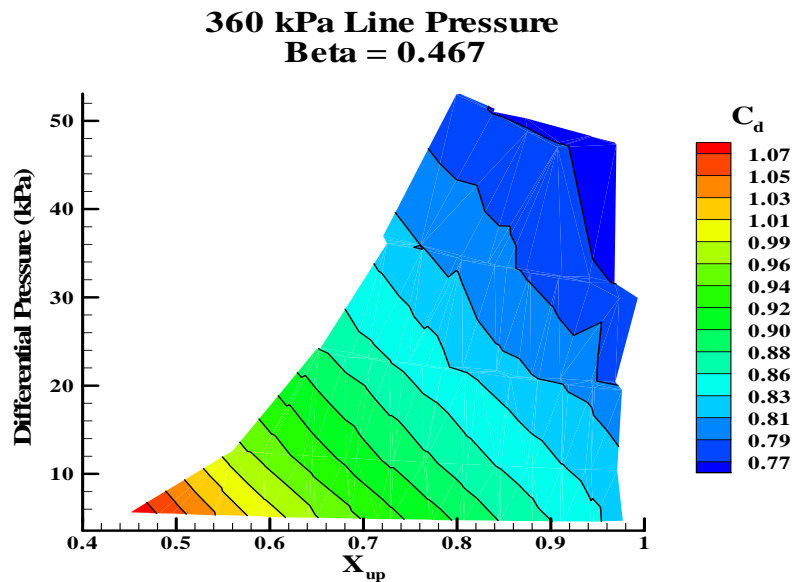
Figure 49   Differential Pressure as a Function of Upstream
             Quality and Coefficient of Discharge,
             360 kPa Upstream Line Pressure, β = 0.467

Case 2 Repeatability
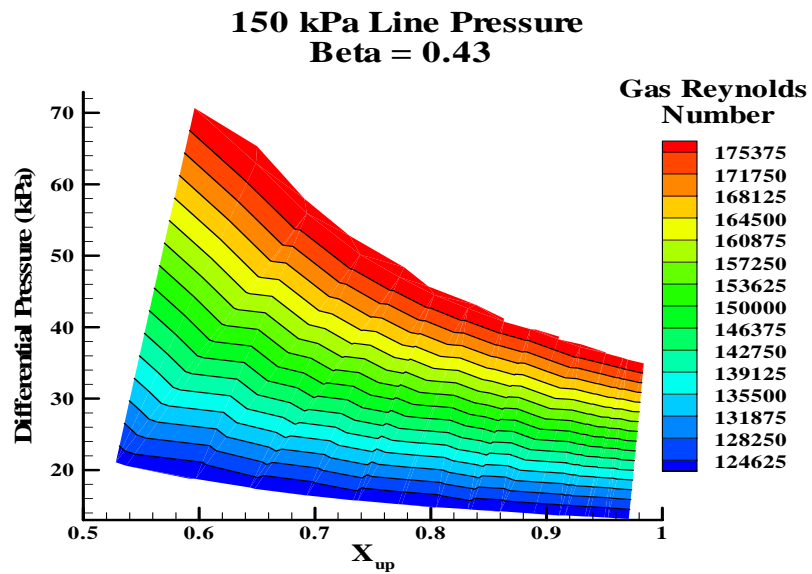
Figure 50 Differential Pressure as a Function of Upstream
Quality and Gas Reynolds Number,
150 kPa Upstream Line Pressure, $\beta = 0.43$
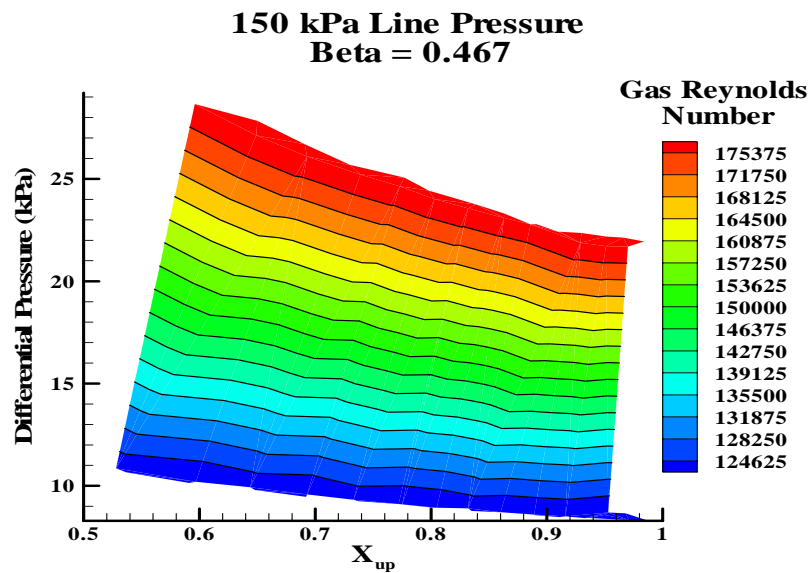
Figure 51 Differential Pressure as a Function of Upstream
Quality and Gas Reynolds Number,
150 kPa Upstream Line Pressure, $\beta = 0.467$

255 kPa Line Pressure
Beta = 0.43
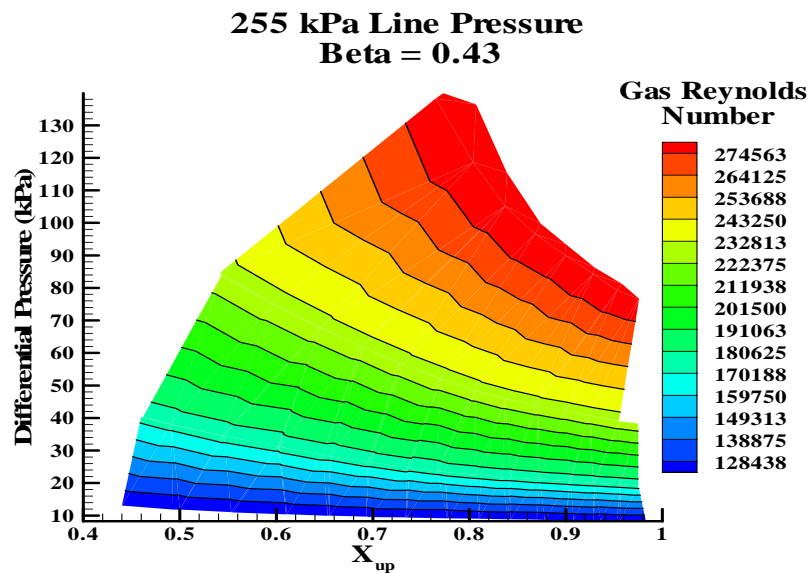
Figure 52　Differential Pressure as a Function of Upstream Quality and Gas Reynolds Number, 255 kPa Upstream Line Pressure, $\beta = 0.43$

255 kPa Line Pressure
Beta = 0.467
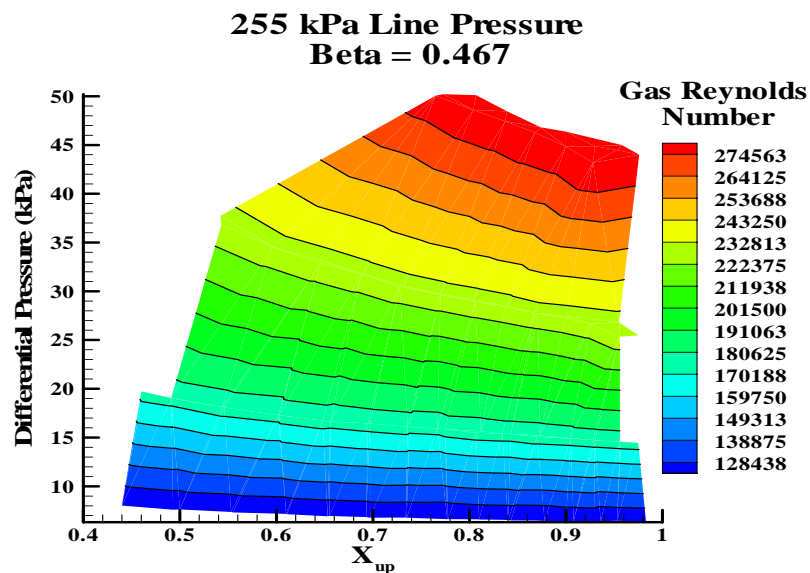
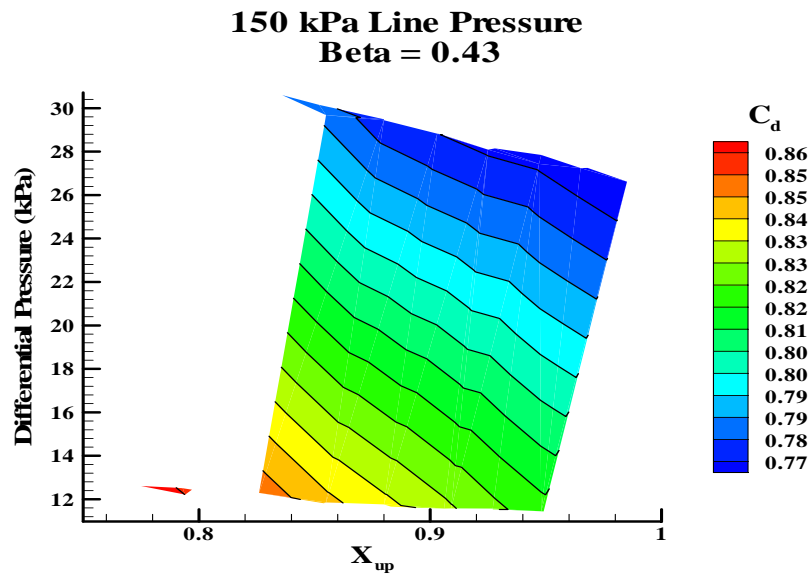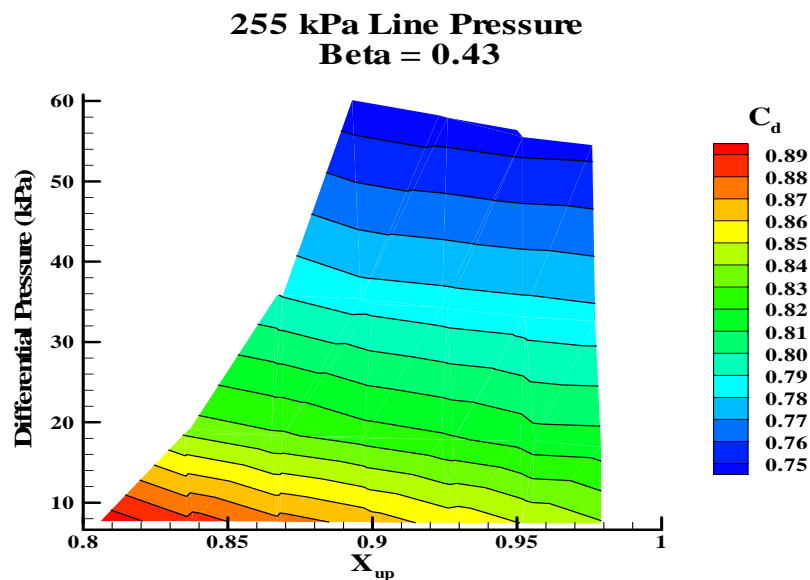Figure 53　Differential Pressure as a Function of Upstream Quality and Gas Reynolds Number, 255 kPa Upstream Line Pressure, $\beta = 0.467$
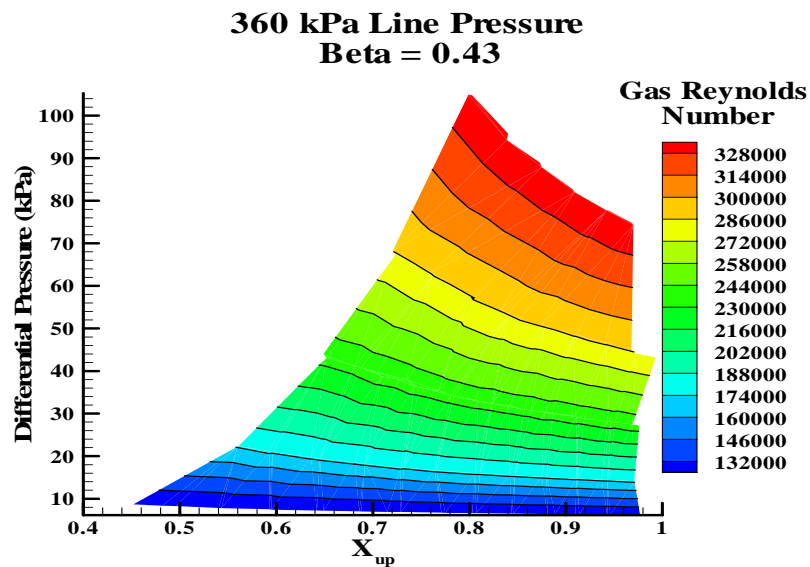
Figure 54   Differential Pressure as a Function of Upstream
Quality and Gas Reynolds Number,
360 kPa Upstream Line Pressure, β = 0.43
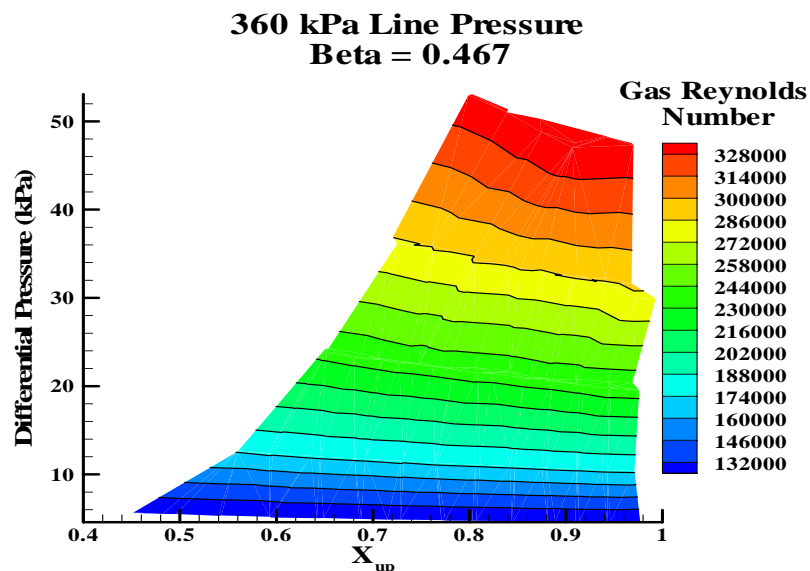
Figure 55   Differential Pressure as a Function of Upstream
Quality and Gas Reynolds Number,
360 kPa Upstream Line Pressure, β = 0.467

dP 0.43 vs dP 0.467
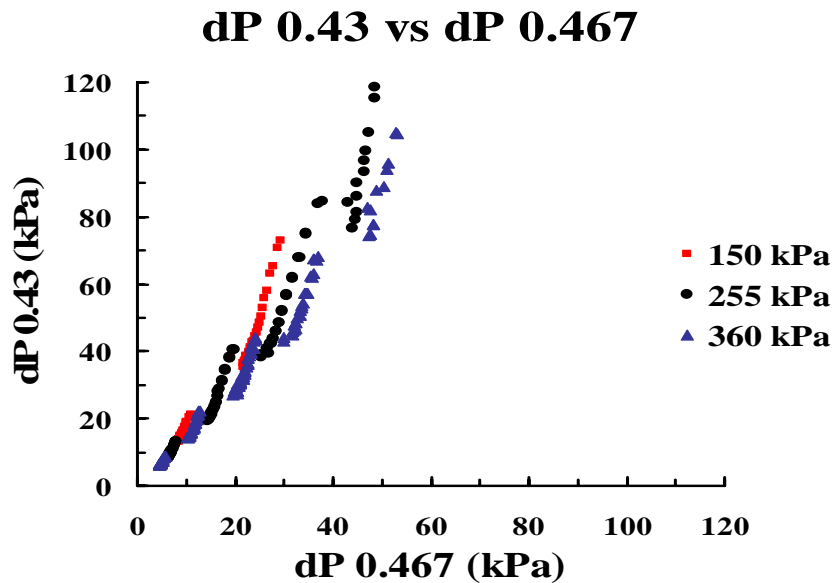
Figure 56   Differential Pressure across β = 0.43 plate as a function
of the Differential Pressure across β = 0.467 plate

Beta = 0.43
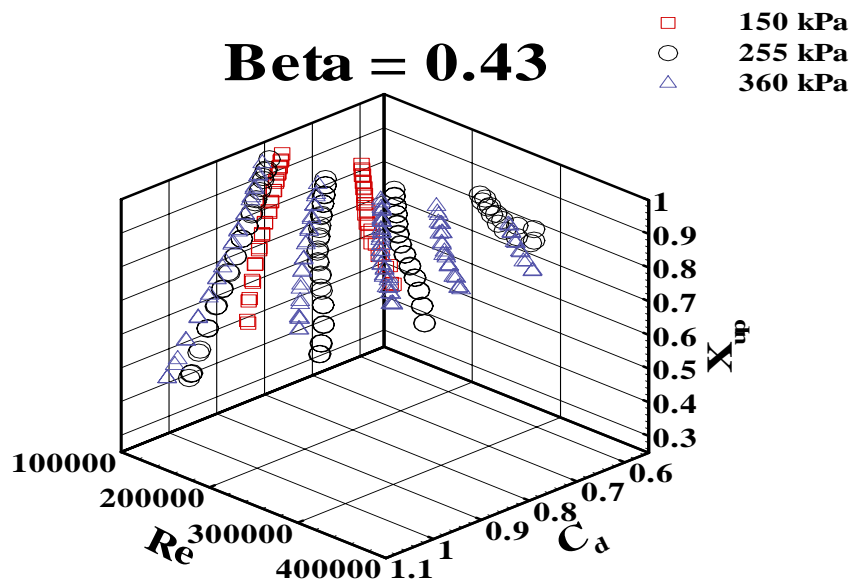
Figure 57   Coefficient of Discharge as a function of
Gas Reynolds Number and Upstream Quality
at different upstream line pressures, β = 0.43

Beta = 0.467
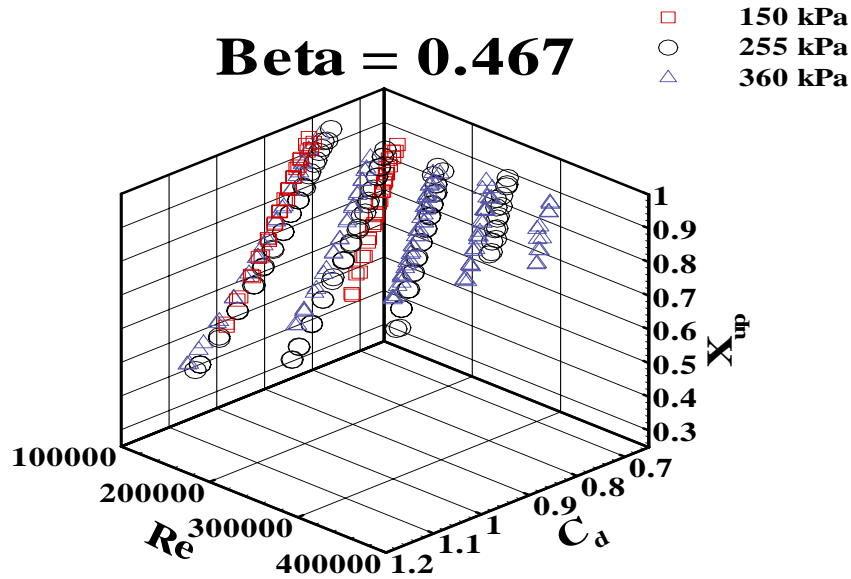
Figure 58   Coefficient of Discharge as a function of
Gas Reynolds Number and Upstream Quality
at different upstream line pressures, β = 0.467

Differential Pressure vs Re
Beta = 0.43
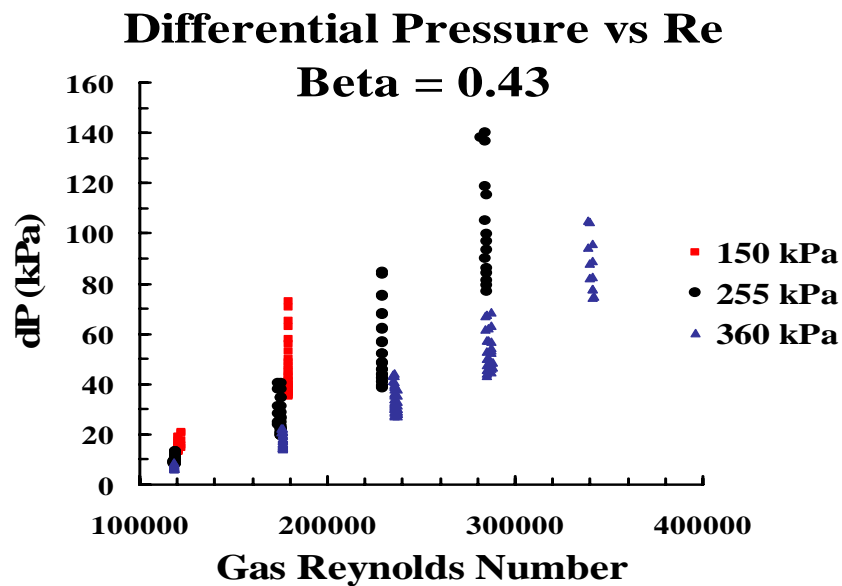
Figure 59   Differential Pressure as a function of
Gas Reynolds Number, β = 0.43
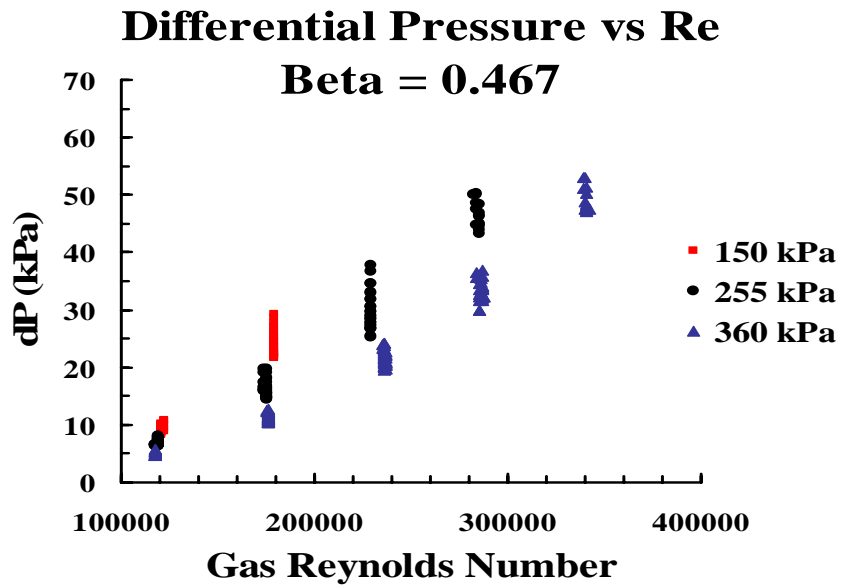
Figure 60   Differential Pressure as a function of
Gas Reynolds Number, β = 0.467
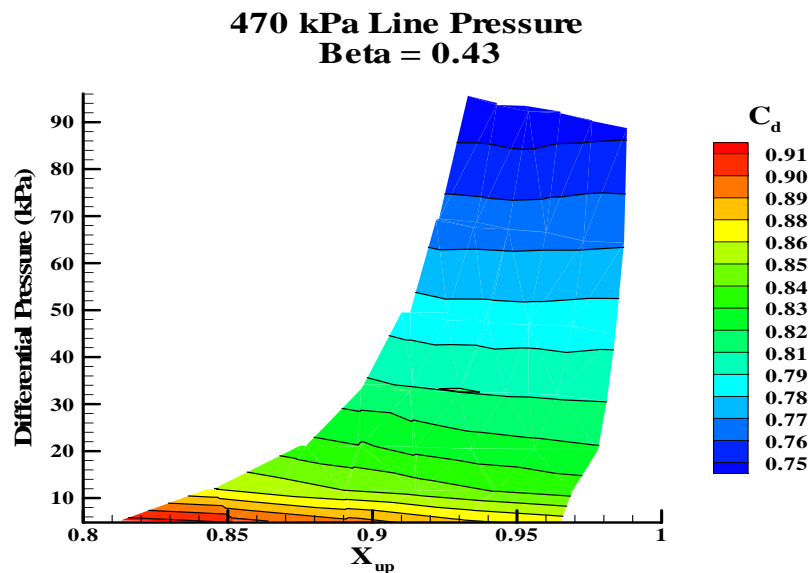
Case 3 Quality Effects at High Air Quality
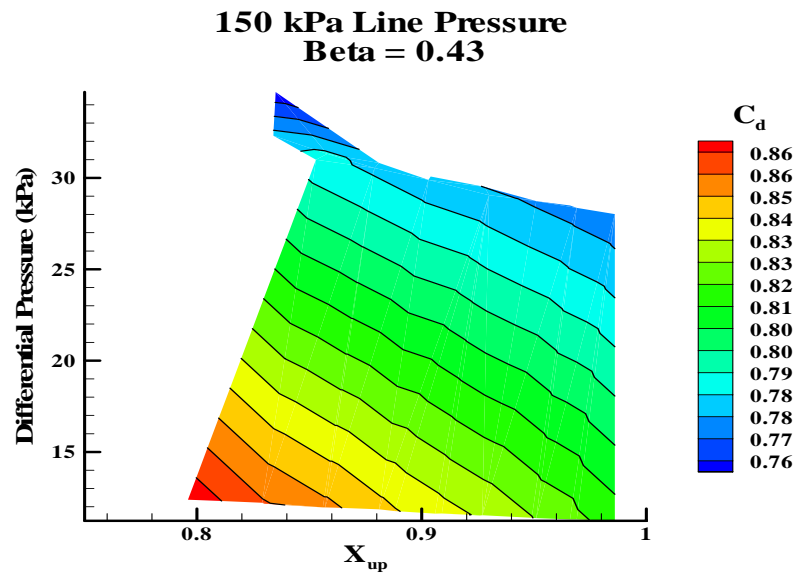
Figure 61   Differential Pressure as a Function of Upstream
Quality and Coefficient of Discharge,
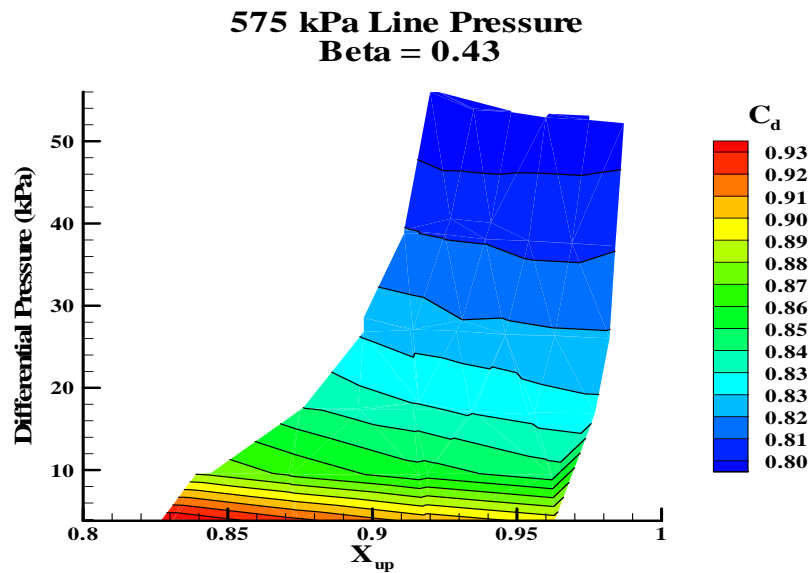150 kPa Upstream Line Pressure, $\beta = 0.43$
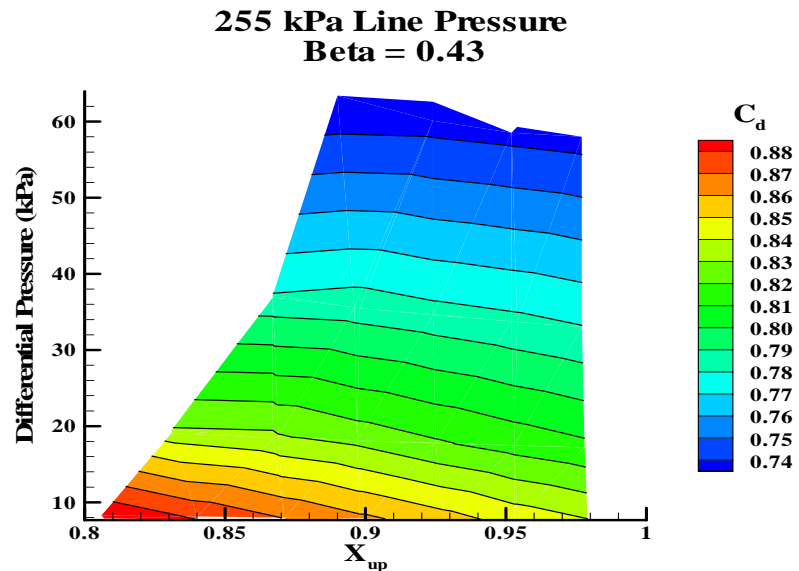
Figure 62   Differential Pressure as a Function of Upstream
Quality and Coefficient of Discharge,
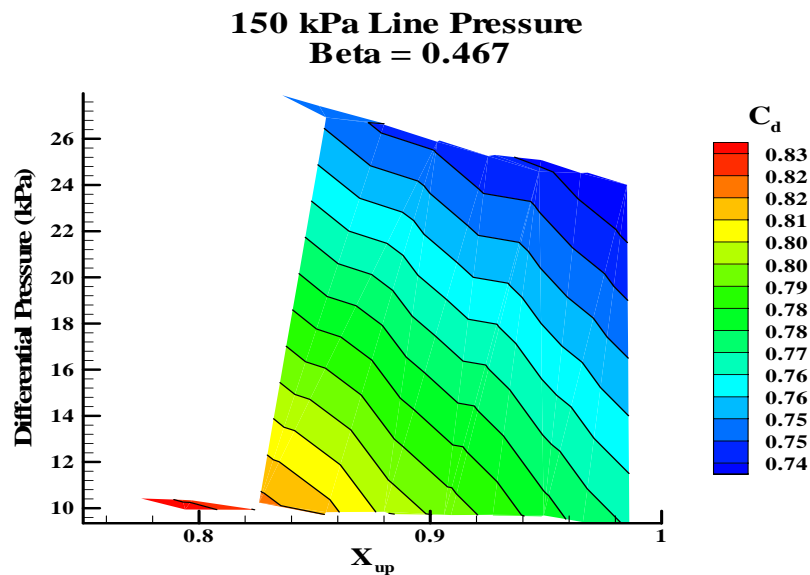255 kPa Upstream Line Pressure, $\beta = 0.43$
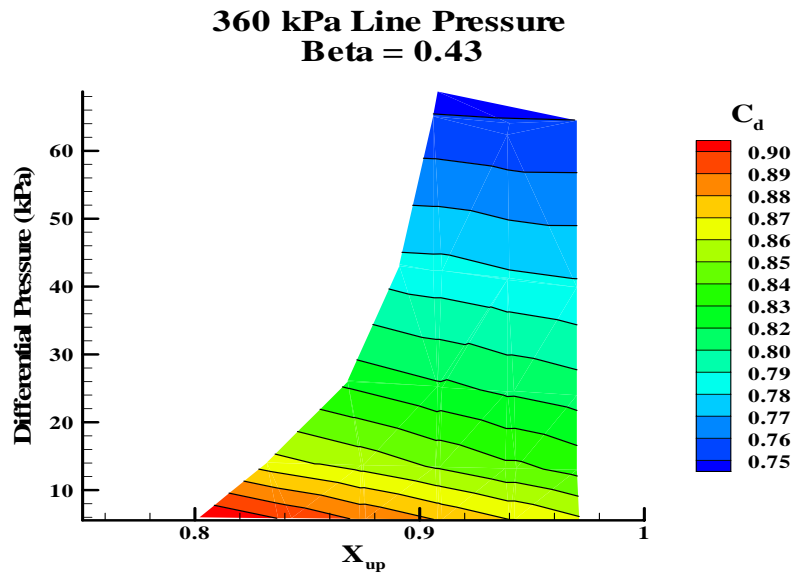
Figure 63   Differential Pressure as a Function of Upstream
Quality and Coefficient of Discharge,
360 kPa Upstream Line Pressure, $\beta = 0.43$
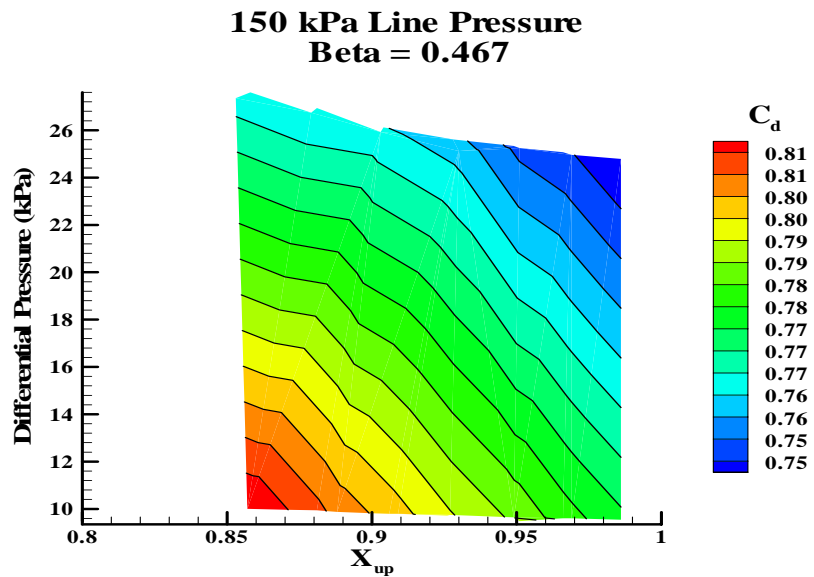
Figure 64   Differential Pressure as a Function of Upstream
Quality and Coefficient of Discharge,
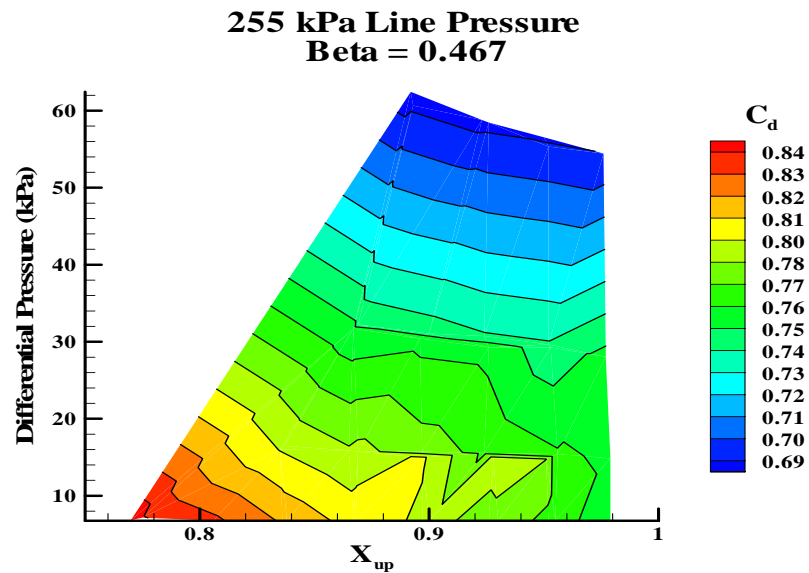150 kPa Upstream Line Pressure, $\beta = 0.467$
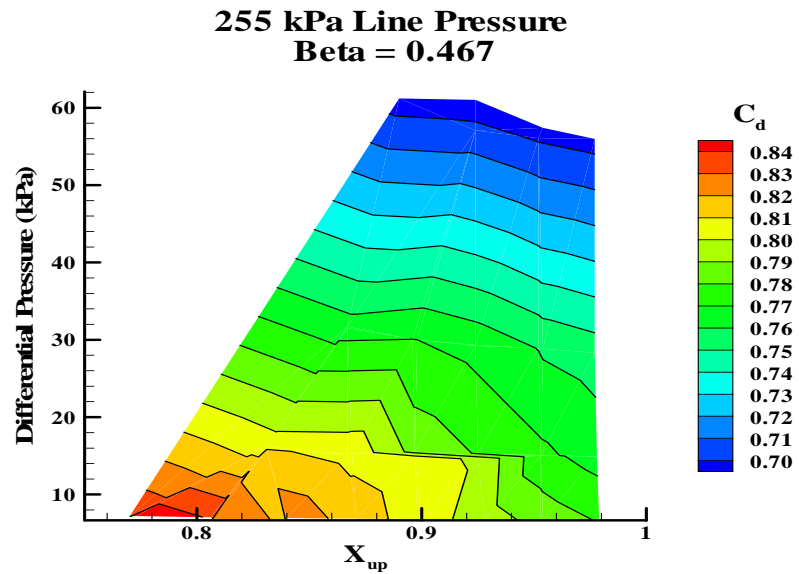
Figure 65   Differential Pressure as a Function of Upstream Quality and Coefficient of Discharge, 255 kPa Upstream Line Pressure, $\beta = 0.467$
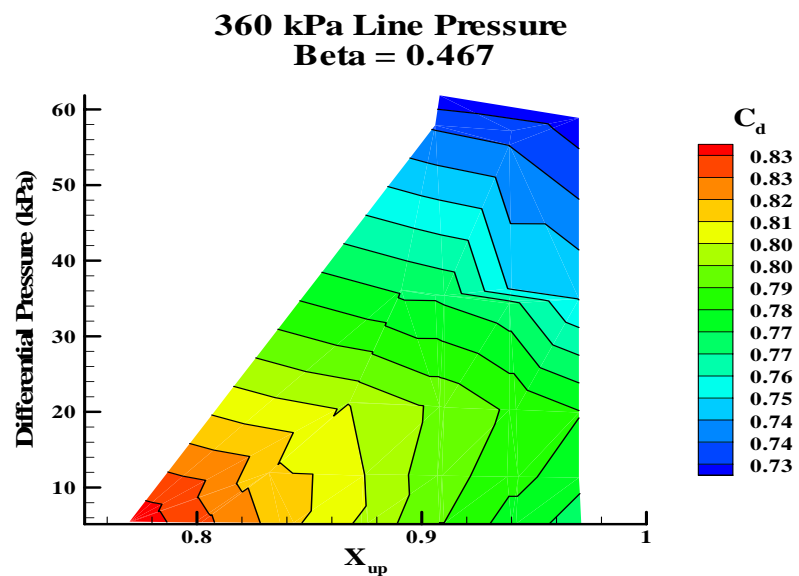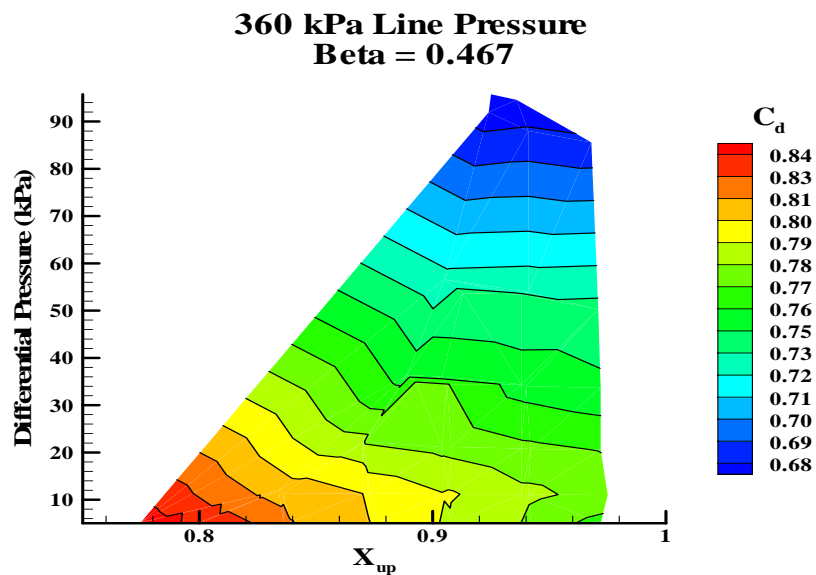

Figure 66   Differential Pressure as a Function of Upstream Quality and Coefficient of Discharge, 360 kPa Upstream Line Pressure, $\beta = 0.467$
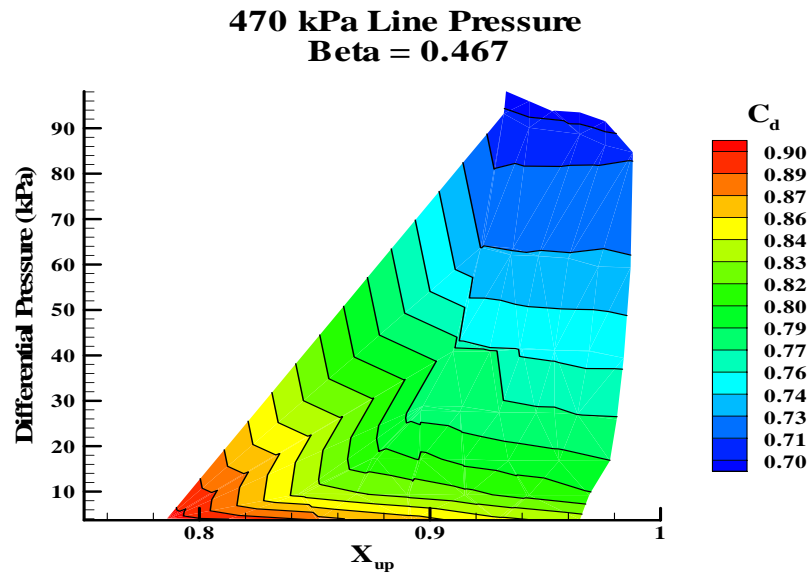
150 kPa Line Pressure
Beta = 0.508
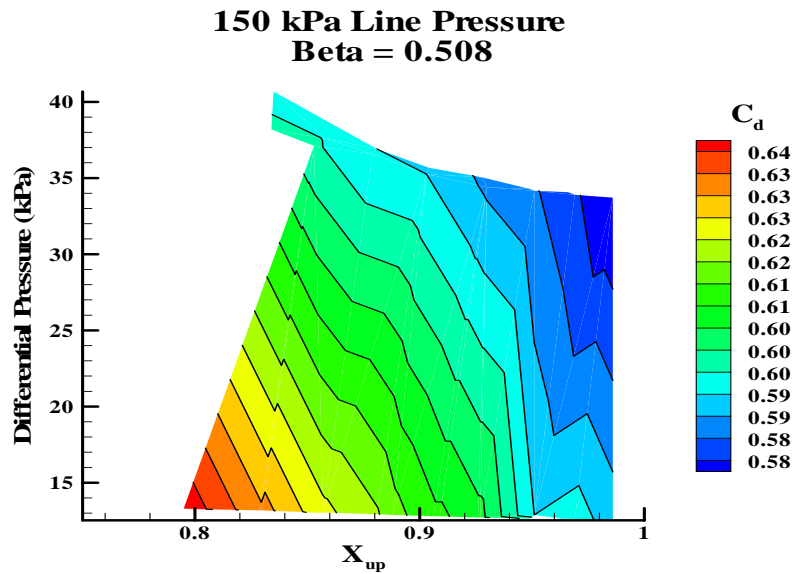
Figure 67   Differential Pressure as a Function of Upstream
Quality and Coefficient of Discharge,
150 kPa Upstream Line Pressure, β = 0.508

255 kPa Line Pressure
Beta = 0.508
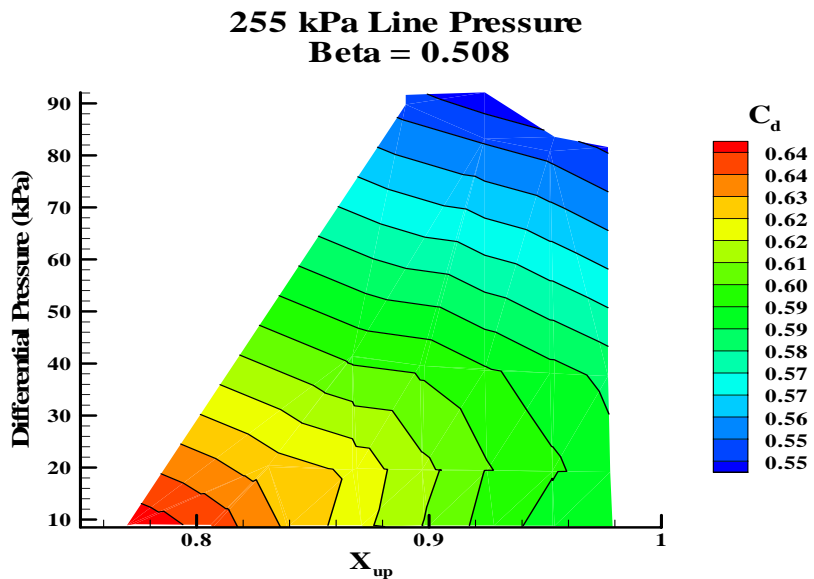
Figure 68   Differential Pressure as a Function of Upstream
Quality and Coefficient of Discharge,
255 kPa Upstream Line Pressure, β = 0.508
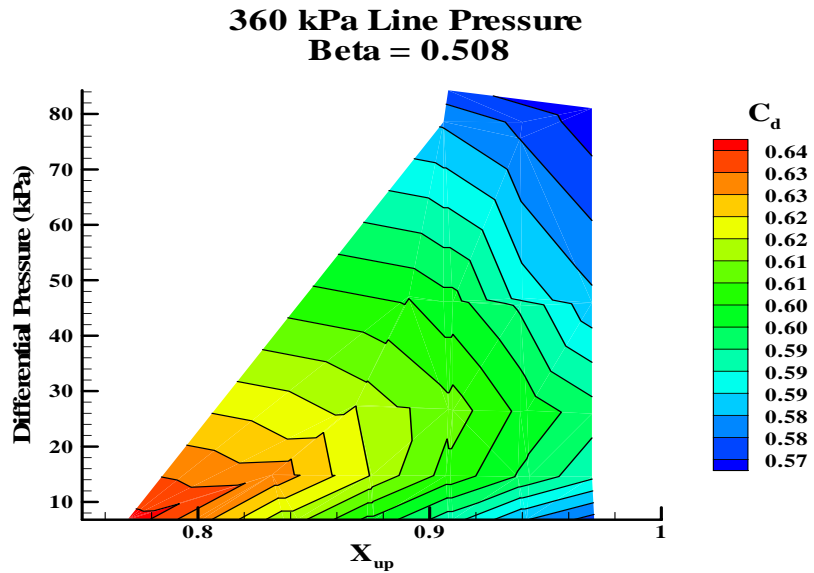
Figure 69   Differential Pressure as a Function of Upstream
             Quality and Coefficient of Discharge,
             360 kPa Upstream Line Pressure, $\beta = 0.508$

Case 3 Quality Effects at Low Air Quality
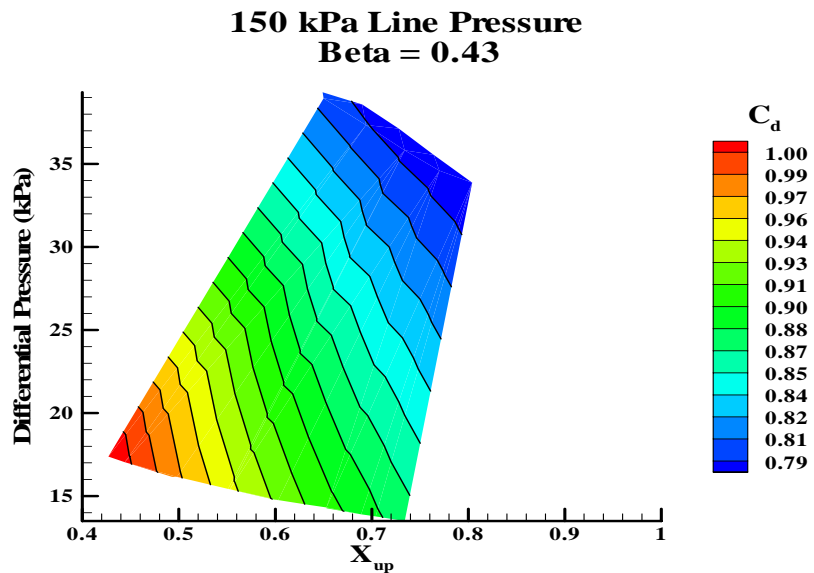
Figure 70   Differential Pressure as a Function of Upstream
             Quality and Coefficient of Discharge,
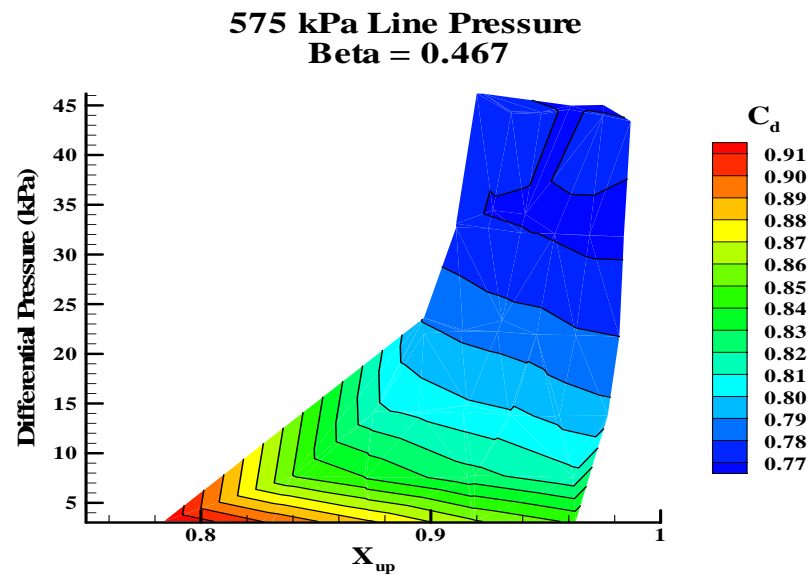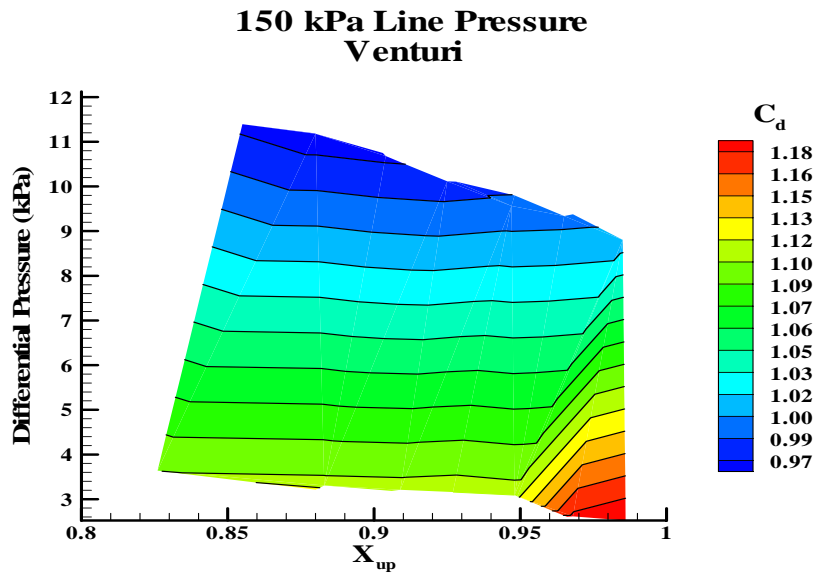   150 kPa Upstream Line Pressure, $\beta = 0.43$
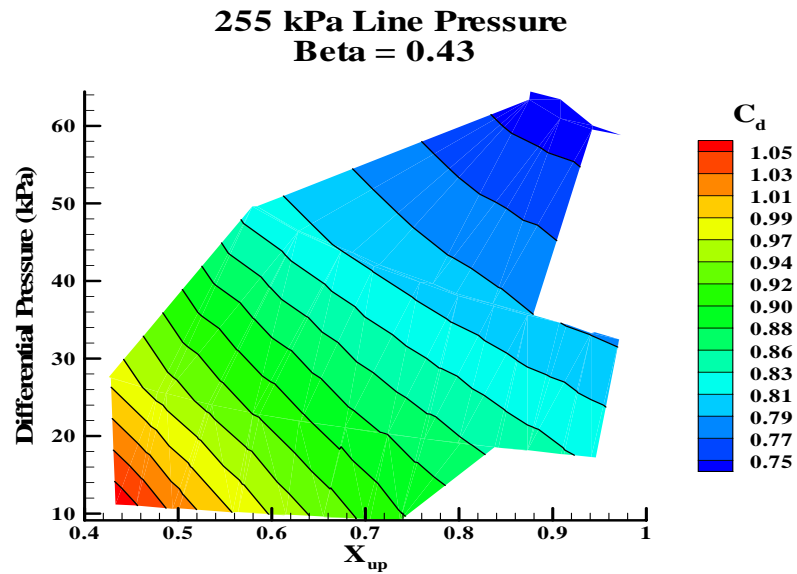
Figure 71   Differential Pressure as a Function of Upstream
             Quality and Coefficient of Discharge,
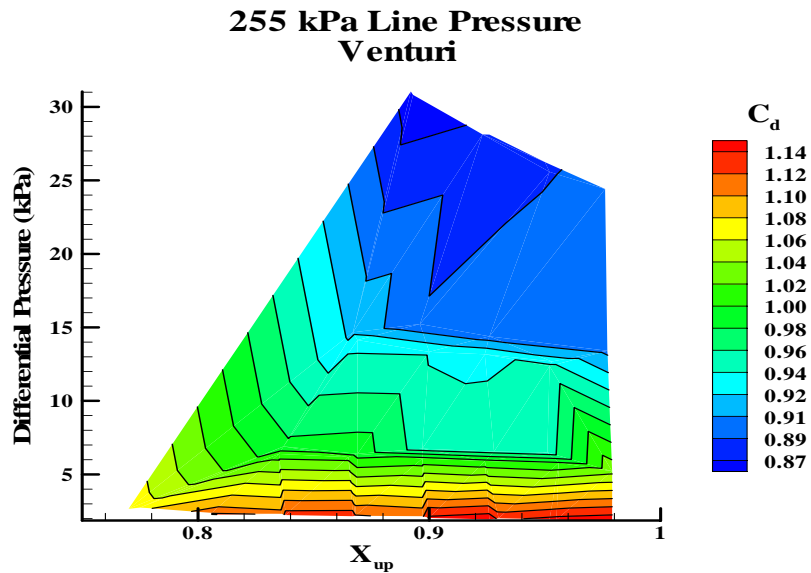   255 kPa Upstream Line Pressure, β = 0.43
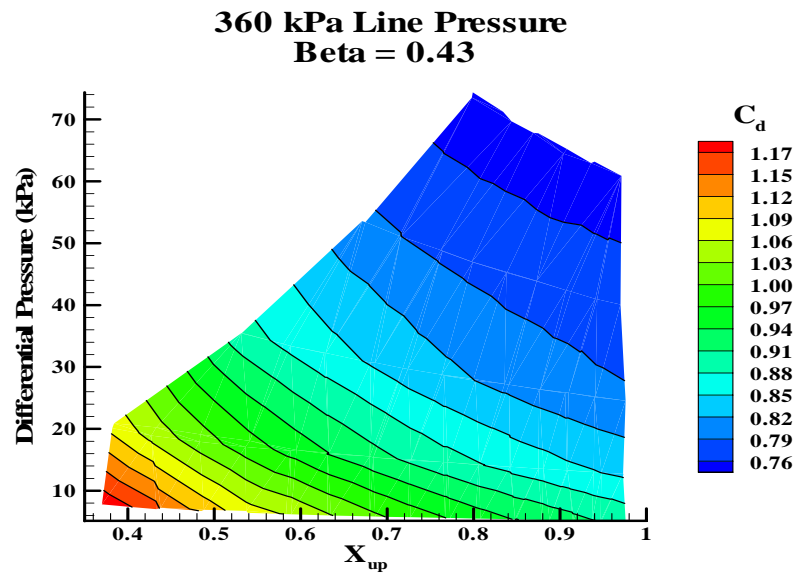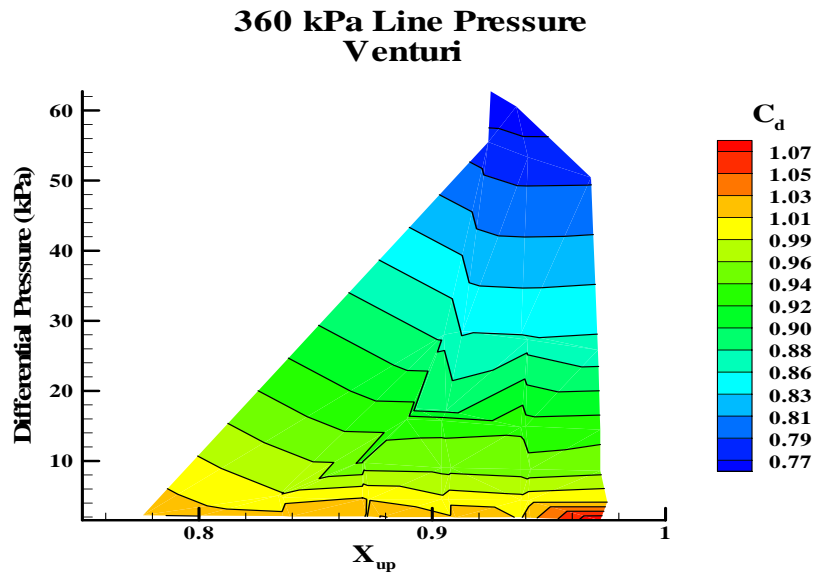

Figure 72   Differential Pressure as a Function of Upstream
             Quality and Coefficient of Discharge,
             360 kPa Upstream Line Pressure, β = 0.43
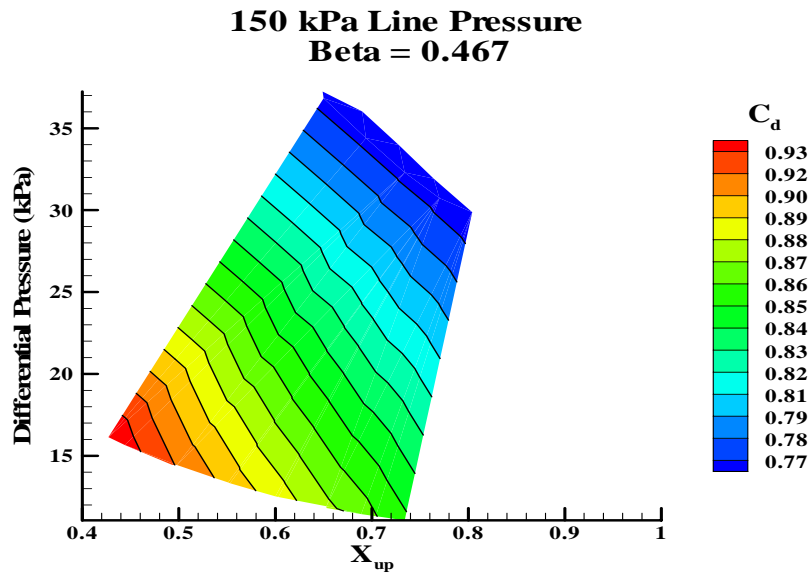
Figure 73   Differential Pressure as a Function of Upstream Quality and Coefficient of Discharge, 150 kPa Upstream Line Pressure, $\beta = 0.467$
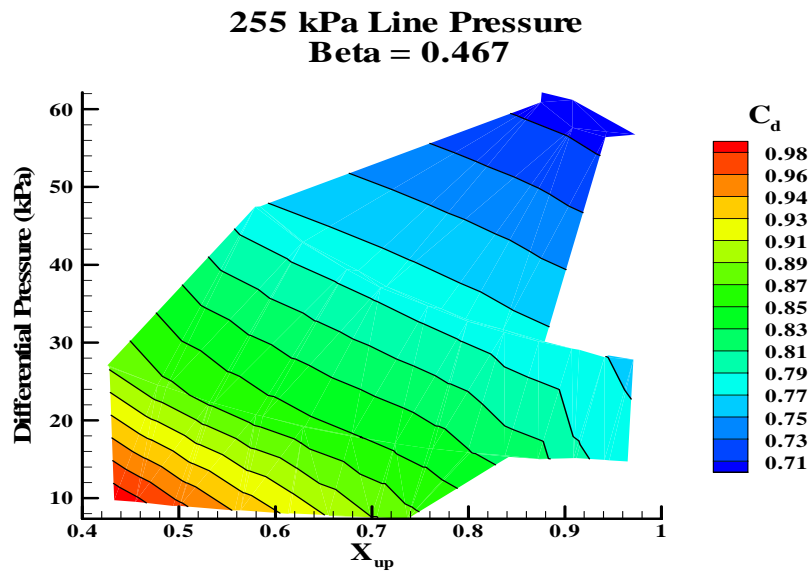
Figure 74   Differential Pressure as a Function of Upstream Quality and Coefficient of Discharge, 255 kPa Upstream Line Pressure, $\beta = 0.467$
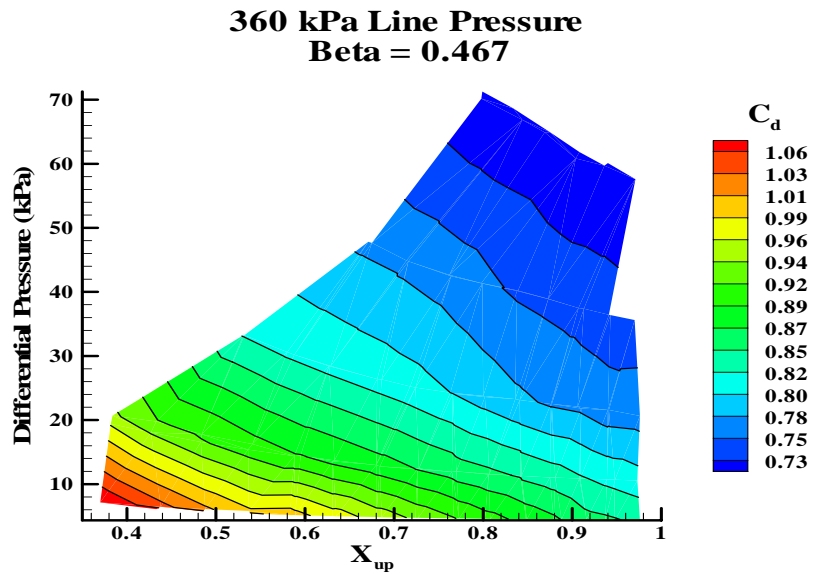
Figure 75   Differential Pressure as a Function of Upstream Quality and Coefficient of Discharge, 360 kPa Upstream Line Pressure, β = 0.467
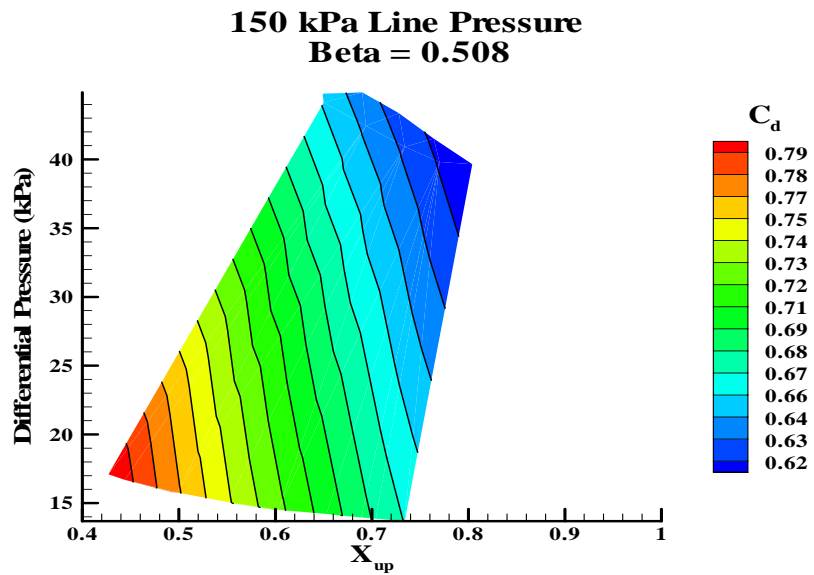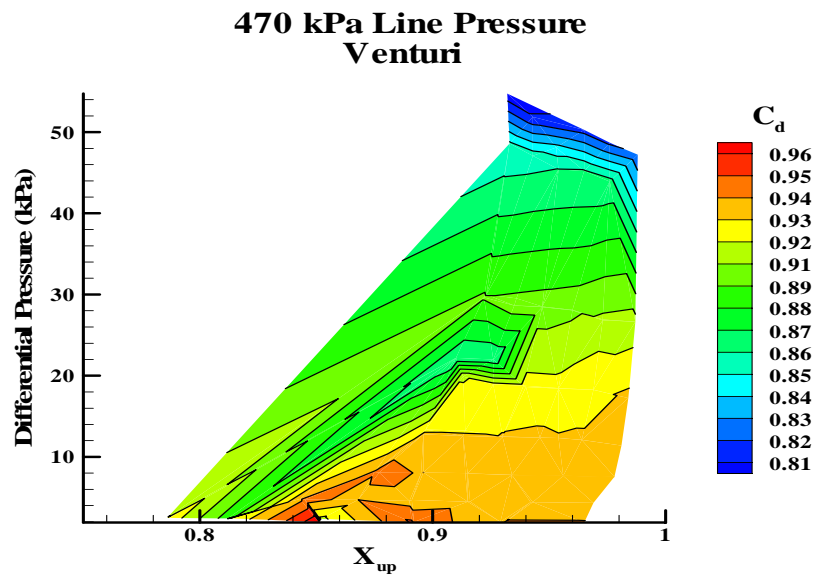

Figure 76   Differential Pressure as a Function of Upstream Quality and Coefficient of Discharge, 150 kPa Upstream Line Pressure, β = 0.508
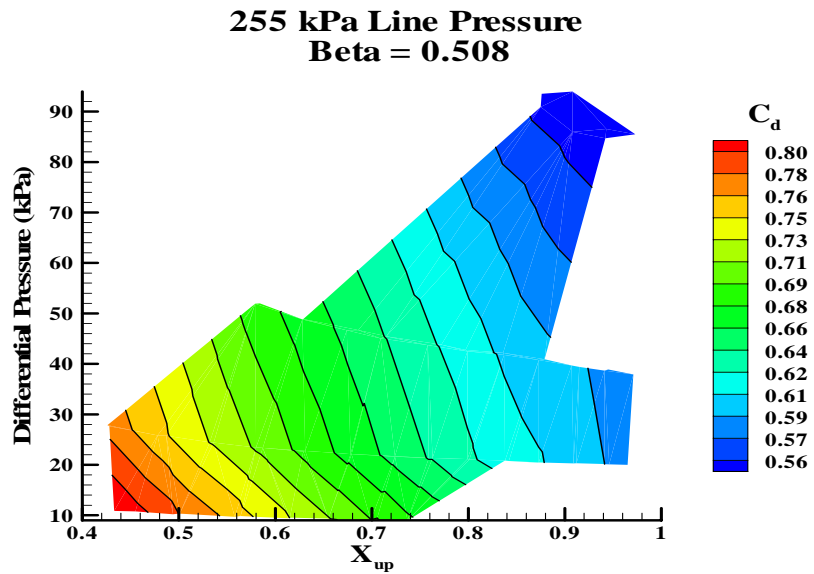
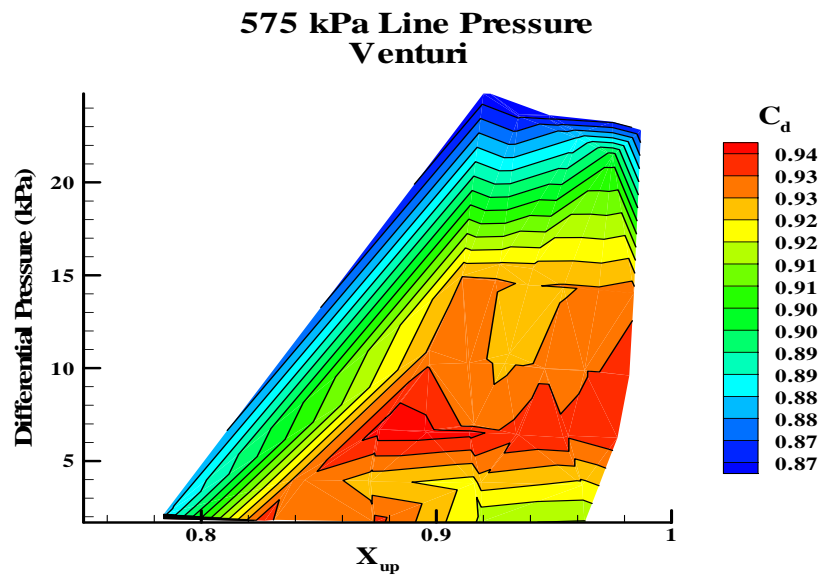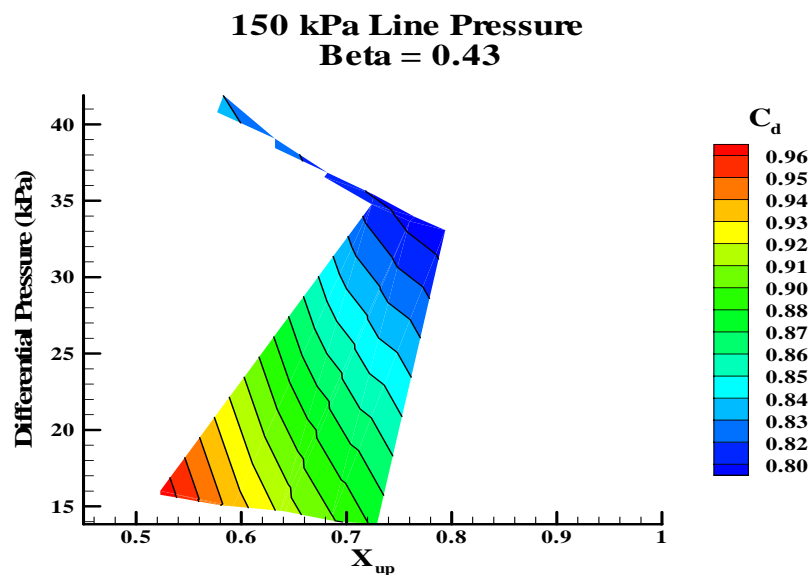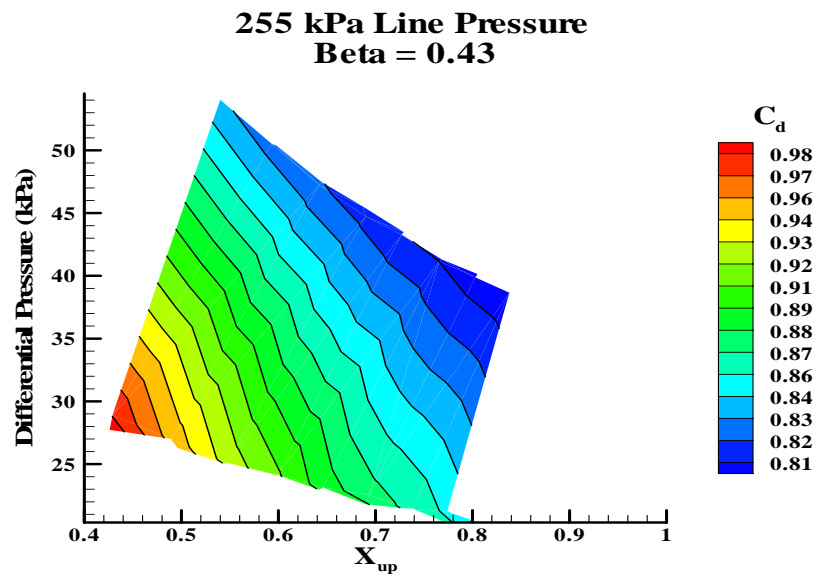Figure 77   Differential Pressure as a Function of Upstream Quality and Coefficient of Discharge, 255 kPa Upstream Line Pressure, $\beta = 0.508$
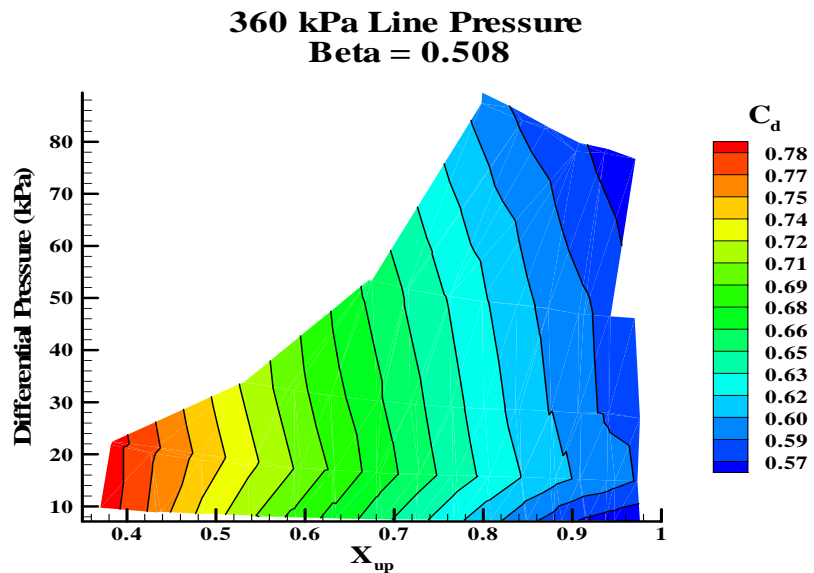
Figure 78   Differential Pressure as a Function of Upstream Quality and Coefficient of Discharge, 360 kPa Upstream Line Pressure, $\beta = 0.508$

Case 3 Repeatability
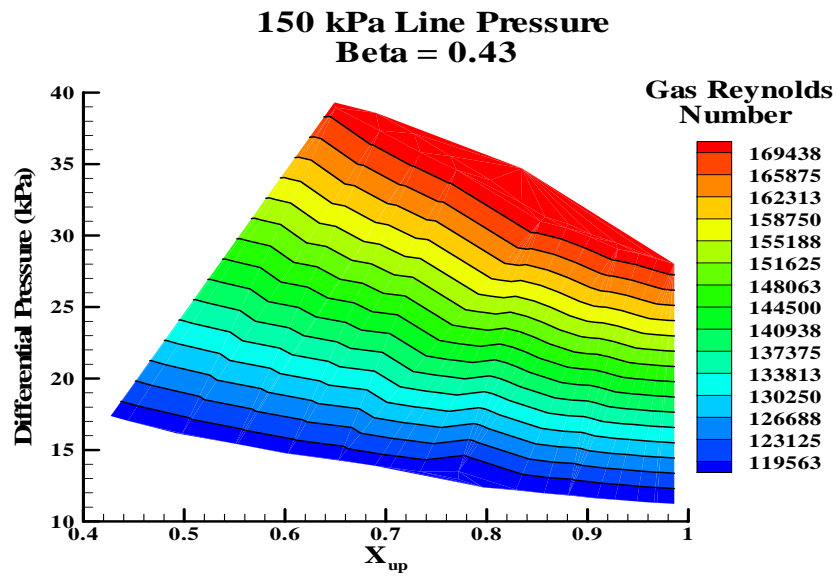
Figure 79   Differential Pressure as a Function of Upstream
Quality and Gas Reynolds Number,
150 kPa Upstream Line Pressure, β = 0.43
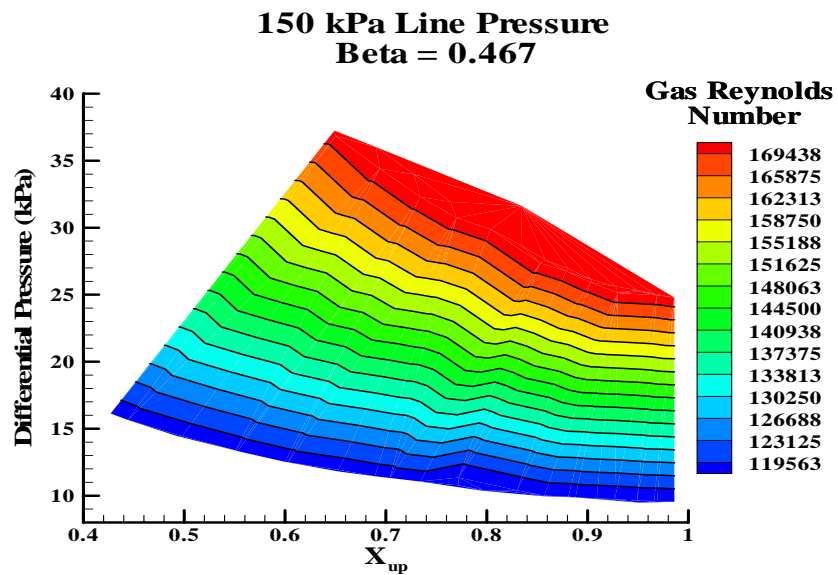
Figure 80   Differential Pressure as a Function of Upstream
Quality and Gas Reynolds Number,
150 kPa Upstream Line Pressure, β = 0.467

150 kPa Line Pressure
Beta = 0.508
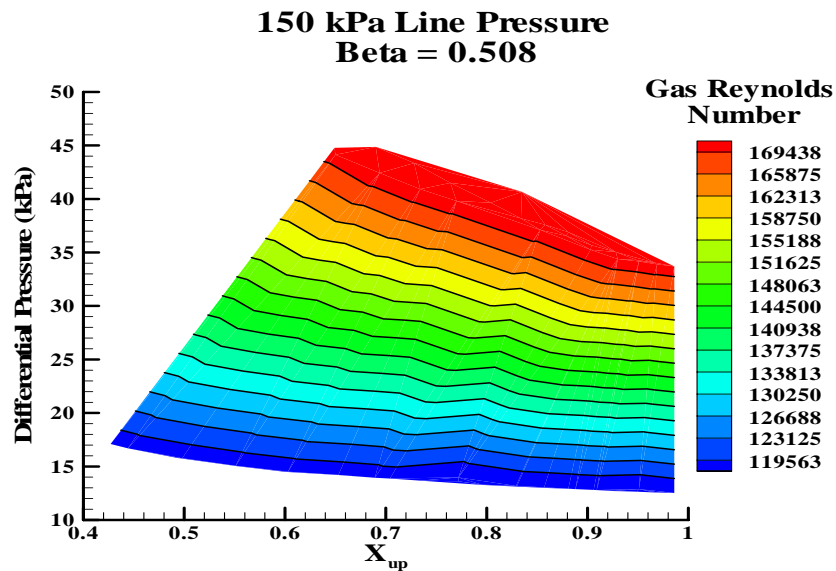
Figure 81   Differential Pressure as a Function of Upstream
            Quality and Gas Reynolds Number,
            150 kPa Upstream Line Pressure, β = 0.508

255 kPa Line Pressure
Beta = 0.43
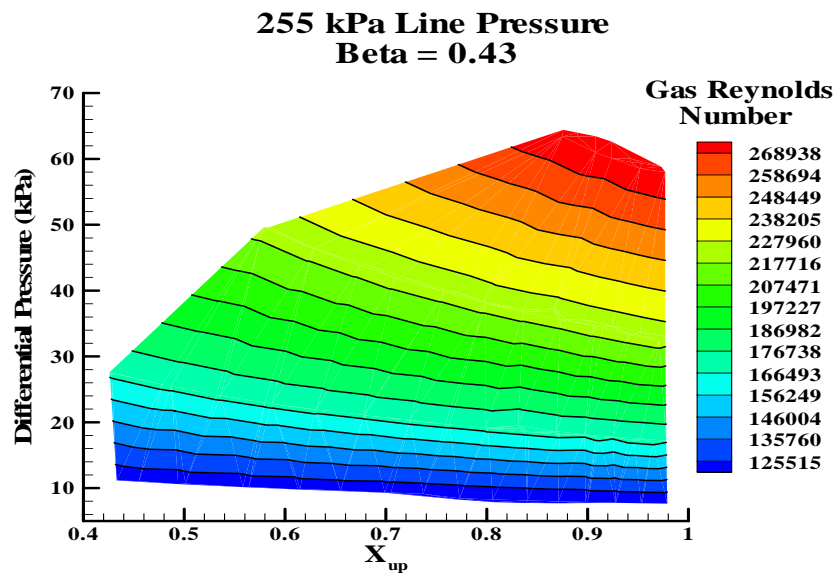
Figure 82   Differential Pressure as a Function of Upstream
            Quality and Gas Reynolds Number,
            255 kPa Upstream Line Pressure, β = 0.43
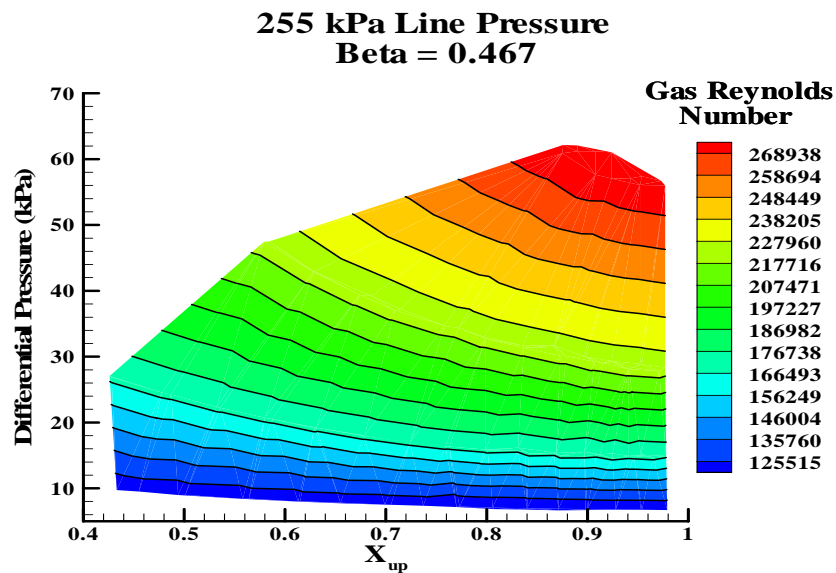
Figure 83   Differential Pressure as a Function of Upstream Quality and Gas Reynolds Number, 255 kPa Upstream Line Pressure, β = 0.467
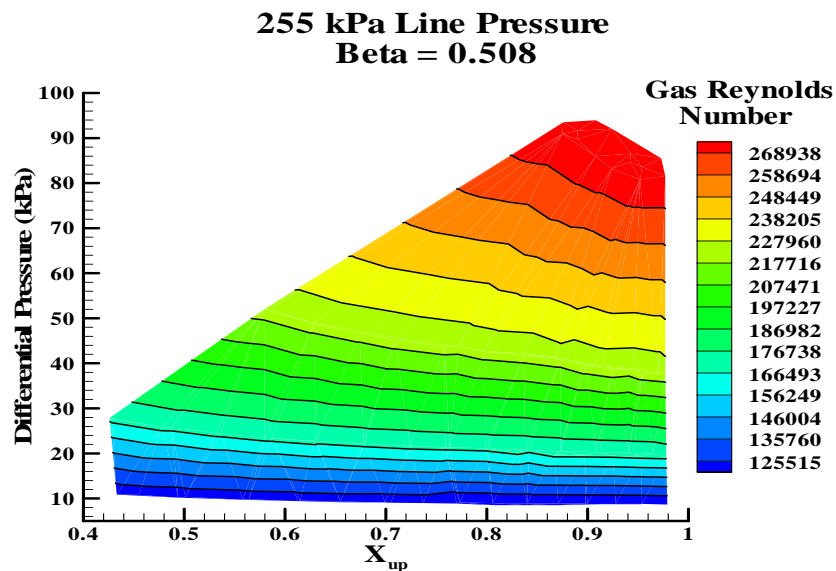
Figure 84   Differential Pressure as a Function of Upstream Quality and Gas Reynolds Number, 255 kPa Upstream Line Pressure, β = 0.508

360 kPa Line Pressure
Beta = 0.43
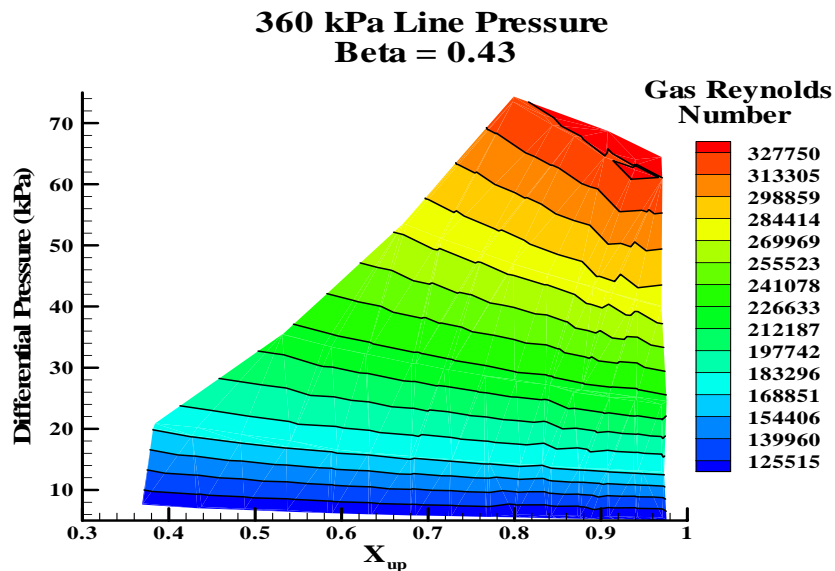
Figure 85   Differential Pressure as a Function of Upstream
              Quality and Gas Reynolds Number,
              360 kPa Upstream Line Pressure, β = 0.43

360 kPa Line Pressure
Beta = 0.467
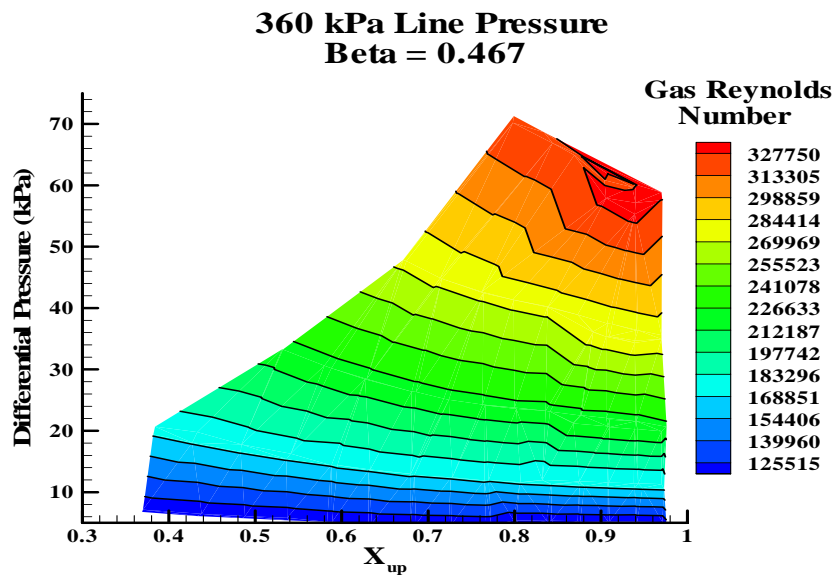
Figure 86   Differential Pressure as a Function of Upstream
              Quality and Gas Reynolds Number,
              360 kPa Upstream Line Pressure, β = 0.467

360 kPa Line Pressure
Beta = 0.508
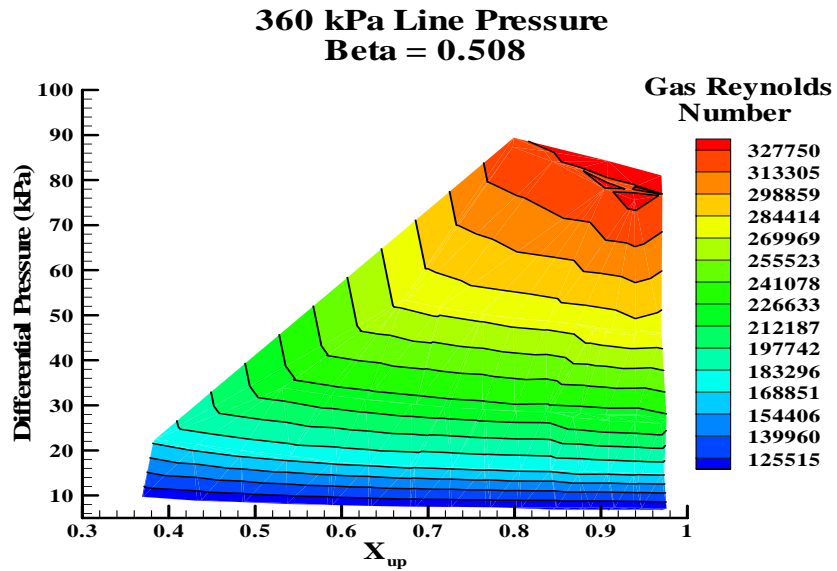
Figure 87   Differential Pressure as a Function of Upstream
Quality and Gas Reynolds Number,
360 kPa Upstream Line Pressure, $\beta = 0.508$

dP 0.43 vs dP 0.467
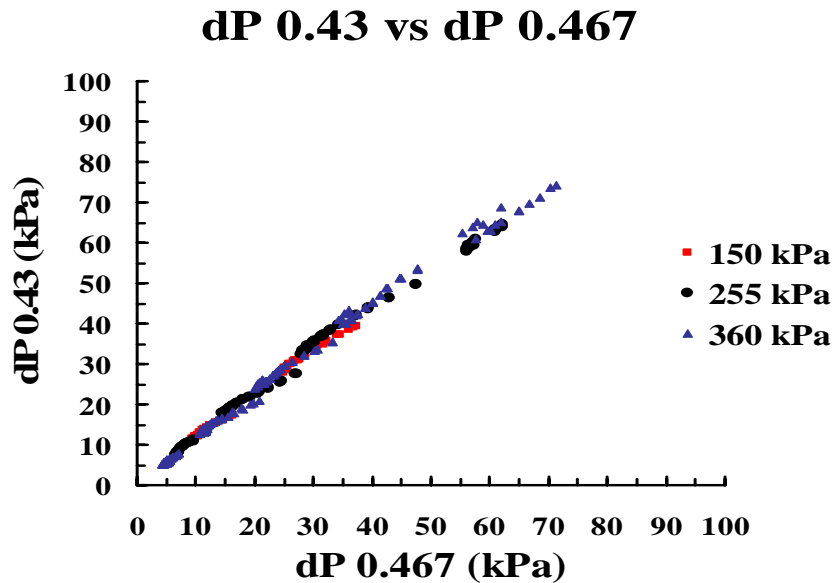
Figure 88   Differential Pressure across $\beta = 0.43$ plate as a function
of the Differential Pressure across $\beta = 0.467$ plate

dP 0.508 vs dP 0.467
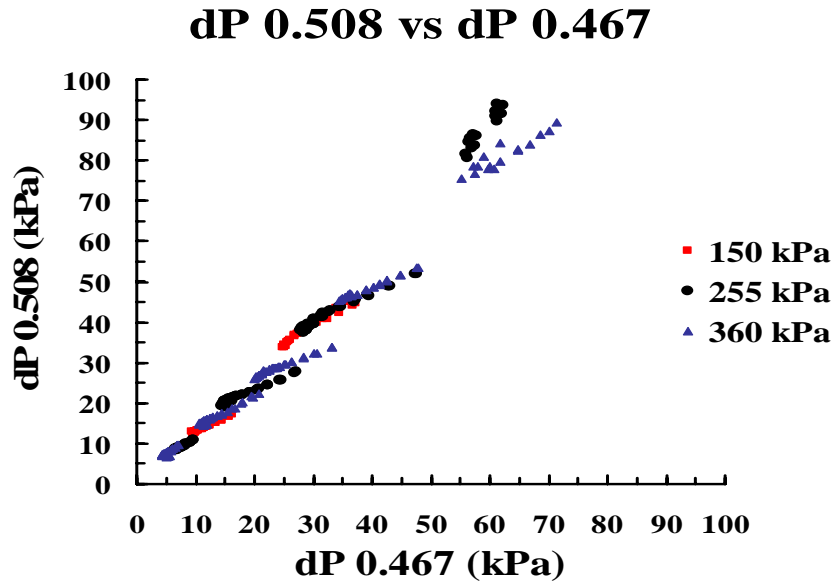
Figure 89   Differential Pressure across $\beta = 0.508$ plate as a function of the Differential Pressure across $\beta = 0.467$ plate
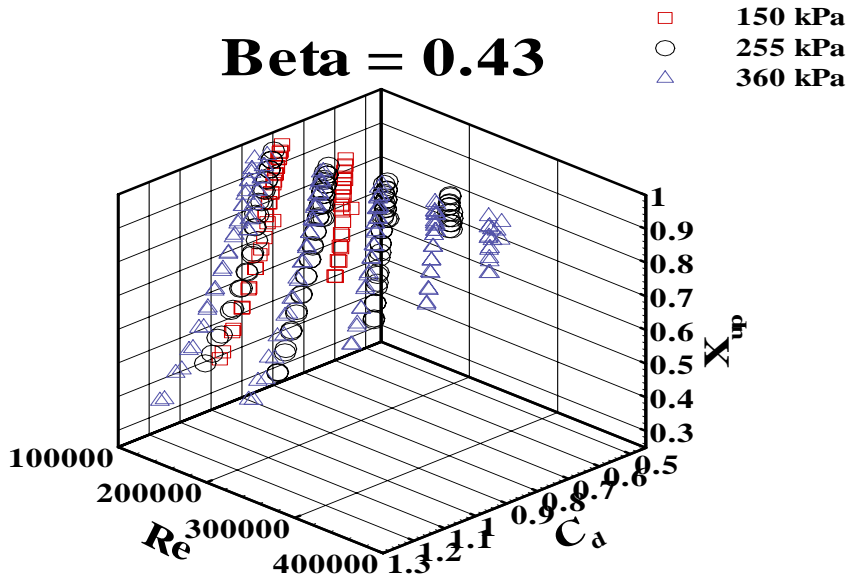
Figure 90   Coefficient of Discharge as a function of Gas Reynolds Number and Upstream Quality at different upstream line pressures, $\beta = 0.43$
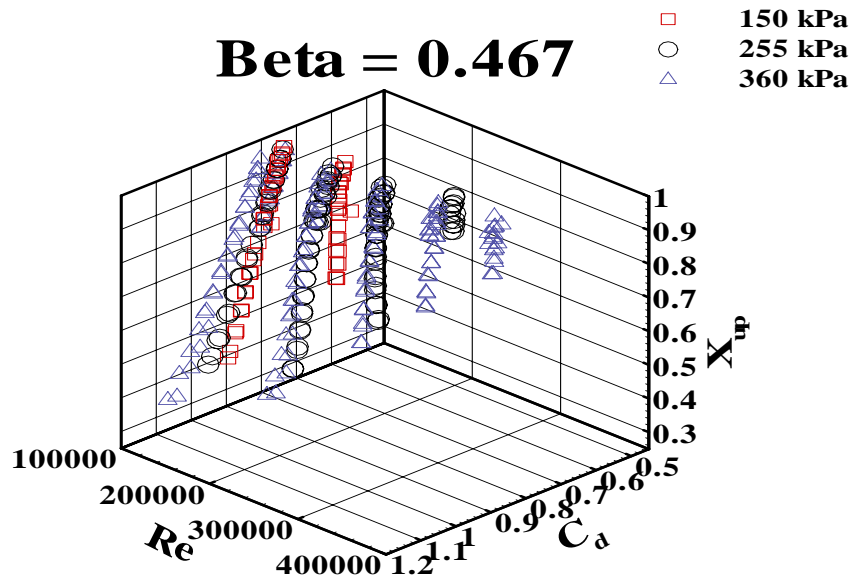
Figure 91   Coefficient of Discharge as a function of
Gas Reynolds Number and Upstream Quality
at different upstream line pressures, β = 0.467
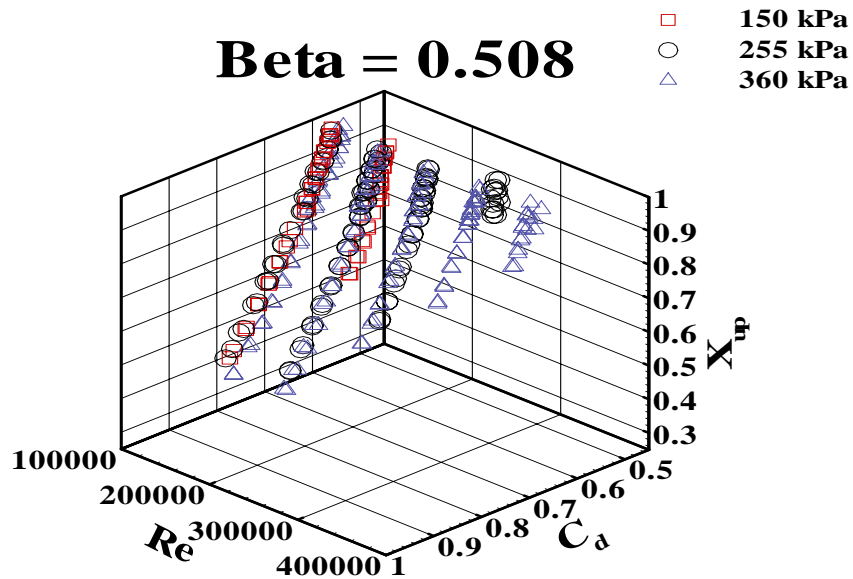
Figure 92   Coefficient of Discharge as a function of
Gas Reynolds Number and Upstream Quality
at different upstream line pressures, β = 0.508
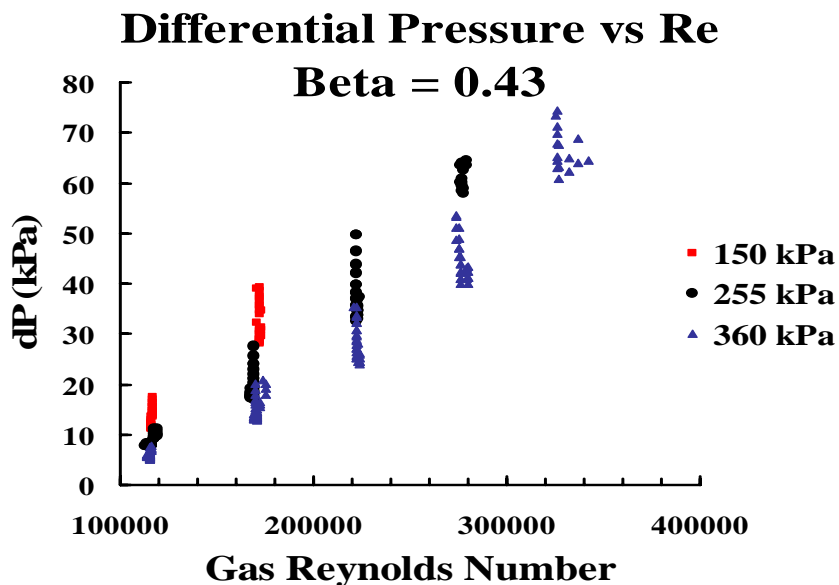
Figure 93　Differential Pressure as a function of
Gas Reynolds Number, β = 0.43
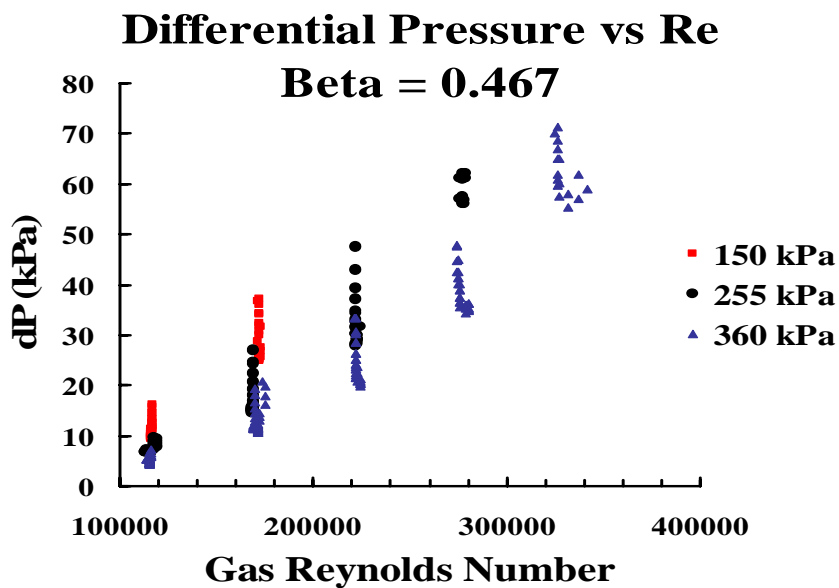
Figure 94　Differential Pressure as a function of
Gas Reynolds Number, β = 0.467
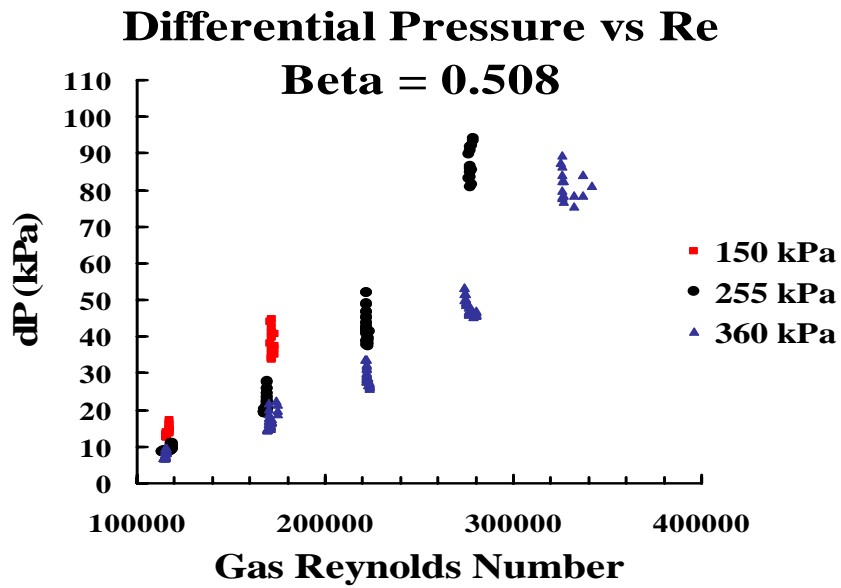
Figure 95 Differential Pressure as a function of
         Gas Reynolds Number, $\beta = 0.508$
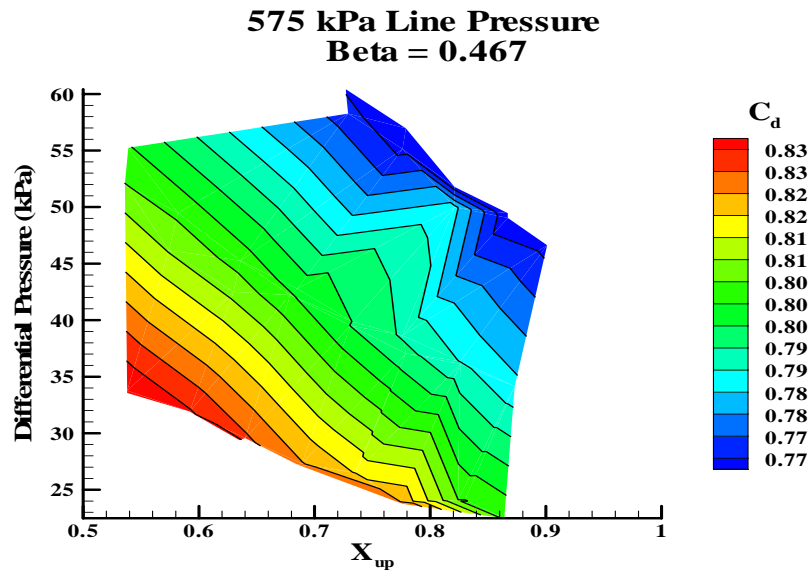
Case 4 Quality Effects at High Air Quality

Figure 96 Differential Pressure as a Function of Upstream Quality and Coefficient of Discharge, 150 kPa Upstream Line Pressure, $\beta = 0.43$

Figure 97 Differential Pressure as a Function of Upstream Quality and Coefficient of Discharge, 255 kPa Upstream Line Pressure, $\beta = 0.43$
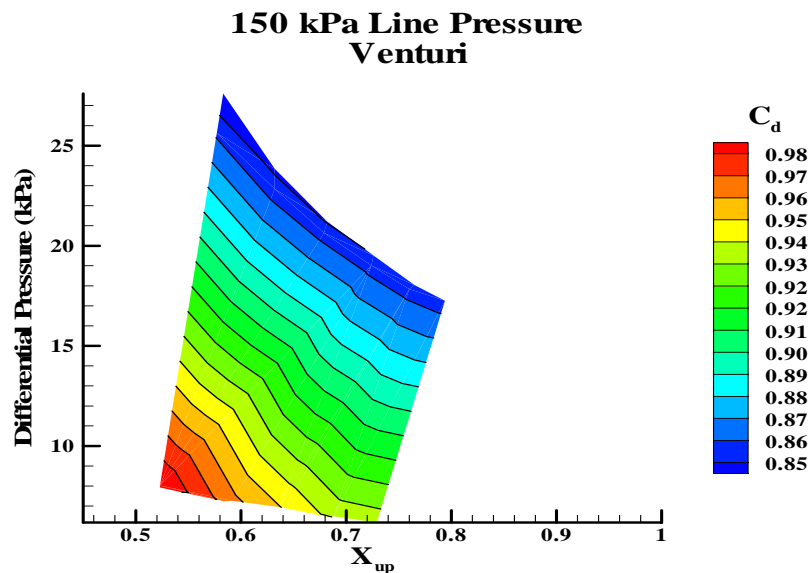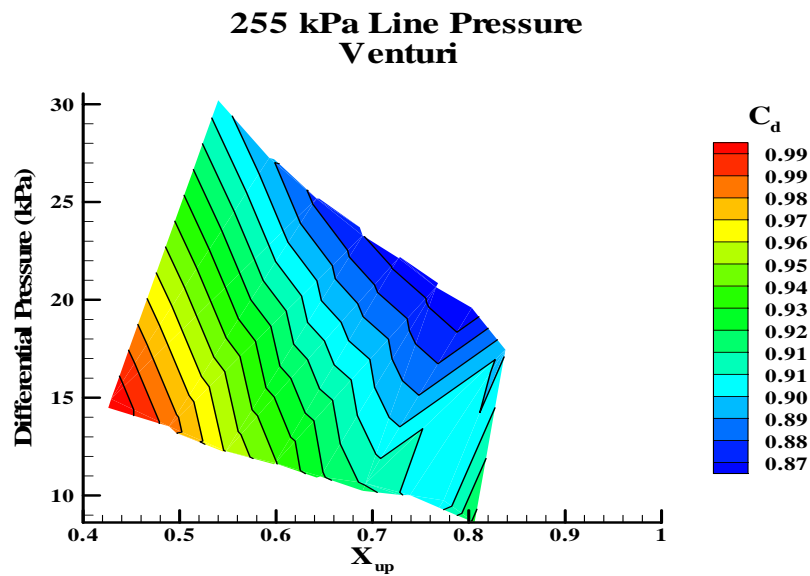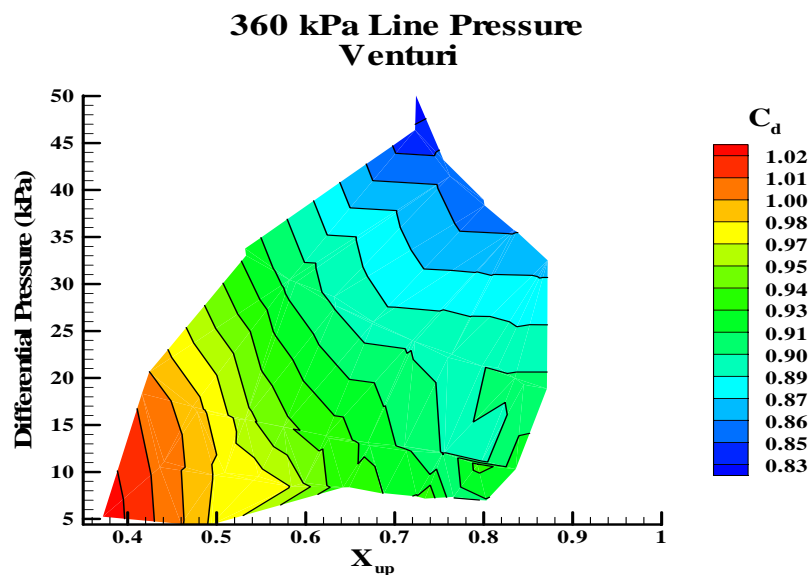
Figure 98   Differential Pressure as a Function of Upstream Quality and Coefficient of Discharge, 360 kPa Upstream Line Pressure, β = 0.43

Figure 99   Differential Pressure as a Function of Upstream Quality and Coefficient of Discharge, 50 kPa Upstream Line Pressure, β = 0.508

Figure 100   Differential Pressure as a Function of Upstream
              Quality and Coefficient of Discharge,
              255 kPa Upstream Line Pressure, β = 0.508

Figure 101   Differential Pressure as a Function of Upstream
              Quality and Coefficient of Discharge,
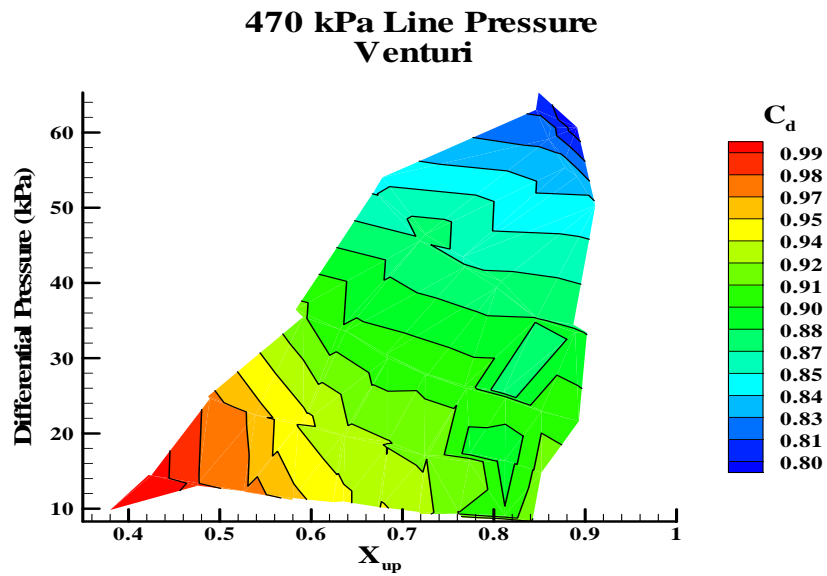   360 kPa Upstream Line Pressure, β = 0.508

Case 4 Quality Effects at Low Air Quality
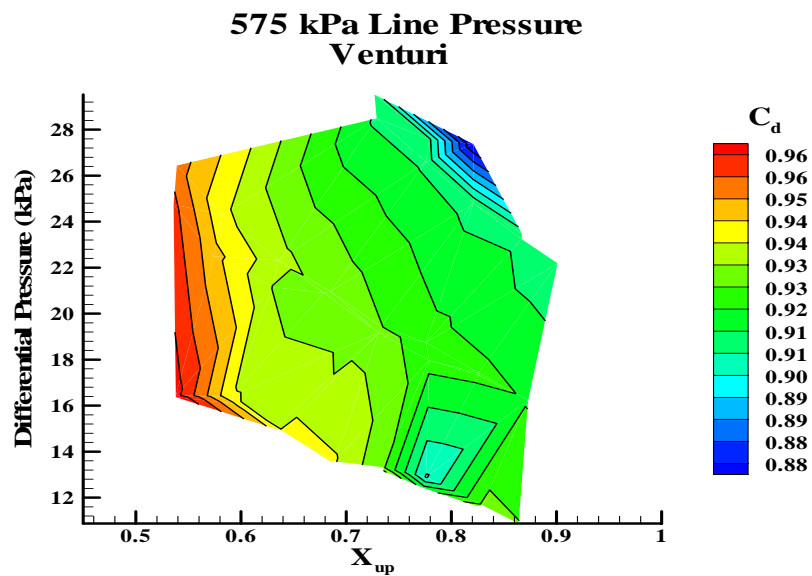

150 kPa Line Pressure
Beta = 0.43

Figure 102   Differential Pressure as a Function of Upstream
Quality and Coefficient of Discharge,
150 kPa Upstream Line Pressure, $\beta = 0.43$

255 kPa Line Pressure
Beta = 0.43

Figure 103   Differential Pressure as a Function of Upstream
Quality and Coefficient of Discharge,
255 kPa Upstream Line Pressure, $\beta = 0.43$

360 kPa Line Pressure
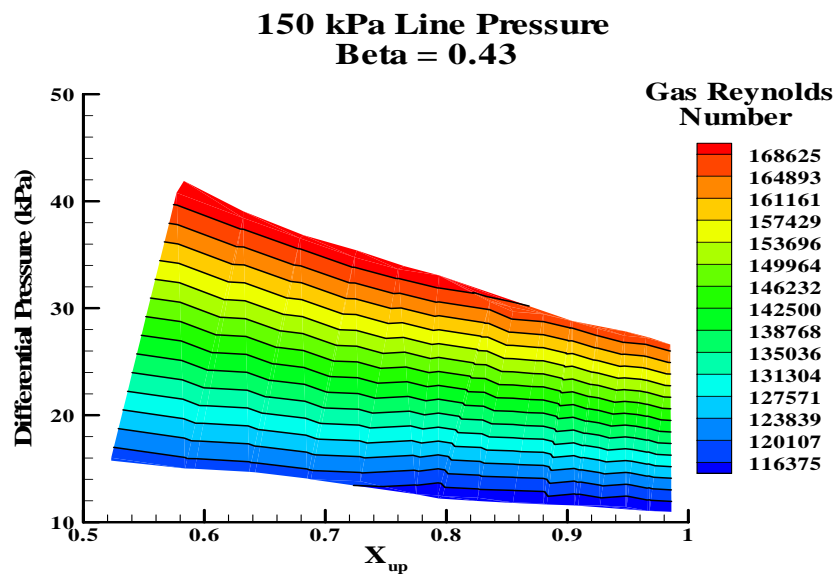**Beta = 0.43**
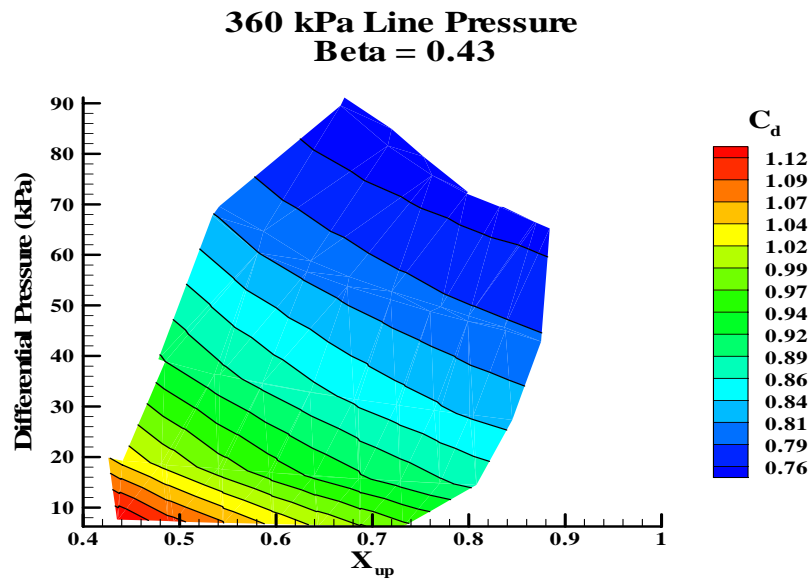
Figure 104　　Differential Pressure as a Function of Upstream
　　　　　　　Quality and Coefficient of Discharge,
　　　　　　　360 kPa Upstream Line Pressure, β = 0.43

150 kPa Line Pressure
Beta = 0.508
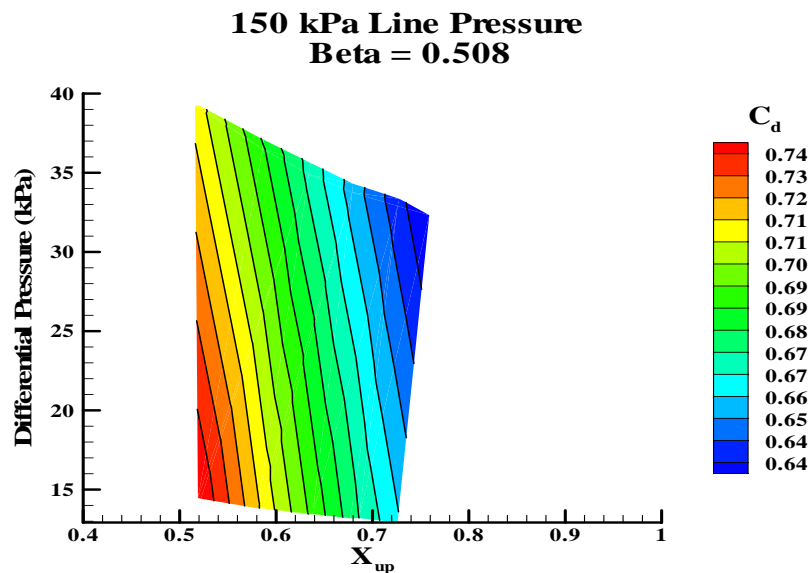
Figure 105　　Differential Pressure as a Function of Upstream
　　　　　　　Quality and Coefficient of Discharge,
　　　　　　　150 kPa Upstream Line Pressure, β = 0.508
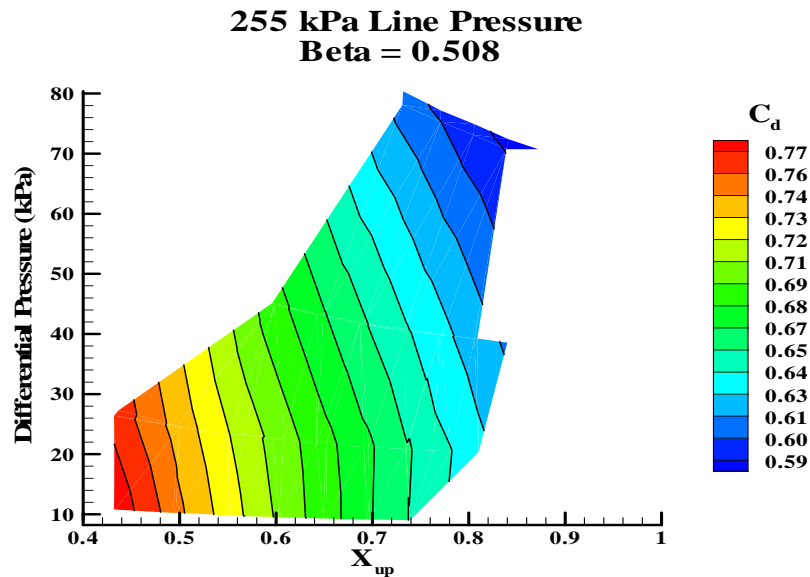
Figure 106 Differential Pressure as a Function of Upstream Quality and Coefficient of Discharge, 255 kPa Upstream Line Pressure, $\beta = 0.508$
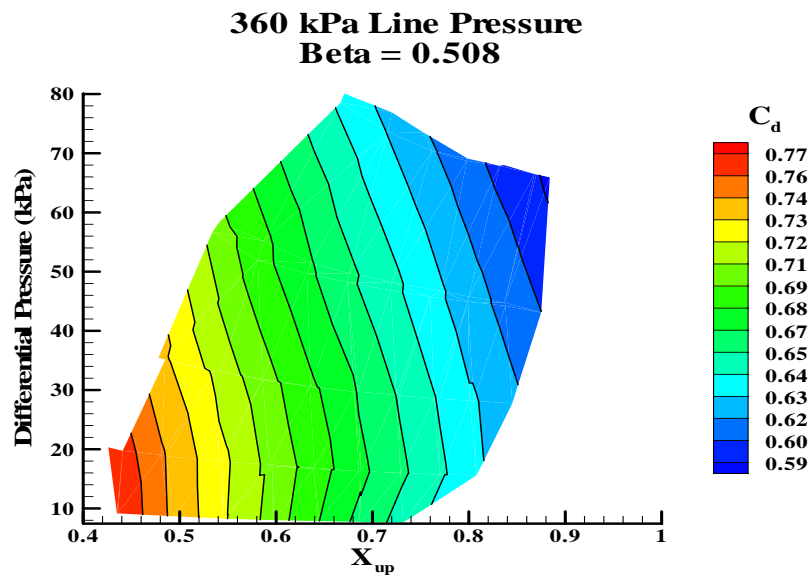
Figure 107 Differential Pressure as a Function of Upstream Quality and Coefficient of Discharge, 360 kPa Upstream Line Pressure, $\beta = 0.508$

Case 4 Repeatability

Figure 108   Differential Pressure as a Function of Upstream
Quality and Gas Reynolds Number,
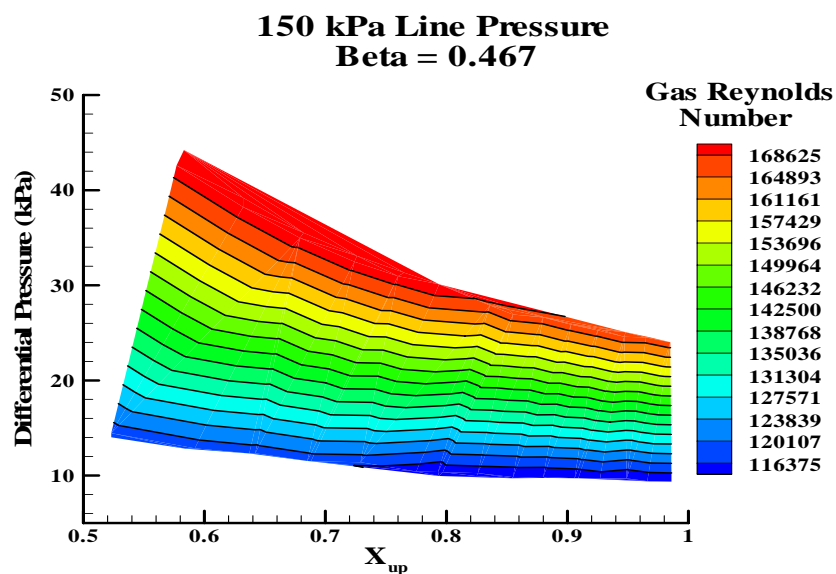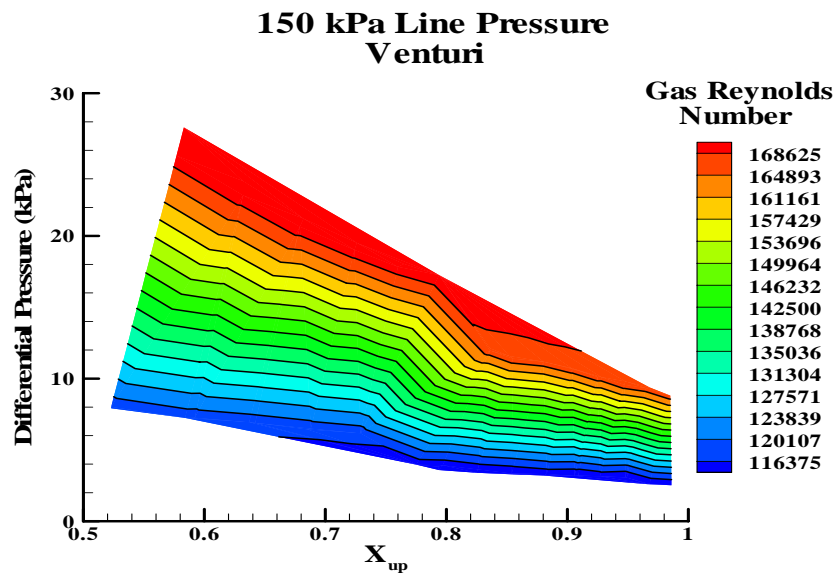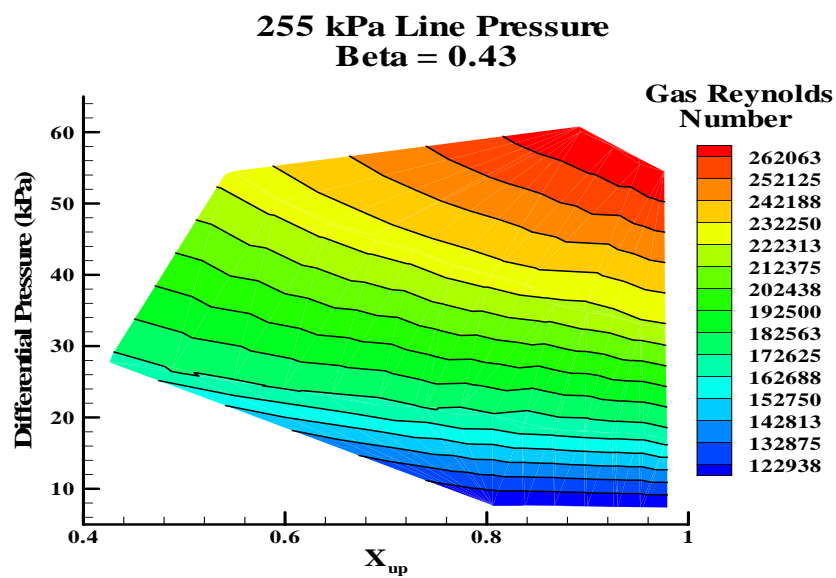150 kPa Upstream Line Pressure, β = 0.43

Figure 109   Differential Pressure as a Function of Upstream
Quality and Gas Reynolds Number,
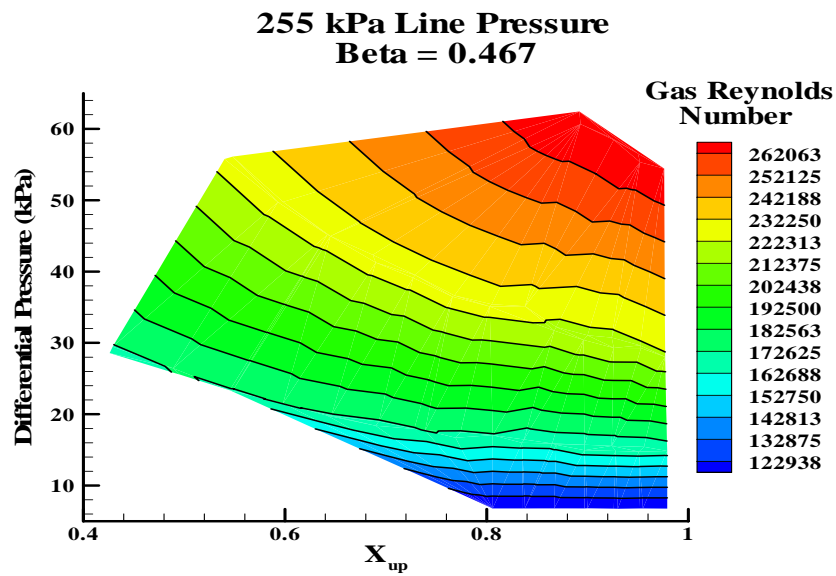150 kPa Upstream Line Pressure, β = 0.508

Figure 110   Differential Pressure as a Function of Upstream
Quality and Gas Reynolds Number,
255 kPa Upstream Line Pressure, $\beta = 0.43$

Figure 111   Differential Pressure as a Function of Upstream
Quality and Gas Reynolds Number,
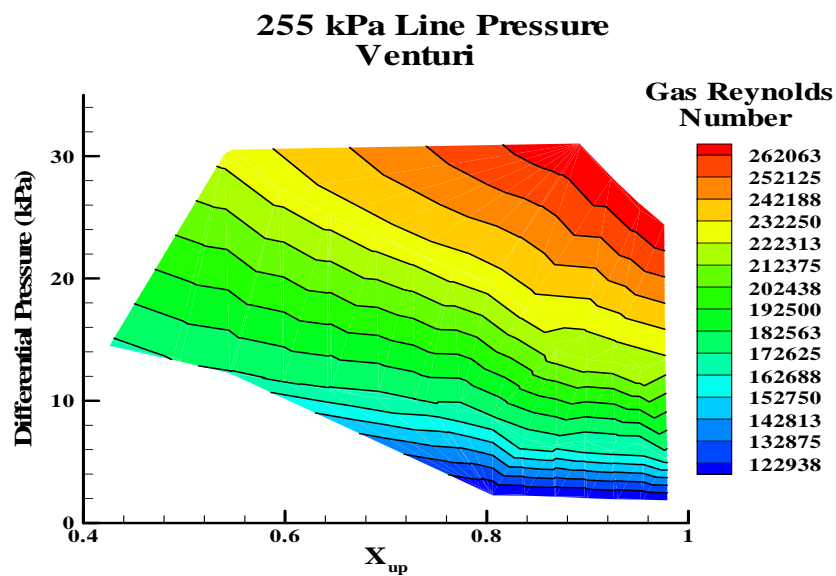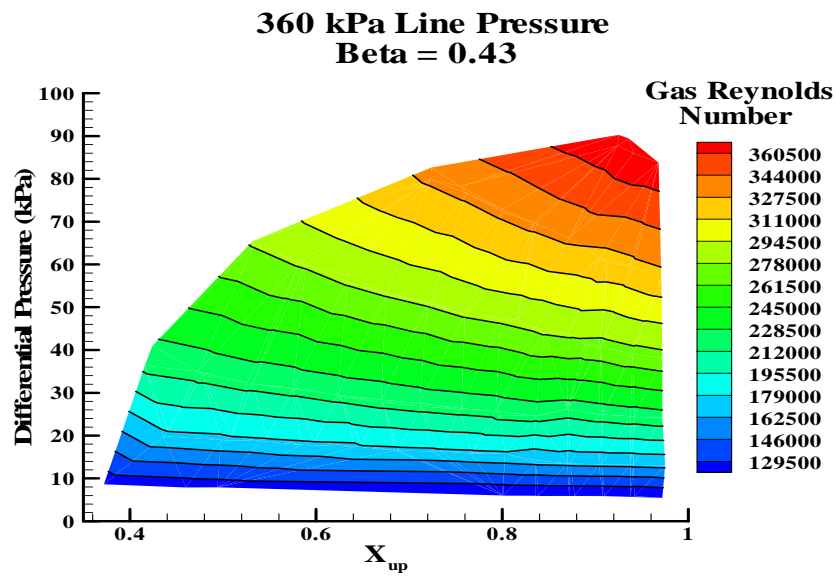255 kPa Upstream Line Pressure, $\beta = 0.508$

Figure 112   Differential Pressure as a Function of Upstream Quality and Gas Reynolds Number, 360 kPa Upstream Line Pressure, β = 0.43
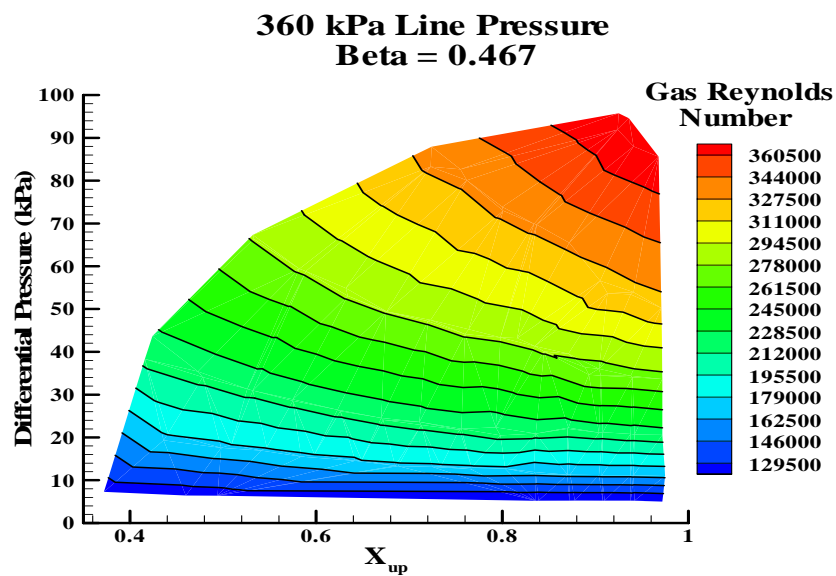

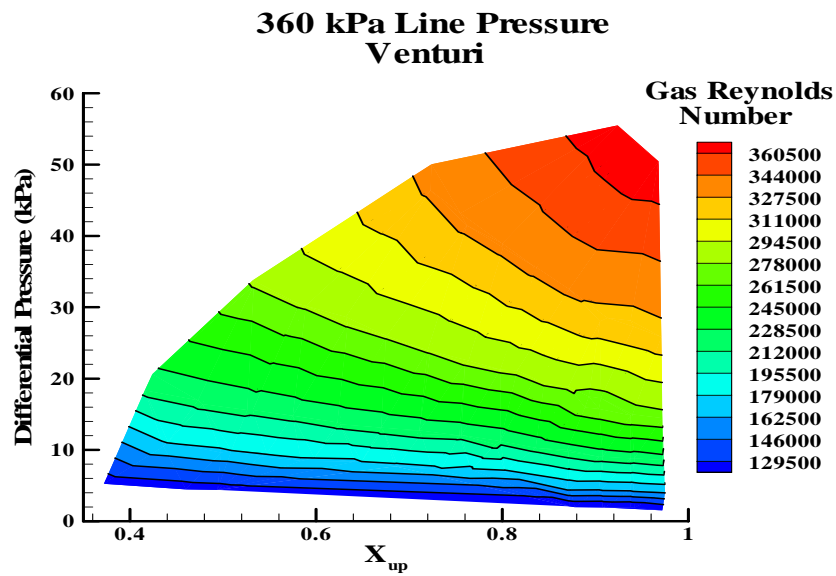Figure 113   Differential Pressure as a Function of Upstream Quality and Gas Reynolds Number, 360 kPa Upstream Line Pressure, β = 0.508

Figure 114 Differential Pressure across $\beta = 0.43$ plate as a function of the Differential Pressure across $\beta = 0.508$ plate
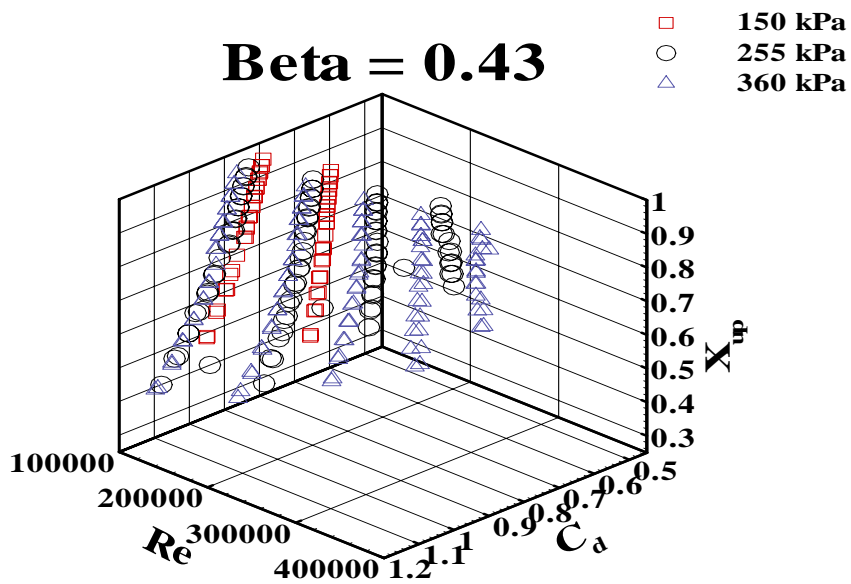
Figure 115 Coefficient of Discharge as a function of Gas Reynolds Number and Upstream Quality at different upstream line pressures, $\beta = 0.43$
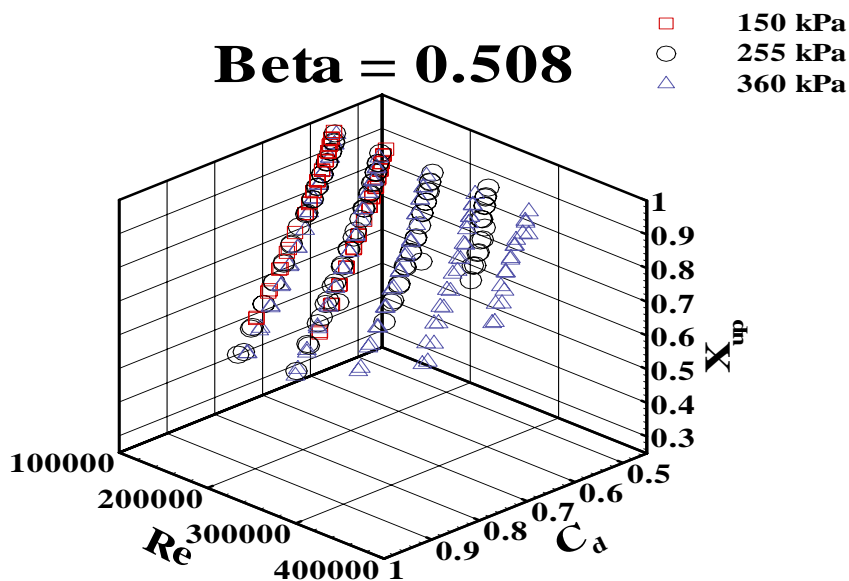
Figure 116   Coefficient of Discharge as a function of
Gas Reynolds Number and Upstream Quality
at different upstream line pressures, $\beta = 0.508$
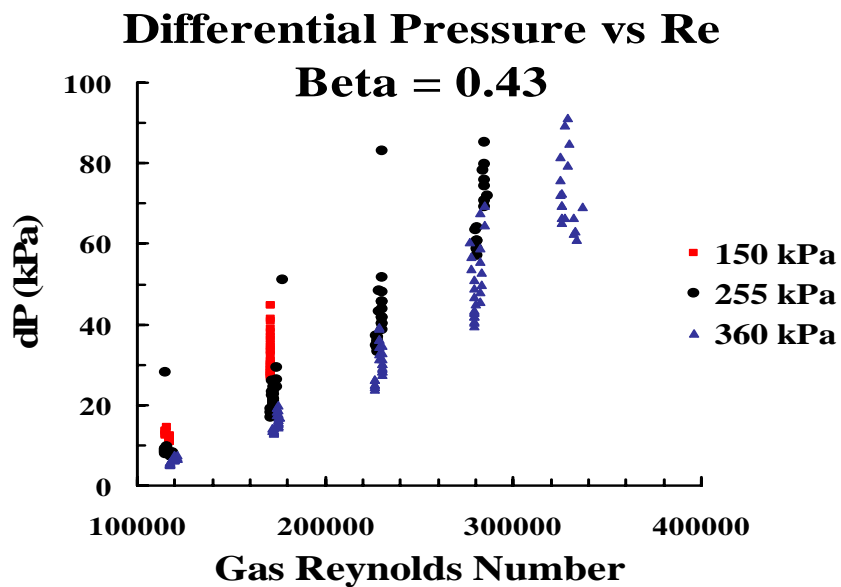
Figure 117   Differential Pressure as a function of
Gas Reynolds Number, $\beta = 0.43$
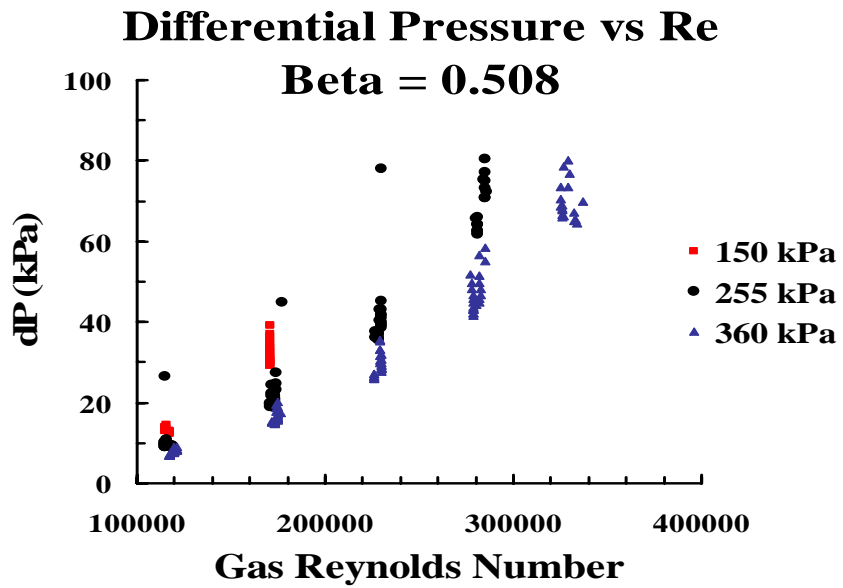
Figure 118   Differential Pressure as a function of
Gas Reynolds Number, β = 0.508

Case 5 Quality Effects at High Air Quality

Figure 119   Differential Pressure as a Function of Upstream
Quality and Coefficient of Discharge,
150 kPa Upstream Line Pressure, β = 0.43

Figure 120   Differential Pressure as a Function of Upstream
Quality and Coefficient of Discharge,
255 kPa Upstream Line Pressure, β = 0.43

360 kPa Line Pressure
Beta = 0.43
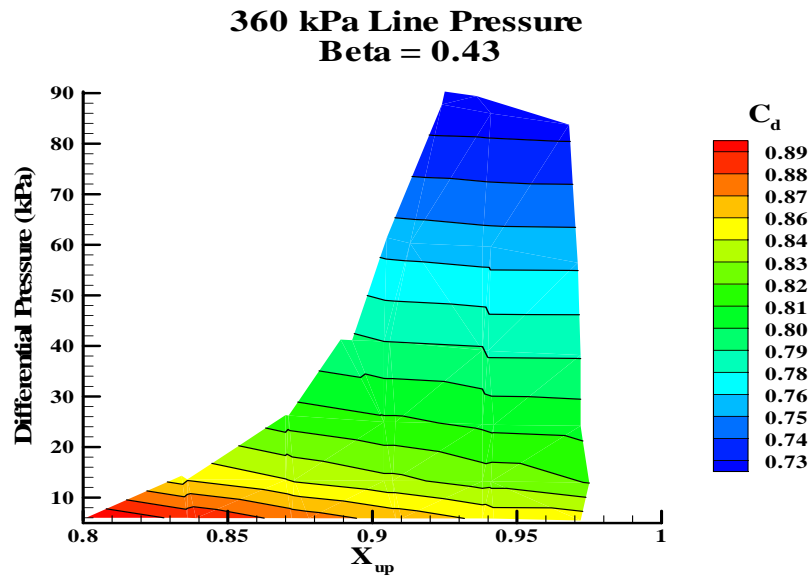
Figure 121   Differential Pressure as a Function of Upstream
Quality and Coefficient of Discharge,
360 kPa Upstream Line Pressure, β = 0.43

470 kPa Line Pressure
Beta = 0.43

Figure 122   Differential Pressure as a Function of Upstream
Quality and Coefficient of Discharge,
470 kPa Upstream Line Pressure, β = 0.43

575 kPa Line Pressure
Beta = 0.43

Figure 123   Differential Pressure as a Function of Upstream
Quality and Coefficient of Discharge,
575 kPa Upstream Line Pressure, β = 0.43

150 kPa Line Pressure
Beta = 0.467

Figure 124   Differential Pressure as a Function of Upstream
Quality and Coefficient of Discharge,
150 kPa Upstream Line Pressure, β = 0.467

255 kPa Line Pressure
Beta = 0.467

Figure 125   Differential Pressure as a Function of Upstream
Quality and Coefficient of Discharge,
255 kPa Upstream Line Pressure, β = 0.467

360 kPa Line Pressure
Beta = 0.467

Figure 126   Differential Pressure as a Function of Upstream
Quality and Coefficient of Discharge,
360 kPa Upstream Line Pressure, β = 0.467

Figure 127   Differential Pressure as a Function of Upstream
Quality and Coefficient of Discharge,
470 kPa Upstream Line Pressure, β = 0.467

Figure 128   Differential Pressure as a Function of Upstream
Quality and Coefficient of Discharge,
575 kPa Upstream Line Pressure, β = 0.467

Figure 129   Differential Pressure as a Function of Upstream
Quality and Coefficient of Discharge,
150 kPa Upstream Line Pressure, Venturi

Figure 130   Differential Pressure as a Function of Upstream
Quality and Coefficient of Discharge,
255 kPa Upstream Line Pressure, Venturi

360 kPa Line Pressure
Venturi

Figure 131   Differential Pressure as a Function of Upstream
             Quality and Coefficient of Discharge,
             360 kPa Upstream Line Pressure, Venturi

470 kPa Line Pressure
Venturi

Figure 132   Differential Pressure as a Function of Upstream
             Quality and Coefficient of Discharge,
             470 kPa Upstream Line Pressure, Venturi

575 kPa Line Pressure
Venturi

Figure 133   Differential Pressure as a Function of Upstream
              Quality and Coefficient of Discharge,
              575 kPa Upstream Line Pressure, Venturi

Case 5 Quality Effects at Low Air Quality

150 kPa Line Pressure
Beta = 0.43

Figure 134   Differential Pressure as a Function of Upstream
              Quality and Coefficient of Discharge,
              150 kPa Upstream Line Pressure, β = 0.43

Figure 135   Differential Pressure as a Function of Upstream
Quality and Coefficient of Discharge,
255 kPa Upstream Line Pressure, β = 0.43
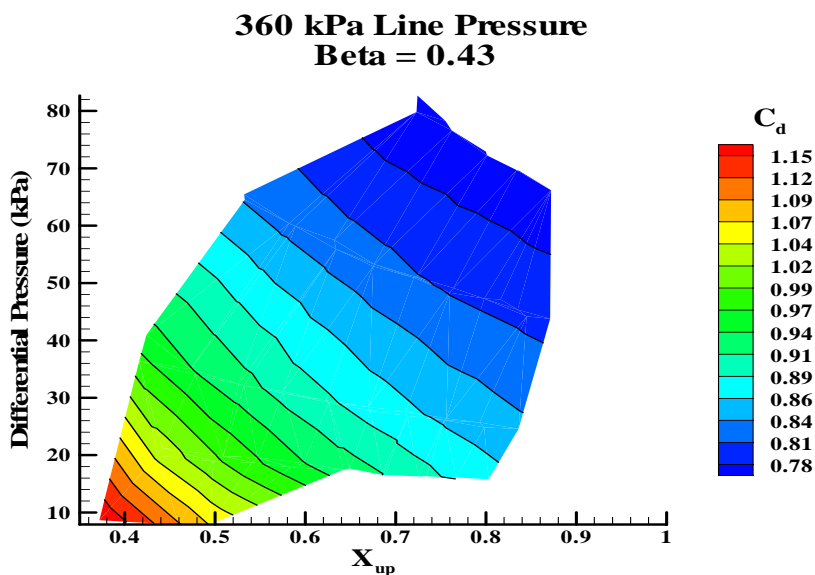
Figure 136   Differential Pressure as a Function of Upstream
Quality and Coefficient of Discharge,
360 kPa Upstream Line Pressure, β = 0.43

470 kPa Line Pressure
Beta = 0.43
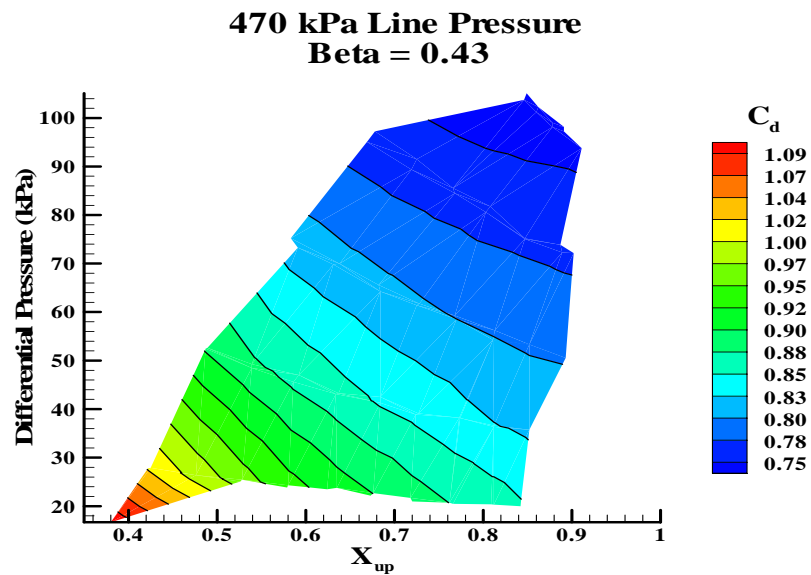
Figure 137   Differential Pressure as a Function of Upstream
             Quality and Coefficient of Discharge,
             470 kPa Upstream Line Pressure, β = 0.43

575 kPa Line Pressure
Beta = 0.43
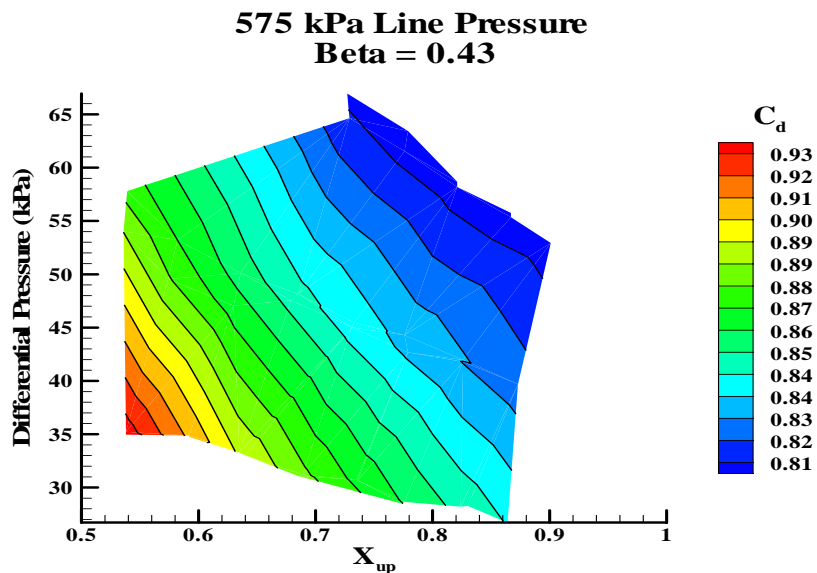
Figure 138   Differential Pressure as a Function of Upstream
             Quality and Coefficient of Discharge,
             575 kPa Upstream Line Pressure, β = 0.43
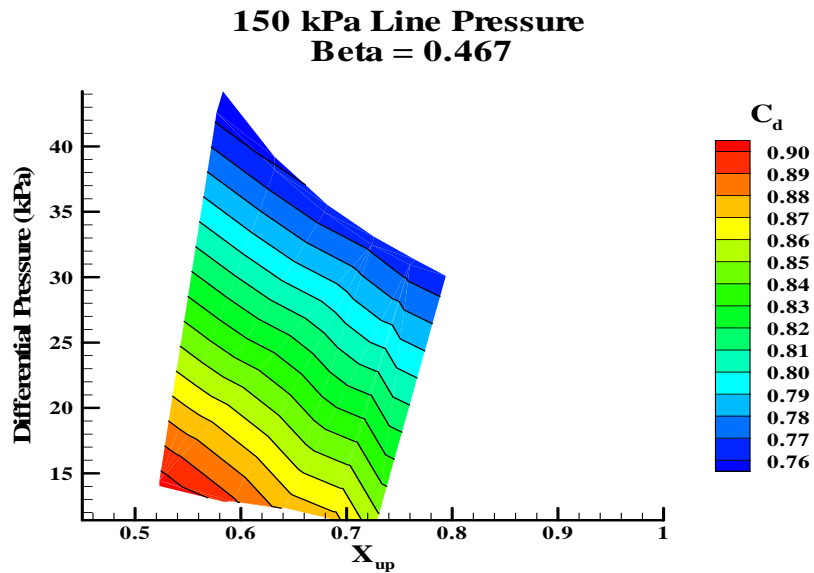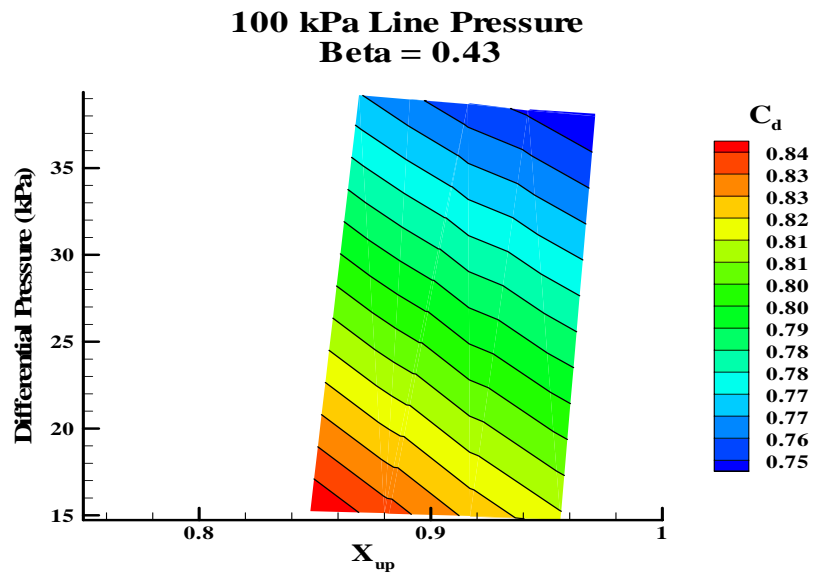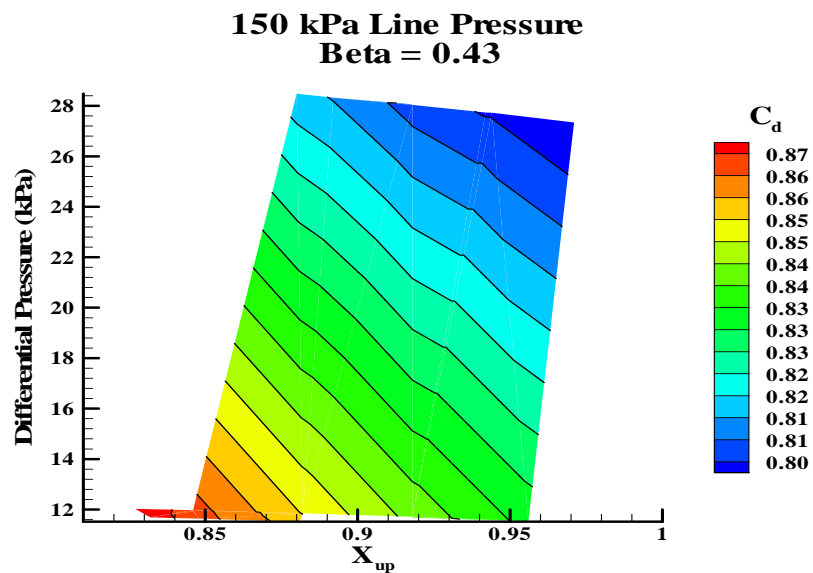
Figure 139   Differential Pressure as a Function of Upstream
              Quality and Coefficient of Discharge,
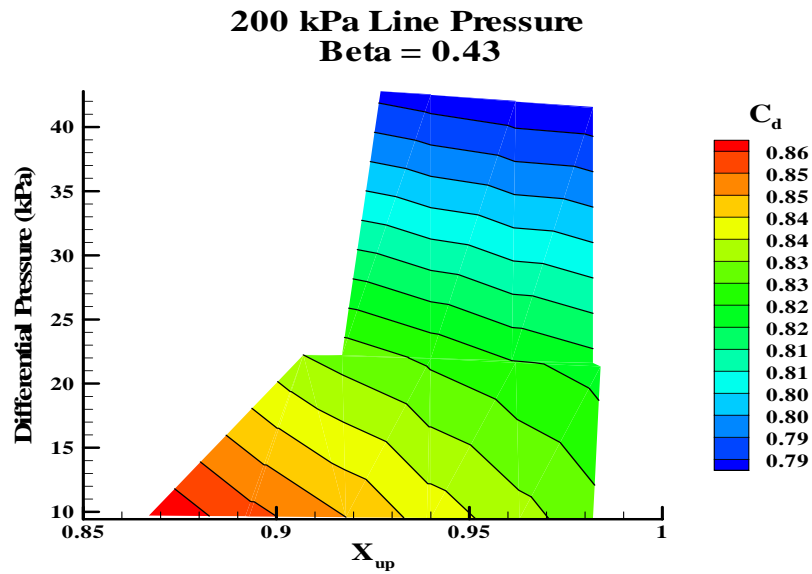   150 kPa Upstream Line Pressure, $\beta = 0.467$
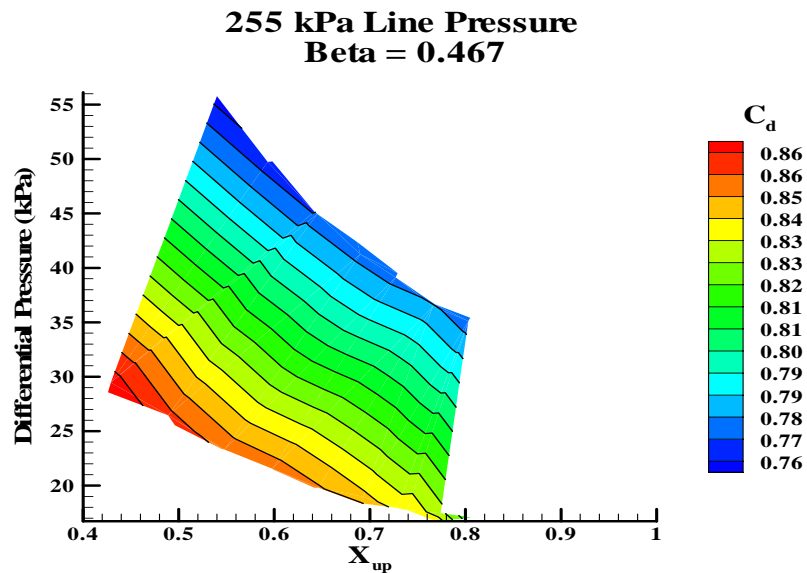
Figure 140   Differential Pressure as a Function of Upstream
              Quality and Coefficient of Discharge,
              255 kPa Upstream Line Pressure, $\beta = 0.467$
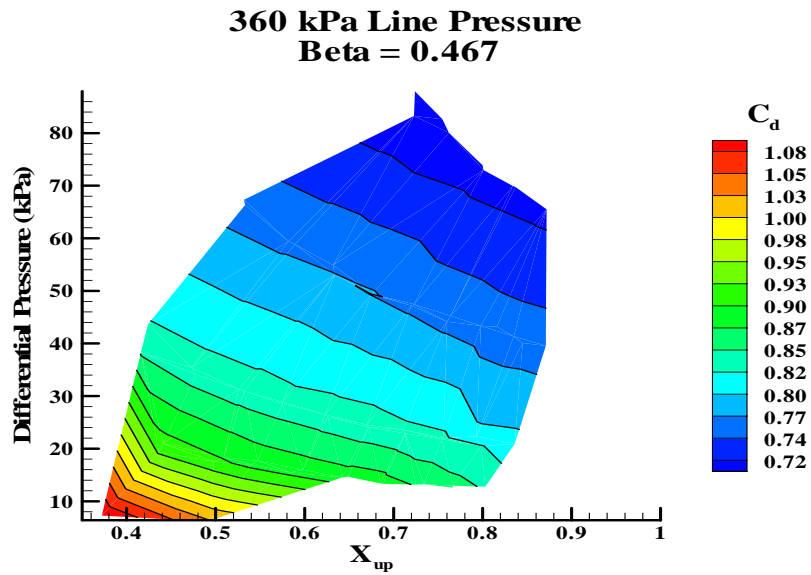
Figure 141 Differential Pressure as a Function of Upstream
Quality and Coefficient of Discharge,
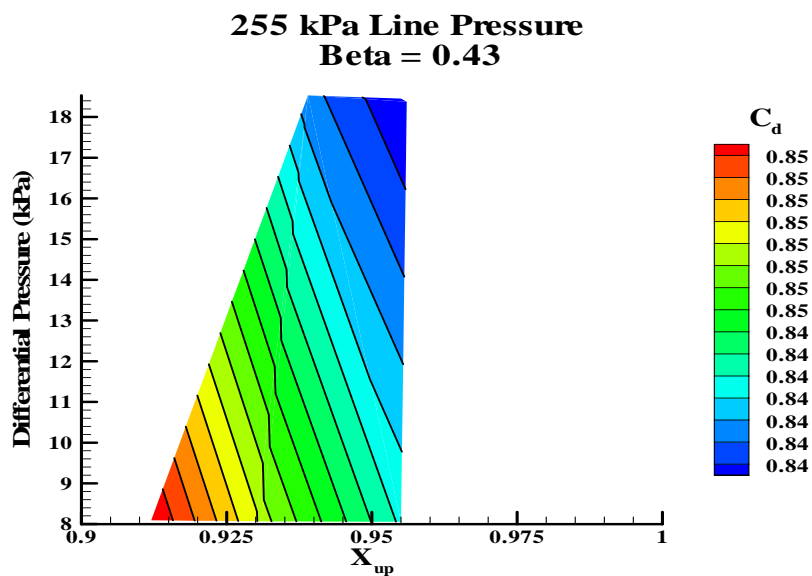360 kPa Upstream Line Pressure, β = 0.467
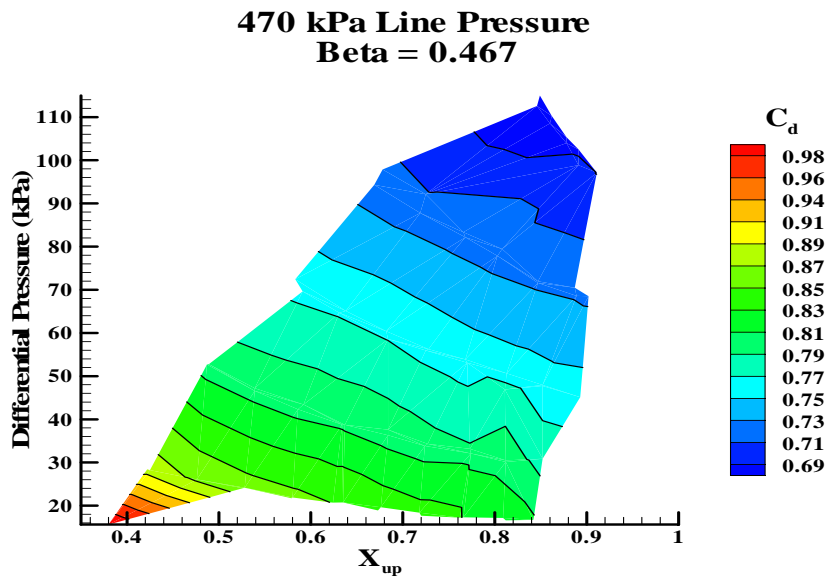
Figure 142 Differential Pressure as a Function of Upstream
Quality and Coefficient of Discharge,
470 kPa Upstream Line Pressure, β = 0.467

Figure 143   Differential Pressure as a Function of Upstream
Quality and Coefficient of Discharge,
575 kPa Upstream Line Pressure, β = 0.467

Figure 144   Differential Pressure as a Function of Upstream
Quality and Coefficient of Discharge,
150 kPa Upstream Line Pressure, Venturi

Figure 145   Differential Pressure as a Function of Upstream
Quality and Coefficient of Discharge,
255 kPa Upstream Line Pressure, Venturi

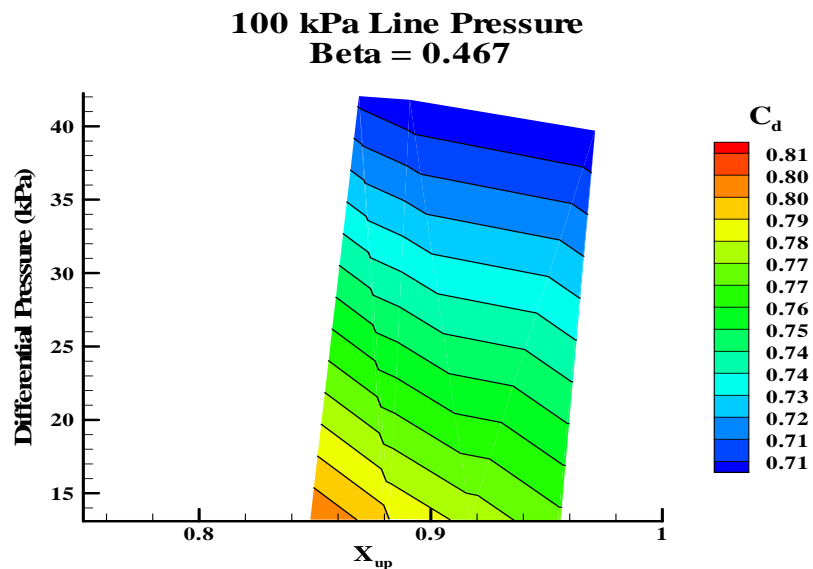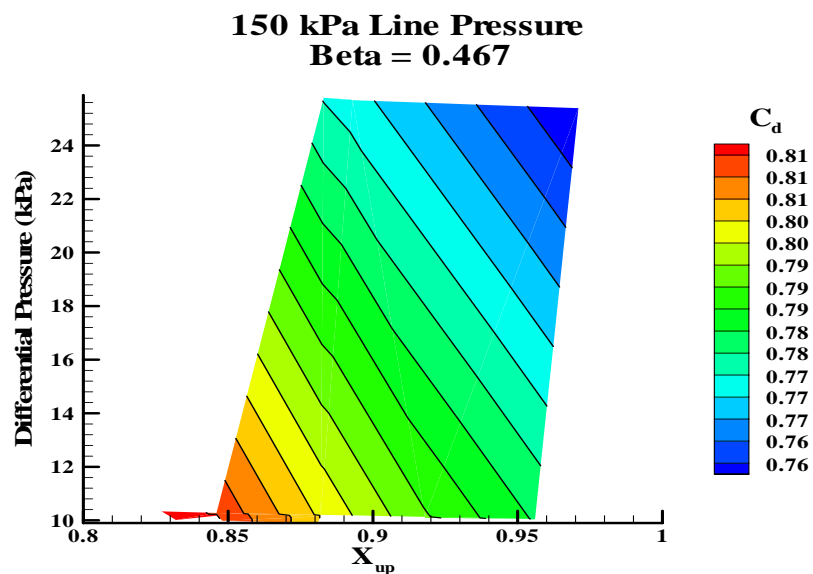Figure 146   Differential Pressure as a Function of Upstream
Quality and Coefficient of Discharge,
360 kPa Upstream Line Pressure, Venturi

Figure 147   Differential Pressure as a Function of Upstream
Quality and Coefficient of Discharge,
470 kPa Upstream Line Pressure, Venturi

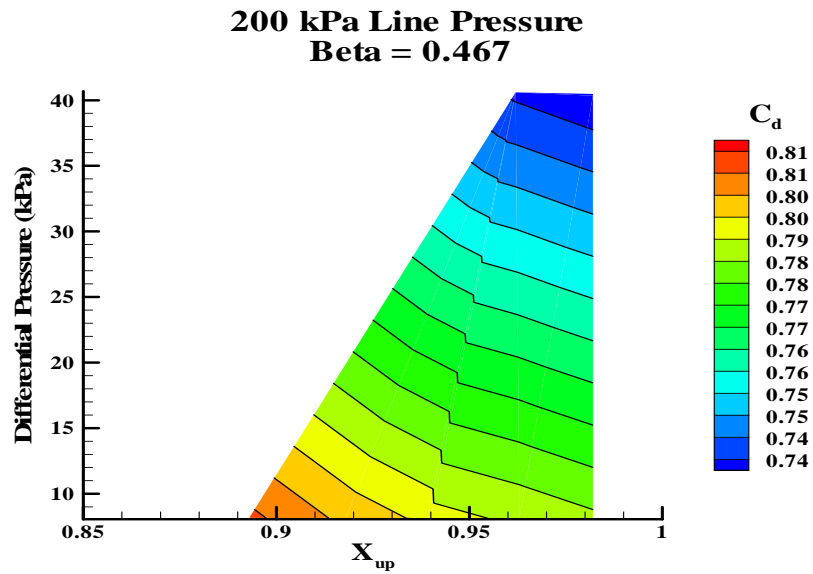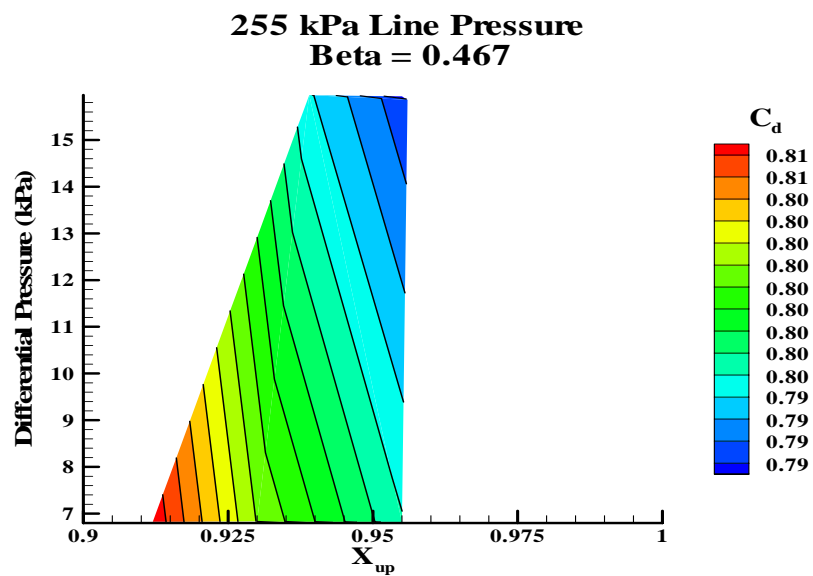

Figure 148   Differential Pressure as a Function of Upstream
Quality and Coefficient of Discharge,
575 kPa Upstream Line Pressure, Venturi

Case 5 Repeatability

**150 kPa Line Pressure
Beta = 0.43**

Figure 149   Differential Pressure as a Function of Upstream
Quality and Gas Reynolds Number
150 kPa Upstream Line Pressure, β = 0.43

**150 kPa Line Pressure
Beta = 0.467**

Figure 150   Differential Pressure as a Function of Upstream
Quality and Gas Reynolds Number
150 kPa Upstream Line Pressure, β = 0.467

**150 kPa Line Pressure
Venturi**

Figure 151   Differential Pressure as a Function of Upstream
Quality and Gas Reynolds Number
150 kPa Upstream Line Pressure, Venturi

**255 kPa Line Pressure
Beta = 0.43**

Figure 152   Differential Pressure as a Function of Upstream
Quality and Gas Reynolds Number
255 kPa Upstream Line Pressure, β = 0.43

Figure 153   Differential Pressure as a Function of Upstream
Quality and Gas Reynolds Number
255 kPa Upstream Line Pressure, β = 0.467

Figure 154   Differential Pressure as a Function of Upstream
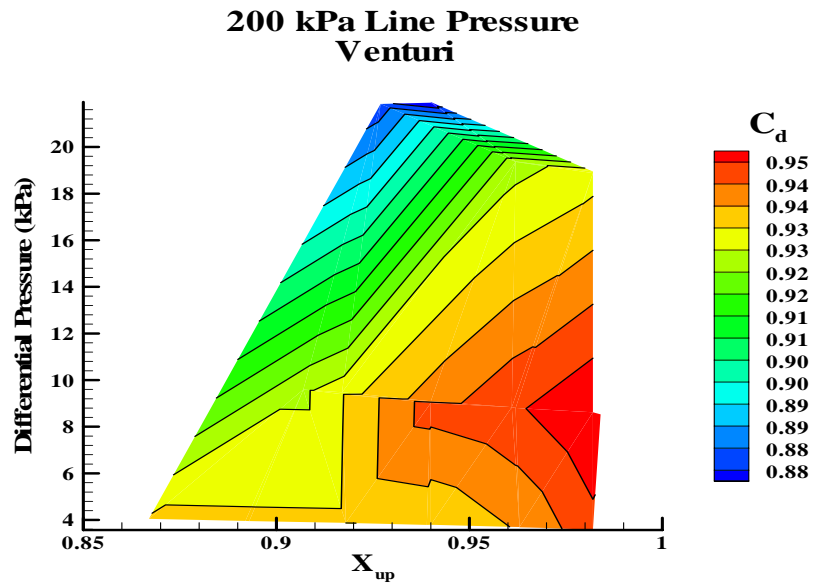Quality and Gas Reynolds Number
255 kPa Upstream Line Pressure, Venturi

360 kPa Line Pressure
Beta = 0.43

Figure 155   Differential Pressure as a Function of Upstream
Quality and Gas Reynolds Number
360 kPa Upstream Line Pressure, $\beta = 0.43$

360 kPa Line Pressure
Beta = 0.467

Figure 156   Differential Pressure as a Function of Upstream
Quality and Gas Reynolds Number
360 kPa Upstream Line Pressure, $\beta = 0.467$

360 kPa Line Pressure
Venturi

Figure 157   Differential Pressure as a Function of Upstream
Quality and Gas Reynolds Number
360 kPa Upstream Line Pressure, Venturi
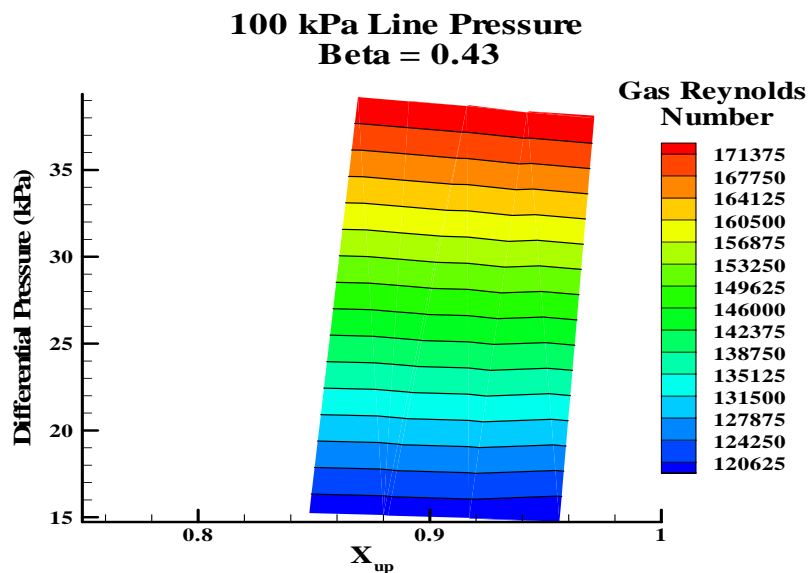
470 kPa Line Pressure
Beta = 0.43
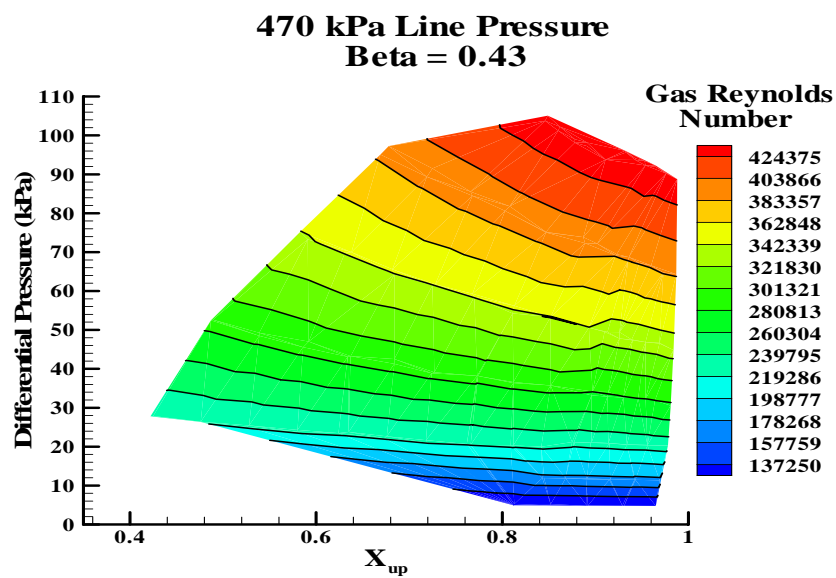
Figure 158   Differential Pressure as a Function of Upstream
Quality and Gas Reynolds Number
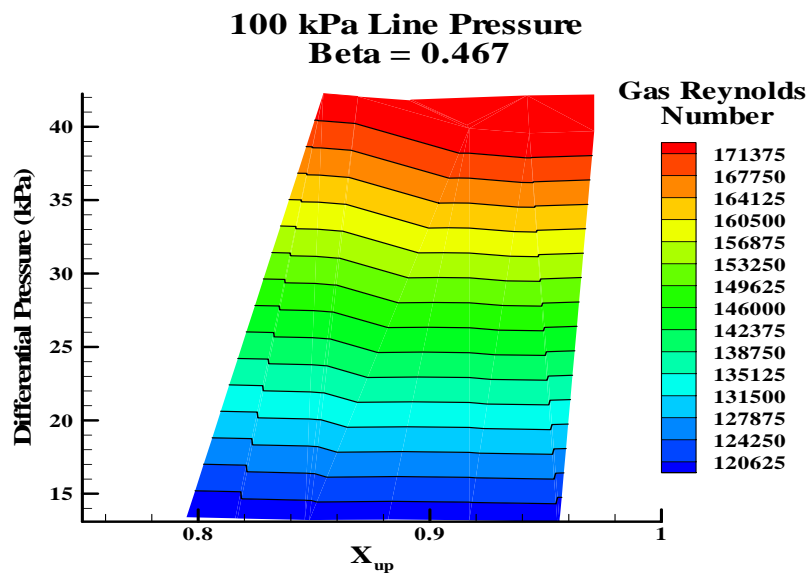470 kPa Upstream Line Pressure, β = 0.43
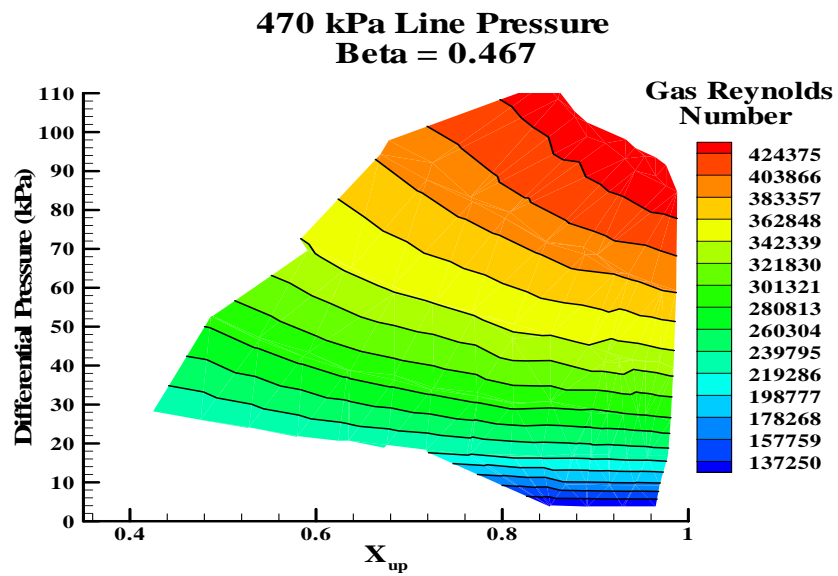
Figure 159   Differential Pressure as a Function of Upstream
               Quality and Gas Reynolds Number
               470 kPa Upstream Line Pressure, β = 0.467
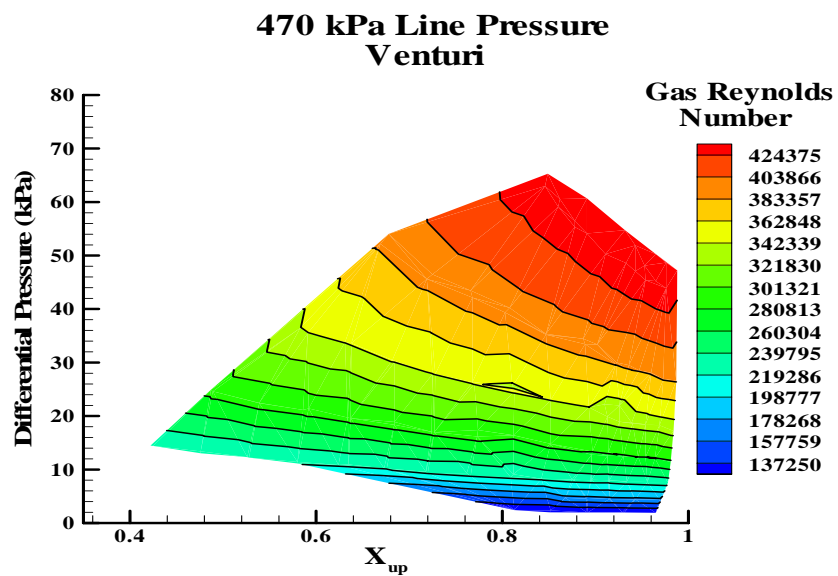
Figure 160   Differential Pressure as a Function of Upstream
               Quality and Gas Reynolds Number
               470 kPa Upstream Line Pressure, Venturi

575 kPa Line Pressure
Beta = 0.43
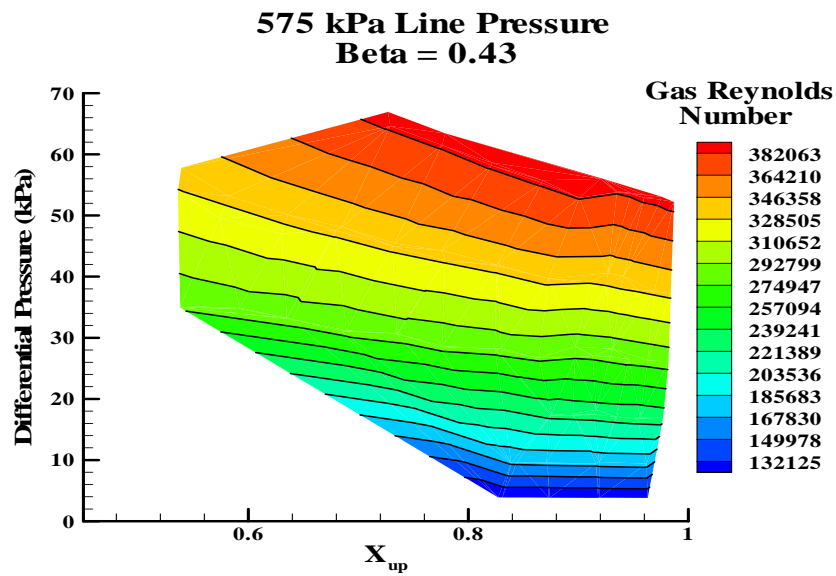
Figure 161   Differential Pressure as a Function of Upstream
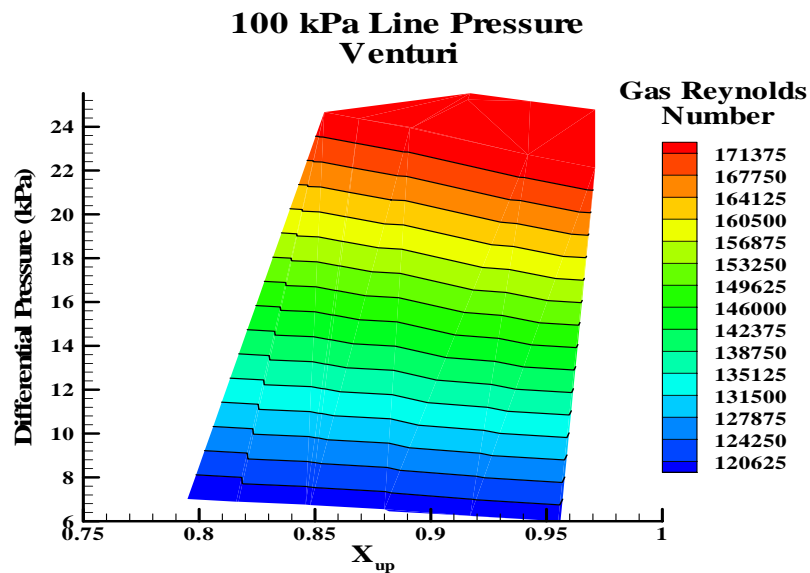Quality and Gas Reynolds Number
575 kPa Upstream Line Pressure, β = 0.43

575 kPa Line Pressure
Beta = 0.467
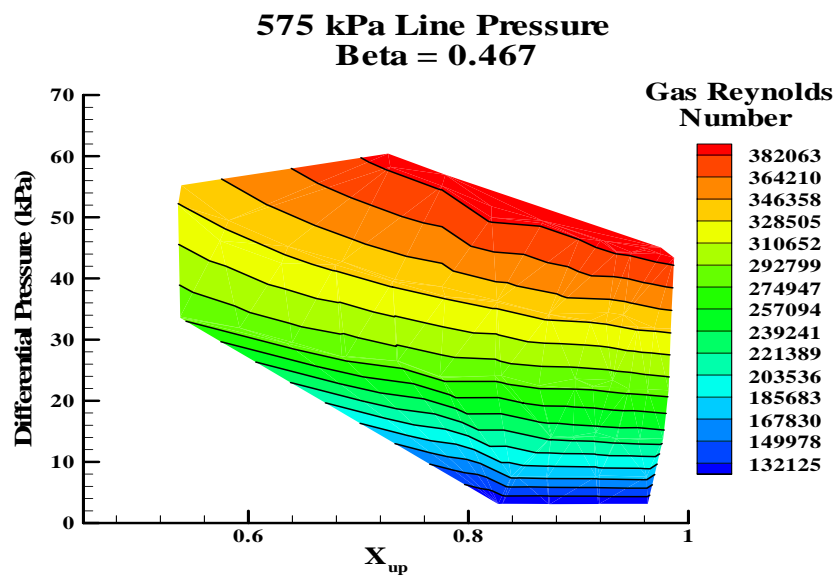
Figure 162   Differential Pressure as a Function of Upstream
Quality and Gas Reynolds Number
575 kPa Upstream Line Pressure, β = 0.467
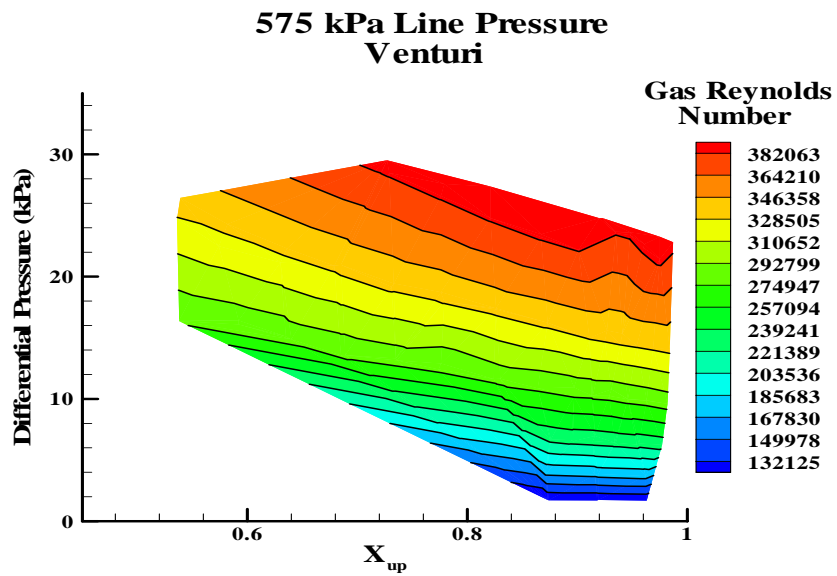
Figure 163   Differential Pressure as a Function of Upstream
Quality and Gas Reynolds Number
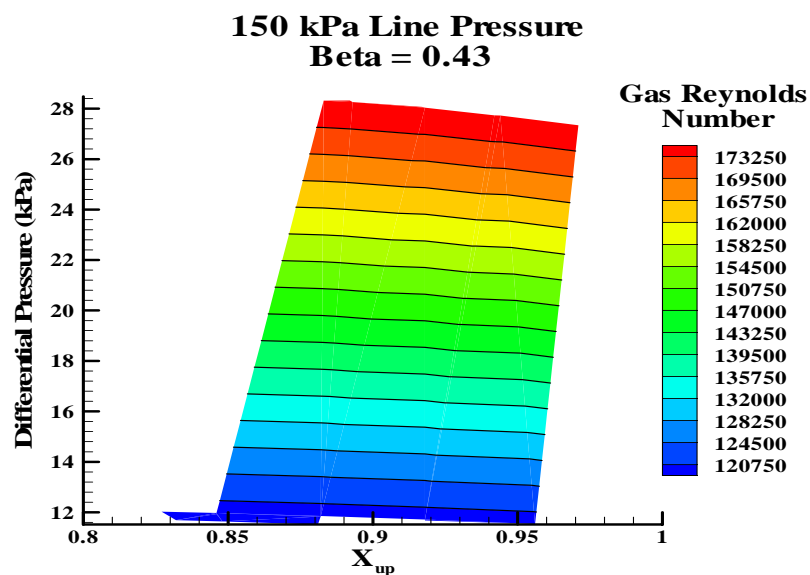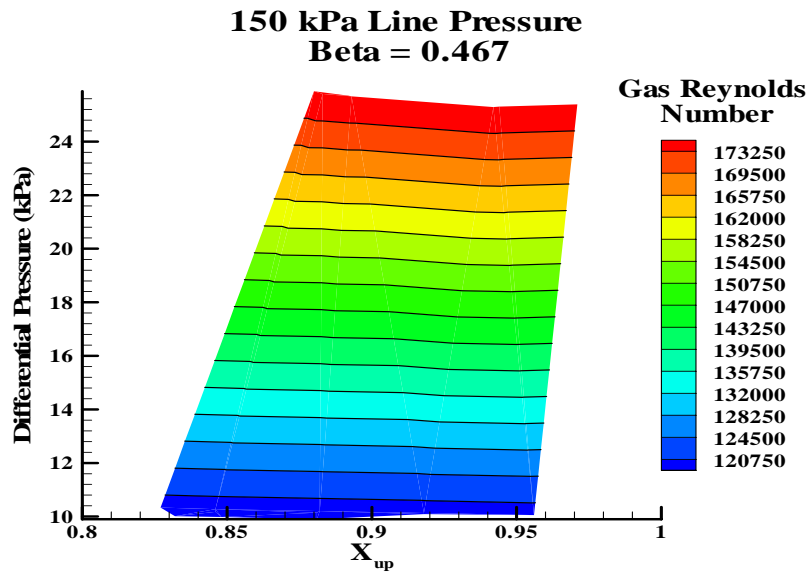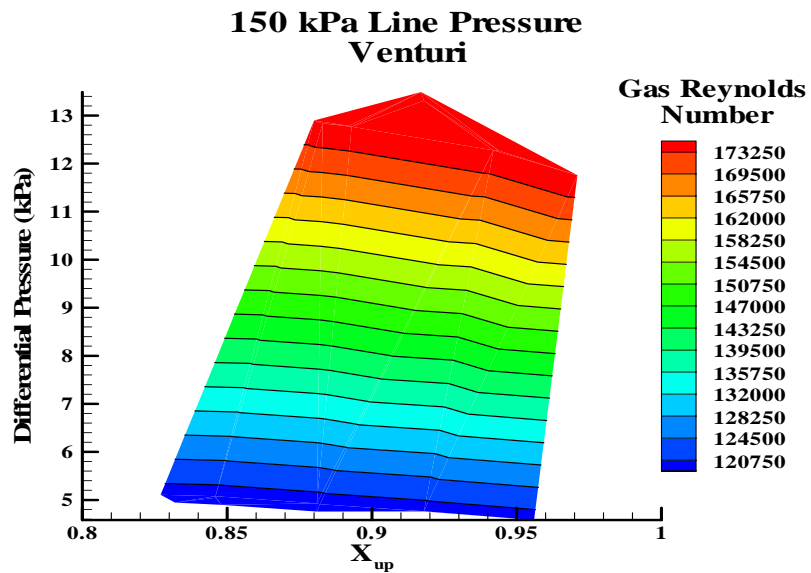575 kPa Upstream Line Pressure, Venturi
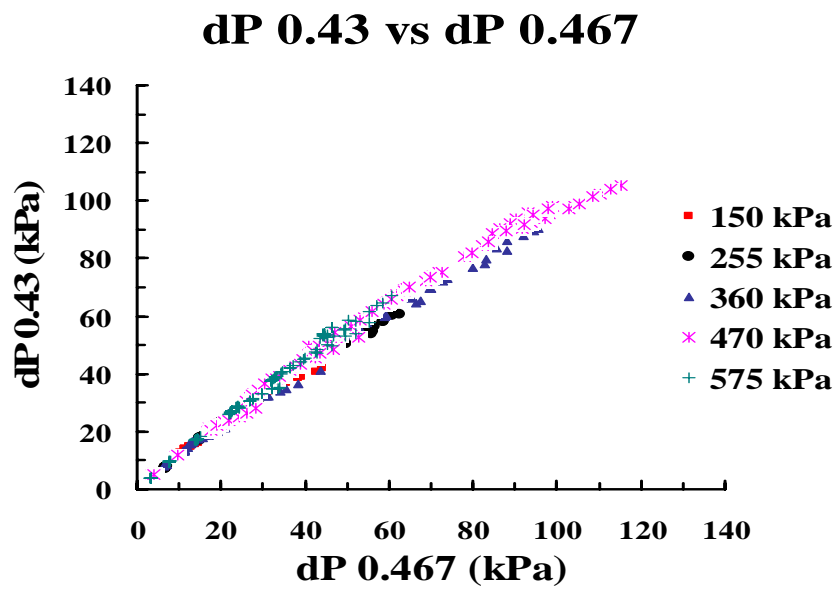
Figure 164   Differential Pressure across $\beta = 0.43$ plate as a function
of the Differential Pressure across $\beta = 0.467$ plate
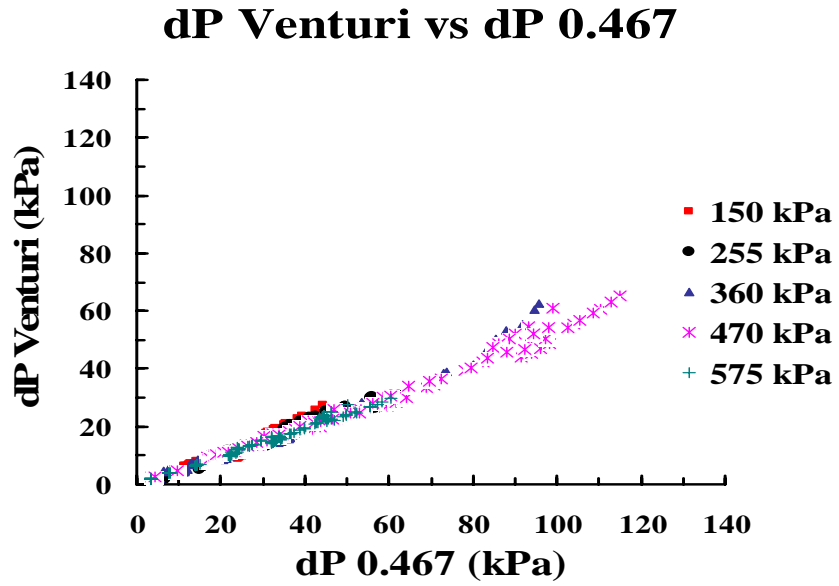
Figure 165   Differential Pressure across the venturi as a function
of the Differential Pressure across β = 0.467 plate
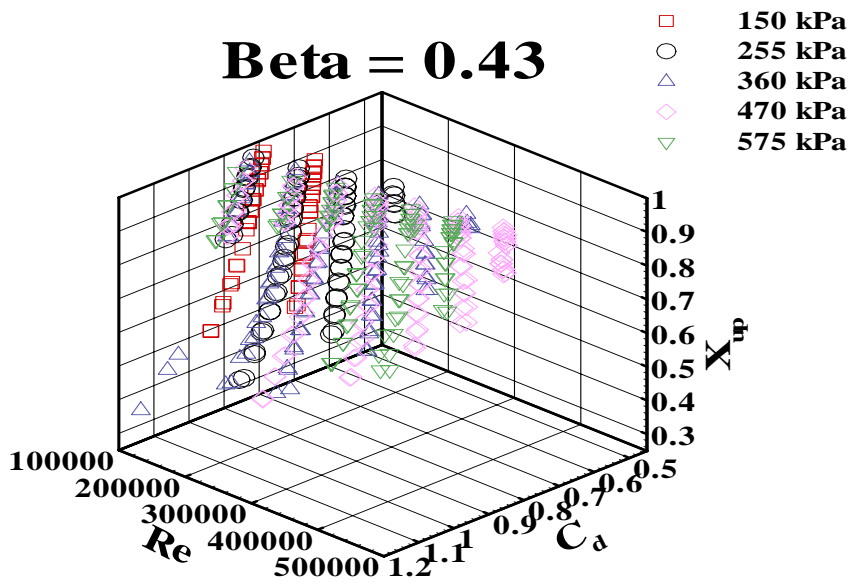
Figure 166   Coefficient of Discharge as a function of
Gas Reynolds Number and Upstream Quality
at different upstream line pressures, β = 0.43
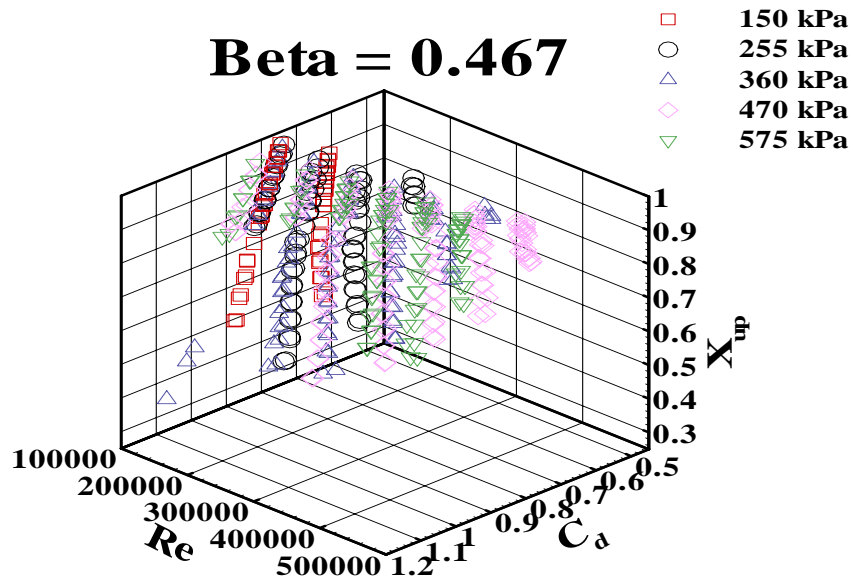
Figure 167   Coefficient of Discharge as a function of
Gas Reynolds Number and Upstream Quality
at different upstream line pressures, β = 0.467
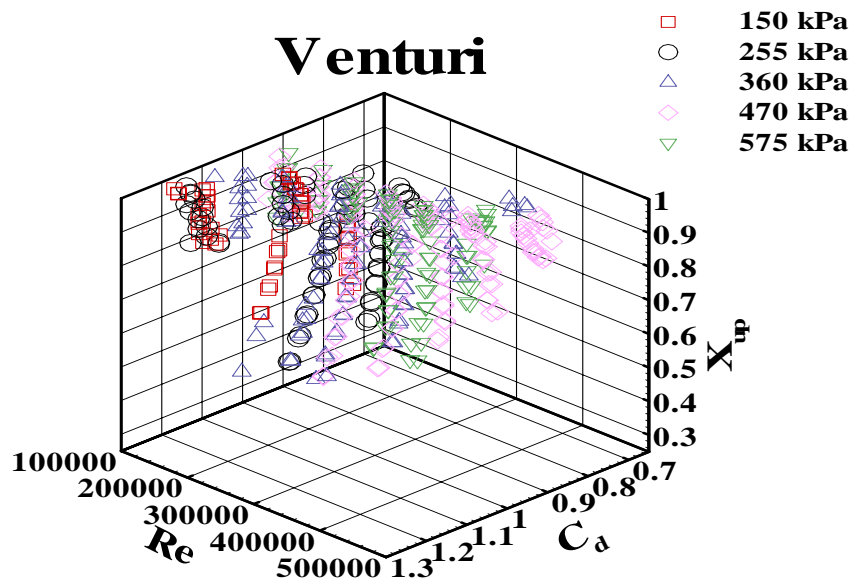
Figure 168   Coefficient of Discharge as a function of
Gas Reynolds Number and Upstream Quality
at different upstream line pressures, Venturi
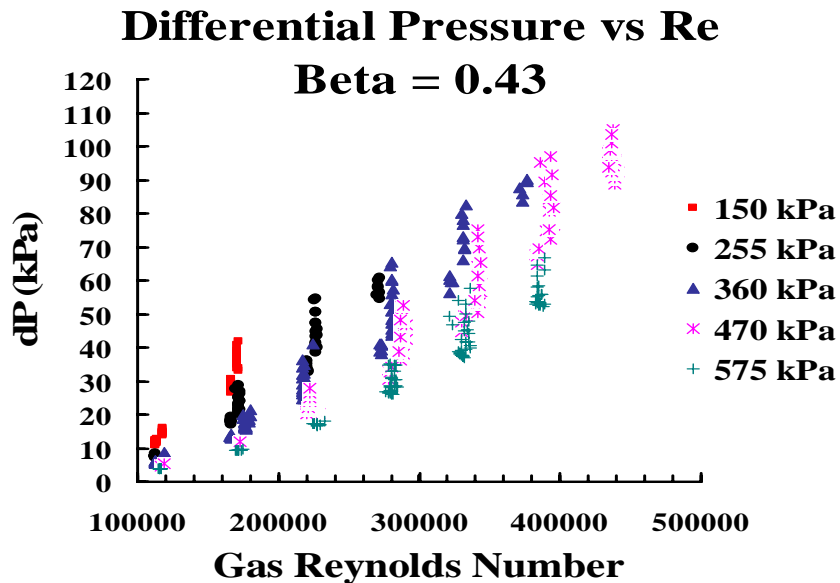
Figure 169   Differential Pressure as a function of
              Gas Reynolds Number, β = 0.43
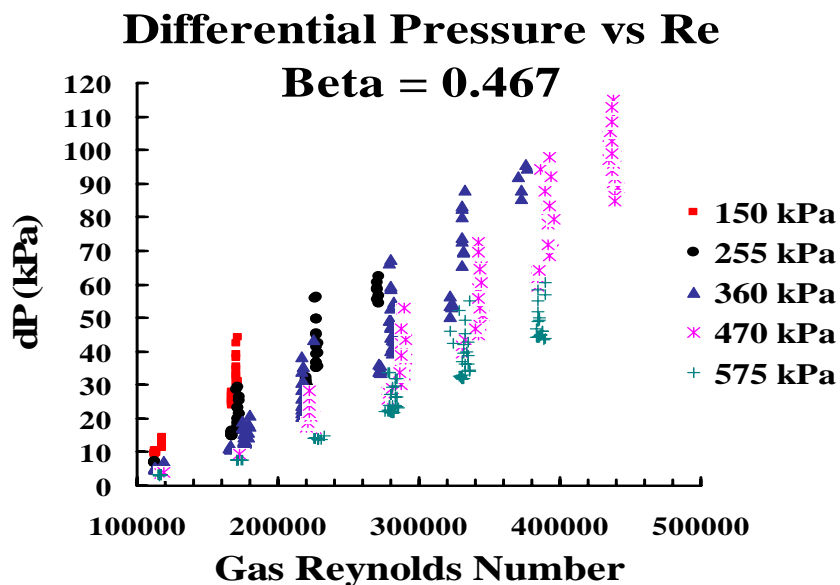
Figure 170   Differential Pressure as a function of
              Gas Reynolds Number, β = 0.467
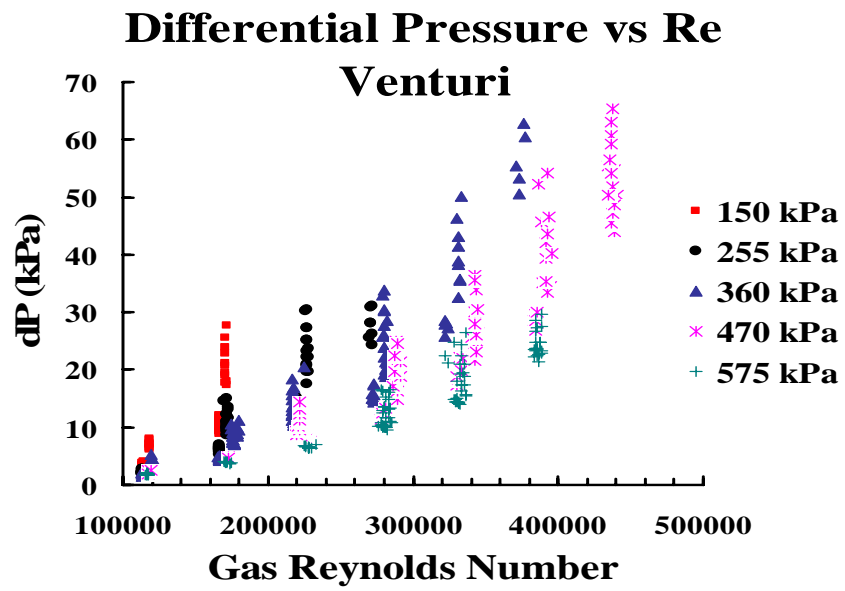
Figure 171   Differential Pressure as a function of
Gas Reynolds Number, Venturi

Case 6 Quality Effects

100 kPa Line Pressure
Beta = 0.43

Figure 172   Differential Pressure as a Function of Upstream
Quality and Coefficient of Discharge,
100 kPa Upstream Line Pressure, β = 0.43

150 kPa Line Pressure
Beta = 0.43

Figure 173   Differential Pressure as a Function of Upstream
Quality and Coefficient of Discharge,
150 kPa Upstream Line Pressure, β = 0.43

200 kPa Line Pressure
Beta = 0.43

Figure 174   Differential Pressure as a Function of Upstream
Quality and Coefficient of Discharge,
200 kPa Upstream Line Pressure, β = 0.43

255 kPa Line Pressure
Beta = 0.43

Figure 175   Differential Pressure as a Function of Upstream
Quality and Coefficient of Discharge,
200 kPa Upstream Line Pressure, β = 0.43

100 kPa Line Pressure
Beta = 0.467

Figure 176   Differential Pressure as a Function of Upstream
Quality and Coefficient of Discharge,
100 kPa Upstream Line Pressure, β = 0.467

150 kPa Line Pressure
Beta = 0.467

Figure 177   Differential Pressure as a Function of Upstream
Quality and Coefficient of Discharge,
150 kPa Upstream Line Pressure, β = 0.467

Figure 178   Differential Pressure as a Function of Upstream
Quality and Coefficient of Discharge,
200 kPa Upstream Line Pressure, β = 0.467

Figure 179   Differential Pressure as a Function of Upstream
Quality and Coefficient of Discharge,
255 kPa Upstream Line Pressure, β = 0.467

**100 kPa Line Pressure
Venturi**
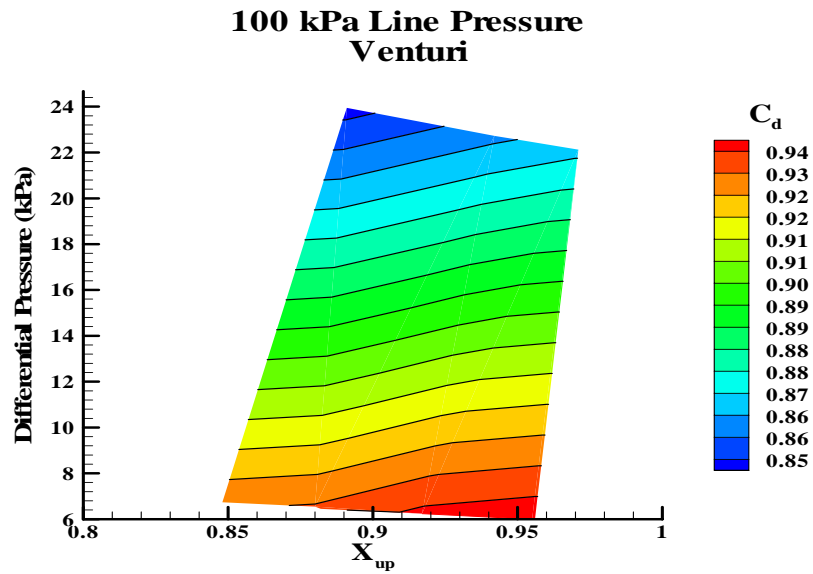
Figure 180   Differential Pressure as a Function of Upstream
Quality and Coefficient of Discharge,
100 kPa Upstream Line Pressure, Venturi

**150 kPa Line Pressure
Venturi**
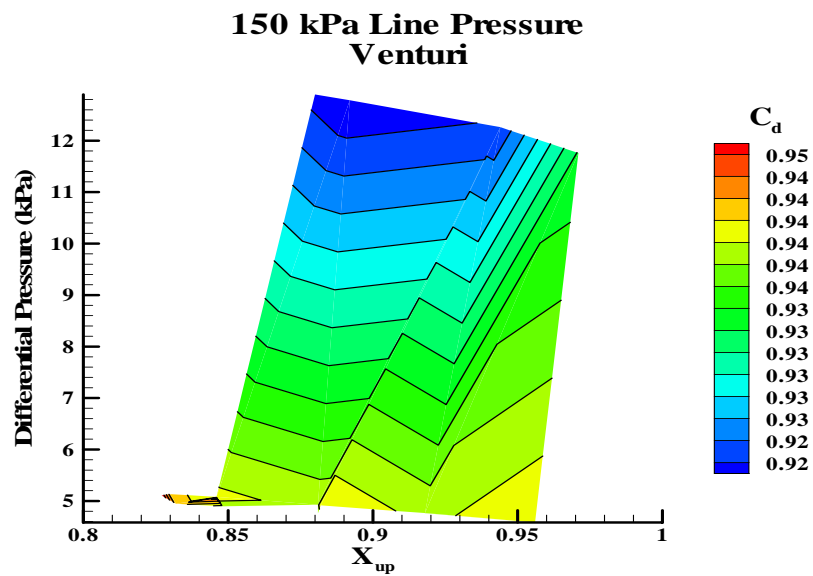
Figure 181   Differential Pressure as a Function of Upstream
Quality and Coefficient of Discharge,
150 kPa Upstream Line Pressure, Venturi

Figure 182   Differential Pressure as a Function of Upstream
              Quality and Coefficient of Discharge,
              200 kPa Upstream Line Pressure, Venturi
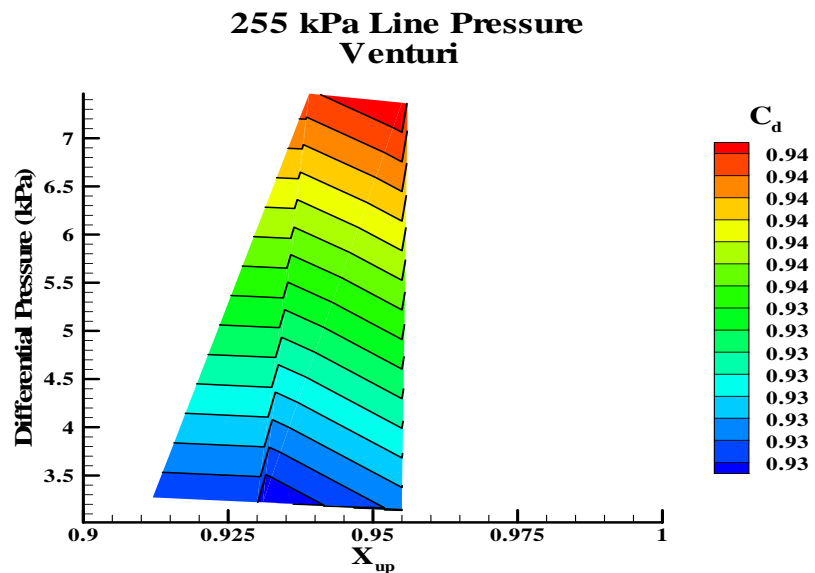
Figure 183   Differential Pressure as a Function of Upstream
              Quality and Coefficient of Discharge,
              255 kPa Upstream Line Pressure, Venturi

Case 6 Repeatability

Figure 184   Differential Pressure as a Function of Upstream Quality and Gas Reynolds Number, 100 kPa Upstream Line Pressure, $\beta = 0.43$

Figure 185   Differential Pressure as a Function of Upstream Quality and Gas Reynolds Number, 100 kPa Upstream Line Pressure, $\beta = 0.467$

Figure 186   Differential Pressure as a Function of Upstream
Quality and Gas Reynolds Number,
100 kPa Upstream Line Pressure, Venturi

Figure 187   Differential Pressure as a Function of Upstream
Quality and Gas Reynolds Number,
150 kPa Upstream Line Pressure, β = 0.43

Figure 188   Differential Pressure as a Function of Upstream
Quality and Gas Reynolds Number,
150 kPa Upstream Line Pressure, $\beta = 0.467$

Figure 189   Differential Pressure as a Function of Upstream
Quality and Gas Reynolds Number,
150 kPa Upstream Line Pressure, Venturi
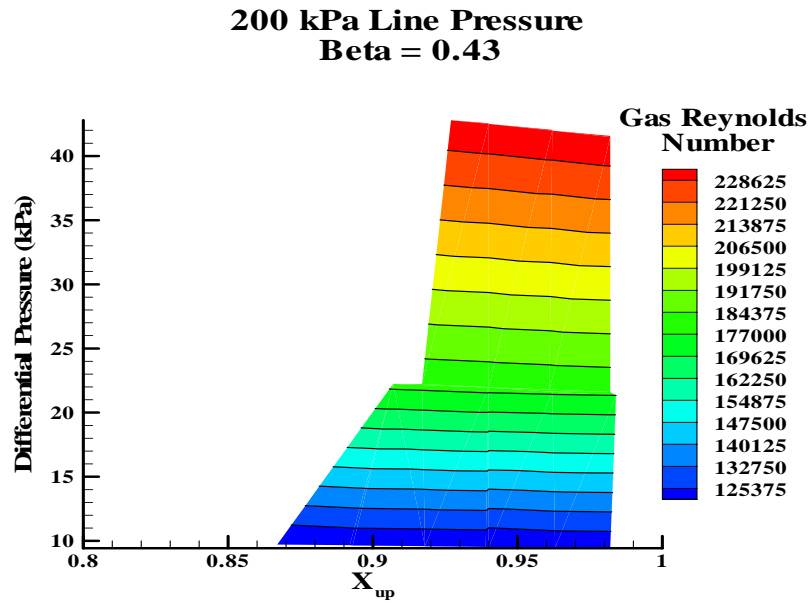
Figure 190   Differential Pressure as a Function of Upstream
Quality and Gas Reynolds Number,
200 kPa Upstream Line Pressure, $\beta = 0.43$
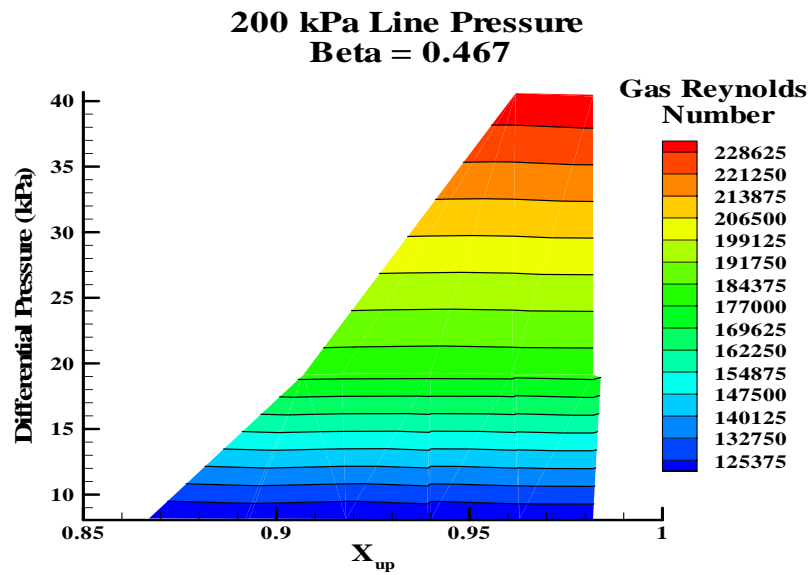
Figure 191   Differential Pressure as a Function of Upstream
Quality and Gas Reynolds Number,
200 kPa Upstream Line Pressure, $\beta = 0.467$

200 kPa Line Pressure
Beta = 0.467
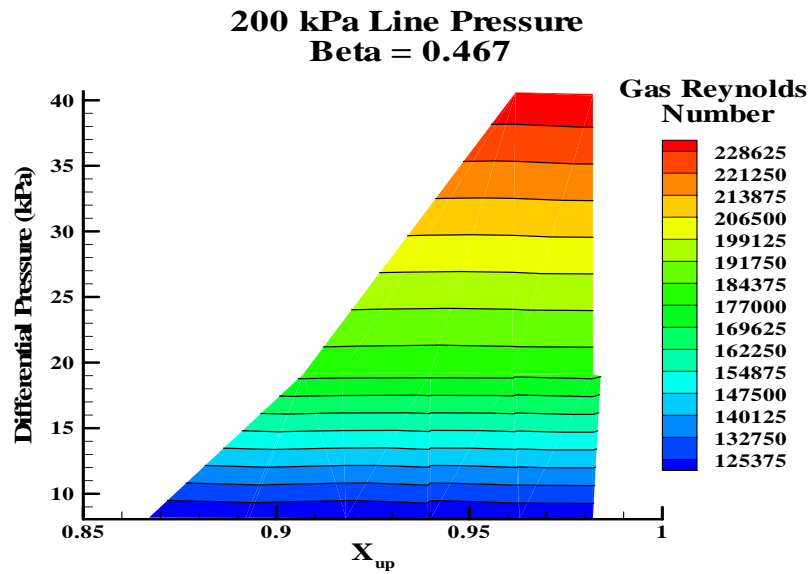
Figure 192   Differential Pressure as a Function of Upstream
Quality and Gas Reynolds Number,
200 kPa Upstream Line Pressure, Venturi

255 kPa Line Pressure
Beta = 0.43
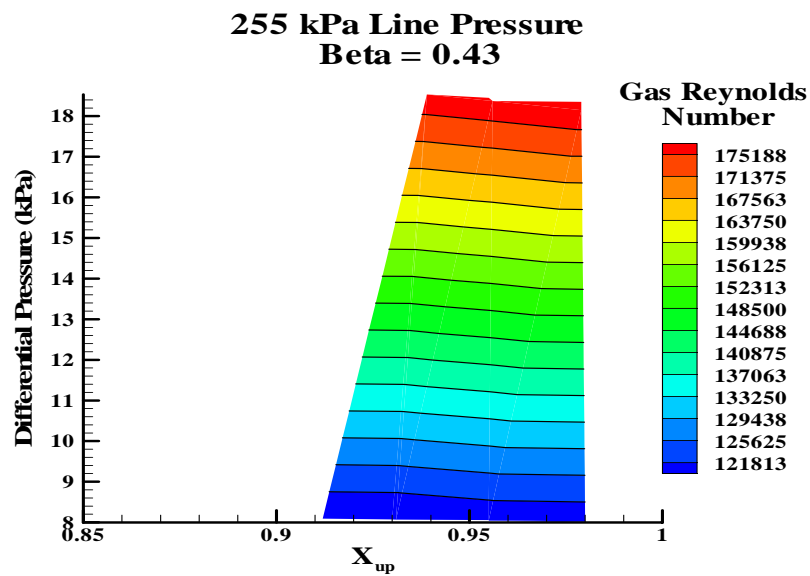
Figure 193   Differential Pressure as a Function of Upstream
Quality and Gas Reynolds Number,
255 kPa Upstream Line Pressure, $\beta = 0.43$
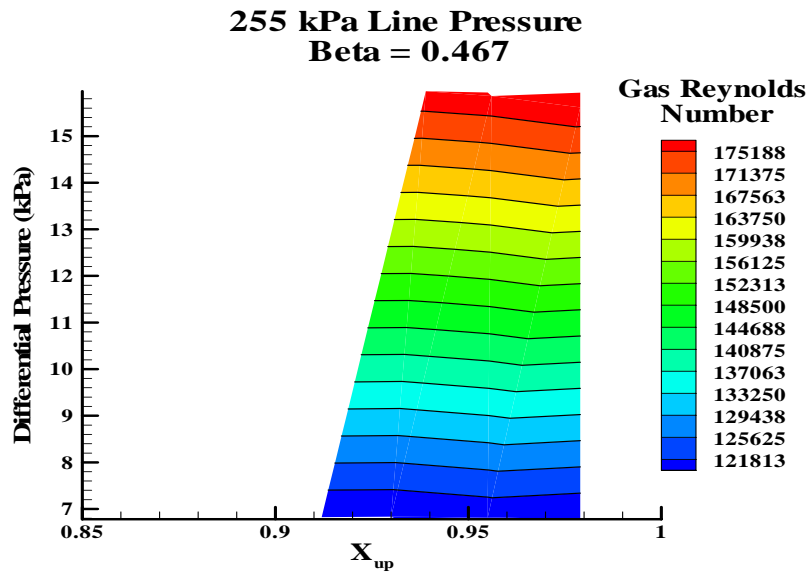
Figure 194   Differential Pressure as a Function of Upstream
Quality and Gas Reynolds Number,
255 kPa Upstream Line Pressure, β = 0.467
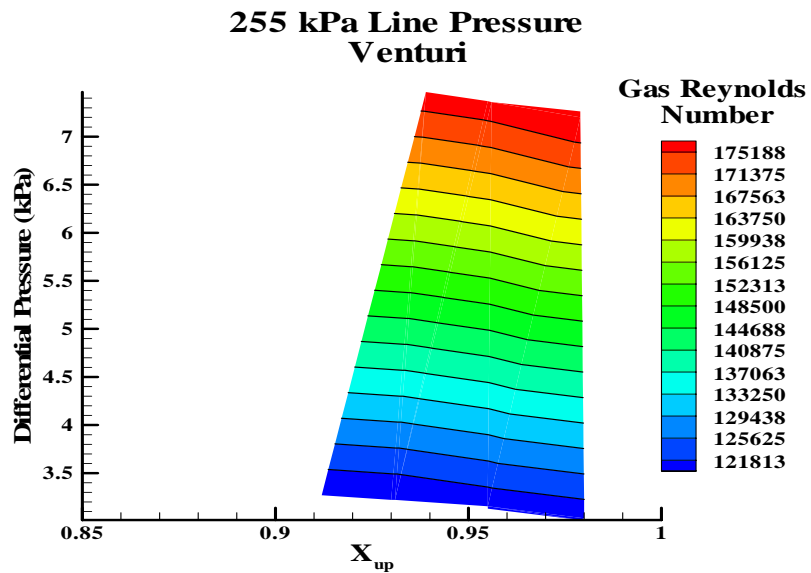
Figure 195   Differential Pressure as a Function of Upstream
Quality and Gas Reynolds Number,
255 kPa Upstream Line Pressure, Venturi
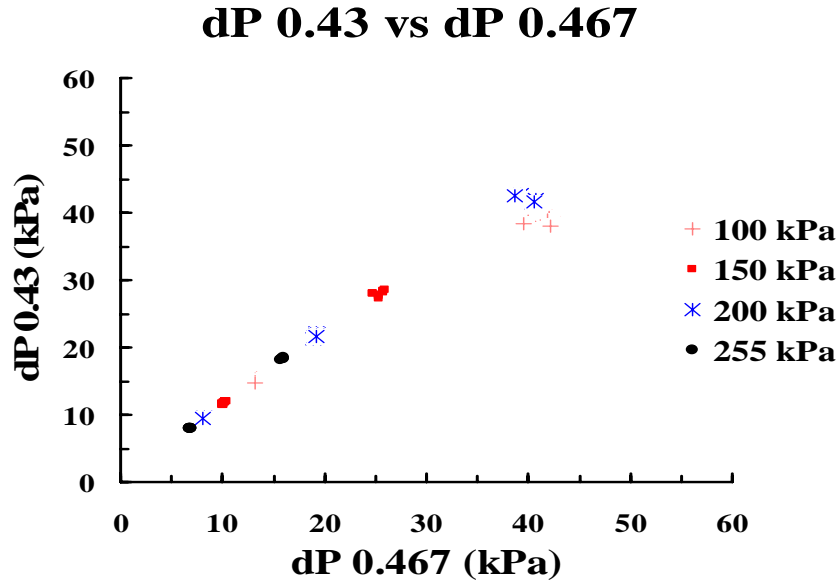
Figure 196   Differential Pressure across $\beta = 0.43$ plate as a function of the Differential Pressure across $\beta = 0.467$ plate
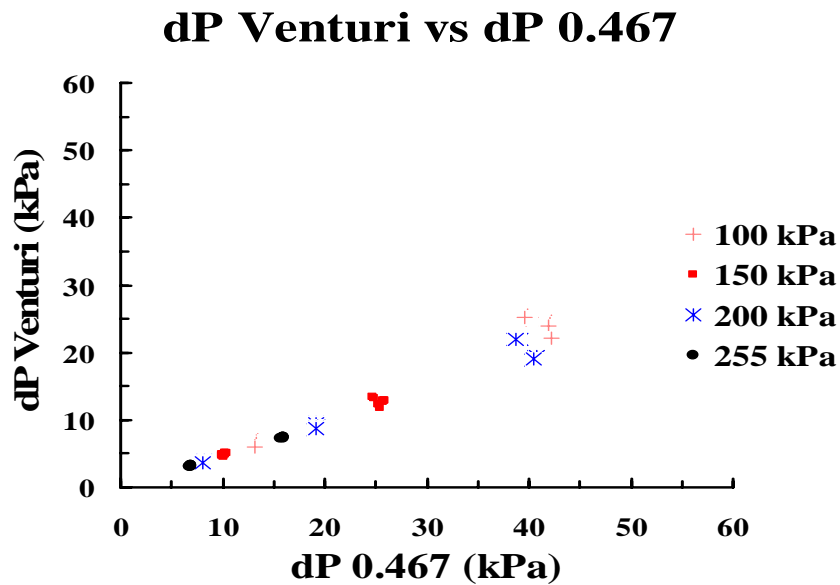
Figure 197   Differential Pressure across the venturi as a function of the Differential Pressure across $\beta = 0.467$ plate
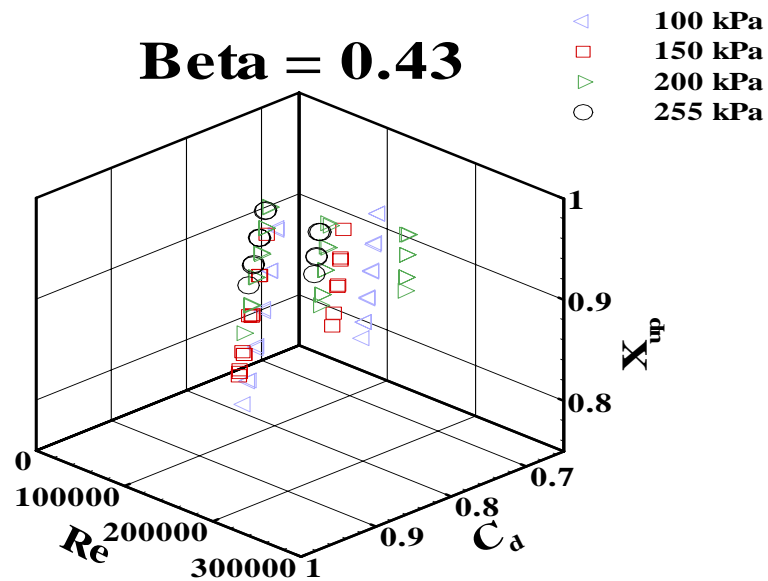
Figure 198   Coefficient of Discharge as a function of
              Gas Reynolds Number and Upstream Quality
              at different upstream line pressures, β = 0.43
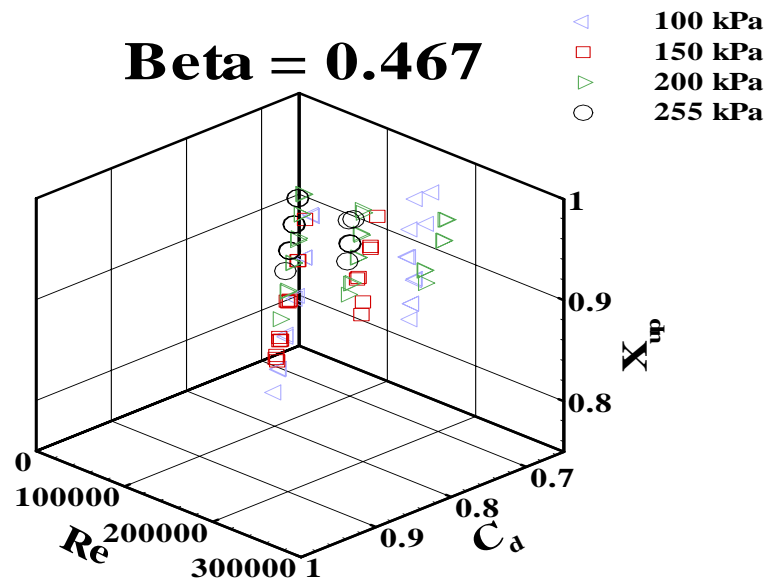
Figure 199   Coefficient of Discharge as a function of
              Gas Reynolds Number and Upstream Quality
              at different upstream line pressures, β = 0.467
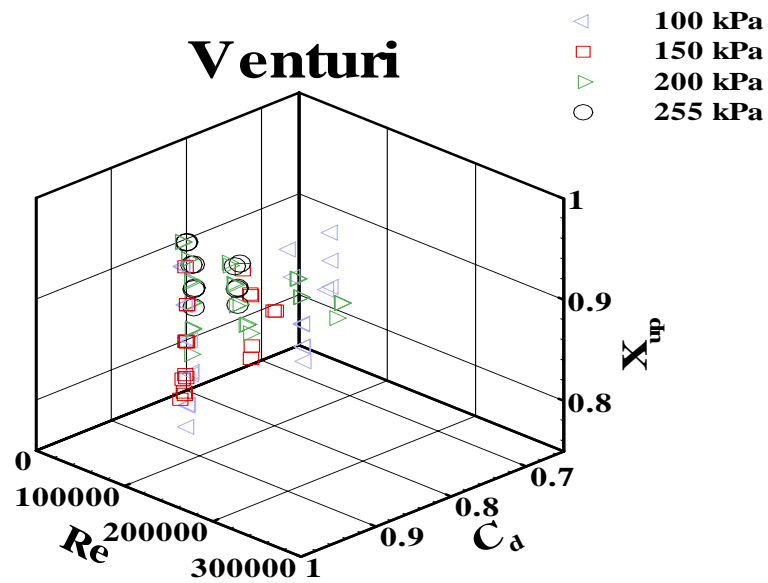
Venturi

Figure 200   Coefficient of Discharge as a function of
Gas Reynolds Number and Upstream Quality
at different upstream line pressures, Venturi

Diferential Pressure vs Re
Beta = 0.43
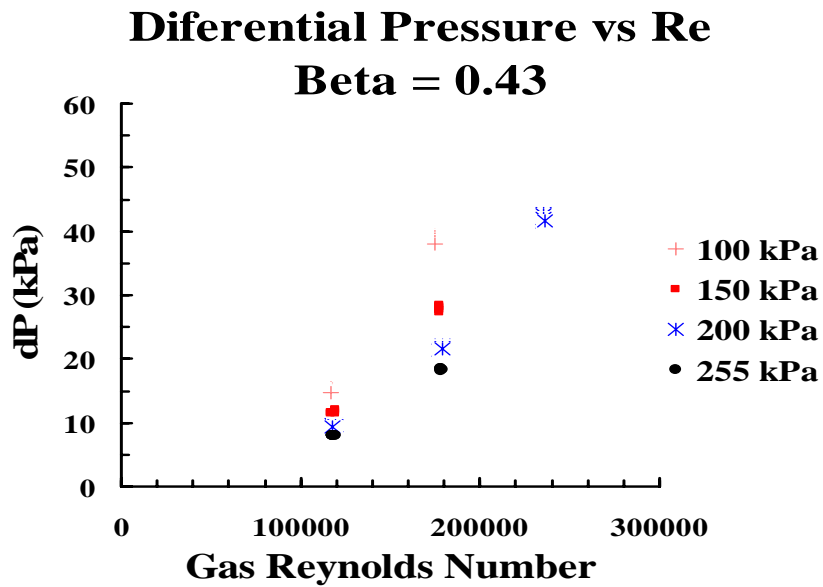
Figure 201   Differential Pressure as a function of
Gas Reynolds Number, $\beta = 0.43$

Differential Pressure vs Re
Beta = 0.467
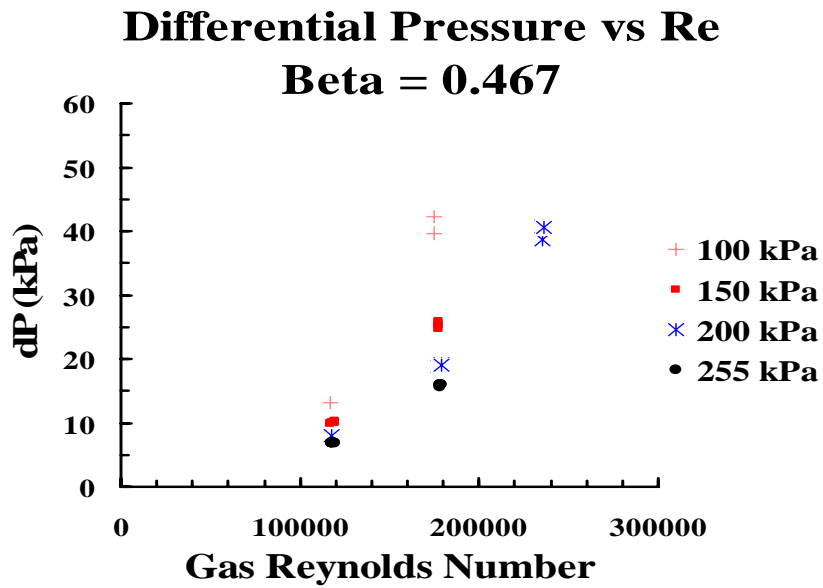
Figure 202   Differential Pressure as a function of
Gas Reynolds Number, β = 0.467

Differential Pressure vs Re
Venturi
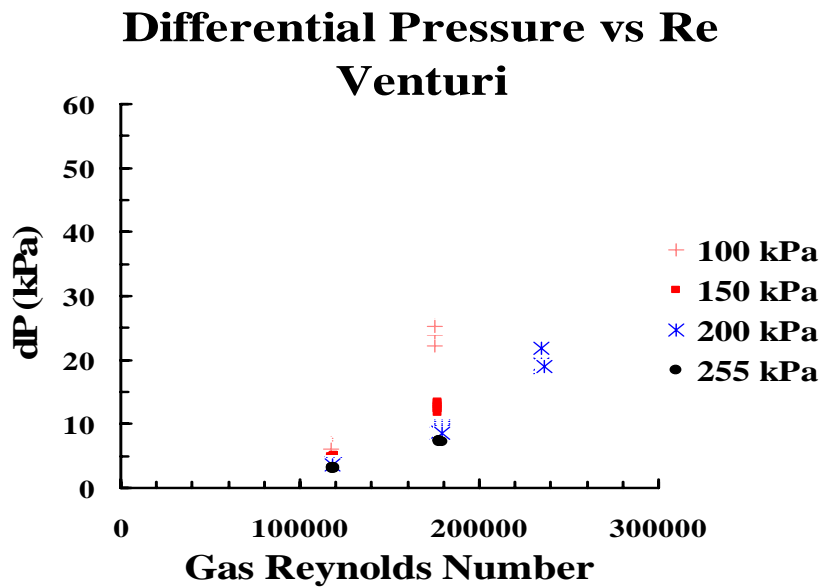
Figure 203   Differential Pressure as a function of
Gas Reynolds Number, Venturi

Reproducibility

Figure 204   Surface plot showing reproducibility
of β = 0.43 slotted plate for all data

Figure 205   Surface plot showing reproducibility
of β = 0.43 slotted plate for all data

Figure 206   Surface plot showing reproducibility
               of β = 0.508 standard plate for all data

Figure 207   Surface plot showing reproducibility
               of β = 0.527 venturi for all data

Figure 208   Surface plot showing reproducibility of $\beta = 0.43$ slotted plate for all data
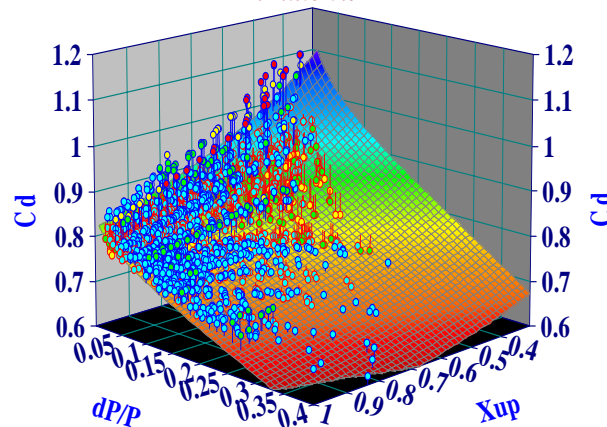

Figure 209   Surface plot showing reproducibility of $\beta = 0.467$ slotted plate for all data

Reproducibility for 0.508 standard plate - All Data
Rank 1 Eqn 302461759 $z^{(-1)}=a+be^{(x/wx)}+cy^2$
$r^2=0.97277645$ DF Adj $r^2=0.97263613$ FitStdErr=0.0093024064 Fstat=10416.142
a=3.0095085 b=-2.1704716
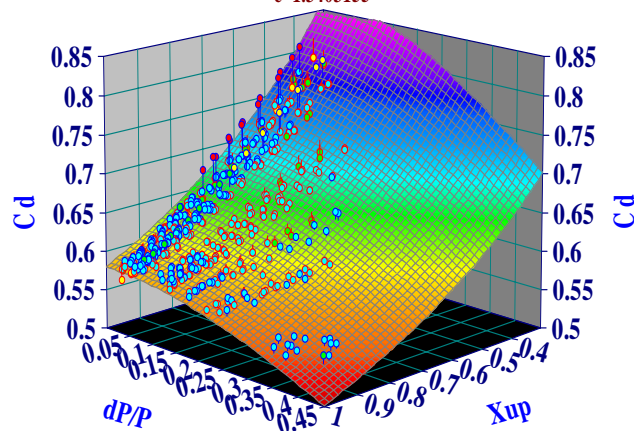c=1.3403155

Figure 210   Surface plot showing reproducibility
of $\beta = 0.508$ standard plate for all data

Reproducibility for 0.527 venturi - All Data
Rank 1 Eqn 3599 $z=a+b\ln x/x^2+cy^{(0.5)}$
$r^2=0.4742254$ DF Adj $r^2=0.47143368$ FitStdErr=0.048554889 Fstat=255.25347
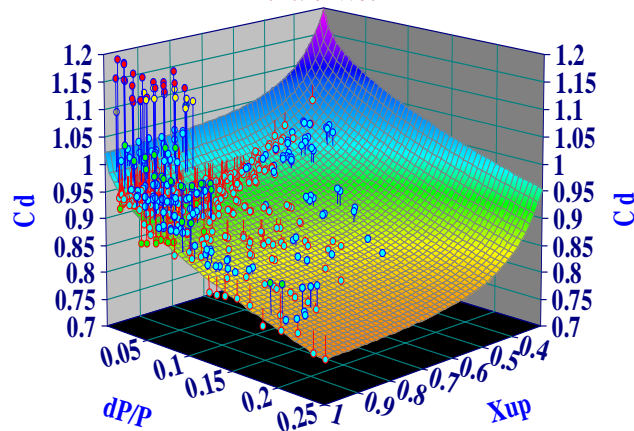a=1.0208939 b=-0.013220637
c=-0.48729936

Figure 211   Surface plot showing reproducibility
of $\beta = 0.527$ venturi for all data

VITA

Vasanth Muralidharan is the son of Mr. R. Muralidharan and Mrs. Vani Muralidharan. He was born on March 25, 1980 in Chennai, Tamil Nadu, India. He has a sister, Ramya. He graduated from P.S.B.B Senior Secondary School in 1997. In 2001, he received his Bachelor of Engineering degree in mechanical engineering from A.C. College of Engineering and Technology, Karaikudi affiliated to the Madurai Kamaraj University, Madurai. He enrolled in the Master of Science program in Mechanical Engineering at Texas A&M University in 2001. His permanent address is A-6 First Block, Sidharth Heights, 55 Arcot Road, Saligramam, Chennai 600093, Tamil Nadu, India.